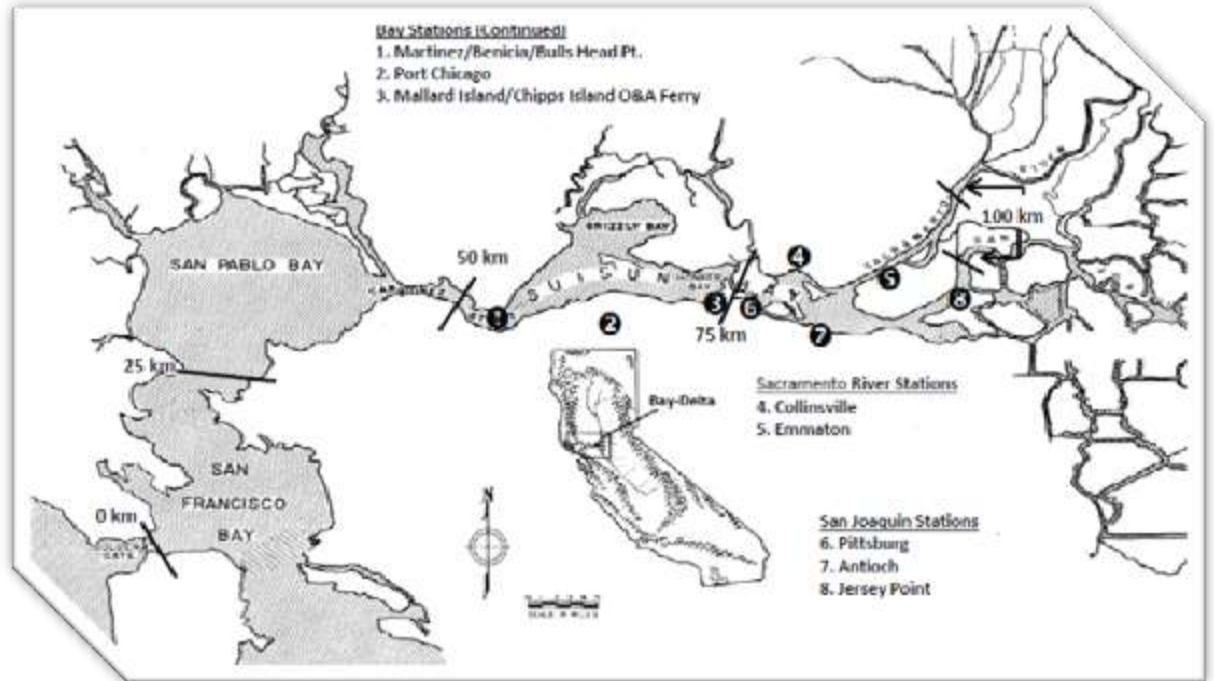


Delta Salinity Gradient (DSG) Model



Version 1.0 Model Documentation

Metropolitan Water District of Southern California

September 9, 2014
Paul H. Hutton, Ph.D., P.E.

Table of Contents

List of Tables	iii
List of Figures	iv
Executive Summary	xv
1. Introduction	1-1
2. Formulation	3-1
2.1 Previous Modeling Efforts	3-1
2.2 Integration of Previous Modeling Efforts	3-2
2.3 Deviations from Self-Similarity	3-4
2.4 Longitudinal Salinity Gradient.....	3-4
2.5 Formulation Summary.....	3-5
3. Calibration & Validation with DSM2 Data.....	5-1
3.1 Data Description.....	5-1
3.2 X2 Parameter Calibration.....	5-1
3.3 S _o Parameter Calibration	5-2
3.4 Salinity & Isohaline Estimates: DSM2 Calibration Period.....	5-3
3.5 Validation Results	5-4
4. Calibration & Validation with Observed Data	7-1
4.1 Data Description.....	7-1
4.2 X2 Parameter Calibration.....	7-1
4.2.1 Sacramento River Branch	7-1
4.2.2 San Joaquin River Branch.....	7-2
4.3 S _o Parameter Calibration	7-2
4.4 Salinity & Isohaline Estimates: Calibration Period.....	7-2
4.5 Validation Results	7-3
4.5.1 X2 Estimates	7-3
4.5.2 Salinity Estimates.....	7-4
4.5.3 Other Isohaline Estimates	7-8
5. Analysis	9-1

5.1 Analysis of Sensitivity	9-1
5.2 Comparison with G-Model Estimates	9-2
5.3 DSG Salinity Estimates Using Interpolated X2 Values	9-3
5.4 Analysis of Salinity Gradient	9-4
5.5 Analysis of Dispersion Coefficients.....	9-5
6. Discussion & Next Steps	11-1
6.1 Discussion	11-1
6.2 Next Steps	11-2
6.2.1 Data Evaluation	11-2
6.2.2 Model Refinement	11- Error! Bookmark not defined.
7. References	13-1
Appendix A: Time Series & Scatter Plots – DSG Model Calibration & Validation with DSM2 Data.....	A-1
Appendix B: Development of Daily Net Delta Outflow for the Period October 1921 through September 1929	B-1
Appendix C: Scatter Plots – DSG Model Calibration with Observed Data	C-1
Appendix D: Time Series Plots – DSG Model Validation with Interpolated X2 Data	D-1
Appendix E: Time Series Plots – DSG Model Validation with Observed Salinity Data	E-1
Appendix F: Time Series Plots – DSG Salinity Predictions Using Interpolated X2 Values	F-1

List of Tables

Table 3-1: Variance of DSG Salinity Predictions with DSM2 Data

Table 4-1: Performance of DSG X2 Predictions by Decade

Table 4-2: Performance of DSG Salinity Predictions at Martinez by Decade

Table 4-3: Performance of DSG Salinity Predictions at Port Chicago by Decade

Table 4-4: Performance of DSG Salinity Predictions at Mallard Island (O&A Ferry) by Decade

Table 4-5: Performance of DSG Salinity Predictions at Collinsville by Decade

Table 4-6: Performance of DSG Salinity Predictions at Emmaton by Decade

Table 4-7: Performance of DSG Salinity Predictions at Pittsburg by Decade

Table 4-8: Performance of DSG Salinity Predictions at Antioch by Decade

Table 4-9: Performance of DSG Salinity Predictions at Jersey Point by Decade

Table 4-10: Performance of DSG 1 ppt Isohaline Predictions by Decade

Table 4-11: Performance of DSG 4 ppt Isohaline Predictions by Decade

Table 4-12: Performance of DSG 6 ppt Isohaline Predictions by Decade

Table 5-1: DSG Model Parameter Sensitivity Analysis: Perturbation by Plus & Minus Ten Percent

Table 5-2: Comparison of α Parameter Values Produced by the DSG and G Models

Table 5-3: Performance of DSG Salinity Predictions Using Interpolated X2 Values: 2000-09

List of Figures

Figure 3-1: DSM2 Interpolated X2 Position as a Function of Antecedent Outflow: 2000-09 Calibration

Figure 3-2: Time Series of DSG Predicted and DSM2 Interpolated X2 Position: 2000-2009

Figure 3-3: Time Series of DSG Predicted and DSM2 Surface Salinity at Martinez: 2000-2009

Figure 3-4: Time Series of DSG Predicted and DSM2 Surface Salinity at Port Chicago: 2000-2009

Figure 3-5: Time Series of DSG Predicted and DSM2 Surface Salinity at Mallard Island: 2000-2009

Figure 3-6: Time Series of DSG Predicted and DSM2 Surface Salinity at Collinsville: 2000-2009

Figure 3-7: Time Series of DSG Predicted and DSM2 Surface Salinity at Emmaton: 2000-2009

Figure 3-8: Time Series of DSG Predicted and DSM2 Interpolated 1 ppt Surface Isohaline Position: 2000-2009

Figure 3-9: Time Series of DSG Predicted and DSM2 Interpolated 4 ppt Surface Isohaline Position: 2000-2009

Figure 3-10: Time Series of DSG Predicted and DSM2 Interpolated 6 ppt Surface Isohaline Position: 2000-2009

Figure 4-1: Interpolated Sacramento Branch X2 Position as a Function of Antecedent Outflow: 2000-09 Calibration

Figure 4-2: Time Series of DSG Predicted and Interpolated Sacramento Branch X2 Position: 2000-2009

Figure 4-3: Interpolated San Joaquin Branch X2 Position as a Function of Antecedent Outflow: 2000-09 Calibration

Figure 4-4: Time Series of DSG Predicted and Interpolated San Joaquin Branch X2 Position: 2000-2009

Figure 4-5: Time Series of DSG Predicted and Observed Surface Salinity at Martinez: 2000-2009

Figure 4-6: Time Series of DSG Predicted and Observed Surface Salinity at Port Chicago: 2000-2009

Figure 4-7: Time Series of DSG Predicted and Observed Surface Salinity at Mallard Island: 2000-2009

Figure 4-8: Time Series of DSG Predicted and Observed Surface Salinity at Collinsville: 2000-2009

Figure 4-9: Time Series of DSG Predicted and Observed Surface Salinity at Emmaton: 2000-2009

Figure 4-10: Time Series of DSG Predicted and Observed Surface Salinity at Pittsburg: 2000-2009

Figure 4-11: Time Series of DSG Predicted and Observed Surface Salinity at Antioch: 2000-2009

Figure 4-12: Time Series of DSG Predicted and Observed Surface Salinity at Jersey Point: 2000-2009

Figure 4-13: Time Series of DSG Predicted and Sacramento River Branch 1 ppt Interpolated Isohaline Position: 2000-2009

Figure 4-14: Time Series of DSG Predicted and Sacramento River Branch 4 ppt Interpolated Isohaline Position: 2000-2009

Figure 4-15: Time Series of DSG Predicted and Sacramento River Branch 6 ppt Interpolated Isohaline Position: 2000-2009

Figure 4-16: Time Series of DSG Predicted and San Joaquin River Branch 1 ppt Interpolated Isohaline Position: 2000-2009

Figure 4-17: Time Series of DSG Predicted and San Joaquin River Branch 4 ppt Interpolated Isohaline Position: 2000-2009

Figure 4-18: Time Series of DSG Predicted and San Joaquin River Branch 6 ppt Interpolated Isohaline Position: 2000-2009

Figure 5-1: DSG and G-Model Predicted Salinity at Collinsville as a Function of Antecedent Outflow: Comparison with Observed Data for 2000-09

Figure 5-2: DSG and G-Model Predicted Salinity at Collinsville as a Function of Antecedent Outflow: Comparison with Observed Data for 1930-39

Figure 5-3: Longitudinal Salinity Gradient as a Function of Distance from Golden Gate and X2 Position

Figure 5-4: Location and Value of Maximum Longitudinal Salinity Gradient as a Function of X2

Figure 5-5: DSG-Predicted Longitudinal Dispersion Coefficient as a Function of Distance along the Estuary

Figure A-1: DSG Predicted vs. DSM2 Surface Salinity at Martinez: 2000-2009

Figure A-2: DSG Predicted vs. DSM2 Surface Salinity at Port Chicago: 2000-2009

Figure A-3: DSG Predicted vs. DSM2 Surface Salinity at Mallard Island: 2000-2009

Figure A-4: DSG Predicted vs. DSM2 Surface Salinity at Collinsville: 2000-2009

Figure A-5: DSG Predicted vs. DSM2 Surface Salinity at Emmaton: 2000-2009

Figure A-6: DSG Predicted vs. DSM2 Interpolated 1 ppt Surface Isohaline Position: 2000-2009

Figure A-7: DSG Predicted vs. DSM2 Interpolated 4 ppt Surface Isohaline Position: 2000-2009

Figure A-8: DSG Predicted vs. DSM2 Interpolated 6 ppt Surface Isohaline Position: 2000-2009

Figure A-9: Time Series of DSG Predicted and DSM2 Interpolated X2 Position: 1990-1999

Figure A-10: DSG Predicted vs. DSM2 Surface Salinity at Martinez: 1990-1999

Figure A-11: DSG Predicted vs. DSM2 Surface Salinity at Port Chicago: 1990-1999

Figure A-12: DSG Predicted vs. DSM2 Surface Salinity at Mallard Island: 1990-1999

Figure A-13: DSG Predicted vs. DSM2 Surface Salinity at Collinsville: 1990-1999

Figure A-14: DSG Predicted vs. DSM2 Surface Salinity at Emmaton: 1990-1999

Figure A-15: DSG Predicted vs. DSM2 Interpolated 1 ppt Surface Isohaline Position: 1990-1999

Figure A-16: DSG Predicted vs. DSM2 Interpolated 4 ppt Surface Isohaline Position: 1990-1999

Figure A-17: DSG Predicted vs. DSM2 Interpolated 6 ppt Surface Isohaline Position: 1990-1999

Figure B-1 Time Series of Delta Inflows: October 1921 – September 1929

Figure B-2 Time Series of Delta Outflow: October 1921 – September 1929

Figure C-1: DSG Predicted vs. Observed Surface Salinity at Martinez: 2000-2009

Figure C-2: DSG Predicted vs. Observed Surface Salinity at Port Chicago: 2000-2009

Figure C-3: DSG Predicted vs. Observed Surface Salinity at Mallard Island: 2000-2009

Figure C-4: DSG Predicted vs. Observed Surface Salinity at Collinsville: 2000-2009

Figure C-5: DSG Predicted vs. Observed Surface Salinity at Emmaton: 2000-2009

Figure C-6: DSG Predicted vs. Observed Surface Salinity at Pittsburg: 2000-2009

Figure C-7: DSG Predicted vs. Observed Surface Salinity at Antioch: 2000-2009

Figure C-8: DSG Predicted vs. Observed Surface Salinity at Jersey Point: 2000-2009

Figure C-9: DSG Predicted vs. Sacramento Branch Interpolated 1 ppt Surface Isohaline: 2000-2009

Figure C-10: DSG Predicted vs. Sacramento Branch Interpolated 4 ppt Surface Isohaline: 2000-2009

Figure C-11: DSG Predicted vs. Sacramento Branch Interpolated 6 ppt Surface Isohaline: 2000-2009

Figure C-12: DSG Predicted vs. San Joaquin Branch Interpolated 1 ppt Surface Isohaline: 2000-2009

Figure C-13: DSG Predicted vs. San Joaquin Branch Interpolated 4 ppt Surface Isohaline: 2000-2009

Figure C-14: DSG Predicted vs. San Joaquin Branch Interpolated 6 ppt Surface Isohaline: 2000-2009

Figure D-1: Time Series of DSG Predicted and Interpolated Sacramento Branch X2 Position: 2010-2013

Figure D-2: Time Series of DSG Predicted and Interpolated Sacramento Branch X2 Position: 1990-1999

Figure D-3: Time Series of DSG Predicted and Interpolated Sacramento Branch X2 Position: 1980-1989

Figure D-4: Time Series of DSG Predicted and Interpolated Sacramento Branch X2 Position: 1970-1979

Figure D-5: Time Series of DSG Predicted and Interpolated Sacramento Branch X2 Position: 1960-1969

Figure D-6: Time Series of DSG Predicted and Interpolated Sacramento Branch X2 Position: 1950-1959

Figure D-7: Time Series of DSG Predicted and Interpolated Sacramento Branch X2 Position: 1940-1949

Figure D-8: Time Series of DSG Predicted and Interpolated Sacramento Branch X2 Position: 1930-1939

Figure D-9: Time Series of DSG Predicted and Interpolated Sacramento Branch X2 Position: 1921-1929

Figure D-10: Time Series of DSG Predicted and Interpolated San Joaquin Branch X2 Position: 2010-2009

Figure D-11: Time Series of DSG Predicted and Interpolated San Joaquin Branch X2 Position: 1990-1999

Figure D-12: Time Series of DSG Predicted and Interpolated San Joaquin Branch X2 Position: 1980-1989

Figure D-13: Time Series of DSG Predicted and Interpolated San Joaquin Branch X2 Position: 1970-1979

Figure D-14: Time Series of DSG Predicted and Interpolated San Joaquin Branch X2 Position: 1960-1969

Figure D-15: Time Series of DSG Predicted and Interpolated San Joaquin Branch X2 Position: 1950-1959

Figure D-16: Time Series of DSG Predicted and Interpolated San Joaquin Branch X2 Position: 1940-1949

Figure D-17: Time Series of DSG Predicted and Interpolated San Joaquin Branch X2 Position: 1930-1939

Figure D-18: Time Series of DSG Predicted and Interpolated San Joaquin Branch X2 Position: 1921-1929

Figure E-1: Time Series of DSG Predicted and Observed Surface Salinity at Martinez: 2010-2013

Figure E-2: Time Series of DSG Predicted and Observed Surface Salinity at Port Chicago: 2010-2013

Figure E-3: Time Series of DSG Predicted and Observed Surface Salinity at Mallard Island: 2010-2013

Figure E-4: Time Series of DSG Predicted and Observed Surface Salinity at Collinsville: 2010-2013

Figure E-5: Time Series of DSG Predicted and Observed Surface Salinity at Emmaton: 2010-2013

Figure E-6: Time Series of DSG Predicted and Observed Surface Salinity at Pittsburg: 2010-2013

Figure E-7: Time Series of DSG Predicted and Observed Surface Salinity at Antioch: 2010-2013

Figure E-8: Time Series of DSG Predicted and Observed Surface Salinity at Jersey Point: 2010-2013

Figure E-9: Time Series of DSG Predicted and Observed Surface Salinity at Martinez: 1990-1999

Figure E-10: Time Series of DSG Predicted and Observed Surface Salinity at Port Chicago: 1990-1999

Figure E-11: Time Series of DSG Predicted and Observed Surface Salinity at Mallard Island: 1990-99

Figure E-12: Time Series of DSG Predicted and Observed Surface Salinity at Collinsville: 1990-1999

Figure E-13: Time Series of DSG Predicted and Observed Surface Salinity at Emmaton: 1990-1999

Figure E-14: Time Series of DSG Predicted and Observed Surface Salinity at Pittsburg: 1990-1999

Figure E-15: Time Series of DSG Predicted and Observed Surface Salinity at Antioch: 1990-1999

Figure E-16: Time Series of DSG Predicted and Observed Surface Salinity at Jersey Point: 1990-1999

Figure E-17: Time Series of DSG Predicted and Observed Surface Salinity at Martinez: 1980-1989

Figure E-18: Time Series of DSG Predicted and Observed Surface Salinity at Port Chicago: 1980-1989

Figure E-19: Time Series of DSG Predicted and Observed Surface Salinity at Mallard Island: 1980-89

Figure E-20: Time Series of DSG Predicted and Observed Surface Salinity at Collinsville: 1980-1989

Figure E-21: Time Series of DSG Predicted and Observed Surface Salinity at Emmaton: 1980-1989

Figure E-22: Time Series of DSG Predicted and Observed Surface Salinity at Pittsburg: 1980-1989

Figure E-23: Time Series of DSG Predicted and Observed Surface Salinity at Antioch: 1980-1989

Figure E-24: Time Series of DSG Predicted and Observed Surface Salinity at Jersey Point: 1980-1989

Figure E-25: Time Series of DSG Predicted and Observed Surface Salinity at Martinez: 1970-1979

Figure E-26: Time Series of DSG Predicted and Observed Surface Salinity at Port Chicago: 1970-1979

Figure E-27: Time Series of DSG Predicted and Observed Surface Salinity at Mallard Island: 1970-79

Figure E-28: Time Series of DSG Predicted and Observed Surface Salinity at Collinsville: 1970-1979

Figure E-29: Time Series of DSG Predicted and Observed Surface Salinity at Emmaton: 1970-1979

Figure E-30: Time Series of DSG Predicted and Observed Surface Salinity at Pittsburg: 1970-1979

Figure E-31: Time Series of DSG Predicted and Observed Surface Salinity at Antioch: 1970-1979

Figure E-32: Time Series of DSG Predicted and Observed Surface Salinity at Jersey Point: 1970-1979

Figure E-33: Time Series of DSG Predicted and Observed Surface Salinity at Martinez: 1960-1969

Figure E-34: Time Series of DSG Predicted and Observed Surface Salinity at Port Chicago: 1960-1969

Figure E-35: Time Series of DSG Predicted and Observed Surface Salinity at Mallard Island: 1960-69

Figure E-36: Time Series of DSG Predicted and Observed Surface Salinity at Collinsville: 1960-1969

Figure E-37: Time Series of DSG Predicted and Observed Surface Salinity at Emmaton: 1960-1969

Figure E-38: Time Series of DSG Predicted and Observed Surface Salinity at Pittsburg: 1960-1969

Figure E-39: Time Series of DSG Predicted and Observed Surface Salinity at Antioch: 1960-1969

Figure E-40: Time Series of DSG Predicted and Observed Surface Salinity at Jersey Point: 1960-1969

Figure E-41: Time Series of DSG Predicted and Observed Surface Salinity at Martinez: 1950-1959

Figure E-42: Time Series of DSG Predicted and Observed Surface Salinity at Port Chicago: 1950-1959

Figure E-43: Time Series of DSG Predicted and Observed Surface Salinity at Mallard Island: 1950-59

Figure E-44: Time Series of DSG Predicted and Observed Surface Salinity at Collinsville: 1950-1959

Figure E-45: Time Series of DSG Predicted and Observed Surface Salinity at Emmaton: 1950-1959

Figure E-46: Time Series of DSG Predicted and Observed Surface Salinity at Pittsburg: 1950-1959

Figure E-47: Time Series of DSG Predicted and Observed Surface Salinity at Antioch: 1950-1959

Figure E-48: Time Series of DSG Predicted and Observed Surface Salinity at Jersey Point: 1950-1959

Figure E-49: Time Series of DSG Predicted and Observed Surface Salinity at Martinez: 1940-1949

Figure E-50: Time Series of DSG Predicted and Observed Surface Salinity at Port Chicago: 1940-1949

Figure E-51: Time Series of DSG Predicted and Observed Surface Salinity at Mallard Island: 1940-49

Figure E-52: Time Series of DSG Predicted and Observed Surface Salinity at Collinsville: 1940-1949

Figure E-53: Time Series of DSG Predicted and Observed Surface Salinity at Emmaton: 1940-1949

Figure E-54: Time Series of DSG Predicted and Observed Surface Salinity at Pittsburg: 1940-1949

Figure E-55: Time Series of DSG Predicted and Observed Surface Salinity at Antioch: 1940-1949

Figure E-56: Time Series of DSG Predicted and Observed Surface Salinity at Jersey Point: 1940-1949

Figure E-57: Time Series of DSG Predicted and Observed Surface Salinity at Martinez: 1930-1939

Figure E-58: Time Series of DSG Predicted and Observed Surface Salinity at Port Chicago: 1930-1939

Figure E-59: Time Series of DSG Predicted and Observed Surface Salinity at Mallard Island: 1930-39

Figure E-60: Time Series of DSG Predicted and Observed Surface Salinity at Collinsville: 1930-1939

Figure E-61: Time Series of DSG Predicted and Observed Surface Salinity at Emmaton: 1930-1939

Figure E-62: Time Series of DSG Predicted and Observed Surface Salinity at Pittsburg: 1930-1939

Figure E-63: Time Series of DSG Predicted and Observed Surface Salinity at Antioch: 1930-1939

Figure E-64: Time Series of DSG Predicted and Observed Surface Salinity at Jersey Point: 1930-1939

Figure E-65: Time Series of DSG Predicted and Observed Surface Salinity at Martinez: 1920-1929

Figure E-66: Time Series of DSG Predicted and Observed Surface Salinity at Port Chicago: 1920-1929

Figure E-67: Time Series of DSG Predicted and Observed Surface Salinity at Mallard Island: 1920-29

Figure E-68: Time Series of DSG Predicted and Observed Surface Salinity at Collinsville: 1920-1929

Figure E-69: Time Series of DSG Predicted and Observed Surface Salinity at Emmaton: 1920-1929

Figure E-70: Time Series of DSG Predicted and Observed Surface Salinity at Pittsburg: 1920-1929

Figure E-71: Time Series of DSG Predicted and Observed Surface Salinity at Antioch: 1920-1929

Figure E-72: Time Series of DSG Predicted and Observed Surface Salinity at Jersey Point: 1920-1929

Figure F-1: Time Series of DSG Predicted (Using Interpolated X2) and Observed Surface Salinity at Martinez: 2000-2009

Figure F-2: Time Series of DSG Predicted (Using Interpolated X2) and Observed Surface Salinity at Port Chicago: 2000-2009

Figure F-3: Time Series of DSG Predicted (Using Interpolated X2) and Observed Surface Salinity at Mallard Island: 2000-2009

Figure F-4: Time Series of DSG Predicted (Using Interpolated X2) and Observed Surface Salinity at Collinsville: 2000-2009

Figure F-5: Time Series of DSG Predicted (Using Interpolated X2) and Observed Surface Salinity at Emmaton: 2000-2009

Figure F-6: Time Series of DSG Predicted (Using Interpolated X2) and Observed Surface Salinity at Pittsburg: 2000-2009

Figure F-7: Time Series of DSG Predicted (Using Interpolated X2) and Observed Surface Salinity at Antioch: 2000-2009

Figure F-8: Time Series of DSG Predicted (Using Interpolated X2) and Observed Surface Salinity at Jersey Point: 2000-2009

Acknowledgements

The author gratefully acknowledged the contributions of Mr. John Rath (Tetra Tech Inc.) for his assistance in articulating the DSG model formulation in Chapter 2 and two independent reviewers (Drs. Edward Gross and Richard Denton) for their valuable comments on an earlier draft of the document. Also, special thanks to Ms. Kandise King and Rachelle Burfict from the MWD Sacramento Office for editorial assistance.

Executive Summary

A new empirical sub-tidal model of daily averaged salinity in Suisun Bay and the western Delta was developed and is reported herein. This model, called the Delta Salinity Gradient (DSG) model, integrates the Eulerian modeling approach of Denton (1993) – focused on a fixed location - and the Lagrangian modeling approach of Monismith et al. (2002) – focused on a fixed salinity – to produce a parsimonious method of estimating X2 and other isohaline positions as well as salinity at fixed locations in the estuary. The formulation allows for prediction of X2 position under sustained low outflow conditions when Delta outflow falls below zero, a condition that occurs frequently under pre-Shasta conditions in the early part of the available salinity record. The model’s ability to predict X2 under extremely low outflow conditions makes it a viable tool for evaluating “without-Project” scenarios that remove the effects of upstream reservoir and Delta export operations from the hydrologic record. No currently available salinity models, neither statically-based nor physically-based, are calibrated to simulate such extreme conditions. The DSG model’s ability to evaluate multiple isohaline positions provides a simple approach to quantify the range of the low salinity zone, thereby allowing broader understanding of the relationship between X2 position and the range of the low salinity zone. Finally, the DSG model’s ability to quantify the estuary’s longitudinal salinity gradient provides a rational method for evaluating the specification of dispersion coefficients and the calibration of one-dimensional salinity transport models.

The DSG model was calibrated with daily averaged salinity and X2 isohaline observations for calendar years 2000 through 2009. The model was also calibrated with simulated data from the DSM2 model for purposes of demonstration. Model validation was accomplished using the recently expanded period of record that was available at the time of development, i.e. October 1921 through September 2012.

DSG model analysis was extended beyond the issues of calibration and validation by (1) evaluating the model’s sensitivity to parameter changes, (2) comparing fixed location salinity predictions with those of the G model, (3) exploring the use of interpolated X2 values rather than predicted values to estimate salinity, thus providing insight into model

uncertainty given “perfect” knowledge of X2 position, and (4) exploring the ramifications of the model’s characterization of longitudinal salinity gradient, considering issues such as value and location of maximum gradient and quantification of dispersion coefficient. Finally, recommendations for future work are discussed.

1. Introduction

The salinity structure of the Bay-Delta estuary, following the fundamental physics of other estuaries, is primarily dependent on freshwater inflows and tidal conditions. Although sophisticated numerical models are available to describe the response of salinity to these and other factors, significant effort and expertise is needed to calibrate, validate and operate these models. Additionally, the processing time associated with running these numerical models can sometimes make it difficult to evaluate a lengthy hydrologic sequence or a large number of management scenarios in a short period of time. Consequently, there remains a need for a fast and reliable method to characterize the salinity structure of the Bay-Delta estuary. This report documents the development, calibration and validation of such a method, a model called the Delta Salinity Gradient (DSG) model.

The initial motivation for developing the DSG model arose from a need to estimate the X2 isohaline position over the entire hydrologic record for the Bay-Delta estuary, going back to October 1929 in the DAYFLOW model. In the early part of the record, particularly during the historic drought of 1928-34, extended periods of low outflow occurred such that net Delta outflow was often negative. The Kimmerer-Monismith (K-M) X2 equation, which is the most widely-accepted statistically-based salinity model of the Bay-Delta estuary, is not defined under such low outflow conditions and none of the currently available physically-based hydrodynamic models of the estuary are calibrated for such extreme conditions.

The method of expressing X2 as a function of antecedent outflow was first applied by the author to the DAYFLOW record and monthly estimates of X2 position were produced (Hutton 2011). The need for a more expansive model became apparent when Metropolitan Water District contracted with Tetra Tech Inc. to assemble a long-term salinity record for the estuary (Roy et al. 2014). In the process of cleaning and filling the salinity record and producing isohaline estimates, a tool was needed to assess the validity of the dataset resulting from the process. The X2 equation was integrated into an early version of the DSG model that was first reported by the author at the 2013 CWEMF annual meeting (Hutton 2013). Since that time, additional refinements have been accomplished and are reported in this document.

Chapter 2 summarizes the mathematical formulation and key assumptions associated with the DSG model. Chapter 3 demonstrates the validity of the formulation by describing a calibration and validation effort using output from the DSM2 model. Chapter 4 presents the steps taken to calibrate and validate the DSG model using the long-term salinity record for the estuary produced by Roy et al. (2014). Supporting materials for Chapters 3 and 4 are provided in Appendices A through E.

Chapter 5 extends the analysis of the DSG model beyond the issues of calibration and validation by first evaluating the model's sensitivity to model parameters. Next, a cursory comparison of the DSG and G models is provided. This chapter then explores the use of interpolated X2 values (rather than values predicted from antecedent outflow) to estimate salinity. This exercise, which provides insight into model uncertainty given "perfect" knowledge of X2 position, highlights the sensitivity of fixed location salinity predictions to X2 predictions. Supporting materials for this exercise are provided in Appendix F. Finally, the ramifications of the DSG model's characterization of longitudinal salinity gradient are explored, considering issues such as value and location of maximum gradient and quantification of dispersion coefficient. Chapter 6 provides a brief discussion on the potential utility of the DSG model and suggests areas of future work.

2. Formulation

2.1 Previous Modeling Efforts

Denton (1993) developed an empirical approach to estimate salinity at fixed location in the estuary, based on a modification of the steady-state solution of the tidally-averaged advection-dispersion equation for salinity transport in a one-dimensional estuary. His approach utilizes boundary conditions representative of the downstream ocean and upstream riverine environments, and a concept called antecedent outflow, representing flow time-history in the Delta. The equation can be represented as:

$$S = (S_o - S_b) * \exp(-\alpha * G) + S_b \dots \dots \dots (2.1)$$

where S is the salinity at a given location, S_o and S_b are the downstream ocean and upstream river boundary salinities, and α is an empirically-determined constant, computed for specific locations in the estuary. Antecedent outflow, G, is defined by the following routing function similar to a relationship used by Harder (1977):

$$\frac{\partial G}{\partial t} = \frac{(Q - G) * G}{\beta} \dots \dots \dots (2.2)$$

where Q is Delta outflow and β is an empirically determined constant. As Denton (1993) points out, the term β/G governs the rate at which G approaches steady state. This approach is commonly referred to as the G Model.

Monismith et. al. (2002) defined X2 position as an autoregressive function of Delta outflow at the current time step and X2 at the previous time step, an approach similar to the Kimmerer-Monismith (K-M) X2 equation described by Jassby et. al. (1995). Monismith et. al. (2002) argues that theoretical predictions for salinity intrusion and flow involve power-law relations rather than logarithms and proposed an X2 function of the following form:

$$X2(t) = \omega_1 * Q(t)^{\omega_2} + \omega_3 * X2(t - 1) \dots \dots \dots (2.3)$$

where ω₁, ω₂ and ω₃ are empirically determined constants.

2.2 Integration of Previous Modeling Efforts

The modeling approaches of Denton (1993) and Monismith et al. (2002) were integrated to develop a flexible tool for diagnostic applications in the salinity data cleaning and filling process described by Roy et al. (2014). The resulting sub-tidal empirical model, capable of estimating surface salinity along the estuary as well as X2 and other isohaline positions on a daily time step, is termed the Delta Salinity Gradient (DSG) model. DSG model formulation is described in the remainder of this section.

First a pseudo steady-state form of Equation (2.3) was defined by setting $X2(t) = X2(t-1)$, substituting antecedent outflow G for $Q(t)$, and re-defining empirical constants $\Phi_1 = \frac{\omega_1}{1 - \omega_3}$ and $\Phi_2 = \omega_2$:

$$X2(t) = \Phi_1 * G^{\Phi_2} \dots \dots \dots (2.4)$$

Substituting Equation (2.4) into Equation (2.1) yields:

$$S = (S_o - S_b) * \exp \left[-\alpha * \left(\frac{\Phi_1}{X2} \right)^{\frac{-1}{\Phi_2}} \right] + S_b \dots \dots \dots (2.5)$$

To motivate the explicit definition of α along the length of the estuary, $\alpha(X)$, the following consistency conditions required by Equation (2.1) are introduced:

Condition 1: $S \rightarrow S_b$, equivalently $\alpha \rightarrow \infty$, as $X \rightarrow \infty$

Condition 2: $S \rightarrow S_o$, equivalently $\alpha \rightarrow 0$, as $X \rightarrow 0$

Condition 3: $S = 2.64$ mS/cm, equivalently $-\alpha * G = \ln \left[\frac{2.64 - S_b}{S_o - S_b} \right]$, when $\frac{X}{X2} = 1$

Monismith et al. (2002) observed that “...for most flow conditions, the mean salinity distribution of the estuary is nearly “self-similar” with a salinity gradient in the center 70% of the region between the Golden Gate and X2 that is proportional to $X2^{-1}$.” This observation can be represented as:

$$S = (S_o - S_b) * f\left(\frac{X}{X2}\right) + S_b \dots \dots \dots (2.6)$$

for some function f , which restates Equation (12) of Monismith et al. (2002) with the addition of an explicit term for a non-zero river boundary salinity, S_b . It then follows that Equation (2.5) represents a self-similar salinity gradient if:

$$\alpha(X) \propto \left(\frac{X}{\Phi_1}\right)^{-\frac{1}{\Phi_2}} \dots \dots \dots (2.7)$$

Consistency conditions 1 and 2 above are satisfied by this form of $\alpha(X)$. The constant of proportionality implied by Equation (2.7) is determined by consistency condition 3, i.e. by substituting $S = 2.64$ mS/cm into Equation (2.5). Introducing the notation $\tau = \ln\left[\frac{2.64-S_b}{S_o-S_b}\right]$ yields:

$$\alpha(X) = -\tau \left(\frac{X}{\Phi_1}\right)^{-\frac{1}{\Phi_2}} \dots \dots \dots (2.8)$$

where $-\tau$ is the constant of proportionality from Equation (2.7). Finally, substituting this expression for $\alpha(X)$ in Equation (2.5) yields:

$$S = (S_o - S_b) * \exp\left[\tau * \left(\frac{X}{X2}\right)^{-\frac{1}{\Phi_2}}\right] + S_b \dots \dots \dots (2.9)$$

This equation can be used to determine salinity (in units of mS/cm) at any longitudinal distance (in units of km) from Golden Gate (X) given $X2$ and Φ_2 and assuming reasonable values for S_o and S_b .

Note that Equation (2.9) can be algebraically rearranged to predict surface salinity isohaline positions as a function of $X2$:

$$X = X2 * \left[\frac{\ln\left(\frac{S - S_b}{S_o - S_b}\right)}{\tau} \right]^{-\Phi_2} \dots \dots \dots (2.10)$$

2.3 Deviations from Self-Similarity

Equation (2.9) describes a perfectly self-similar salinity structure when S_o and S_b are defined as model constants. However, as noted by Monismith et al. (2002), the estuary's salinity structure is not perfectly self-similar but rather changes under high flow conditions. To address this observed response to flow, S_o is re-defined from a model constant representing ocean salinity to an empirically-determined value that varies with antecedent outflow. To motivate this new definition, it can be reasoned that S_o varies with $X2$ such that:

- as $X2 \rightarrow 0$ km, $S_o \rightarrow 2.64$ mS/cm
- as $X2 \rightarrow \infty$, $S_o \rightarrow$ ocean salinity ≈ 53 mS/cm = \hat{S}

These conditions can be satisfied by the following relationship:

$$S_o = \hat{S} + (2.64 - \hat{S}) * \exp(-\gamma * X2^\delta) \dots \dots \dots (2.11)$$

where γ and δ are empirically determined constants.

2.4 Longitudinal Salinity Gradient

The longitudinal salinity gradient of the estuary is defined as the partial derivative of Equation (2.9) with respect to distance X . Thus,

$$\frac{\partial S}{\partial X} = \frac{-\tau}{\phi_2 * X} * (S_o - S_b) * \left(\frac{X}{X2}\right)^{\frac{-1}{\phi_2}} * \exp\left[\tau * \left(\frac{X}{X2}\right)^{\frac{-1}{\phi_2}}\right] \dots \dots \dots (2.12)$$

A rudimentary analysis of this equation and the resulting definition of a one-dimensional dispersion coefficient is provided in Chapter 5.

2.5 Formulation Summary

The Delta Salinity Gradient (DSG) model, as presented above, is a statistically-based sub-tidal empirical model capable of estimating surface salinity along the longitudinal axis of the estuary as well as the position of $X2$ and other isohalines on a daily time step. Model logic is summarized as follows:

- Antecedent outflow (G), in units of cfs, is calculated per Denton (1993) from Equation (2.2) given Delta outflow and the empirically determined constant β .

- X_2 position (in units of km) is calculated from [Equation \(2.4\)](#) given antecedent outflow and empirically determined fitting constants Φ_1 and Φ_2 .
- S_o , in units of mS/cm, is calculated from [Equation \(2.11\)](#) given X_2 position and empirically determined constants γ and δ , and assuming a reasonable value for ocean salinity \hat{S} , also in units of mS/cm.
- Surface salinity (S), in units of mS/cm, is calculated from [Equation \(2.9\)](#) at any longitudinal distance along the estuary (X) given X_2 , S_o , Φ_2 , and assuming a reasonable value for the river boundary salinity S_b , also in units of mS/cm.
- Surface isohaline position (X), in units of km, is calculated for any surface salinity (S) from [Equation \(2.10\)](#), which is a simple algebraic rearrangement of [Equation \(2.9\)](#).

3. Calibration & Validation with DSM2 Data

3.1 Data Description

The DSG model was calibrated with DSM2 simulation data as a formulation proof of concept. DSM2 data covering the period of January 1990 through February 2012 were provided by DWR Bay-Delta Office¹. Daily averaged salinity outputs were reported at the following key locations in Suisun Bay and the lower Sacramento River branch, with DSM2 longitudinal distances from Golden Gate provided in parentheses:

- Martinez (54.3 km)
- Port Chicago (63.5 km)
- Mallard Island (73.5 km)
- Collinsville (80.6 km)
- Emmaton (91.7 km)

Additionally, salinity outputs were reported at 1 km increments. X2 and other isohaline positions were estimated from these data through log-linear interpolation. Similar analyses were not conducted for the lower San Joaquin River branch. The period January 1990 through June 1990 span the model warm-up period and were therefore not utilized in the evaluation.

3.2 X2 Parameter Calibration

Equation (2.4) was calibrated with X2 position interpolated from DSM2 salinity data for the period January 2000 – December 2009. Antecedent outflow was calculated from Equation (2.2) assuming a nominal value for β of 475 cfs-years and assuming adjusted daily Delta outflows from the DAYFLOW model (CDWR 2014). For consistency with the DSM2 simulated hydrology, DAYFLOW outflow values were adjusted to reflect net channel depletions generated by the Delta Island Consumptive Use (DICU) model. A scatter plot of X2 versus antecedent outflow is provided in Figure 3-1. Best fit parameter values $\Phi_1 = 564$

¹ Data from DSM2-QUAL Version 8.1.1 were provided by Tara Smith in a September 11, 2012 email.

± 4.9 (mean ± 1 SE) and $\Phi_2 = -0.215 \pm 0.001$ result from the regression analysis. The coefficient of determination $R^2 = 0.94$ and the standard error of estimate is 2.4 km. The resulting DSG predictions are compared with DSM2 interpolated X2 data as time series in [Figure 3-2](#) for the calibration period.

3.3 S_o Parameter Calibration

This section describes the procedure that was followed to calibrate the relationship between S_o and X2, [Equation \(2.11\)](#), with DSM2 data spanning the period January 2000 through December 2009.

The first step of the calibration procedure was to calculate daily values of S_o associated with each of the five salinity stations. This calculation was accomplished by algebraically manipulating [Equation \(2.9\)](#) to solve for S_o :

$$S_o = \exp \left[\frac{\left(\frac{X}{X2}\right)^{\frac{-1}{\Phi_2}} * \ln(2.64 - S_b) - \ln(S - S_b)}{\left(\frac{X}{X2}\right)^{\frac{-1}{\Phi_2}} - 1} \right] + S_b \dots\dots\dots(3.1)$$

given daily interpolated X2 values, the calibrated value of Φ_2 reported above, DSM2 salinity values (S), and assuming $S_b = 0.2$ mS/cm. Note that S_o is not defined by [Equation \(3.1\)](#) when $S \leq S_b$ and when $X/X2 = 1$. Data for a given time step were removed from this analysis if $S \leq S_b$ or if $X/X2 \geq 0.9$. This latter constraint limited the use of much of the upstream station data; in fact, no data from the Emmaton station were used. Best fit parameter values $\gamma = 3.98 \times 10^{-5} \pm 8 \times 10^{-6}$ and $\delta = 2.22 \pm 0.04$ result from the regression analysis.

The data analysis suggests that S_o also varies by longitudinal distance; however, this refinement was not incorporated into the model. It was also observed that [Equation \(3.1\)](#) could be modified to eliminate the discontinuity at $X/X2=1$ by de-scaling (i.e. redefining it as a function of $1/X2$). This modification resulted in a larger and less noisy data set; however, the re-scaled values did not appear to provide a significantly better model. Finally, it was observed that the calibrated [Equation \(2.9\)](#) is approximately linear with respect to X2 in the typical range of 50 to 100 km.

3.4 Salinity & Isohaline Estimates: DSM2 Calibration Period

DSM2-calibrated DSG surface salinity predictions are compared with DSM2 data as time series in [Figures 3-3 through 3-7](#) and as scatter plots in [Figures A-1 through A-5](#) for the calibration period. DSG model variance with DSM2 data, as measured by standard error and coefficient of variation, is provided by station in [Table 3-1](#). Both time series and scatter plots reveal a significant bias to overestimate Emmaton salinity under low outflow conditions. A formal residual analysis was not conducted.

DSM2-calibrated DSG surface isohaline predictions at 1 ppt (1.7 mS/cm), 4 ppt (6.8 mS/cm), and 6 ppt (10.0 mS/cm) are compared with DSM2 interpolated values as time series in [Figures 3-8 through 3-10](#) and as scatter plots in [Figures A-6 through A-8](#) for the calibration period. DSG model variances with DSM2 interpolated values, as measured by standard error, are similar to the error associated with the X2 prediction: 2.4 km for the 1 ppt and 4 ppt estimates and 2.5 km for the 6 ppt estimate. Neither time series nor scatter plots reveal significant bias in the isohaline estimates. However, a formal residual analysis was not conducted.

Table 3-1. Variance of DSG Salinity Predictions with DSM2 Data

Station	2000-09 Calibration		1990-99 Validation	
	Standard Error (mS/cm)	Coefficient of Variation	Standard Error (mS/cm)	Coefficient of Variation
Martinez	2.1	0.13	2.4	0.17
Port Chicago	1.7	0.16	2.1	0.23
Mallard Island	1.0	0.17	1.1	0.19
Collinsville	0.8	0.25	0.8	0.23
Emmaton	0.3	0.45	0.5	0.48

3.5 Validation Results

The DSG model, as calibrated with DSM2 data, was applied to a validation period July 1990 through December 1999. Model results for this validation period are discussed below.

DSG X2 predictions are compared with DSM2 interpolated X2 data as a time series in [Figure A-9](#) for the validation period. Standard error of the DSG predictions is 2.4 km for the validation period.

DSG surface salinity predictions are compared with DSM2 salinity data at five stations as scatter plots in [Figures A-10 through A-14](#) for the validation period. DSG model variance with DSM2 data, as measured by standard error and coefficient of variation, is provided by station in [Table 3-1](#). Similar to the calibration period, scatter plots reveal a significant bias to overestimate Emmaton salinity under low outflow conditions. Performance of the DSG model was weakest during the extended drought spanning the July 1990 through December 1992 period.

DSG surface isohaline predictions at 1 ppt (1.7 mS/cm), 4 ppt (6.8 mS/cm), and 6 ppt (10.0 mS/cm) are compared with DSM2 interpolated values as scatter plots in [Figures A-15 through A-17](#) for the validation period. DSG model variances with DSM2 interpolated values, as measured by standard error, are somewhat higher than the error associated with the X2 prediction: 2.9 km for the 1 ppt and 2.6 km for the 4 ppt and 6 ppt estimates. Scatter plots do not reveal significant bias in the isohaline estimates. However, a formal residual analysis was not conducted.

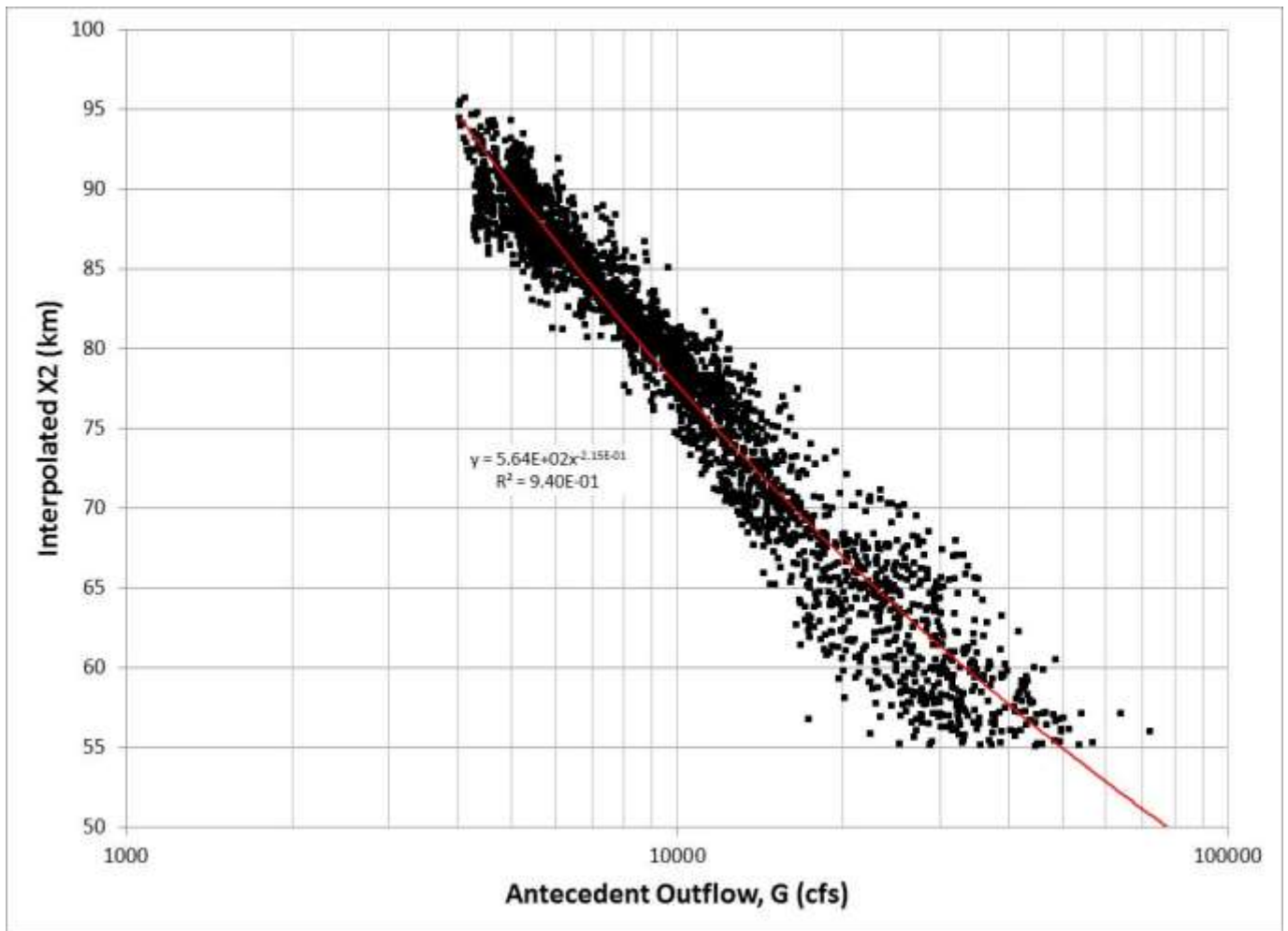


Figure 3-1. DSM2 Interpolated X2 Position as a Function of Antecedent Outflow: 2000-09 Calibration

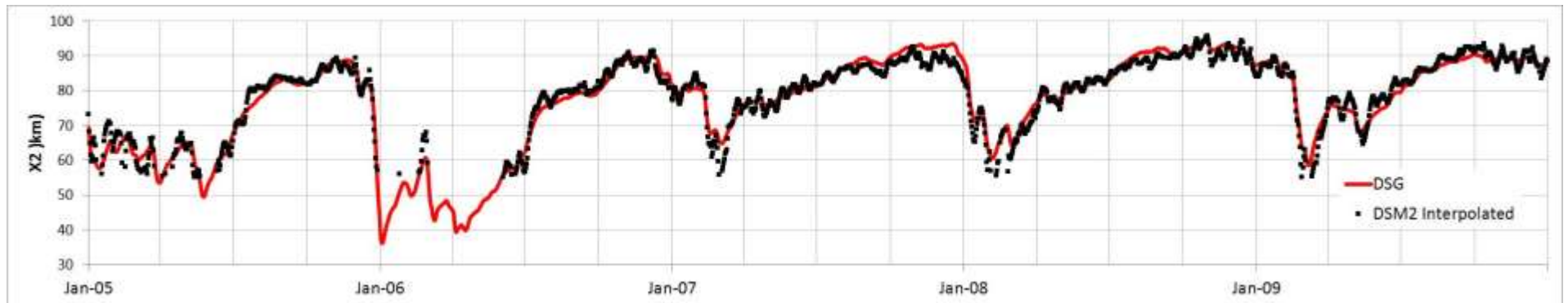
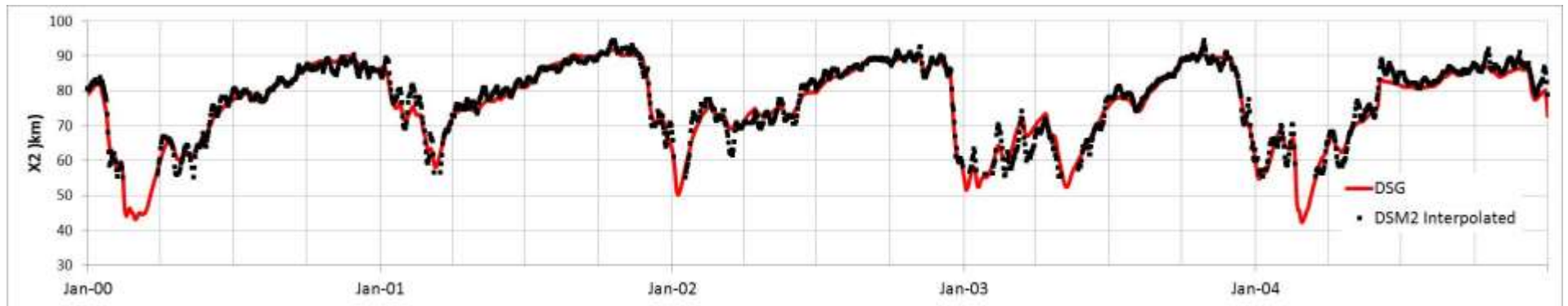


Figure 3-2: Time Series of DSG Predicted and DSM2 Interpolated X2 Position: 2000-2009

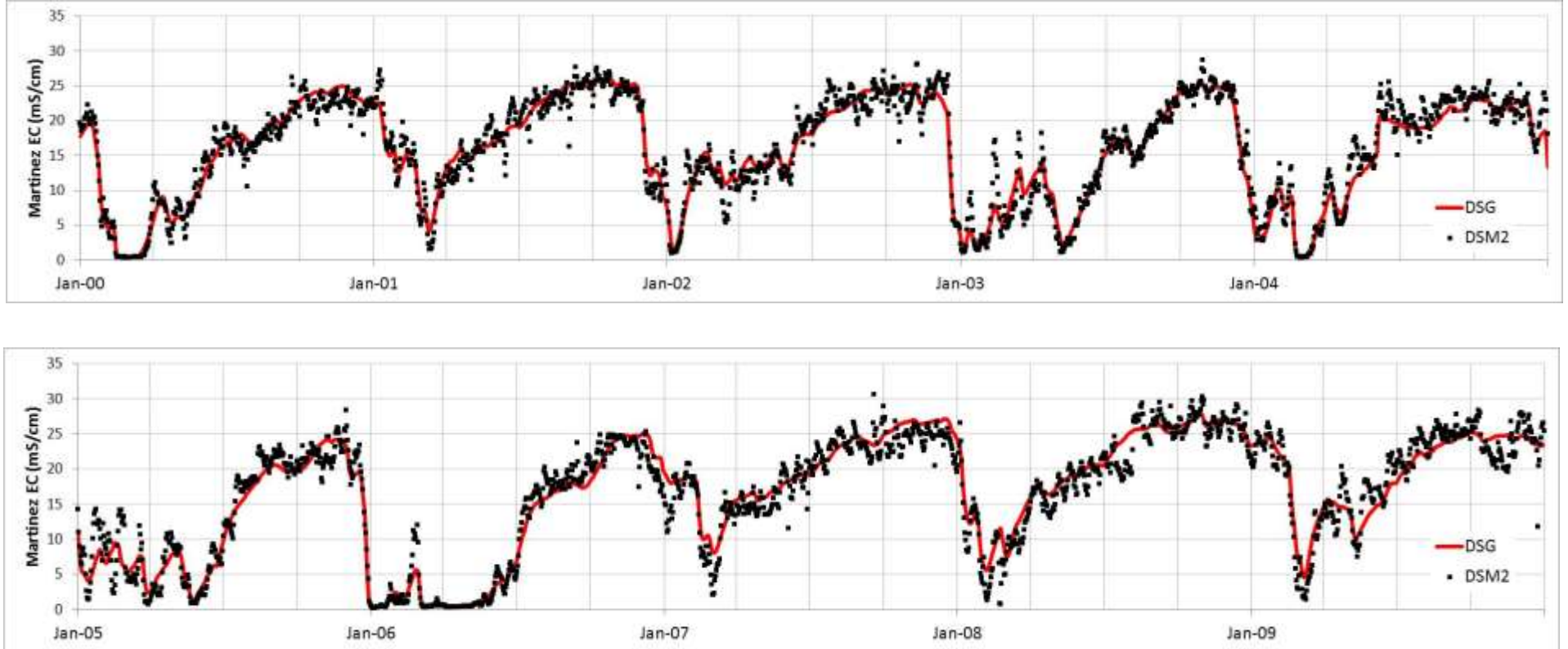


Figure 3-3: Time Series of DSG Predicted and DSM2 Surface Salinity at Martinez: 2000-2009

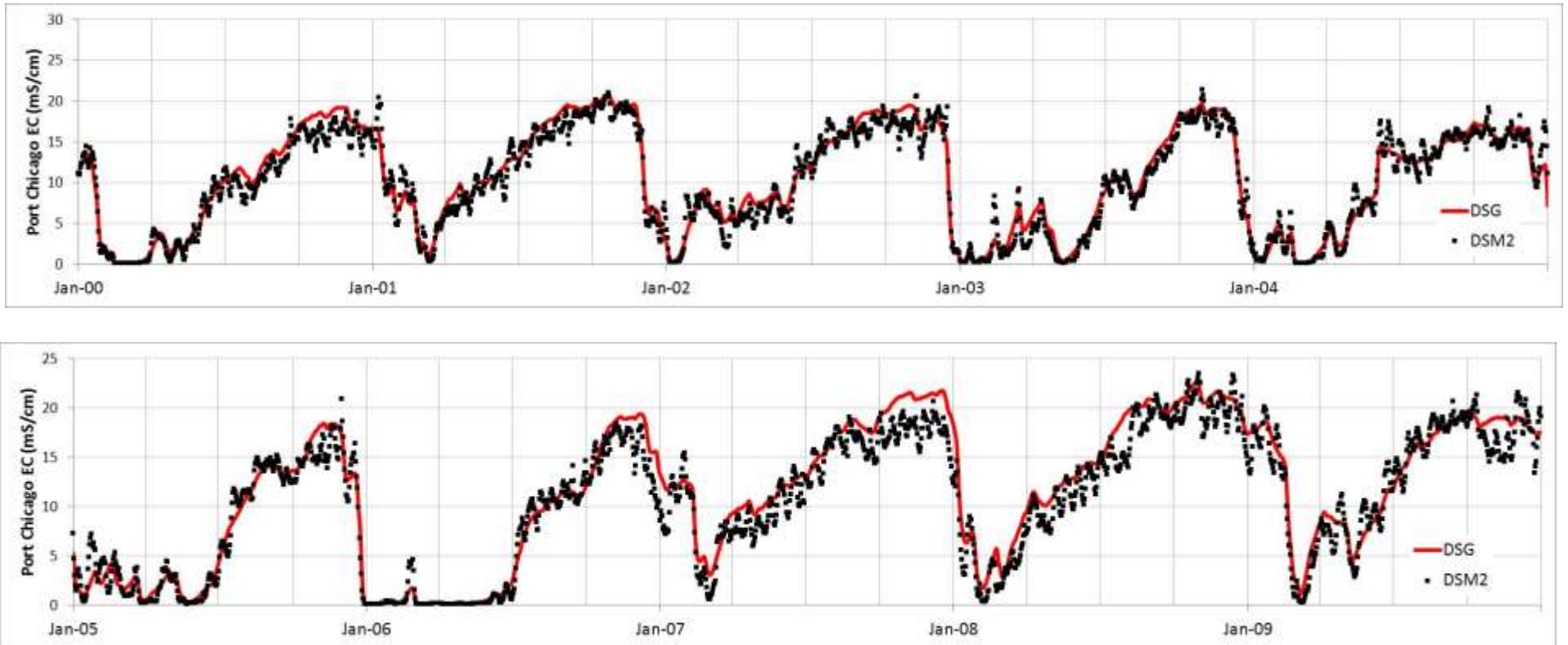


Figure 3-4: Time Series of DSG Predicted and DSM2 Surface Salinity at Port Chicago: 2000-2009

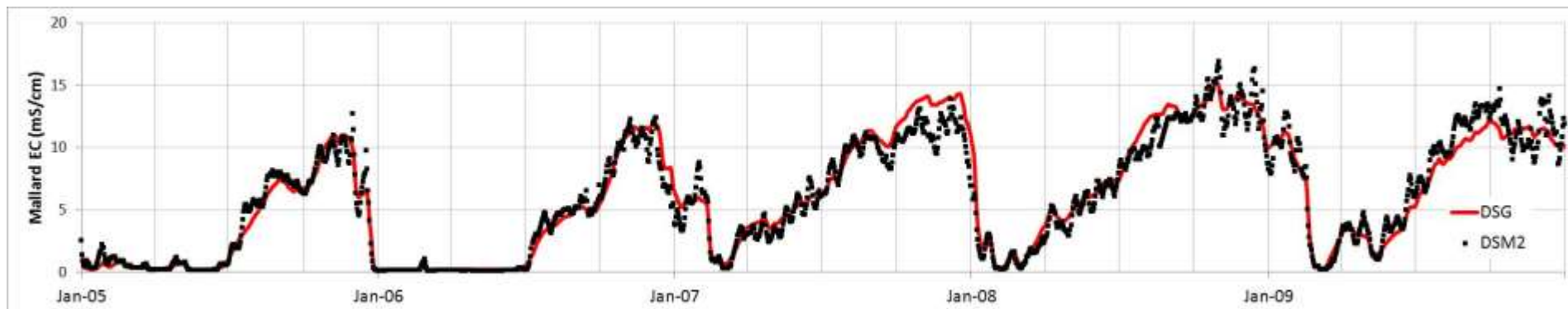
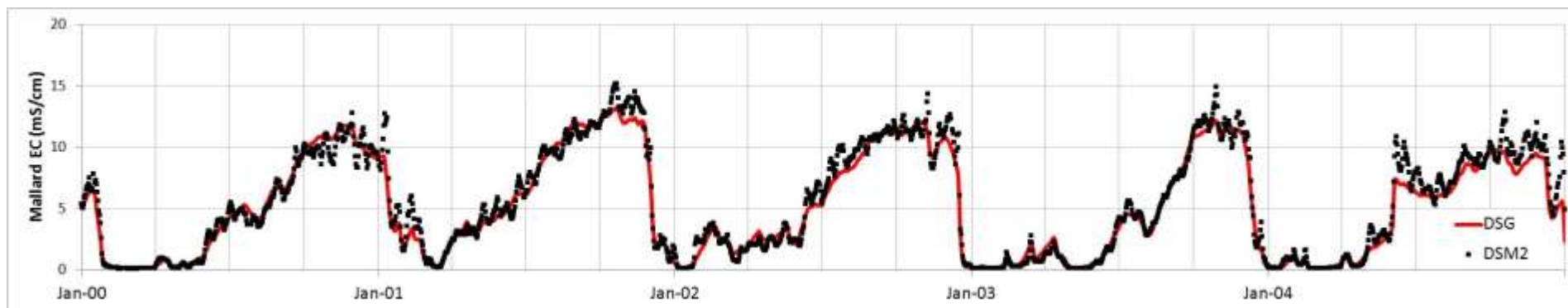


Figure 3-5: Time Series of DSG Predicted and DSM2 Surface Salinity at Mallard Island: 2000-2009

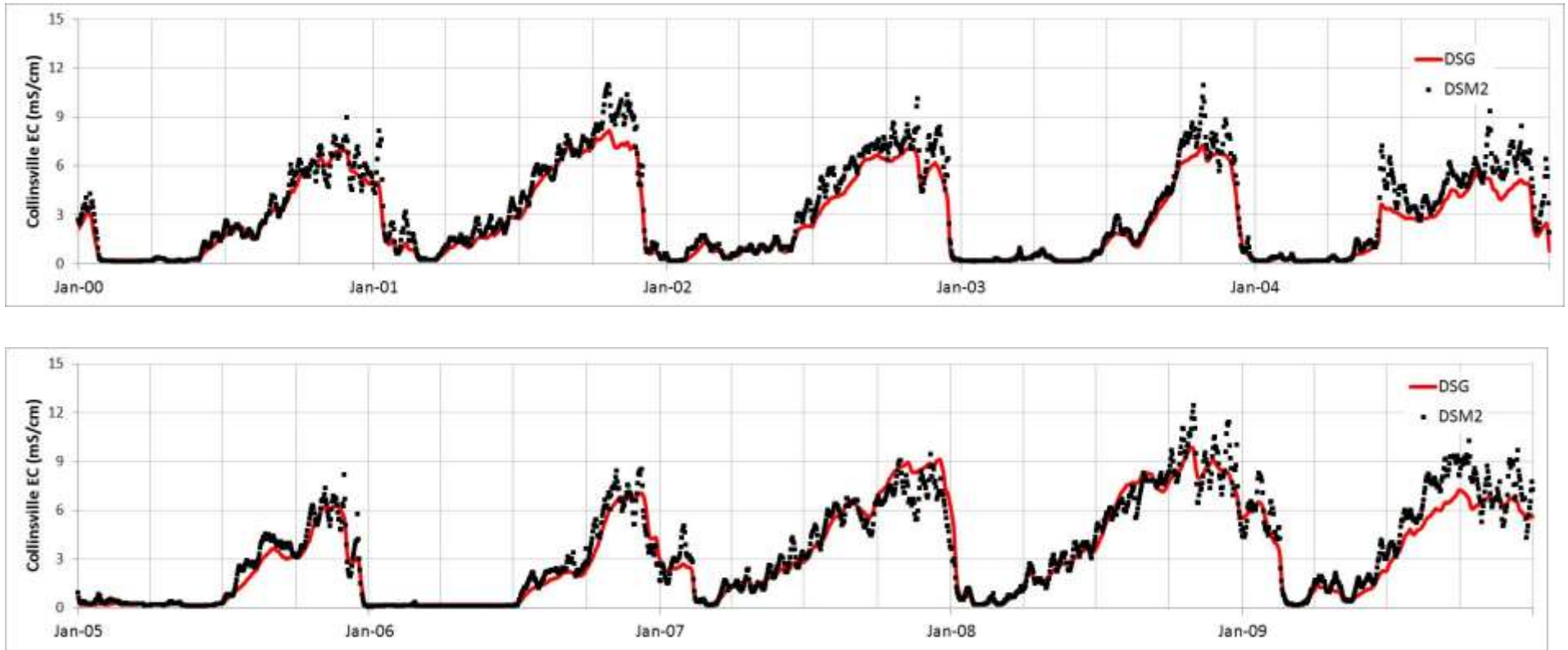


Figure 3-6: Time Series of DSG Predicted and DSM2 Surface Salinity at Collinsville: 2000-2009

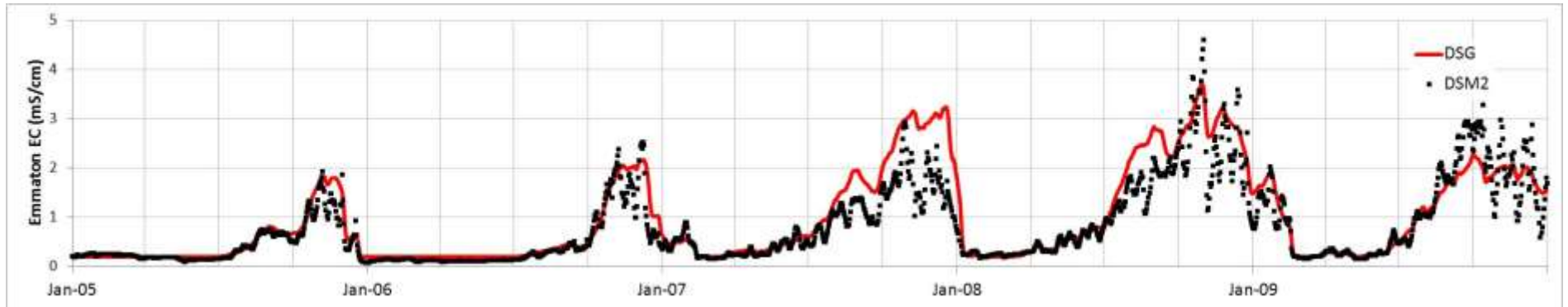
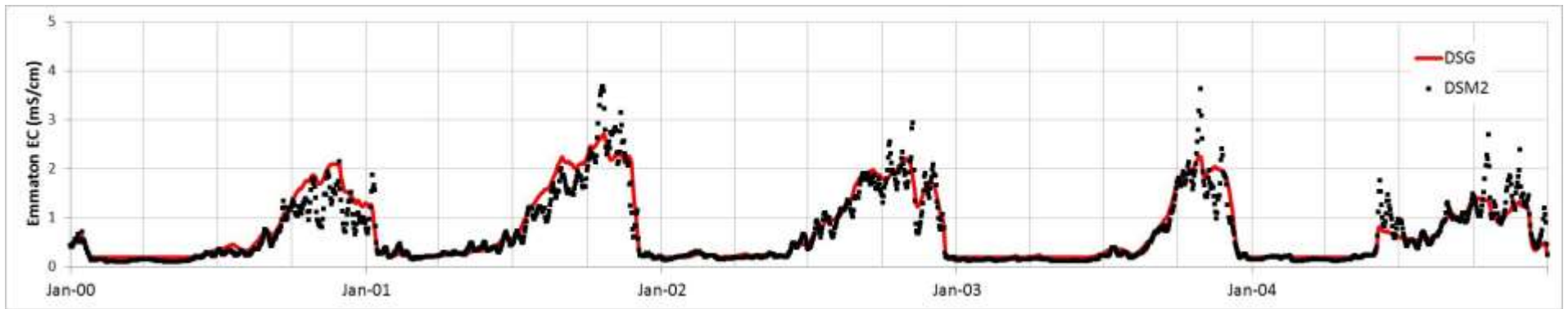


Figure 3-7: Time Series of DSG Predicted and DSM2 Surface Salinity at Emmaton: 2000-2009

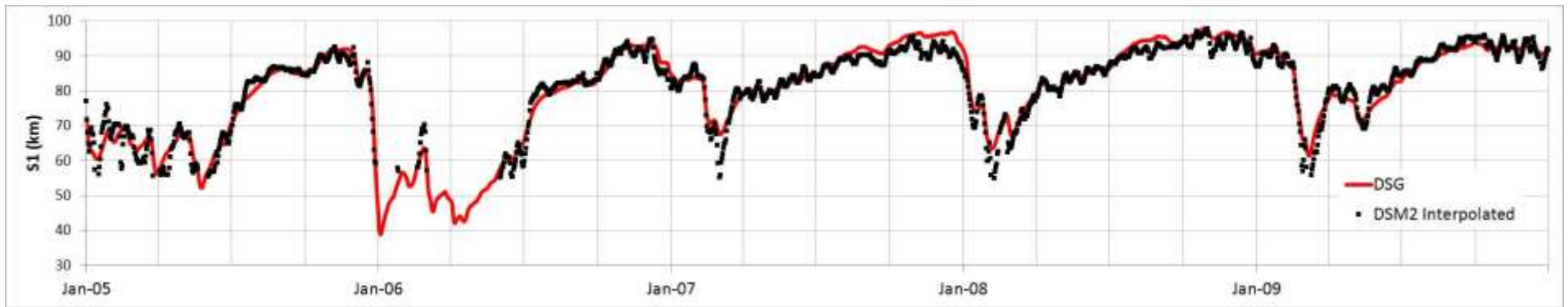
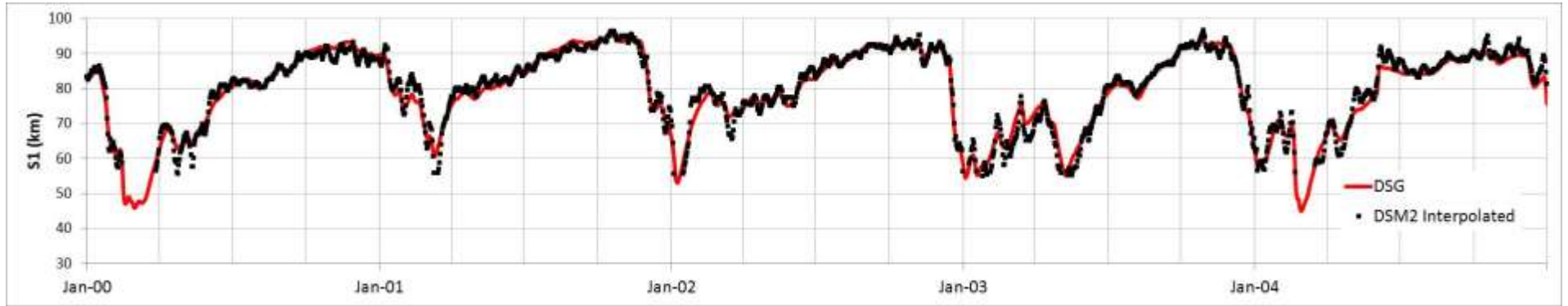


Figure 3-8: Time Series of DSG Predicted and DSM2 Interpolated 1 ppt Surface Isohaline Position: 2000-2009

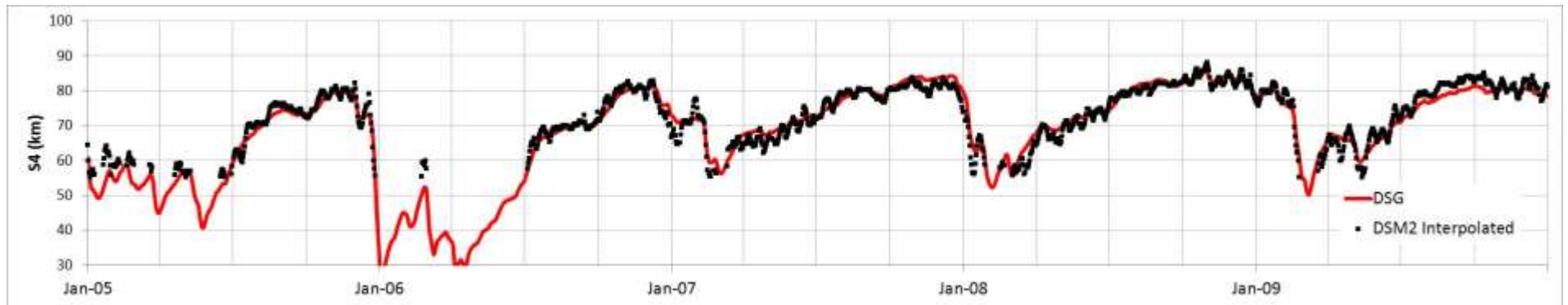
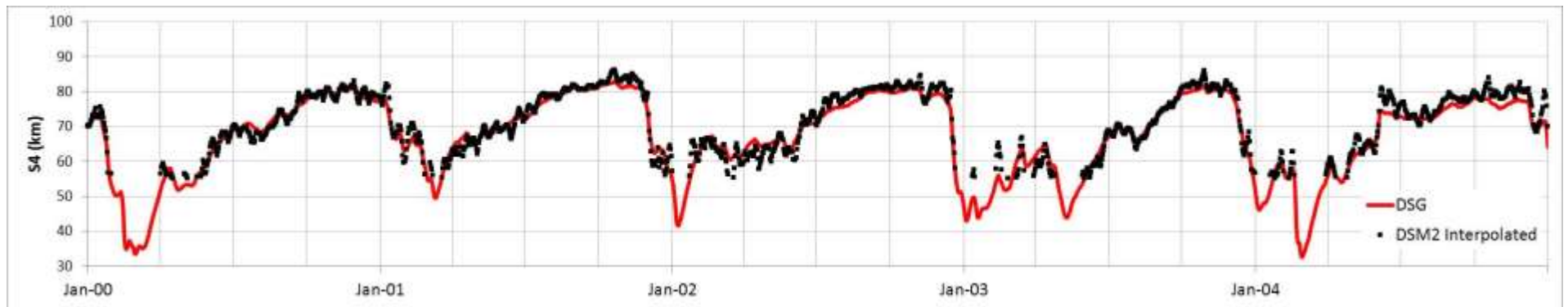


Figure 3-9: Time Series of DSG Predicted and DSM2 Interpolated 4 ppt Surface Isohaline Position: 2000-2009

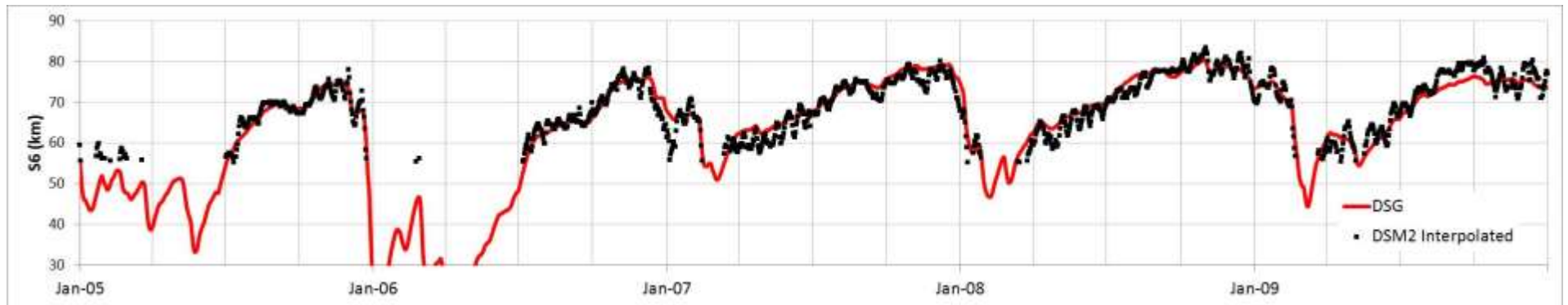
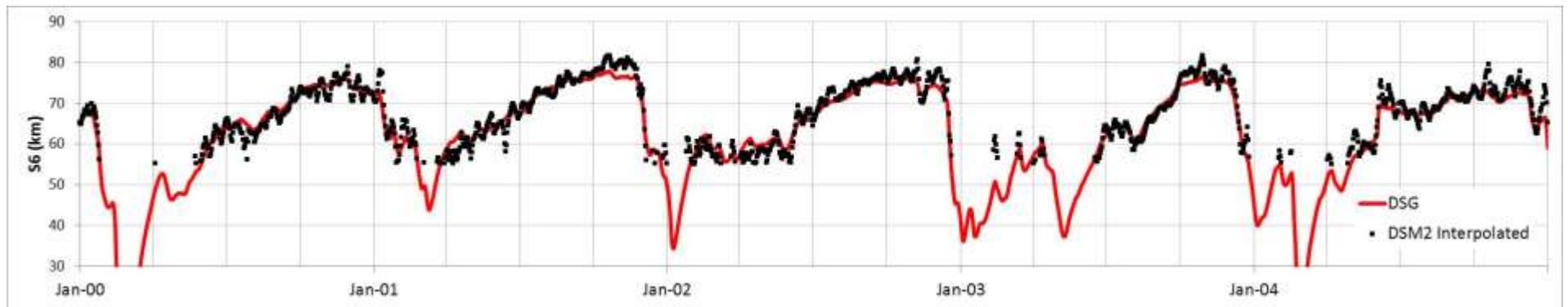


Figure 3-10: Time Series of DSG Predicted and DSM2 Interpolated 6 ppt Surface Isohaline Position: 2000-2009

4. Calibration & Validation with Observed Data

4.1 Data Description

Daily averaged salinity and isohaline position data were taken from work reported by Roy et al. (2014). Daily net Delta outflow data were obtained from DAYFLOW for the period October 1929 through September 2012. The outflow record was extended back to October 1921. Average monthly outflow were based on data provided by DWR (DWR 1957). The development of daily outflow estimates from these monthly values is described in Appendix B. The period spanning calendar years 2000-09 was selected as the calibration period.

4.2 X2 Parameter Calibration

Antecedent outflow was calculated from [Equation \(2.2\)](#) assuming a nominal value for β of 475 cfs-years and assuming daily Delta outflows (Q) from the DAYFLOW model (CDWR 2014). X2 values along the San Joaquin River branch are typically higher (i.e. further upstream) than those along the Sacramento River branch, due in large part to smaller freshwater inflow volumes from the San Joaquin River available to repel salinity. Thus, [Equation \(2.4\)](#) was calibrated for both the Sacramento and San Joaquin River branches.

4.2.1 Sacramento River Branch

A scatter plot of interpolated X2 along the Sacramento River branch versus antecedent outflow is provided in [Figure 4-1](#). Best fit parameter values $\Phi_1 = 457 \pm 3.9$ (mean \pm 1 SE) and $\Phi_2 = -0.193 \pm 0.0009$ resulted after data points representing extremely high outflow events (X2 < 38 km) were removed from the analysis. The coefficient of determination $R^2 = 0.93$ and the standard error of estimate is 3.3 km. Our parameter estimates are similar to those reported by Gross et. al. (2010) for various steady fit models they considered, when recalibrated assuming antecedent outflow in comparable units (m^3/sec). Differences in parameter estimates are attributed primarily to the use of a different calibration period. The resulting DSG predictions are compared with interpolated X2 data as time series in [Figure 4-2](#) for the calibration period.

4.2.2 San Joaquin River Branch

Best fit parameter values were also calibrated for the San Joaquin River branch, resulting in $\Phi_1 = 502 \pm 4.5$ and $\Phi_2 = -0.203 \pm 0.001$ with $R^2 = 0.92$ and a 3.6 km standard error of estimate. See [Figure 4-3](#). The resulting DSG predictions are compared with interpolated X2 data as time series in [Figure 4-4](#) for the calibration period.

4.3 S_0 Parameter Calibration

[Equation \(2.11\)](#) was calibrated with observed salinity data and interpolated X2 data in a manner similar to that reported earlier for the DSM2 data calibration. Salinity data were limited to the Martinez station, and data for a given time step were removed from this analysis if $S \leq S_b$ or if $X/X_2 \geq 0.8$. Best fit parameter values $\gamma = 2.29 \times 10^{-4} \pm 4.0 \times 10^{-5}$ and $\delta = 1.83 \pm 0.04$ result from the regression analysis. Similar to the calibration with DSM2 data, it was observed that the calibrated [Equation \(2.9\)](#) is approximately linear with respect to X2 in the typical range of 50 to 100 km.

4.4 Salinity & Isohaline Estimates: Calibration Period

DSG surface salinity predictions are compared with observed data as time series in [Figures 4-5 through 4-12](#) and as scatter plots in [Figures C-1 through C-8](#) for the calibration period. A formal residual analysis was not conducted.

DSG surface isohaline predictions at 1 ppt (1.7 mS/cm), 4 ppt (6.8 mS/cm), and 6 ppt (10.0 mS/cm) are compared with Sacramento River branch interpolated values as time series in [Figure 4-13 through 4-15](#) and as scatter plots in [Figures C-9 through C-11](#) for the calibration period. Similarly, predictions are compared with San Joaquin River branch interpolated values as time series in [Figure 4-16 through 4-18](#) and as scatter plots in [Figures C-12 through C-14](#).

DSG model variances with Sacramento River branch interpolated values, as measured by standard error, are similar to or greater than the error associated with the X2 prediction: 3.3 km for the 1 ppt estimate, 3.4 km for the 4 ppt estimate, and 3.6 km for the 6 ppt estimate. DSG model variances with San Joaquin River branch interpolated values, as measured by standard error, are similar to or greater than the error associated with the X2 prediction: 3.9 km for the 1 ppt estimate, 3.6 km for the 4 ppt estimate, and 3.7 km for the 6 ppt estimate.

Neither time series nor scatter plots reveal significant bias in the isohaline estimates. However, a formal residual analysis was not conducted.

4.5 Validation Results

The DSG model estimates for X2 position, surface salinity and surface isohaline positions were compared with data developed by Roy et al. (2014). Comparisons are provided in this section through time series plots and tabulated statistics. Statistics are aggregated by decade. The earliest decade (1920-29) does not include observed data prior to October 1921. The most recent decade (2010-12) does not include observed data after September 2012.

4.5.1 X2 Estimates

DSG X2 predictions are compared with observed data as time series in Appendix D by decade for the Sacramento and San Joaquin branches. The Sacramento branch time series plots are provided in [Figures D-1 through D-9](#). The San Joaquin branch time series plots are provided in [Figures D-10 through D-18](#). Measures of DSG model variance and bias with interpolated X2 data are provided in [Table 4-1](#) by decade.

Table 4-1. Performance of DSG X2 Predictions by Decade
 $\text{Predicted} = C1 + C2 * \text{Interpolated}$

Decade	Sacramento Branch				San Joaquin Branch			
	Standard Error (km)	C1	C2	R2	Standard Error (km)	C1	C2	R2
2010-12	2.64	5.64	0.93	0.94	2.85	6.58	0.90	0.94
2000-09	3.29	5.59	0.93	0.92	3.57	6.05	0.92	0.92
1990-99	3.57	3.75	0.94	0.95	4.05	1.68	0.97	0.94
1980-89	3.74	-3.81	1.06	0.93	3.98	-3.38	1.05	0.92
1970-79	2.99	-3.30	1.05	0.96	3.02	-3.02	1.04	0.96
1960-69	3.50	-1.04	1.02	0.92	3.67	-2.32	1.03	0.93
1950-59	4.02	4.28	0.95	0.92	4.54	6.95	0.93	0.93
1940-49	4.03	-2.33	1.04	0.92	4.04	-0.56	1.00	0.92
1930-39	5.19	1.03	0.70	0.95	5.98	13.7	0.81	0.94
1920-29	4.68	-2.04	1.06	0.94	4.12	6.94	0.91	0.94

Model variance associated with X2 prediction generally decreases with time. This result is consistent with known changes over time such as sea level rise and bathymetric changes, both of which have changed the flow-salinity relationship of the estuary. However, the

model variance associated salinity estimates (as provided in the following section) does not consistently reflect such a temporal trend. Therefore, its significance is unclear.

4.5.2 Salinity Estimates

DSG salinity predictions are compared with observed data as time series in Appendix E (see [Figures E-1 through E-72](#)) by decade at the locations listed below. Assumed longitudinal distances to Golden Gate are provided in parentheses for each location. These locations are as reported by Roy et al. (2014) and therefore maintain consistency with interpolated X2 positions. The first distance is associated with the recent (CDEC) data and was applied to the decades beginning with 1960-69 (CDEC 2013). The second distance is associated with older (Bulletin 23) data and was applied to decades previous to 1960-69 (CDPW, 1924-55, CDWR 1956-62, CDWR 1962, CDWR 1963-71). This approach introduces some error into the analysis of the 1960-69 decade, as this decade is described by both Bulletin 23 and CDEC data. The Mallard Island location was reported at O&A Ferry in the earlier Bulletin 23 data. Roy et al. (2014) found anomalies in the Bulletin 23 Pittsburg data; thus, results are not provided at this location prior to the 1960-69 decade.

- Martinez (54/54 km)
- Port Chicago (64/66 km)
- Mallard Island (75 km) or O&A Ferry (74.8 km)
- Collinsville (81/81.8 km)
- Emmaton (92/92.9 km)
- Pittsburg (77 km)
- Antioch (85.75/88.4 km)
- Jersey Point (95.75/98.8 km)

Measures of DSG model variance and bias with observed salinity data are provided for each location in [Tables 4-2 through 4-9](#) by decade.

Table 4-2. Performance of DSG Salinity Predictions at Martinez by Decade
 Predicted = C1 + C2 * Observed

Decade	Standard Error (mS/cm)	Coefficient of Variation	C1	C2	R2
2010-12	2.3	0.14	1.3	0.87	0.93
2000-09	2.2	0.12	1.1	0.93	0.93
1990-99	2.4	0.14	0.3	0.95	0.94
1980-89	3.2	0.20	1.2	0.96	0.89
1970-79	2.6	0.18	0.4	1.0	0.92
1960-69	3.4	0.25	-1.0	1.1	0.85
1950-59	3.3	0.29	0.4	1.1	0.91
1940-49	3.3	0.25	-0.3	1.2	0.90
1930-39	5.8	0.42	-0.4	1.3	0.91
1920-29	5.0	0.38	0.2	1.2	0.91

Table 4-3 Performance of DSG Salinity Predictions at Port Chicago by Decade
 Predicted = C1 + C2 * Observed

Decade	Standard Error (mS/cm)	Coefficient of Variation	C1	C2	R2
2010-12	2.0	0.23	0.6	0.96	0.91
2000-09	2.9	0.28	1.2	0.99	0.86
1990-99	2.2	0.19	0.0	0.97	0.93
1980-89	3.1	0.33	0.3	1.1	0.88
1970-79	2.3	0.24	-0.4	1.1	0.94
1960-69	2.0	0.25	-0.3	1.1	0.94
1950-59	1.6	0.22	-0.5	1.0	0.95
1940-49	2.1	0.23	-0.6	0.97	0.94
1930-39	2.9	0.24	-1.1	1.1	0.93
1920-29	2.3	0.18	-0.7	1.0	0.94

Table 4-4 Performance of DSG Salinity Predictions at Mallard Island (O&A Ferry)
by Decade Predicted = C1 + C2 * Observed

Decade	Standard Error (mS/cm)	Coefficient of Variation	C1	C2	R2
2010-12	1.3	0.33	0.1	0.84	0.91
2000-09	1.6	0.28	0.0	0.92	0.88
1990-99	1.8	0.32	-0.0	0.96	0.88
1980-89	2.1	0.46	0.1	1.1	0.86
1970-79	1.3	0.30	-0.0	1.1	0.95
1960-69	1.2	0.33	-0.1	1.1	0.94
1950-59	1.1	0.35	0.1	1.1	0.94
1940-49	1.1	0.79	-0.1	1.0	0.95
1930-39	2.1	0.29	-0.1	1.1	0.97
1920-29	1.4	0.20	0.2	1.0	0.98

Table 4-5 Performance of DSG Salinity Predictions at Collinsville by Decade
Predicted = C1 + C2 * Observed

Decade	Standard Error (mS/cm)	Coefficient of Variation	C1	C2	R2
2010-12	0.8	0.43	0.2	0.79	0.88
2000-09	1.2	0.37	0.2	0.87	0.85
1990-99	1.7	0.50	0.3	0.88	0.79
1980-89	1.6	0.66	0.1	1.2	0.83
1970-79	1.3	0.56	0.1	1.2	0.94
1960-69	0.9	0.47	0.2	1.0	0.92
1950-59	0.8	0.53	0.2	0.93	0.90
1940-49	0.9	0.48	0.2	0.98	0.92
1930-39	1.8	0.39	0.1	1.1	0.95
1920-29	1.3	0.29	0.1	1.0	0.96

Table 4-6 Performance of DSG Salinity Predictions at Emmaton by Decade
 Predicted = C1 + C2 * Observed

Decade	Standard Error (mS/cm)	Coefficient of Variation	C1	C2	R2
2010-12	0.3	0.79	0.1	0.83	0.54
2000-09	0.5	0.68	0.2	0.77	0.64
1990-99	0.8	0.73	0.2	0.73	0.64
1980-89	0.8	1.12	0.1	1.2	0.65
1970-79	0.4	0.56	0.1	1.0	0.90
1960-69	0.3	0.65	0.1	0.99	0.83
1950-59	0.5	1.14	0.2	0.69	0.53
1940-49	0.4	0.73	0.0	1.1	0.86
1930-39	1.5	0.70	0.2	1.1	0.92
1920-29	1.1	0.60	0.2	1.1	0.94

Table 4-7 Performance of DSG Salinity Predictions at Pittsburg by Decade
 Predicted = C1 + C2 * Observed

Decade	Standard Error (mS/cm)	Coefficient of Variation	C1	C2	R2
2010-12	1.1	0.38	0.1	0.95	0.87
2000-09	1.2	0.37	0.3	0.92	0.82
1990-99	2.1	0.41	-0.0	0.92	0.82
1980-89	2.0	0.50	0.1	1.1	0.83
1970-79	1.4	0.41	0.0	1.1	0.94
1960-69	1.0	0.45	-0.1	1.2	0.94
1950-59	n/a	n/a	n/a	n/a	n/a
1940-49	n/a	n/a	n/a	n/a	n/a
1930-39	n/a	n/a	n/a	n/a	n/a
1920-29	n/a	n/a	n/a	n/a	n/a

Table 4-8 Performance of DSG Salinity Predictions at Antioch by Decade
 Predicted = C1 + C2 * Observed

Decade	Standard Error (mS/cm)	Coefficient of Variation	C1	C2	R2
2010-12	0.6	0.49	0.1	0.77	0.82
2000-09	0.9	0.47	0.1	0.88	0.78
1990-99	1.3	0.59	-0.0	0.98	0.73
1980-89	1.4	0.81	-0.0	1.2	0.75
1970-79	0.9	0.55	-0.2	1.2	0.93
1960-69	0.7	0.64	-0.0	1.2	0.92
1950-59	0.5	0.54	0.1	0.82	0.90
1940-49	0.6	0.48	0.0	0.87	0.92
1930-39	1.5	0.38	-0.2	1.0	0.95
1920-29	1.2	0.34	-0.2	0.93	0.96

Table 4-9 Performance of DSG Salinity Predictions at Jersey Point by Decade
 Predicted = C1 + C2 * Observed

Decade	Standard Error (mS/cm)	Coefficient of Variation	C1	C2	R2
2010-12	0.3	0.67	0.1	0.43	0.73
2000-09	0.4	0.56	0.1	0.68	0.62
1990-99	0.6	0.76	0.0	0.85	0.50
1980-89	0.6	0.87	-0.0	1.1	0.61
1970-79	0.4	0.60	-0.1	1.1	0.86
1960-69	0.3	0.67	-0.0	1.2	0.79
1950-59	0.2	0.52	0.1	0.65	0.86
1940-49	0.2	0.43	-0.0	0.88	0.90
1930-39	1.0	0.55	-0.1	1.0	0.94
1920-29	0.6	0.40	-0.1	1.0	0.96

4.5.3 Other Isohaline Estimates

The DSG model was run to predict surface isohaline locations at 1 ppt (1.7 mS/cm), 4 ppt (6.8 mS/cm) and 6 ppt (10.0 mS/cm). Measures of DSG model variance and bias with interpolated surface isohaline data are provided in [Tables 4-10 through 4-12](#) by decade.

Table 4-10 Performance of DSG 1 ppt Isohaline Predictions by Decade
 Predicted = C1 + C2 * Interpolated

Decade	Sacramento Branch				San Joaquin Branch			
	Standard Error (km)	C1	C2	R2	Standard Error (km)	C1	C2	R2
2010-12	2.70	4.89	0.94	0.94	3.21	9.15	0.87	0.94
2000-09	3.25	4.93	0.94	0.93	3.86	7.98	0.89	0.92
1990-99	3.51	2.97	0.96	0.95	4.52	3.41	0.94	0.93
1980-89	3.77	-3.91	1.06	0.93	4.02	-0.40	1.00	0.93
1970-79	2.99	-3.51	1.06	0.96	3.08	-0.39	1.00	0.96
1960-69	3.49	-2.33	1.03	0.93	3.75	-1.18	1.01	0.93
1950-59	4.13	1.60	0.99	0.91	3.88	3.67	0.95	0.93
1940-49	4.20	-5.00	1.07	0.92	4.35	1.63	0.96	0.92
1930-39	5.34	-1.78	1.06	0.95	6.81	15.6	0.79	0.91
1920-29	5.00	-5.34	1.10	0.94	4.19	6.32	0.92	0.93

Table 4-11 Performance of DSG 4 ppt Isohaline Predictions by Decade
 Predicted = C1 + C2 * Interpolated

Decade	Sacramento Branch				San Joaquin Branch			
	Standard Error (km)	C1	C2	R2	Standard Error (km)	C1	C2	R2
2010-12	2.66	5.00	0.92	0.94	2.73	0.41	0.99	0.93
2000-09	3.42	5.67	0.92	0.91	3.63	2.41	0.97	0.90
1990-99	3.61	2.05	0.96	0.94	3.80	-1.58	1.01	0.94
1980-89	4.14	-6.37	1.11	0.91	4.48	-8.64	1.13	0.91
1970-79	3.32	-6.03	1.10	0.94	3.74	-9.84	1.15	0.94
1960-69	3.83	0.24	0.99	0.90	4.09	-3.25	1.04	0.90
1950-59	4.63	11.6	0.84	0.92	4.34	9.20	0.87	0.92
1940-49	4.18	9.77	0.86	0.93	3.94	7.61	0.89	0.94
1930-39	5.25	7.19	0.93	0.94	5.03	11.1	0.84	0.96
1920-29	4.39	6.04	0.94	0.95	4.23	9.54	0.87	0.96

Table 4-12 Performance of DSG 6 ppt Isohaline Predictions by Decade
 Predicted = C1 + C2 * Interpolated

Decade	Sacramento Branch				San Joaquin Branch			
	Standard Error (km)	C1	C2	R2	Standard Error (km)	C1	C2	R2
2010-12	2.78	0.74	0.98	0.93	2.98	-2.88	1.03	0.93
2000-09	3.60	3.52	0.95	0.90	3.72	0.48	0.99	0.89
1990-99	3.72	0.45	0.98	0.93	3.93	-2.91	1.03	0.93
1980-89	4.57	-7.13	1.13	0.90	4.84	-9.46	1.15	0.89
1970-79	3.78	-7.46	1.12	0.93	4.22	-11.6	1.18	0.93
1960-69	4.35	1.13	0.98	0.87	4.63	-2.70	1.03	0.87
1950-59	4.95	12.2	0.82	0.93	4.48	9.25	0.86	0.93
1940-49	4.59	11.1	0.84	0.93	4.25	8.40	0.87	0.93
1930-39	5.44	9.30	0.89	0.95	5.07	10.3	0.86	0.96
1920-29	4.61	8.30	0.90	0.95	4.30	8.63	0.88	0.95

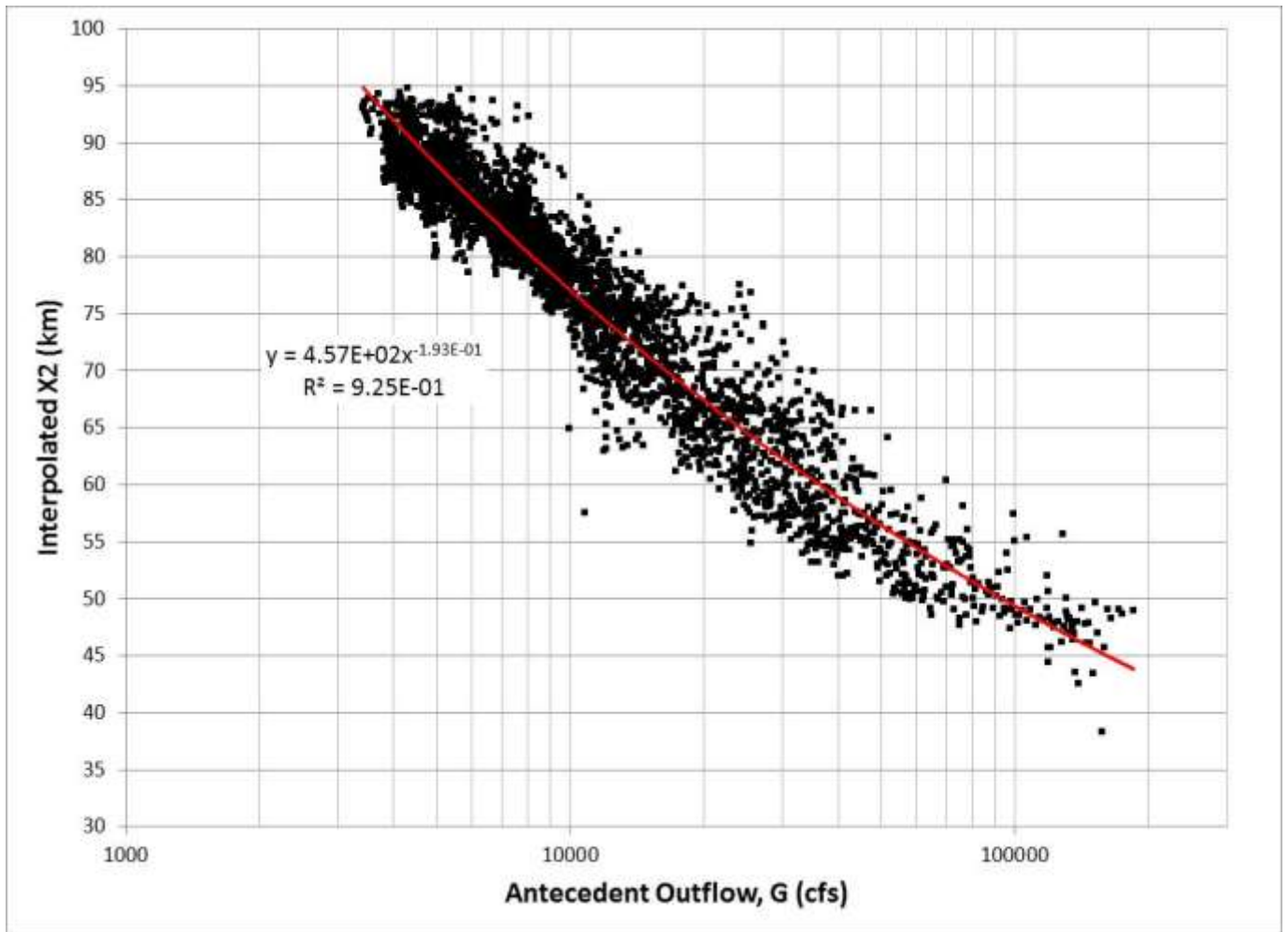


Figure 4-1. Interpolated Sacramento Branch X2 Position as a Function of Antecedent Outflow: 2000-09 Calibration

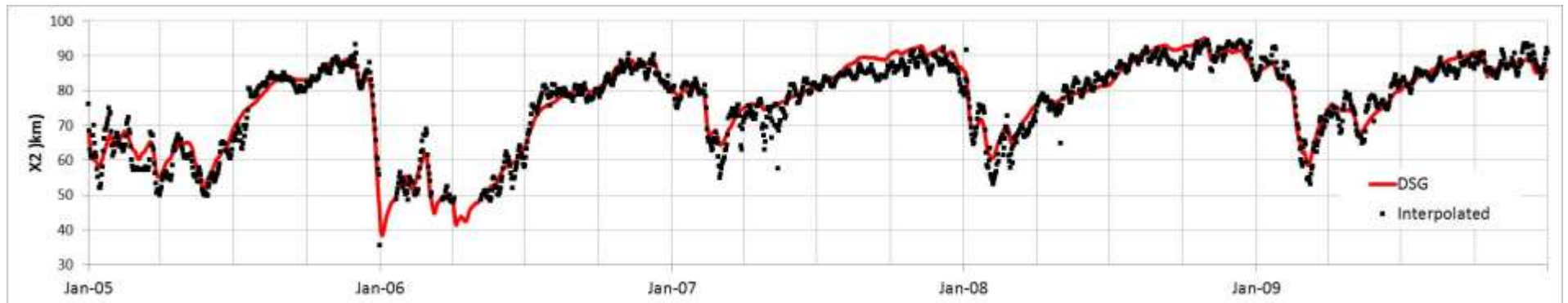
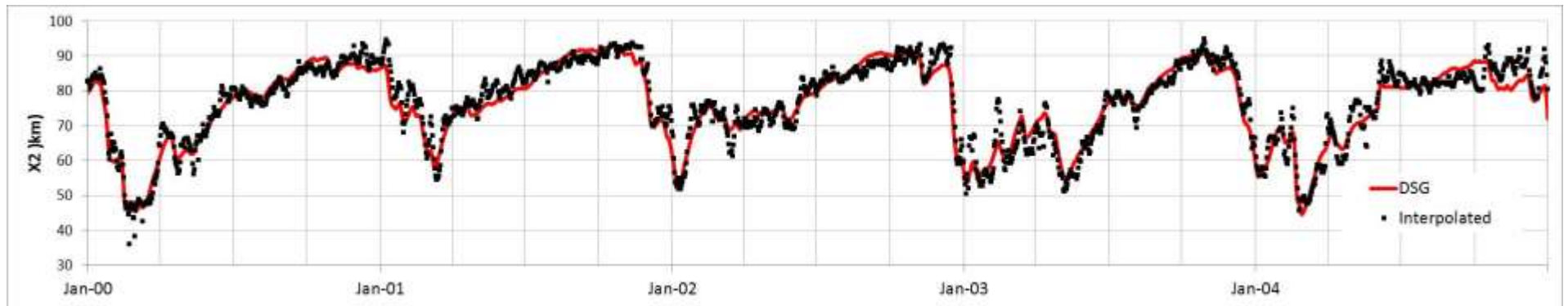


Figure 4-2: Time Series of DSG Predicted and Interpolated Sacramento Branch X2 Position: 2000-2009

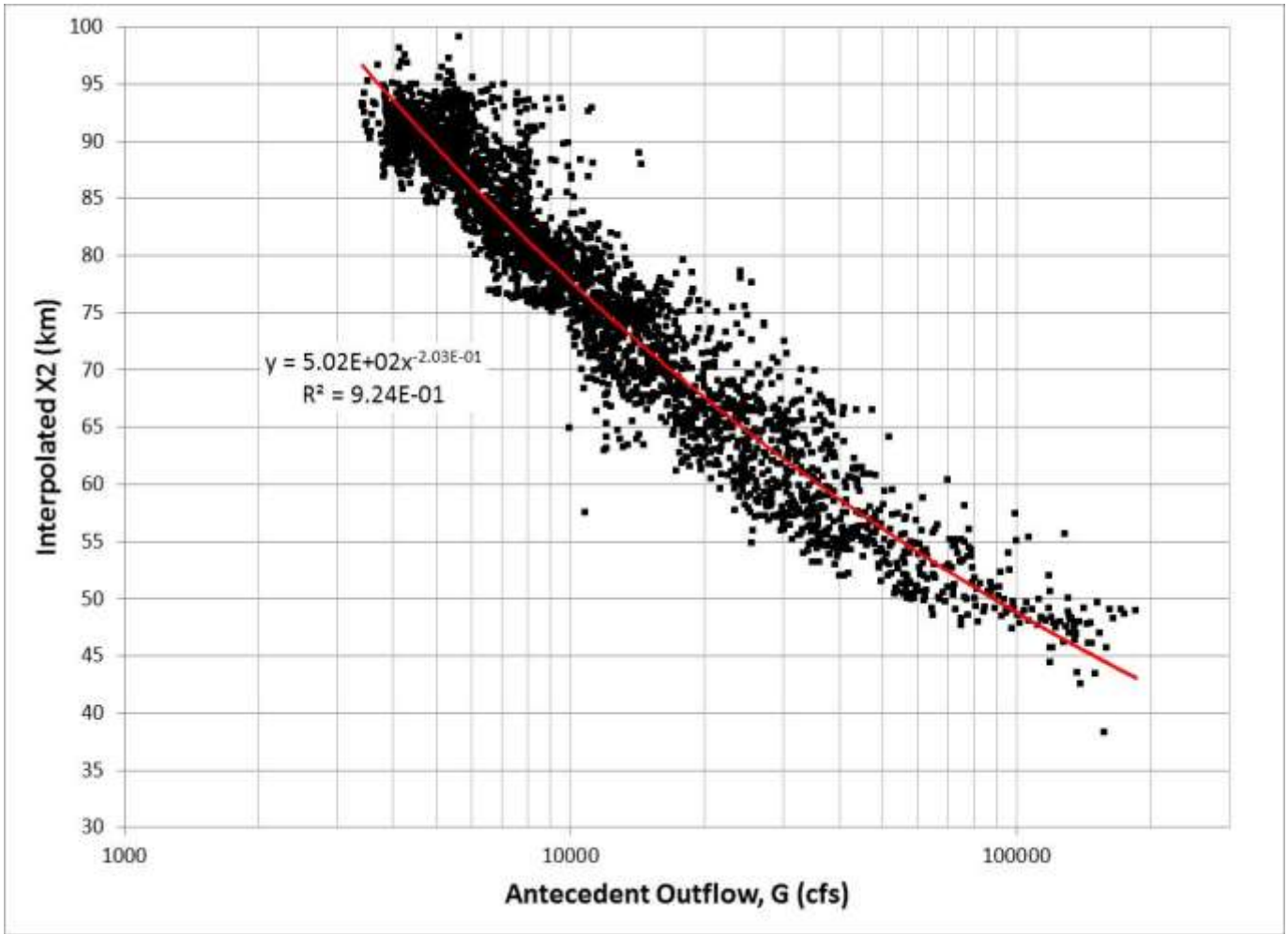


Figure 4-3. Interpolated San Joaquin Branch X2 Position as a Function of Antecedent Outflow: 2000-09 Calibration

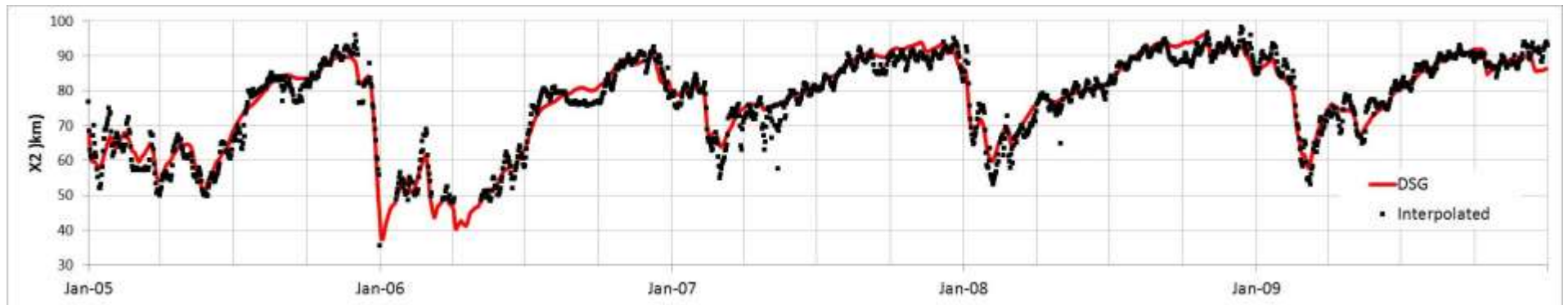
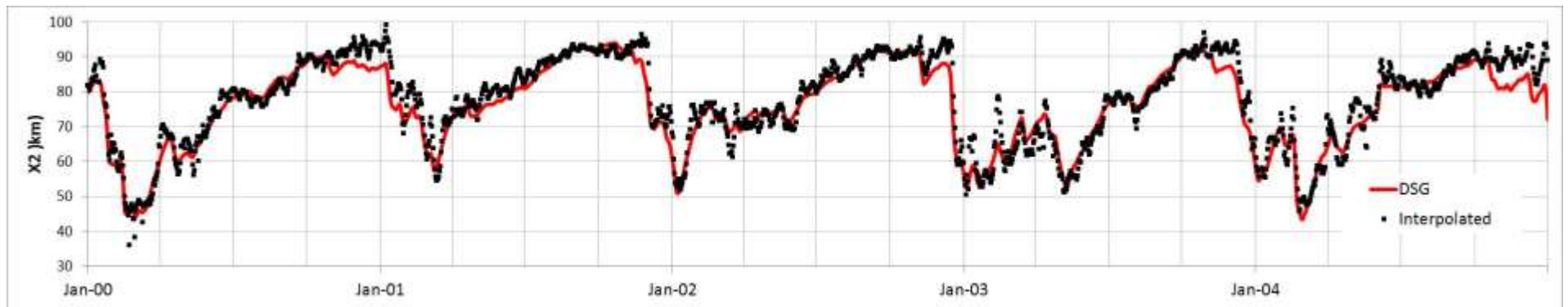


Figure 4-4: Time Series of DSG Predicted and Interpolated San Joaquin Branch X2 Position: 2000-2009

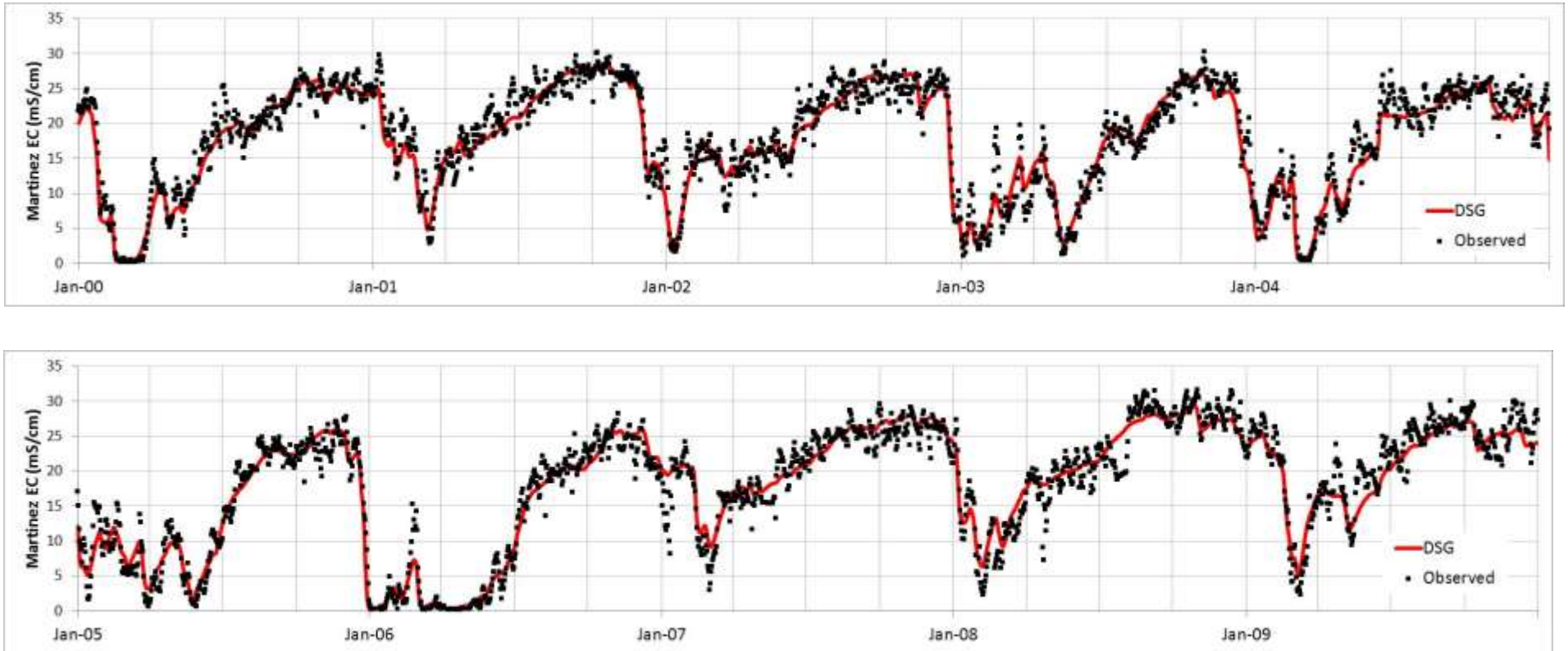


Figure 4-5: Time Series of DSG Predicted and Observed Surface Salinity at Martinez: 2000-2009

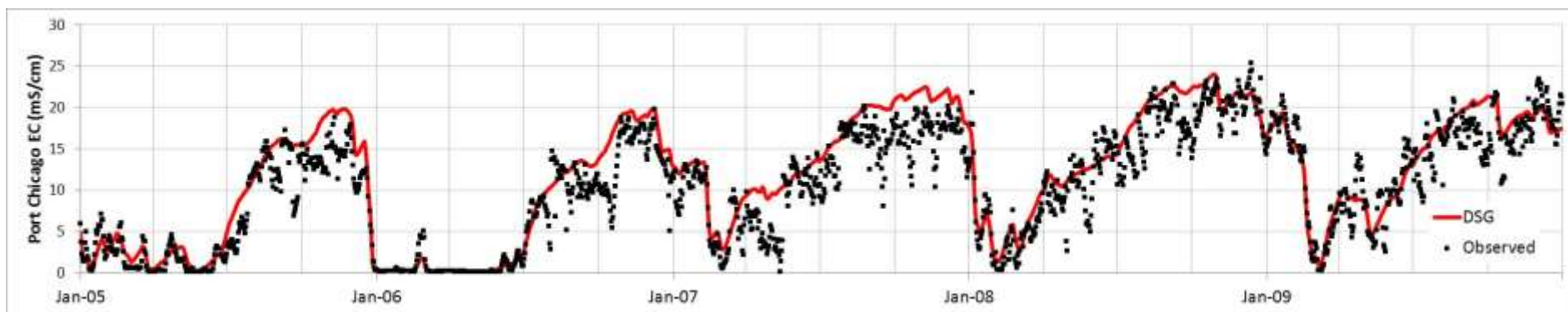
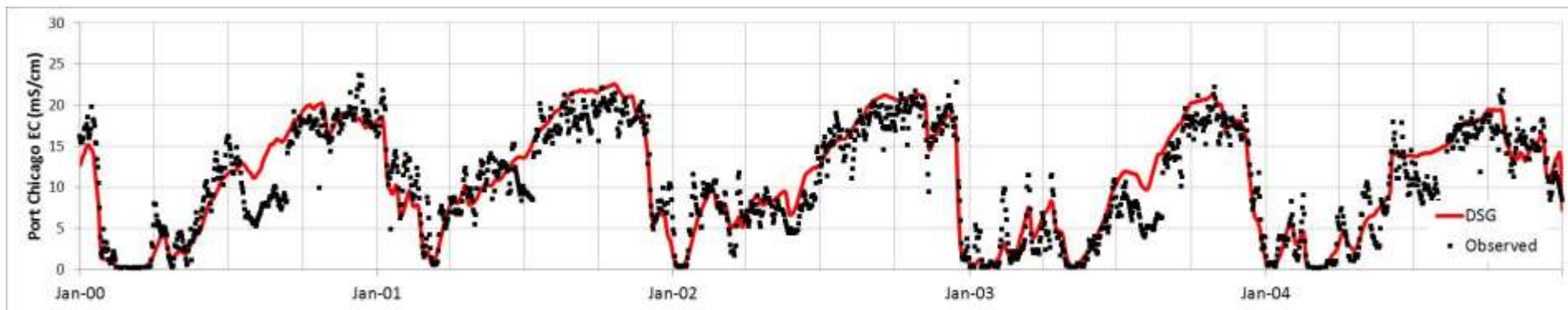


Figure 4-6: Time Series of DSG Predicted and Observed Surface Salinity at Port Chicago: 2000-2009

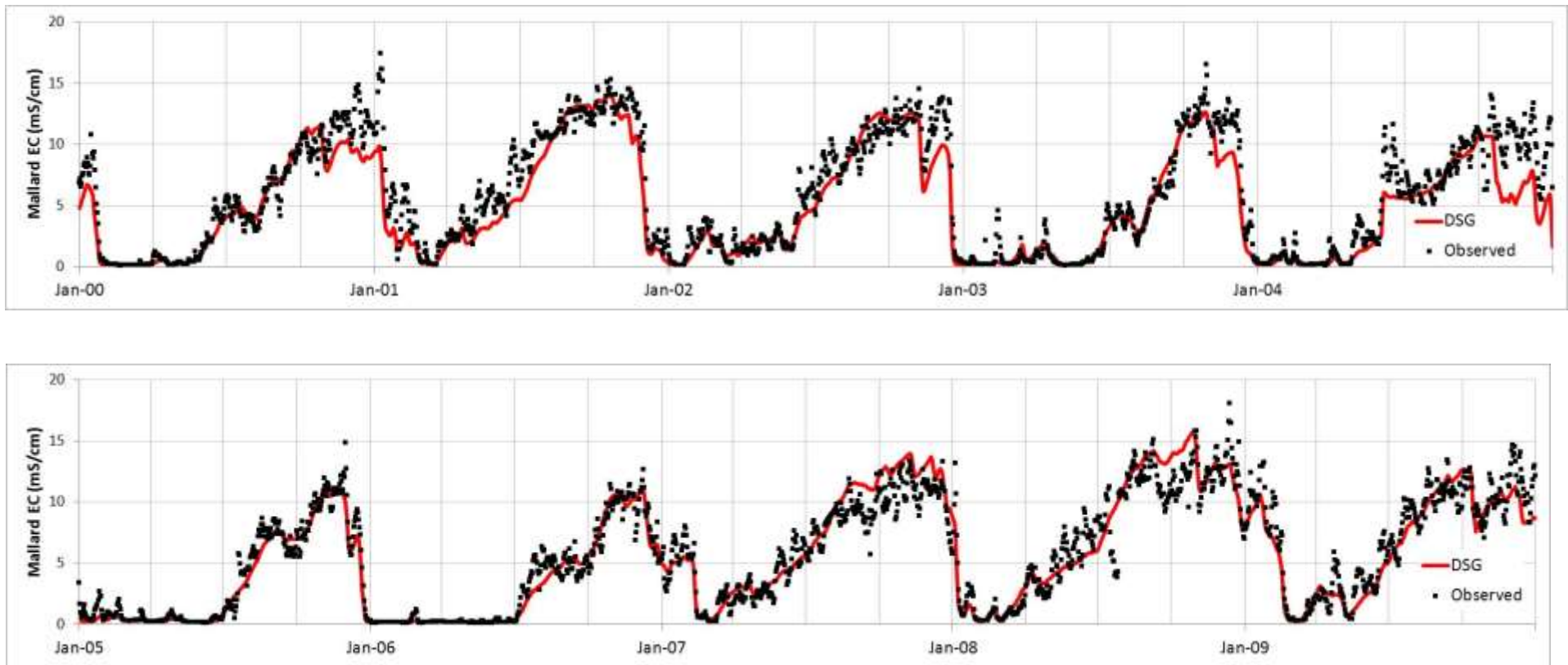


Figure 4-7: Time Series of DSG Predicted and Observed Surface Salinity at Mallard Island: 2000-2009

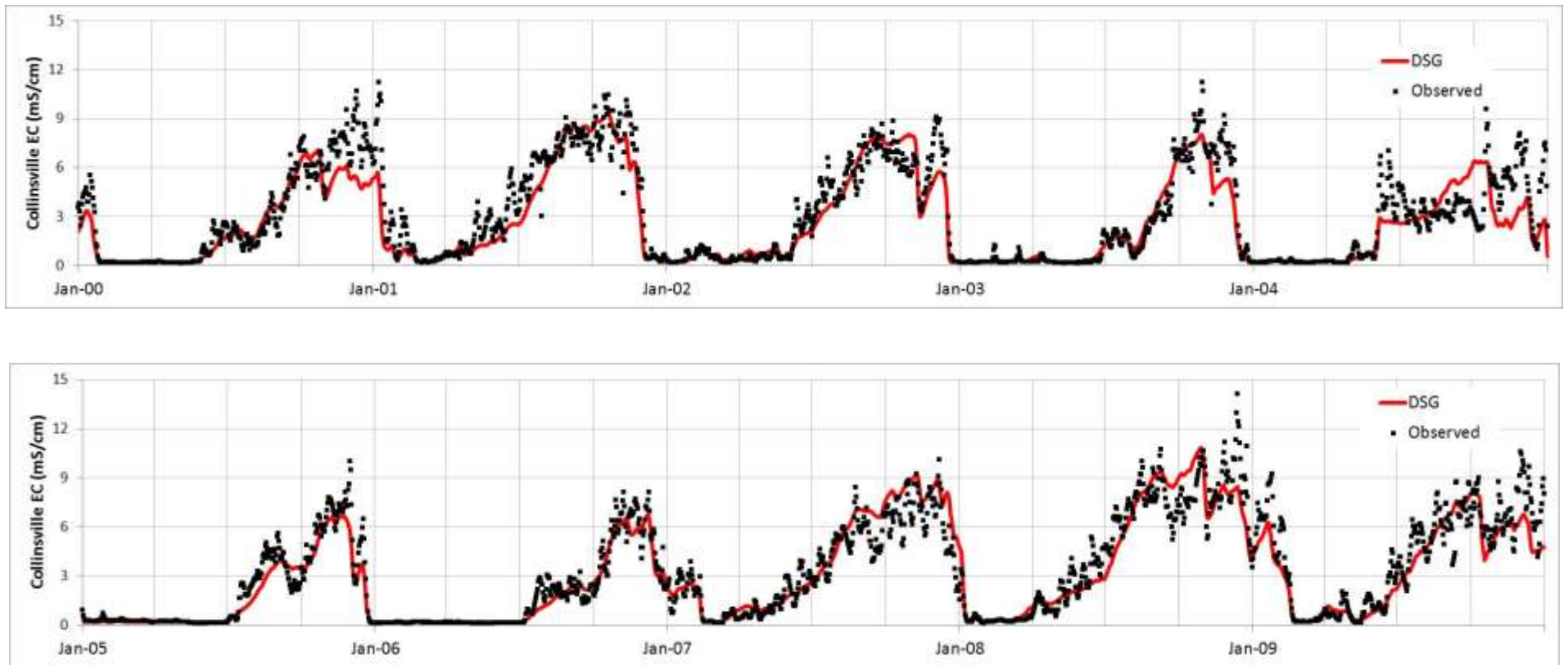


Figure 4-8: Time Series of DSG Predicted and Observed Surface Salinity at Collinsville: 2000-2009

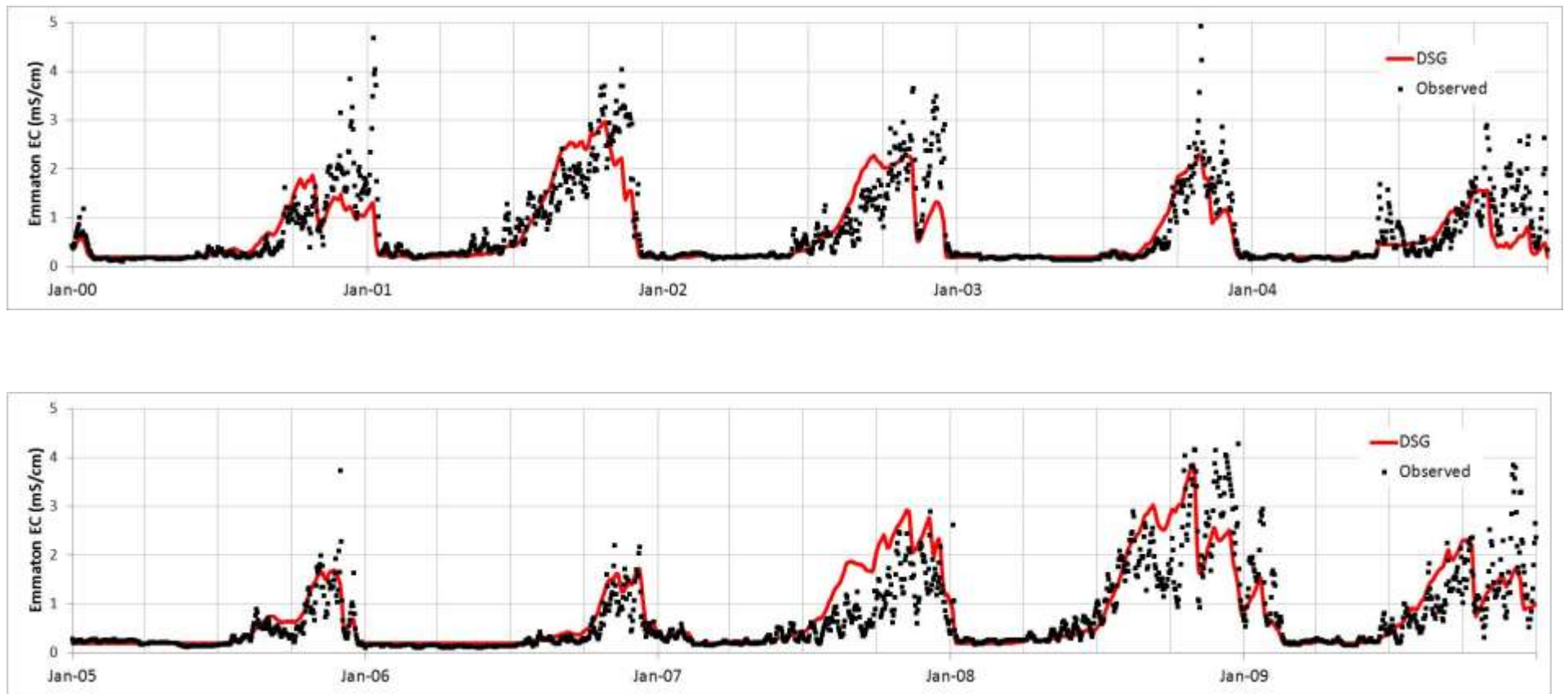


Figure 4-9: Time Series of DSG Predicted and Observed Surface Salinity at Emmaton: 2000-2009

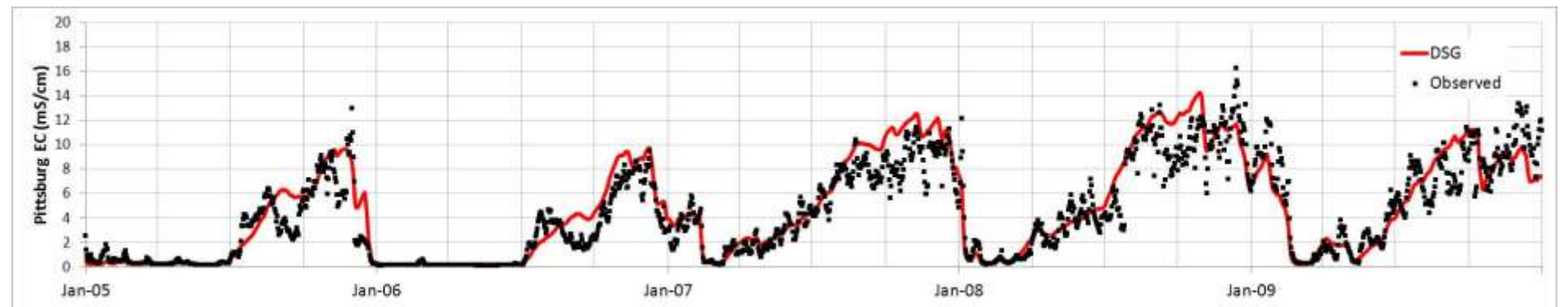
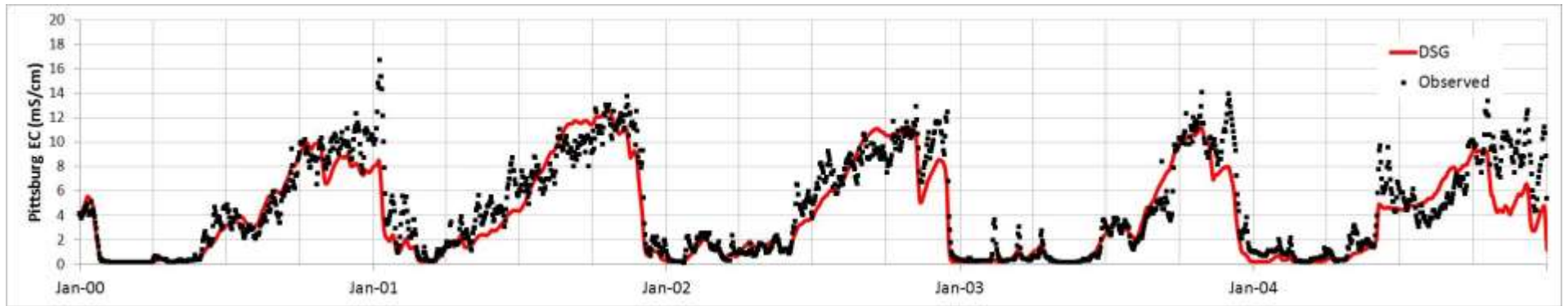


Figure 4-10: Time Series of DSG Predicted and Observed Surface Salinity at Pittsburg: 2000-2009

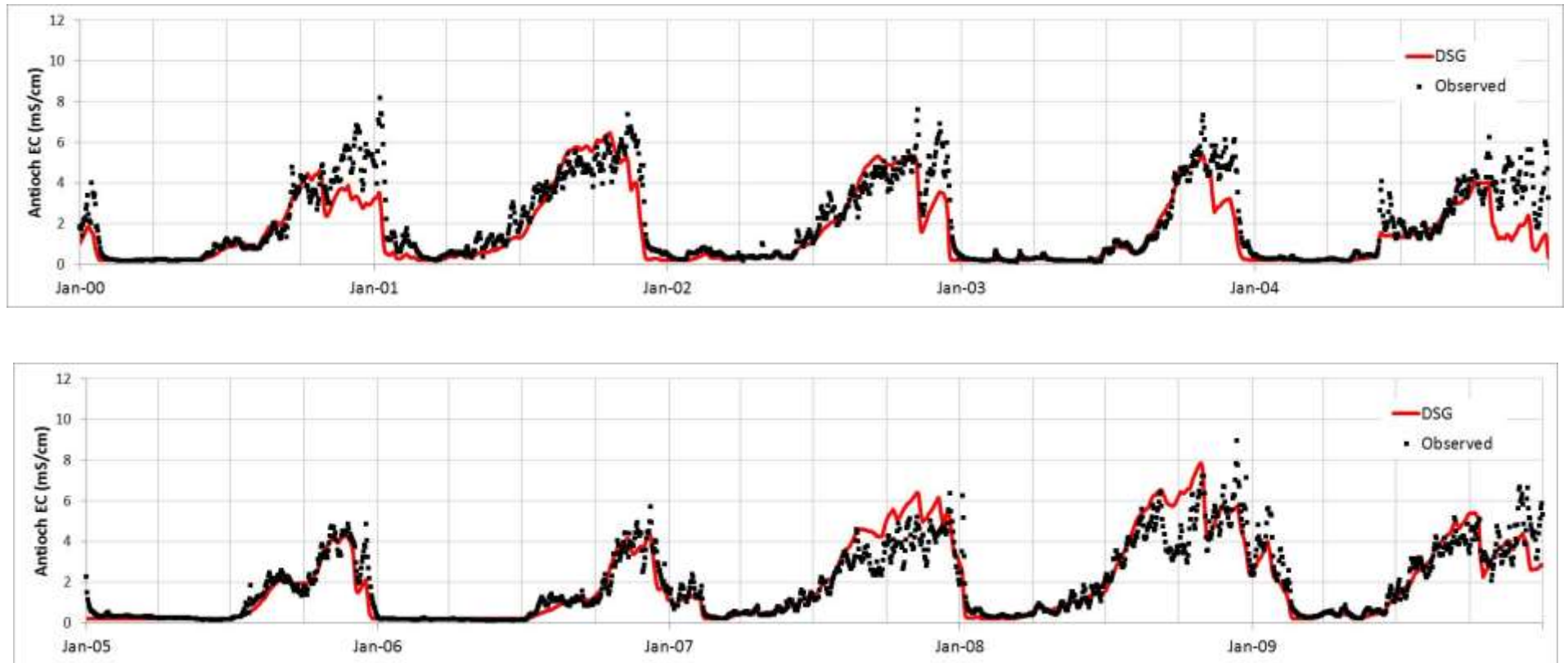


Figure 4-11: Time Series of DSG Predicted and Observed Surface Salinity at Antioch: 2000-2009

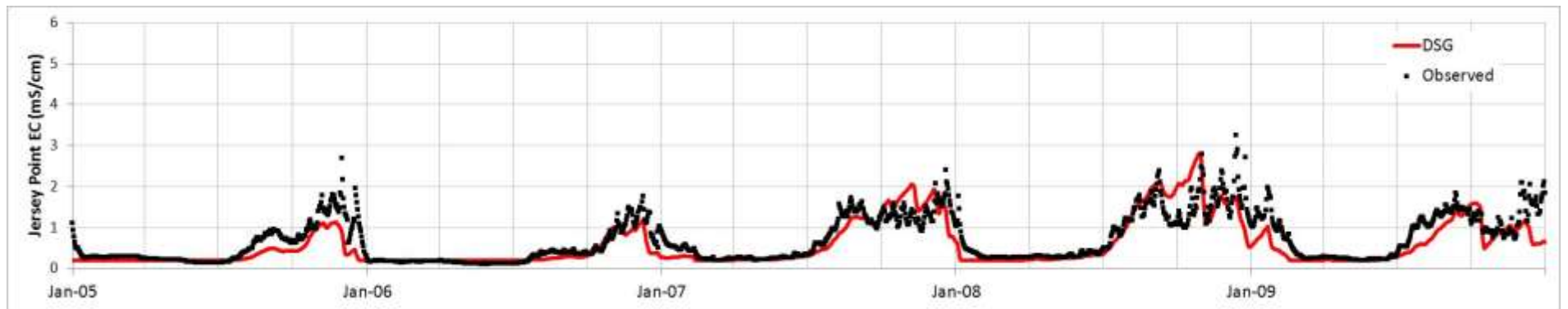
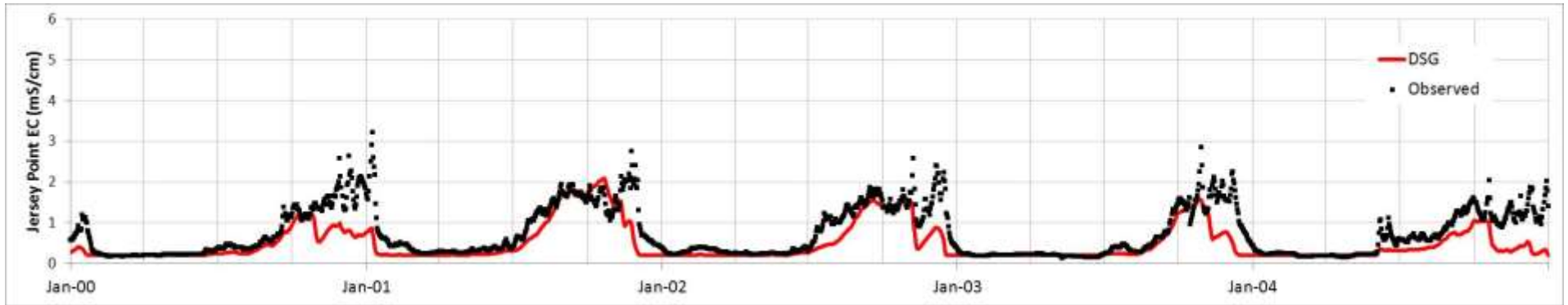


Figure 4-12: Time Series of DSG Predicted and Observed Surface Salinity at Jersey Point: 2000-2009

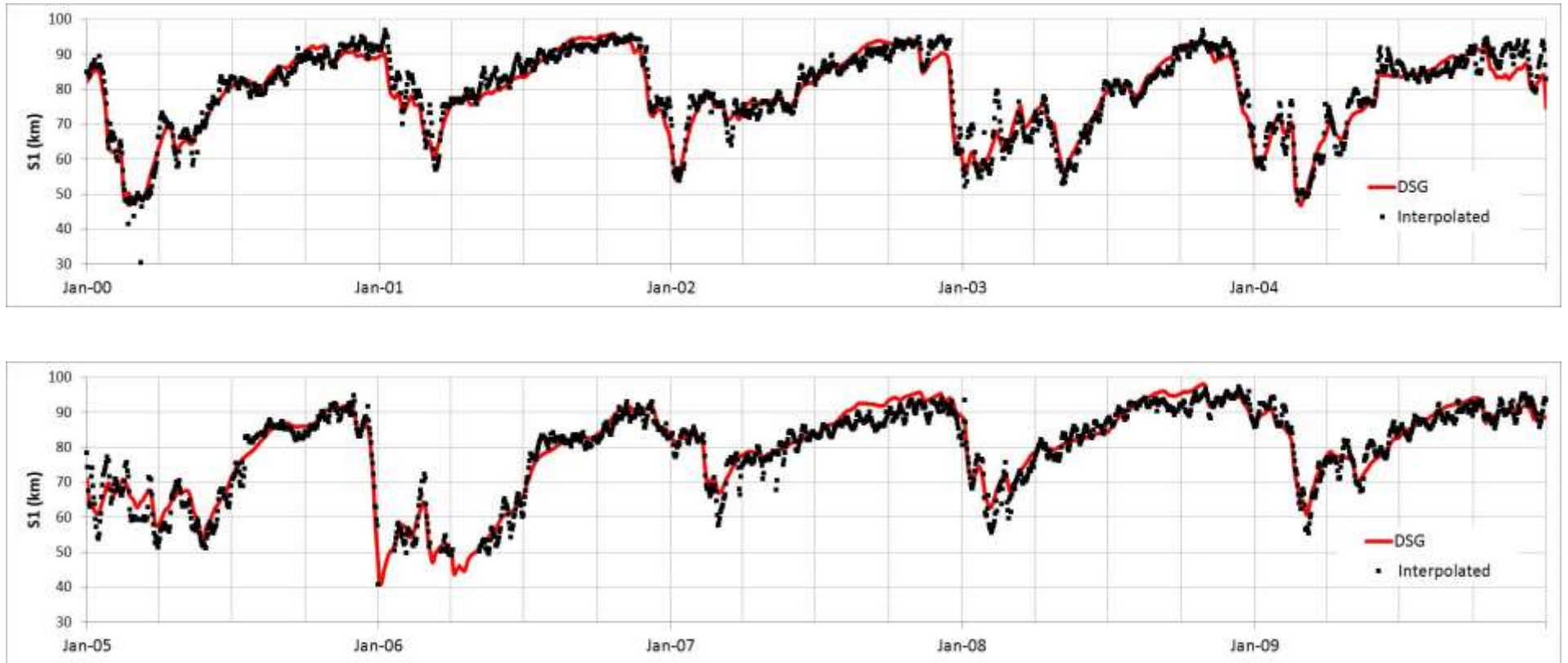


Figure 4-13: Time Series of DSG Predicted and Sacramento River Branch Interpolated 1 ppt Surface Isohaline Position: 2000-2009

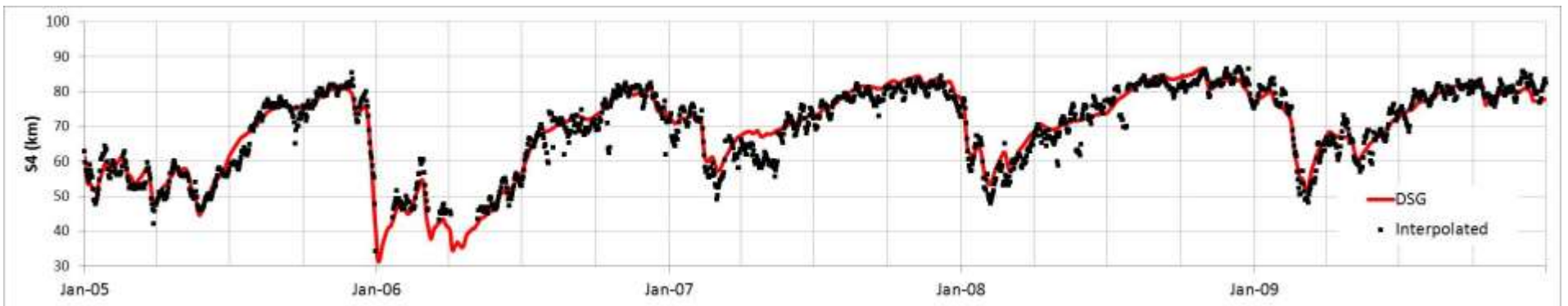
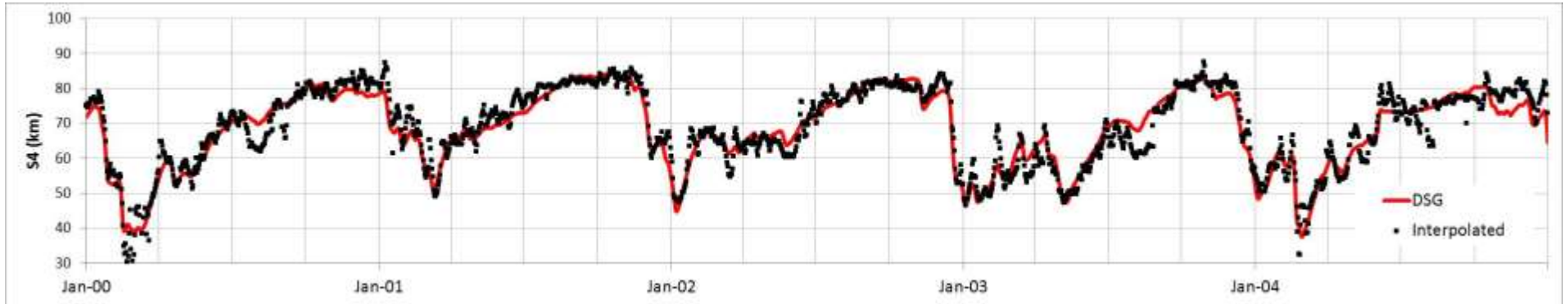


Figure 4-14: Time Series of DSG Predicted and Sacramento River Branch Interpolated 4 ppt Surface Isohaline Position: 2000-2009

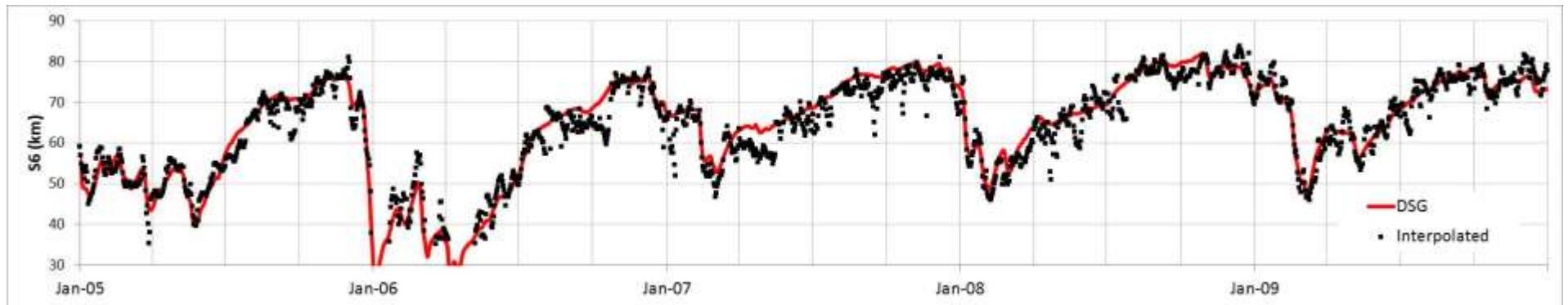
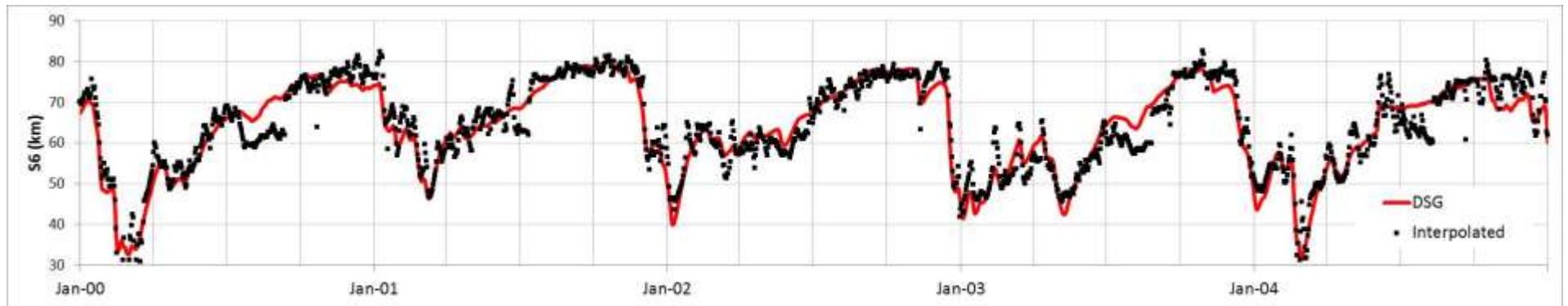


Figure 4-15: Time Series of DSG Predicted and Sacramento River Branch Interpolated 6 ppt Surface Isohaline Position: 2000-2009

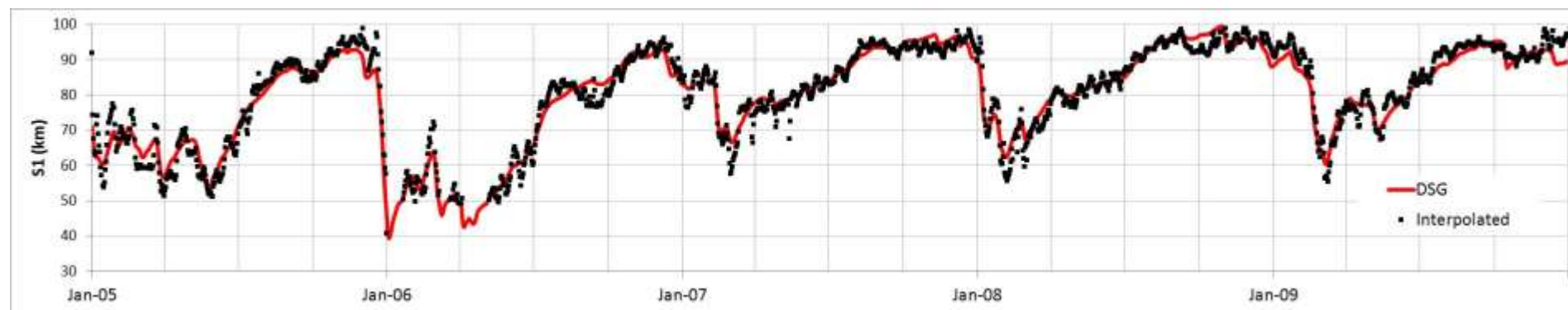
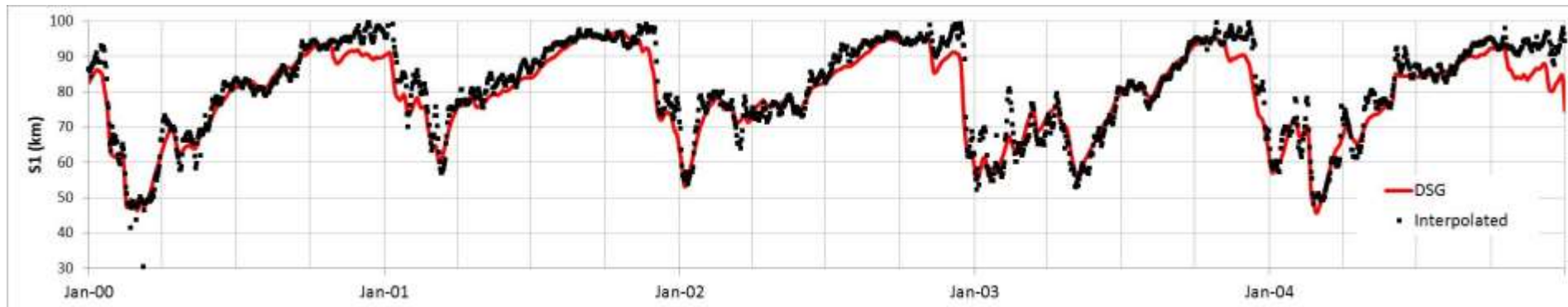


Figure 4-16: Time Series of DSG Predicted and San Joaquin River Branch Interpolated 1 ppt Surface Isohaline Position: 2000-2009

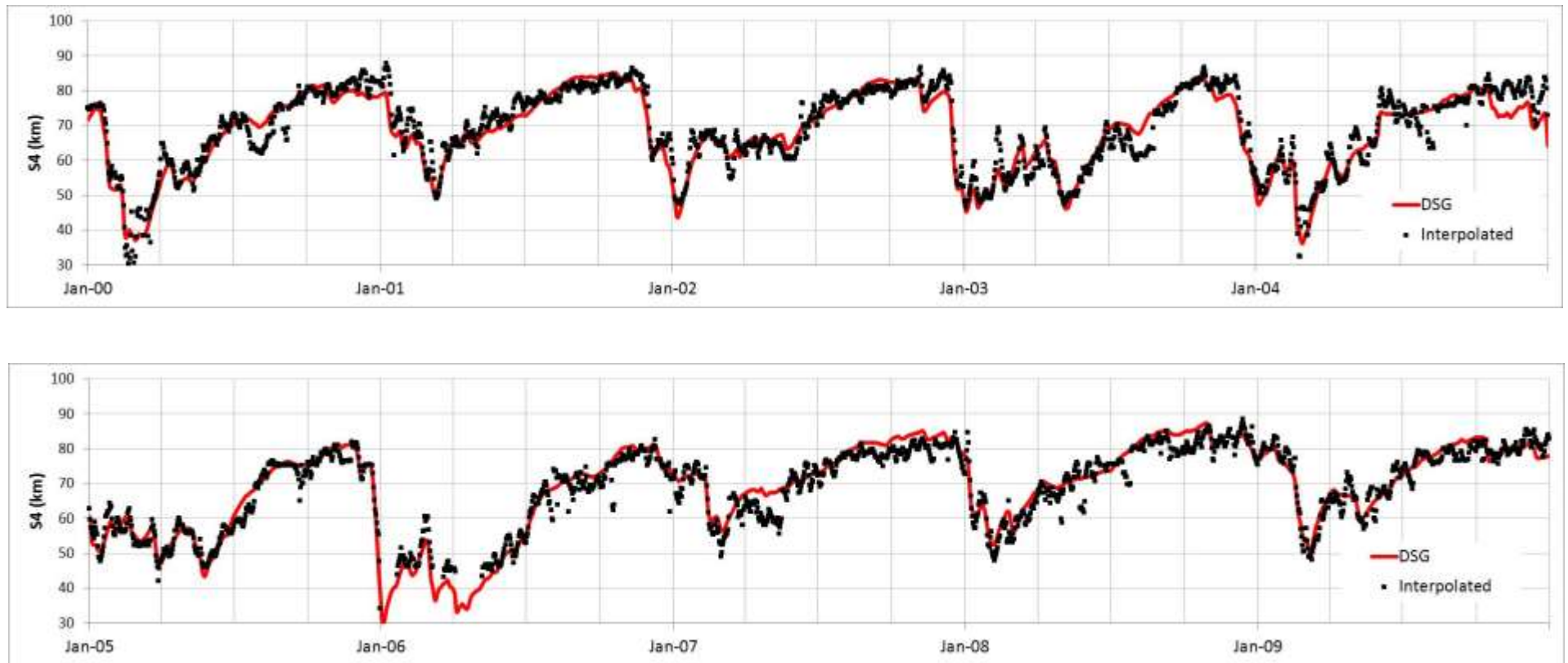


Figure 4-17: Time Series of DSG Predicted and San Joaquin River Branch Interpolated 4 ppt Surface Isohaline Position: 2000-2009

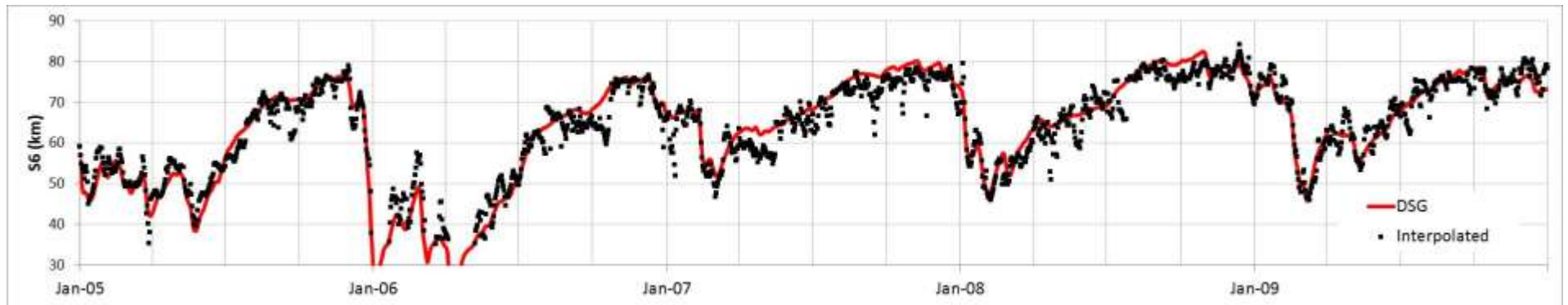
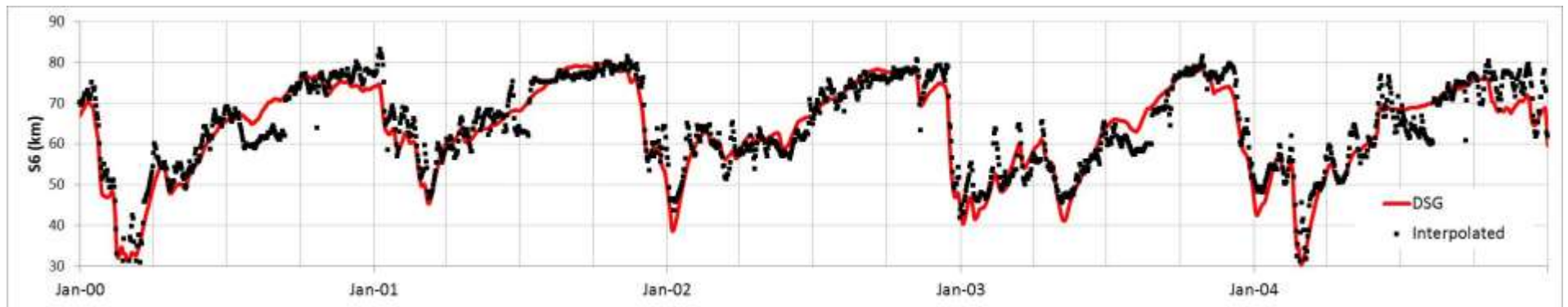


Figure 4-18: Time Series of DSG Predicted and San Joaquin River Branch Interpolated 6 ppt Surface Isohaline Position: 2000-2009

5. Analysis

The preceding chapters demonstrate the robustness of the DSG model in representing the subtidal salinity structure of the Bay-Delta estuary. The model effectively predicts the daily average position of X2 as well as other isohalines as a function of antecedent outflow over a nine decade period of record. It is particularly noteworthy that the formulation allows for X2 predictions during periods when Delta outflow is less than zero, a condition that occurred frequently in the early part of the historical record. The model also effectively predicts daily average salinity at fixed locations along the estuary. The DSG model relies on the specification of five empirically-determined constants to produce isohaline and salinity estimates.

This chapter extends the analysis of the DSG model beyond the issues of calibration and validation by first evaluating the model's sensitivity to model parameters. Next, a cursory comparison of the DSG and G models is provided. This chapter then explores the use of interpolated X2 values (rather than values predicted from antecedent outflow) to estimate salinity. This exercise, which provides insight into model uncertainty given "perfect" knowledge of X2 position, highlights the sensitivity of fixed location salinity predictions to X2 predictions. Finally, the ramifications of the DSG model's characterization of longitudinal salinity gradient are explored, considering issues such as value and location of maximum gradient and quantification of dispersion coefficient.

5.1 Analysis of Sensitivity

The sensitivity of DSG salinity predictions to calibrated model parameters was explored through a simple perturbation analysis. Each of the five DSG model parameters was perturbed +10% and -10%, and 2000-09 period average salinity was predicted at five locations along the Sacramento River branch and compared with baseline predictions. The analysis, summarized in [Table 5-1](#), clearly shows that the DSG model is highly sensitive to the parameters associated with the X2 prediction, i.e. Φ_1 and Φ_2 and is relatively insensitive to the β parameter. Model sensitivity to the δ term is greater at more downstream locations.

Table 5-1. DSG Model Parameter Sensitivity Analysis:
Perturbation by Plus & Minus Ten Percent

X (km)	Difference with Baseline (%)									
	β		Φ ₁		Φ ₂		γ		δ	
	-10%	+10%	-10%	+10%	-10%	+10%	-10%	+10%	-10%	+10%
54	0.4%	-0.4%	-27.8%	26.1%	55.4%	-47.9%	-5.4%	5.0%	-36.7%	40.9%
64	0.7%	-0.7%	-40.9%	43.4%	95.4%	-62.9%	-4.4%	4.0%	-31.4%	32.1%
75	1.5%	-1.4%	-58.2%	80.0%	185.1%	-77.0%	-2.8%	2.5%	-20.8%	18.9%
81	2.0%	-1.9%	-66.3%	113.2%	272.8%	-81.1%	-1.5%	1.4%	-11.6%	10.1%
92	2.9%	-2.8%	-64.2%	193.7%	526.6%	-69.9%	1.2%	-1.1%	12.0%	-6.4%

5.2 Comparison with G-Model Estimates

The DSG model, as calibrated for the Sacramento River branch, was compared with the G-Model (Denton 1993). The first comparison was with the empirically-determined α parameter reported by Denton and Sullivan (1993). To accomplish this comparison, the calibrated values for Φ_1 and Φ_2 were substituted into Equation (2.8) yielding:

$$\alpha(X) = -\ln\left(\frac{2.64 - S_b}{S_o - S_b}\right) * \left(\frac{X}{457}\right)^{5.181} \dots \dots \dots (5.1)$$

By substituting values for X, S_o and S_b as assumed by Denton and Sullivan (1993), α was computed from Equation (5.1) and shown in Table 5-2. Differences between α estimates range from 8% (at Collinsville) to 16% (at Chipps Island). Note that the DSG model assumes that the parameter $\beta = 475$ cfs-years for all values of X, while the G-model for Port Chicago assumes a smaller value of 400 cfs-years.

A second comparison was made with the S_o parameter. Denton and Sullivan (1993) report a range of S_o values between 31-36 mS/cm for the locations listed in Table 5-2. The DSG model produces S_o values that range between 20.7-34.4 mS/cm for antecedent outflows ranging between 30,000 cfs and 3000 cfs (equivalent to an X2 range of 62.5-97.5 km per the DSG model).

Table 5-2. Comparison of α Parameter Values Produced by the DSG and G Models

Location	Parameters per Denton & Sullivan (1993)					α per DSG Model ($\text{cfs}^{-1} \times 10^{-4}$)
	X (km)	α ($\text{cfs}^{-1} \times 10^{-4}$)	B (cfs-years)	S_o (mS/cm)	S_b (mS/cm)	
Port Chicago	64	1.05	400	31	0.17	0.95
Chippis Island	74	2.5	475	36	0.18	2.1
Collinsville	81	3.6	475	32	0.15	3.3

As a third and final comparison, the trace of salinity as a function of antecedent outflow was produced for the Collinsville location using the DSG and G models. The trace is compared with observed salinity data for the 2000-09 period in [Figure 5-1](#) and for the 1930-39 period in [Figure 5-2](#). One observation common to both graphs is that the DSG model consistently predicts higher salinity than the G model at Collinsville. The graphs also suggest a change in the estuary's salinity regime over time, i.e. the estuary is getting saltier in the vicinity of Collinsville for the same level of outflow. This important observation, while intuitively consistent with known changes in the estuary (e.g. sea level rise and bathymetric changes), was not explored further in this work.

5.3 DSG Salinity Estimates Using Interpolated X2 Values

DSG model performance was explored further by using interpolated X2 values (rather than values predicted from antecedent outflow) to estimate salinity. This exercise, which was performed over the model calibration period 2000-2009 as a proof of concept, provides insight into model uncertainty given “perfect” knowledge of X2 position. Extending this analysis to other periods could assist in identifying limitations in the current formulation and/or calibration, as well as demonstrate the value of improving models to estimate X2 position.

DSG salinity predictions are compared with observed data as time series in Appendix F (see [Figures F-1 through F-8](#)) at each location. Measures of DSG model variance and bias with observed salinity data are provided for each location in [Table 5-3](#). This exercise suggests that, if X2 is known or can be predicted with a high level of confidence, salinity can also be predicted with a high level of confidence throughout the range of the low salinity zone. Predictions at Jersey Point are the weakest among all tested, with some under-prediction bias and the highest coefficient of variation.

Table 5-3. Performance of DSG Salinity Predictions Using Interpolated X2 Values:
2000-09 Predicted = C1 + C2 * Observed

Station	Standard Error (mS/cm)	Coefficient of Variation	C1	C2	R2
Martinez	1.7	0.10	0.4	0.97	0.96
Port Chicago	2.4	0.23	0.9	1.0	0.92
Mallard Island	0.8	0.14	-0.0	0.94	0.98
Collinsville	0.6	0.20	0.1	0.89	0.97
Emmaton	0.3	0.19	0.1	0.90	0.98
Pittsburg	1.0	0.23	0.0	1.1	0.95
Antioch	0.4	0.19	-0.1	1.1	0.97
Jersey Point	0.2	0.28	-0.1	0.93	0.92

5.4 Analysis of Salinity Gradient

A rudimentary analysis of the salinity gradient, as characterized by the DSG model, was conducted and is summarized here. The longitudinal salinity gradient $\frac{\partial s}{\partial x}$ defined in [Equation \(2.12\)](#) is presented as a function of longitudinal distance (X) and X2 position in [Figure 5-3](#). This figure shows that, under a typical range of hydrology (X2 between 60-90 km), the function is convex with larger absolute values within the low salinity zone and smaller values near the downstream and upstream boundaries of the estuary.

The location of the maximum (absolute value) salinity gradient (X*) was defined by setting the first derivative of [Equation \(2.12\)](#) equal to zero, resulting in the following relationship:

$$X^* = \left(\frac{1+\Phi_2}{-\tau} \right)^{-\Phi_2} * X2 \dots\dots\dots (5.2)$$

Figure 5-4 plots the location of the maximum salinity gradient (X^*) as a function of $X2$. The graph illustrates that X^* increases with increasing $X2$ in an approximately linear manner and is roughly 10 to 20 km downstream of the $X2$ location. The figure also plots the associated value of the maximum salinity gradient as a function of $X2$.

5.5 Analysis of Dispersion Coefficients

The tidally-averaged advection-dispersion equation for salinity transport, assuming a one-dimensional estuary and steady state conditions, is given by:

$$\frac{-Q}{A(X)} * S = K_x * \frac{\partial S}{\partial X} \dots\dots\dots (5.3)$$

where $A(X)$ is the cross-sectional area at longitudinal location X , K_x is the longitudinal dispersion coefficient (in dimensional units of L^2/T), with other terms previously defined. The dispersion coefficient is used in one-dimensional constituent transport models such as DSM2 to parameterize a variety of physical mechanisms and is therefore an important quantity to estimate. The DSG model provides a method for estimating appropriate values of K_x , given known values for the longitudinal salinity gradient - see Equation (2.12) - and cross-sectional area.

By assuming $S \gg S_b$, substituting antecedent outflow (G) for Q and representing S and $\frac{\partial S}{\partial X}$ by Equations (2.1) and (2.12) respectively, Equation (5.3) can be re-written as follows:

$$K_x = \frac{-\Phi_2 * X}{A(X) * \alpha} \dots\dots\dots (5.4)$$

The above equation is dimensionally correct, as Φ_2 is dimensionless and α - see Equation (2.8) - has the dimensions of T/L^3 . However, the DSG model as described herein was calibrated in mixed English and metric units and does not directly allow for a correct evaluation of K_x . To address this issue of inconsistent units, Equation (2.4) was recalibrated with $X2$ in units of meters (rather than kilometers) and G in units of m^3/sec (rather than cfs), resulting in $\Phi_1 = 2.30 \times 10^5 \text{ sec}/m^2$ and $\Phi_2 = -0.193$ (unchanged).

Substituting Equation (2.8) into Equation (5.4) yields:

$$K_x = \frac{\Phi_1^{-\frac{1}{\Phi_2}} * \Phi_2 * X^{1+\frac{1}{\Phi_2}}}{A(X) * \tau} \dots \dots \dots (5.5)$$

where X is also in meters. Note that since τ varies with S_o , and S_o varies with X^2 (and therefore outflow), K_x varies with outflow as well as with longitudinal distance along the estuary. However, the DSG model suggests that the sensitivity of K_x to outflow is small, as τ does not vary greatly with flow (e.g $\tau = -2.64$ for $G = 3000$ cfs and $\tau = -2.13$ for $G = 30,000$ cfs).

The resulting range of dispersion coefficients were evaluated assuming values of $A(X)$ from Peterson et al. (1975) and a range of outflows, resulting in values shown in Figure 5-5. According to this analysis, values in Suisun Bay (X ranging from 60 to 80 km) are approximately 150 to 300 m^2/sec , compared with the value of 200 m^2/sec typically cited for estuaries (Fischer et al. 1979).

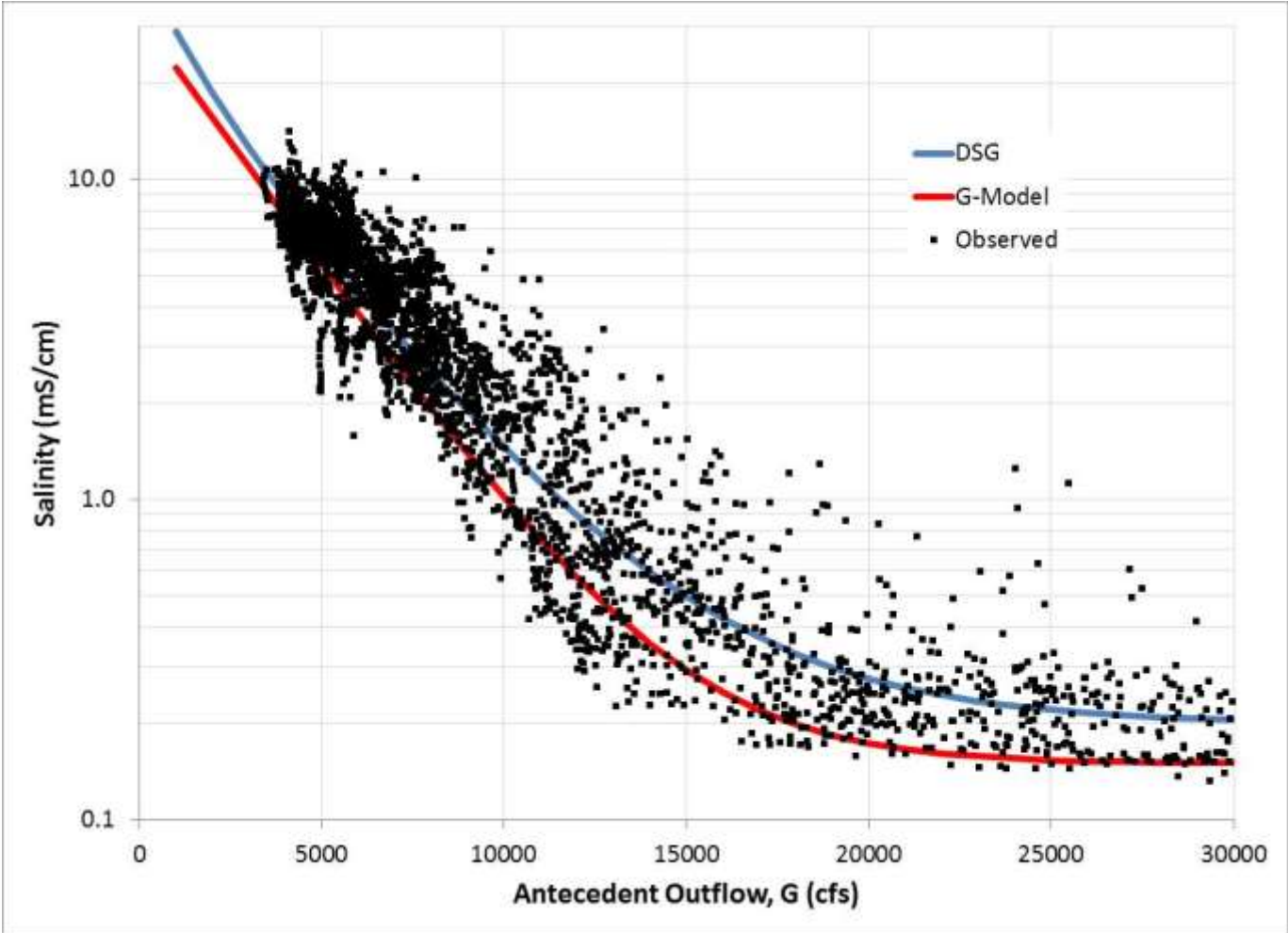


Figure 5-1. DSG and G-Model Predicted Salinity at Collinsville as a Function of Antecedent Outflow: Comparison with Observed Data for 2000-09

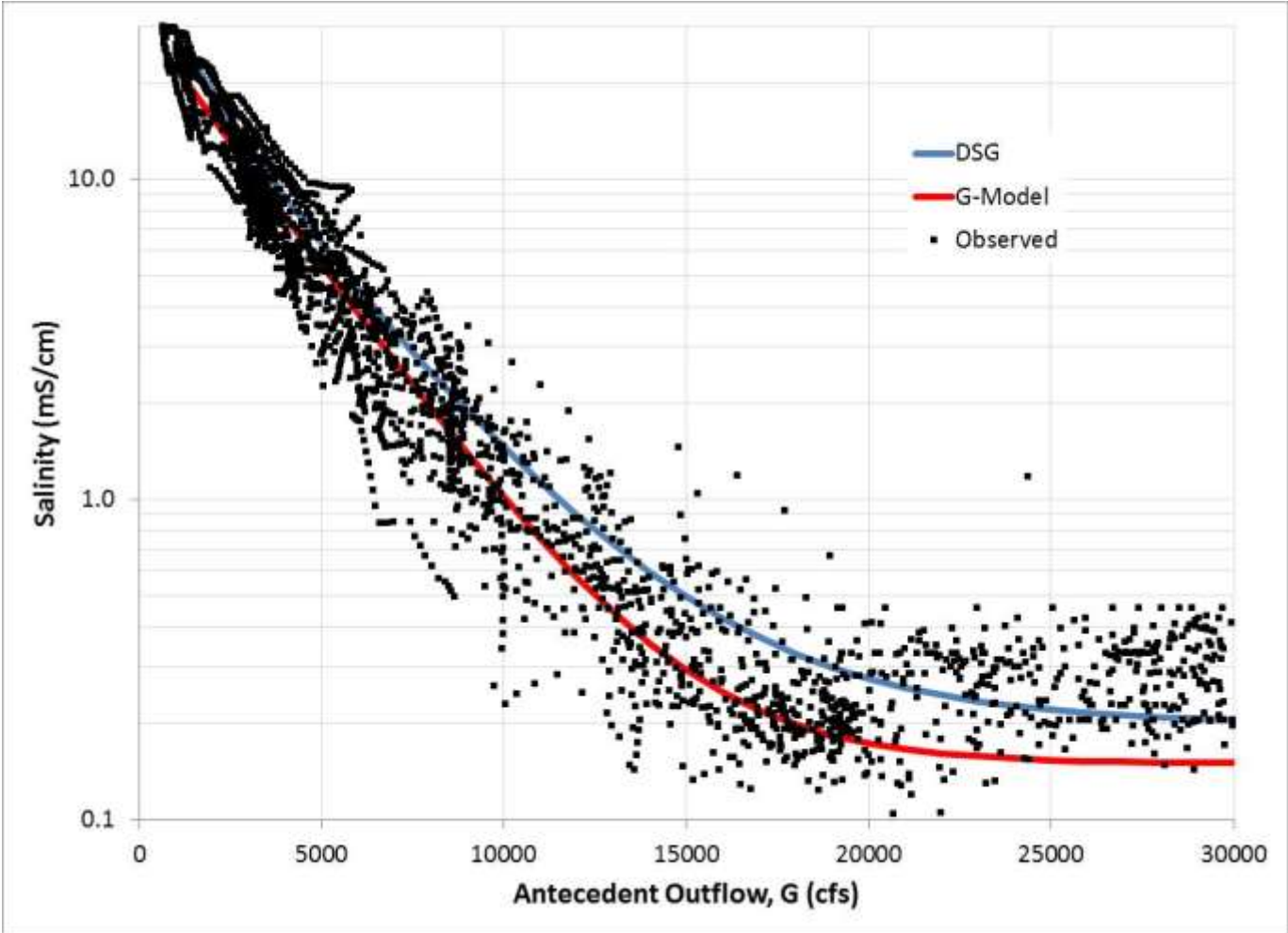


Figure 5-2. DSG and G-Model Predicted Salinity at Collinsville as a Function of Antecedent Outflow: Comparison with Observed Data for 1930-39

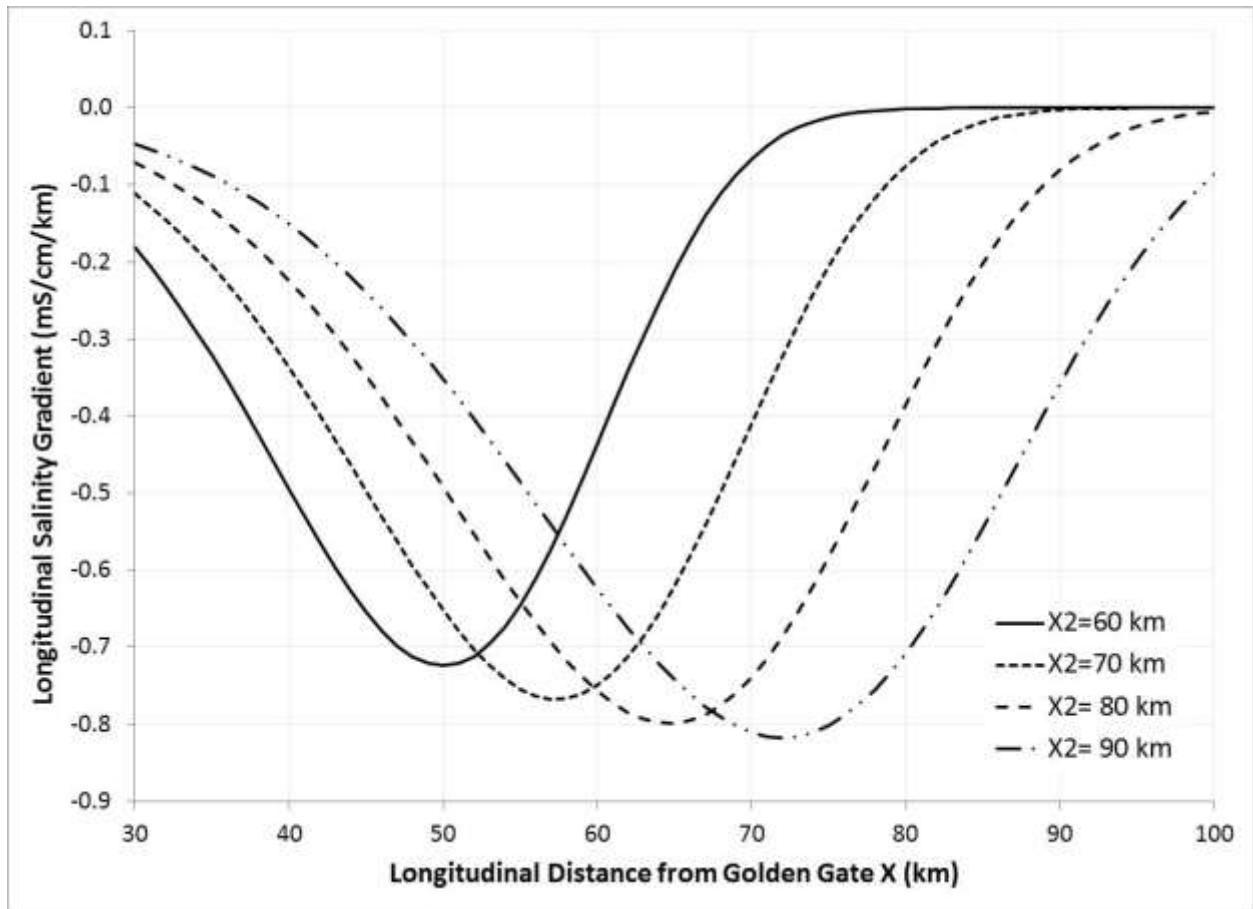


Figure 5-3: Longitudinal Salinity Gradient as a Function of Distance from Golden Gate and X2 Position

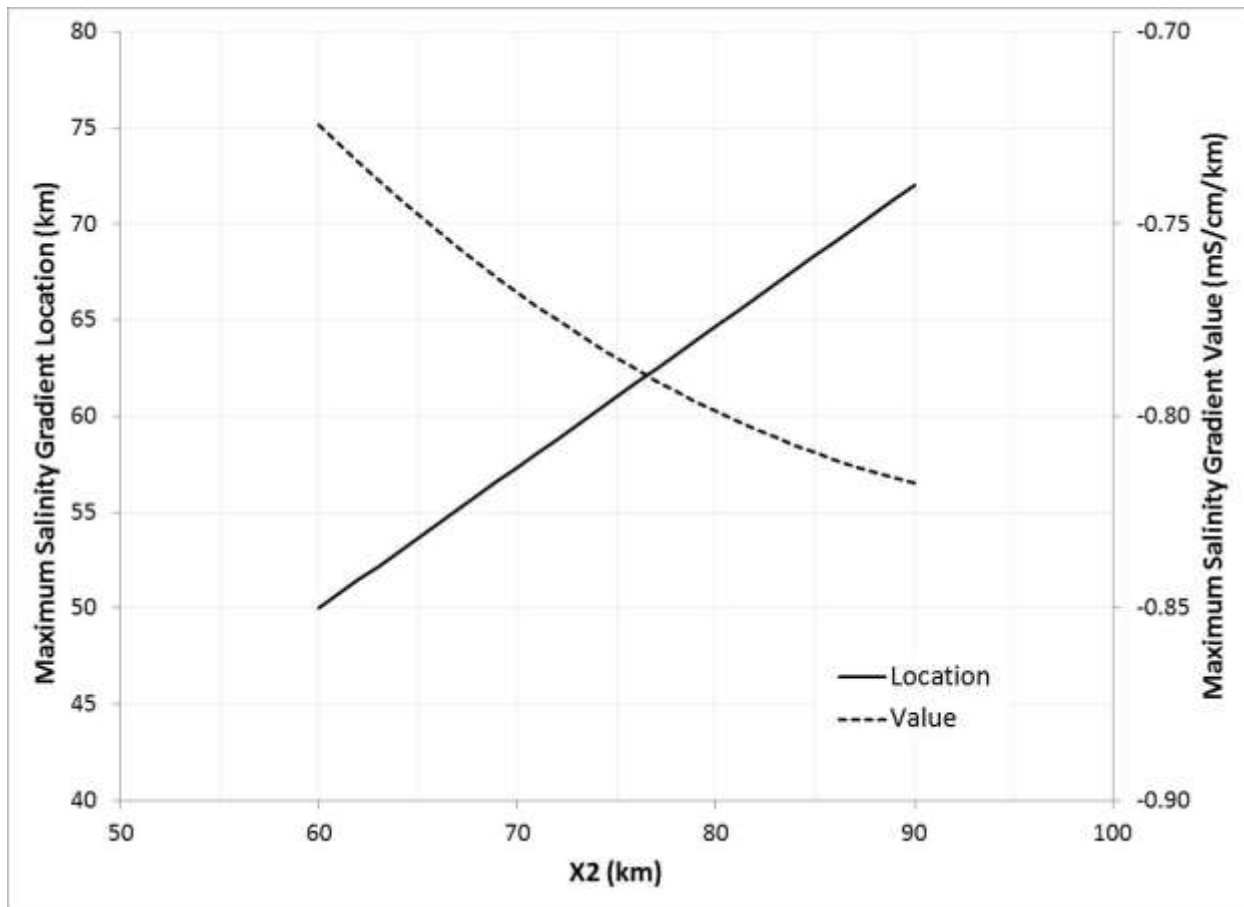


Figure 5-4: Location and Value of Maximum Longitudinal Salinity Gradient as a Function of X2

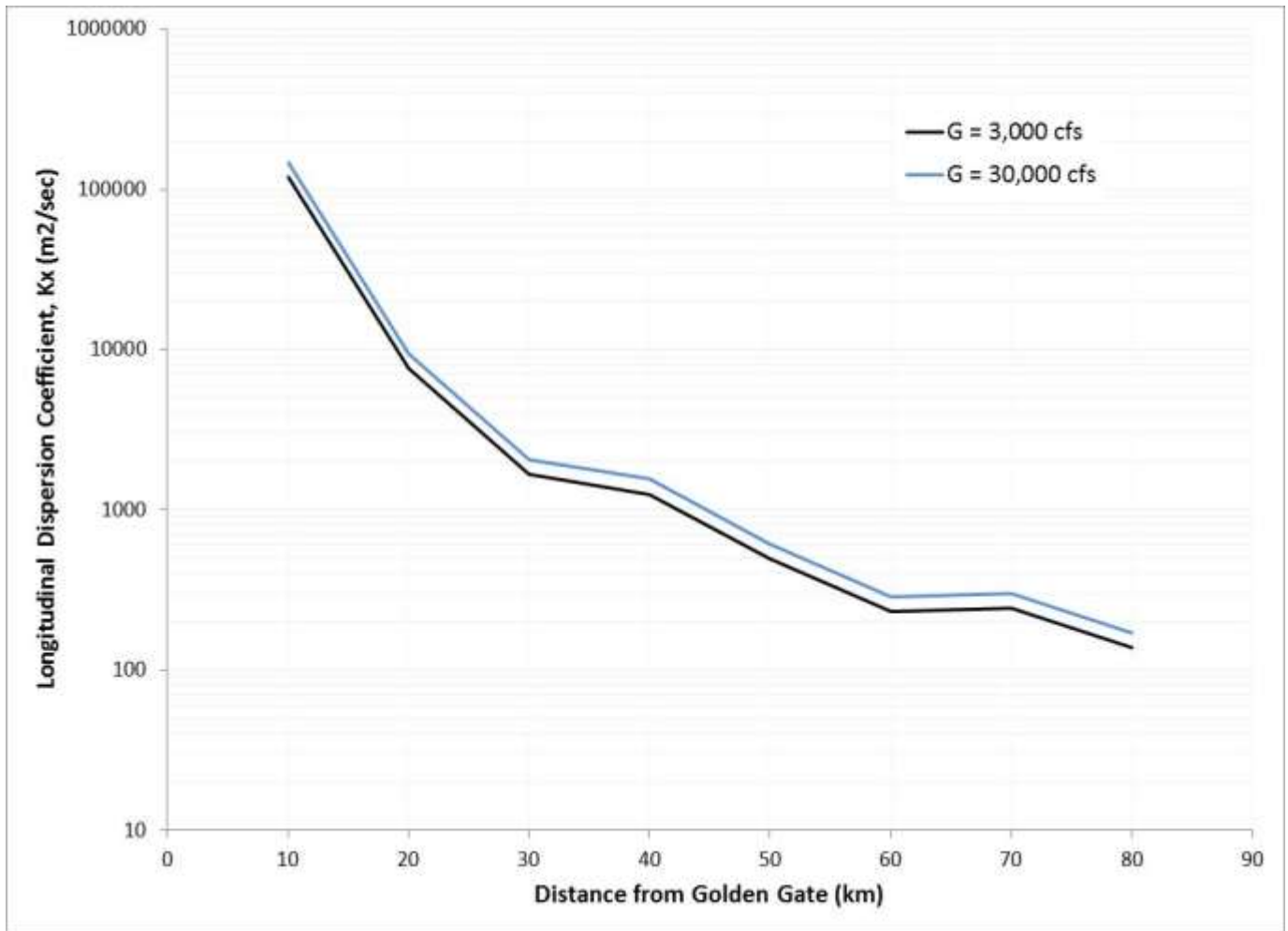


Figure 5-5. DSG-Predicted Longitudinal Dispersion Coefficient as a Function of Distance along the Estuary

6. Discussion & Next Steps

This chapter provides a brief discussion on the potential utility of the DSG model. The chapter concludes by suggesting areas of future work.

6.1 Discussion

The DSG model integrates the Eulerian modeling approach of Denton (1993) – focused on a fixed location - and the Lagrangian modeling approach of Monismith et al. (2002) – focused on a fixed salinity – to produce a parsimonious method of estimating X2 and other isohaline positions as well as salinity at fixed locations in the estuary. The formulation allows for prediction of X2 position under sustained low outflow conditions when Delta outflow falls below zero, a condition that occurs frequently under pre-Shasta conditions in the early part of the available salinity record. The model’s ability to predict X2 under extremely low outflow conditions makes it a viable tool for evaluating “without-Project” scenarios with current level Delta hydrology unimpaired for upstream reservoir operations. No currently available salinity models, neither statically-based nor physically-based, are calibrated to simulate such conditions. The DSG model’s ability to evaluate multiple isohaline positions provides a simple approach to quantify the range of the low salinity zone, thereby allowing broader understanding of the relationship between X2 position and the range of the low salinity zone. Finally, the DSG model’s ability to quantify the estuary’s longitudinal salinity gradient provides a rational method for evaluating the specification of dispersion coefficients and the calibration of one-dimensional salinity transport models.

Given historically-observed sea level rise and known changes to channel bathymetry, it is reasonable to assume that the estuary’s flow-salinity regime has changed over the period of record. The DSG model analysis presented in this report does not conclusively reveal such a temporal trend. Noise associated with the salinity and isohaline data may be sufficiently high to mask changes to the estuary’s flow-salinity regime over time.

6.2 Next Steps

Using the DSG model to predict location-specific salinity with interpolated X2 values (rather than X2 values predicted from antecedent outflow), as demonstrated in Chapter 5, produces very accurate estimates. This finding demonstrates the critical importance of the X2 prediction in the model's ability to predict the estuary's salinity structure and suggests that refinements to the X2 prediction should be given highest priority in any subsequent model refinement. Some potential high-priority model refinements are listed below:

- The existing X2 formulation could be refined to include a tidal term. Tides are known to have a significant influence on salinity, particularly under low flow conditions, and are a critical component of more sophisticated hydrodynamic models. Tidal terms have been proposed by others as part of simplified empirical salinity models (Denton and Sullivan 1993; Morel-Seytoux 1999, Morel-Seytoux 2002).
- Re-calibrating the existing X2 formulation (i.e. Equation 2.4) in a piece-wise manner could be explored. Visual inspection of Figure 4-1 suggests that the current calibration tends to underestimate X2 position in the range of 75-85 km, a range critical for water quality compliance in the estuary. As with any piece-wise model implementation, special care will need to be taken at the interface of the segments. In the extreme case, the calibration data could be limited to the lower flow periods, thereby providing a better fit for these conditions at the expense of the higher flow periods. To improve the robustness of the X2 prediction under extremely low outflow conditions, the calibration data set could be expanded to include low-flow observations from the 1920s and 1930s.
- The existing X2 formulation could be refined to include a QWEST term, thereby accounting for known effects of Delta cross channel operations and in-Delta diversions and exports on salinity in the lower Sacramento and San Joaquin Rivers upstream of the confluence. Denton (2006) has explored the use of a QWEST term in refinements to the G model at upstream locations.
- The existing DSG formulation could be refined to increase the degrees of freedom associated with Equation 2.1 through the addition of another variable, i.e. G^n . Denton (1994) observed that a simple exponential relationship does not have sufficient flexibility to fit the salinity data over the full range of outflows and proposed such a modification to the G model. Although not presented in this report, the current DSG

formulation does not appear to reliably predict salinity at locations downstream of Martinez and could benefit from such a modification.

- Artificial neural networks (ANNs) could be incorporated into the DSG model to provide estimates of X2 position and other DSG model parameters as functions of multiple hydrologic and hydrodynamic inputs. Metropolitan Water District has been pursuing the use of ANNs to predict isohaline position and salinity in Suisun Bay and the western Delta (Chen et al. 2014). Work completed to date, as well as ongoing work, explores the use of the general DSG formulation to constrain ANN predictions, with the goal of minimizing extrapolation problems that must be addressed when developing ANN-based models. This work also explores the use of tidal terms to predict salinity more precisely on a daily basis.

7. References

California Data Exchange Center (CDEC) (2013). Salinity data available online at: <http://cdec.water.ca.gov>

California Department of Public Works (CDPW) (1924-55). Report of the Sacramento-San Joaquin Water Supervisor for the Period 1924-1954, Bulletin 23.

California Department of Public Works (CDPW) (1931). Variation and Control of Salinity in Sacramento-San Joaquin Delta and Upper San Francisco Bay, Bulletin 27.

California Department of Water Resources (CDWR) (1956-62). Report of the Sacramento-San Joaquin Water Supervisor for the Period 1955-1961, Bulletin 23.

California Department of Water Resources (CDWR) (1957). Joint Hydrology Study: Sacramento River and Sacramento-San Joaquin River Delta, Division of Planning, July.

California Department of Water Resources (CDWR) (1962). Hydrologic Data for 1962, Bulletin 65.

California Department of Water Resources (CDWR) (1963-71). Hydrologic Data for the Period 1963-1971, Bulletin 130.

California Department of Water Resources (CDWR) (2014). DAYFLOW model data available online at: <http://www.water.ca.gov/dayflow/>

Chen, L., Rath, J.S. and Roy, S.B. (2014). Modeling Salinity in Suisun Bay and the Western Delta Using Artificial Neural Networks, Prepared for Metropolitan Water District of Southern California, Tetra Tech Inc., April 18.

Denton, R.A. (1993). Accounting for Antecedent Conditions in Seawater Intrusion Modeling – Applications for the San Francisco Bay-Delta, Proceedings of the 1993 Hydraulic Division National Conference, American Society of Civil Engineers, San Francisco, Calif., H.W. Shen, Ed. 821-826.

Denton, R.A. and Sullivan, G.D. (1993). Antecedent flow-salinity relations: Application to Delta Planning Models, CCWD Technical Memorandum.

Denton, R.A. (2006). Refining CCWD's Salinity-Outflow Model, Presentation to DSM2 Users Group Meeting, Sacramento, April 25.

Fischer, H.B., List, E.J., Imberger, J., Koh, C.Y. and Brooks, N.H. (1979). Mixing in Inland and Coastal Waters, Academic Press, 483 pp.

Harder, J.A. (1977). Predicting estuarine salinity from river inflows, Journal of the Hydraulics Division, Proceedings of the American Society of Civil Engineers, Vol. 103, No. HY8, August, pp. 877-888.

Hutton, P.H. (2011). Declaration in Support of Plaintiffs' Motion for Injunctive Relief, U.S. District Court Case 1:09-cv-00407-OWW-DLB, Document 927-2, filed June 20.

Hutton, P. (2013). A new empirical Bay-Delta salinity model, presented at the Calif. Water & Environmental Modeling Forum Annual Meeting, Folsom, Calif., April 24, available online at: <http://www.cwemf.org/>

Jassby, A. D., Kimmerer, W.J., Monismith, S.G., Armor, C., Cloern, J.E., Powell, T.M., Schubel, J.R. and Vendlinski, T.J. (1995). Isohaline position as a habitat indicator for estuarine populations. Ecological Applications, 5: 272–289.

Monismith, S. G., Kimmerer, W., Burau, J. R., & Stacey, M. T. (2002). Structure and flow-induced variability of the subtidal salinity field in northern San Francisco Bay. Journal of Physical Oceanography, 32(11), 3003–3019.

Morel-Seytoux, H.J. (1999). Relationship between flows into the Sacramento-San Joaquin Delta Estuary and salinity intrusion into the Delta, Report to the U.S. Bureau of Reclamation, September 9.

Morel-Seytoux, H.J. (2002). Basic description and results of the H-model for salt movement in the Delta, Report to the U.S. Bureau of Reclamation, June 12.

Peterson, D.H., Conomos, T.J., Broenkow, W.W. and Doherty, P.C. (1975). Location of the non-tidal current null zone in northern San Francisco Bay, *Estuarine and Coastal Marine Science*, 3, 1-11.

Roy, S.B., Rath, J., Chen, L., Unga, M.J. and Guerrero, M. (2014). *Salinity Trends in Suisun Bay and the Western Delta (October 1921 – September 2012)*, Prepared for the San Luis and Delta Mendota Water Authority and State Water Contractors, Tetra Tech Inc., January 16.

Schemel, L. (2001). Simplified Conversions Between Specific Conductance and Salinity Units for Use with Data from Monitoring Stations, IEP Newsletter, Volume 14, No. 1.

Appendix A: Time Series & Scatter Plots – DSG Model Calibration & Validation with DSM2 Data

This appendix provides time series and scatter plots comparing DSG and DSM2 estimates of isohaline position and salinity at the following locations for the 2000-09 calibration period and the 1990-99 validation period: Martinez, Port Chicago, Mallard Island, Collinsville, Emmaton, Pittsburg, Antioch and Jersey Point.

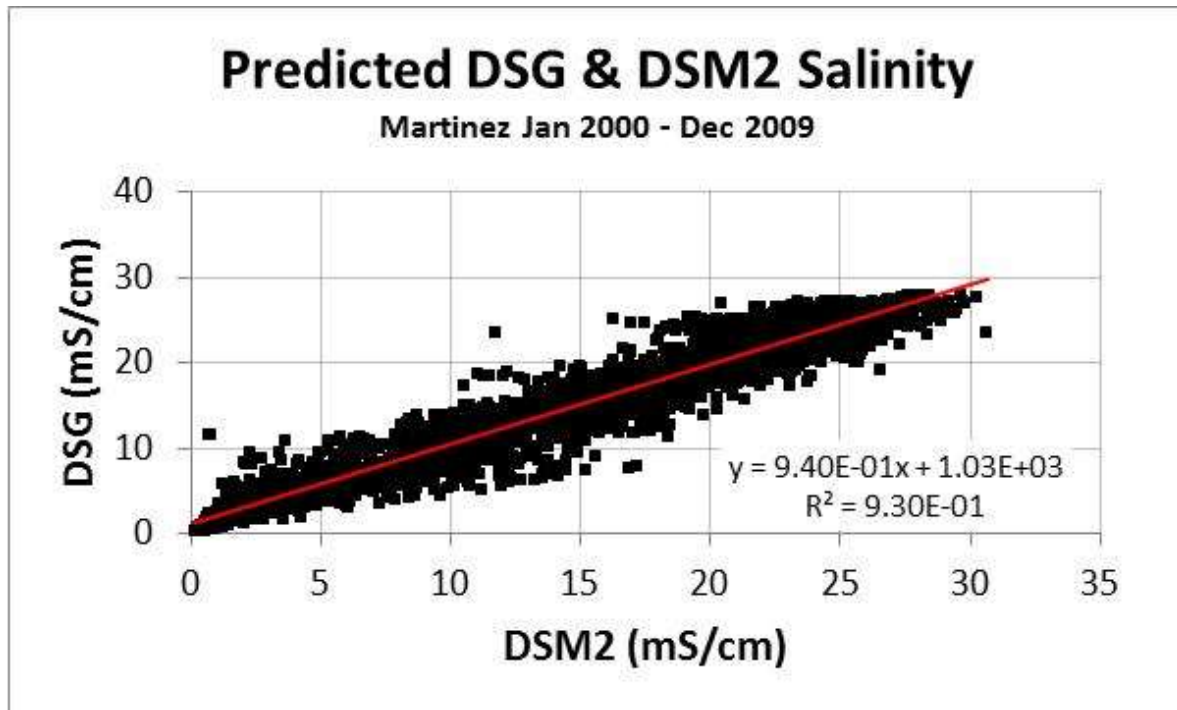


Figure A-1: DSG Predicted vs. DSM Surface Salinity at Martinez: 2000-2009

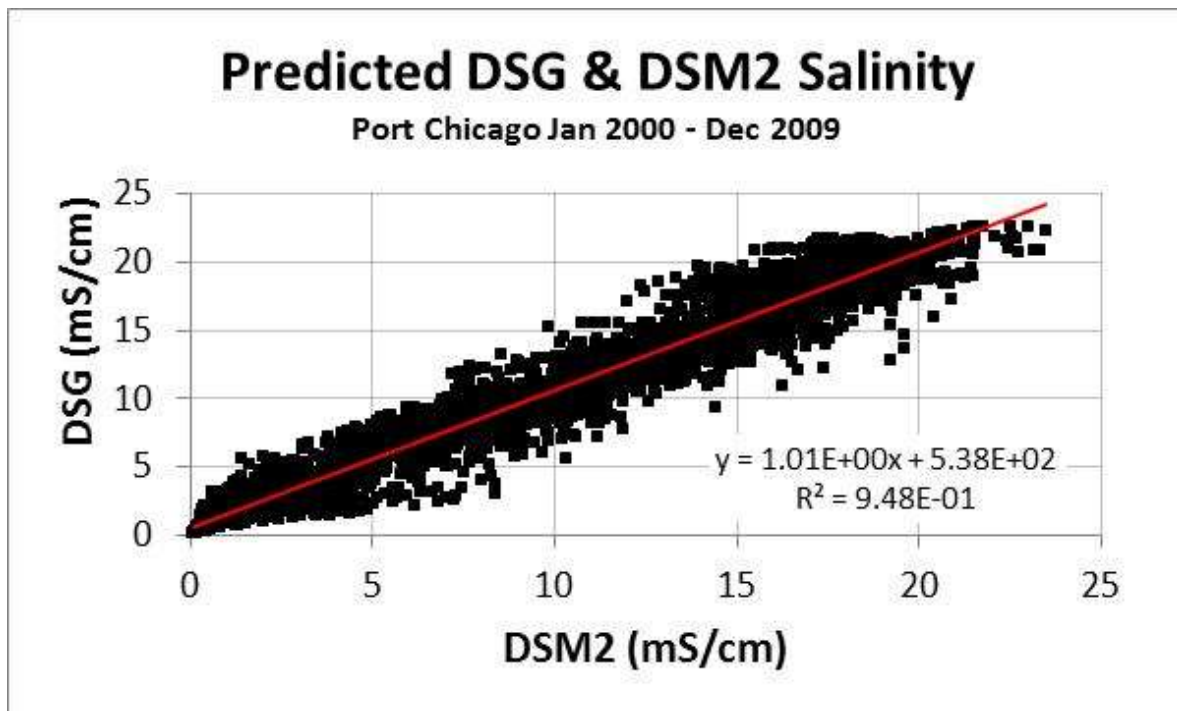


Figure A-2: DSG Predicted vs. DSM Surface Salinity at Port Chicago: 2000-2009

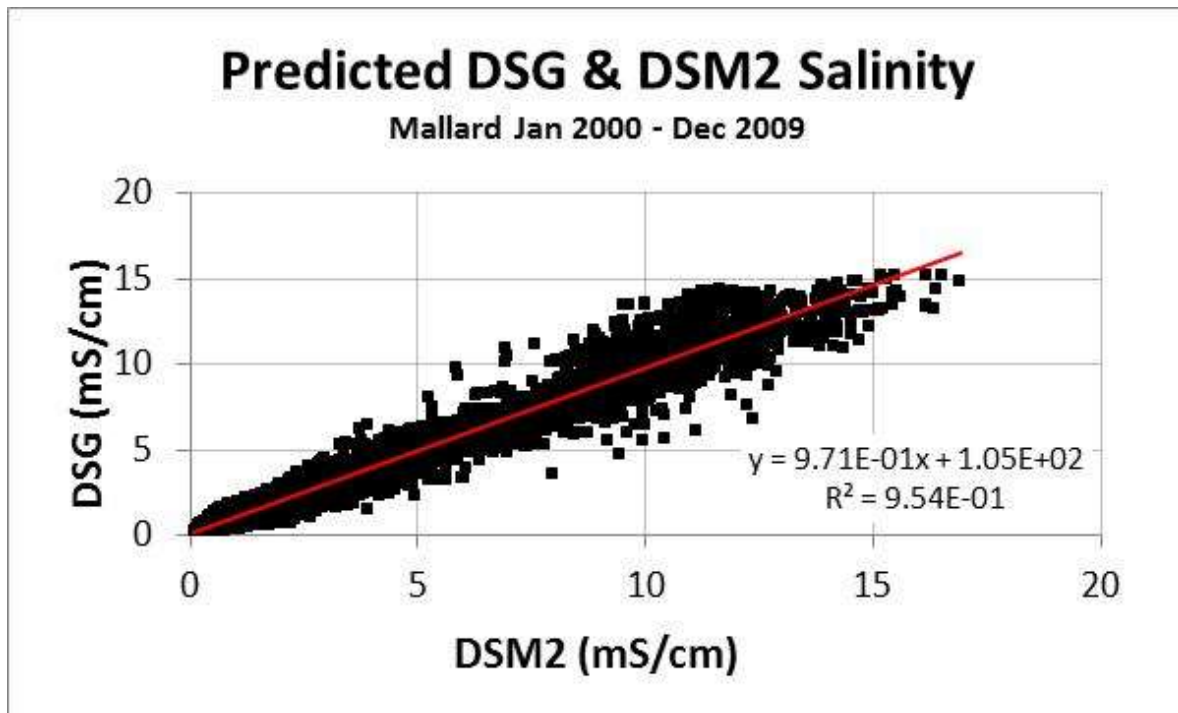


Figure A-3: DSG Predicted vs. DSM Surface Salinity at Mallard Island: 2000-2009

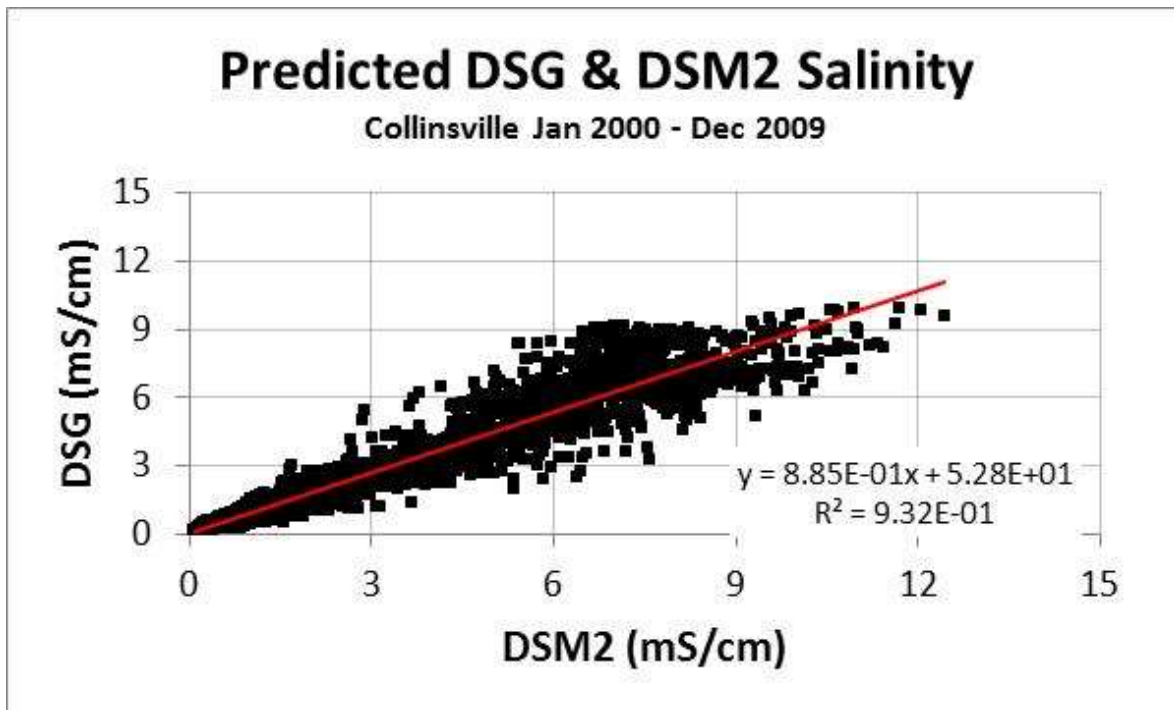


Figure A-4: DSG Predicted vs. DSM Surface Salinity at Collinsville: 2000-2009

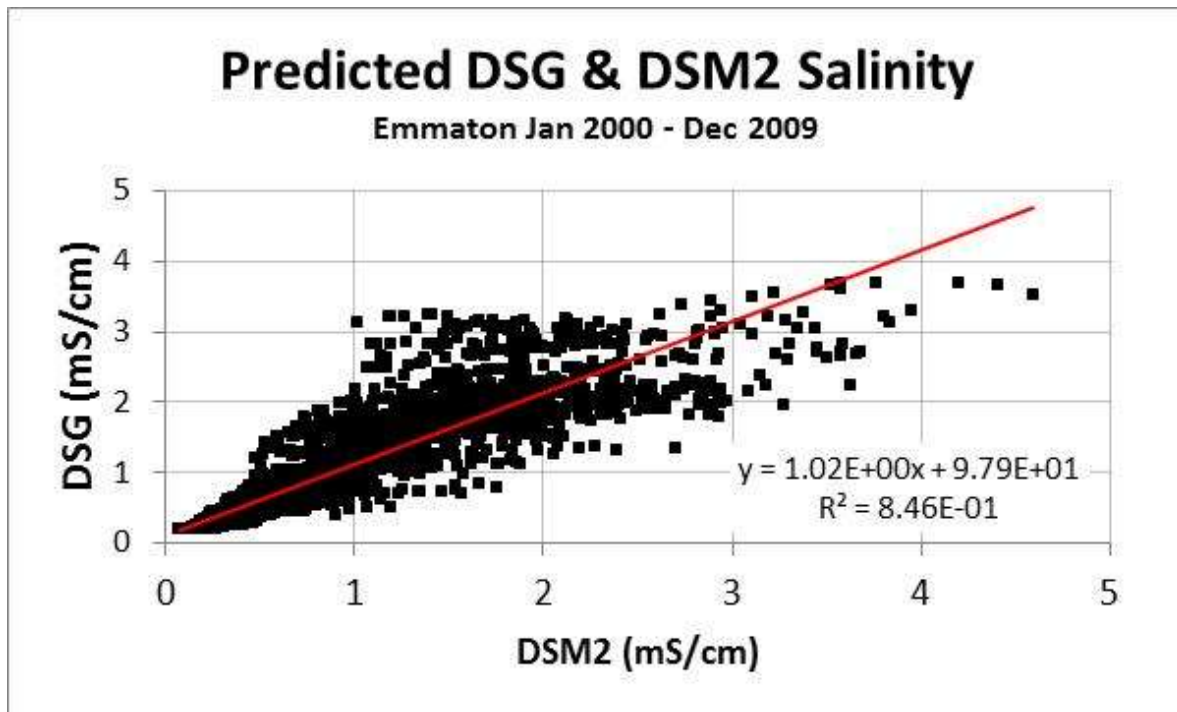


Figure A-5: DSG Predicted vs. DSM Surface Salinity at Emmaton: 2000-2009

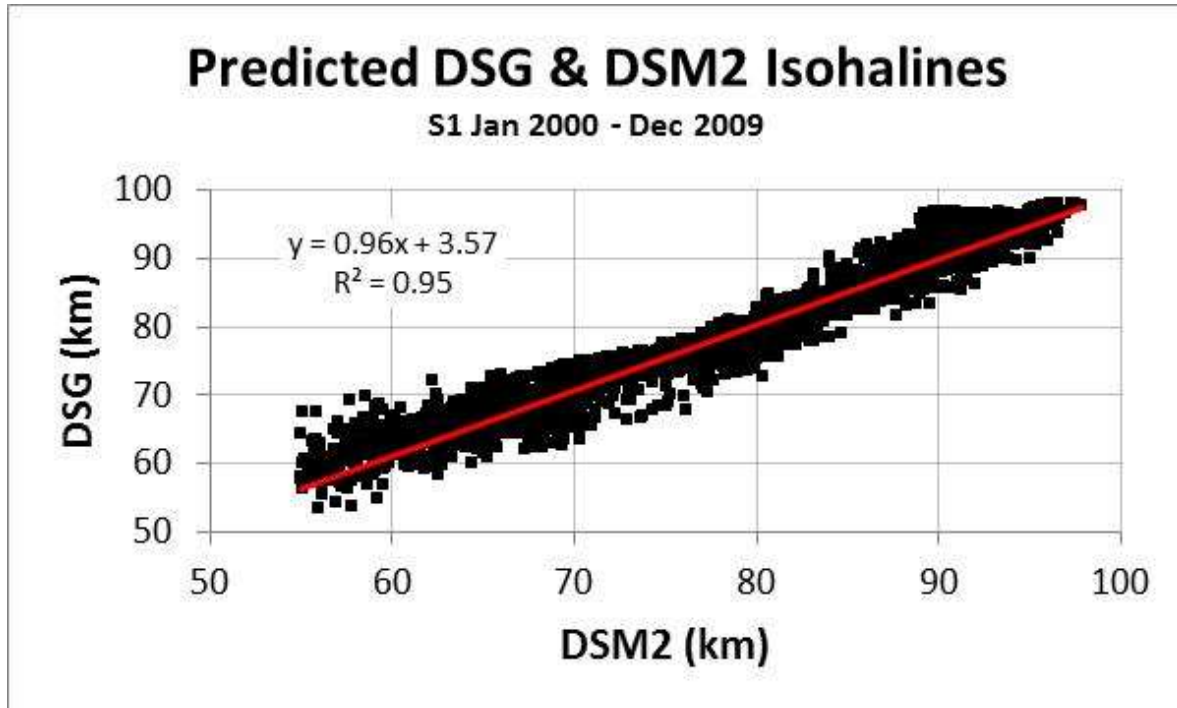


Figure A-6: DSG Predicted vs. DSM2 Interpolated 1 ppt Surface Isohaline Position: 2000-2009

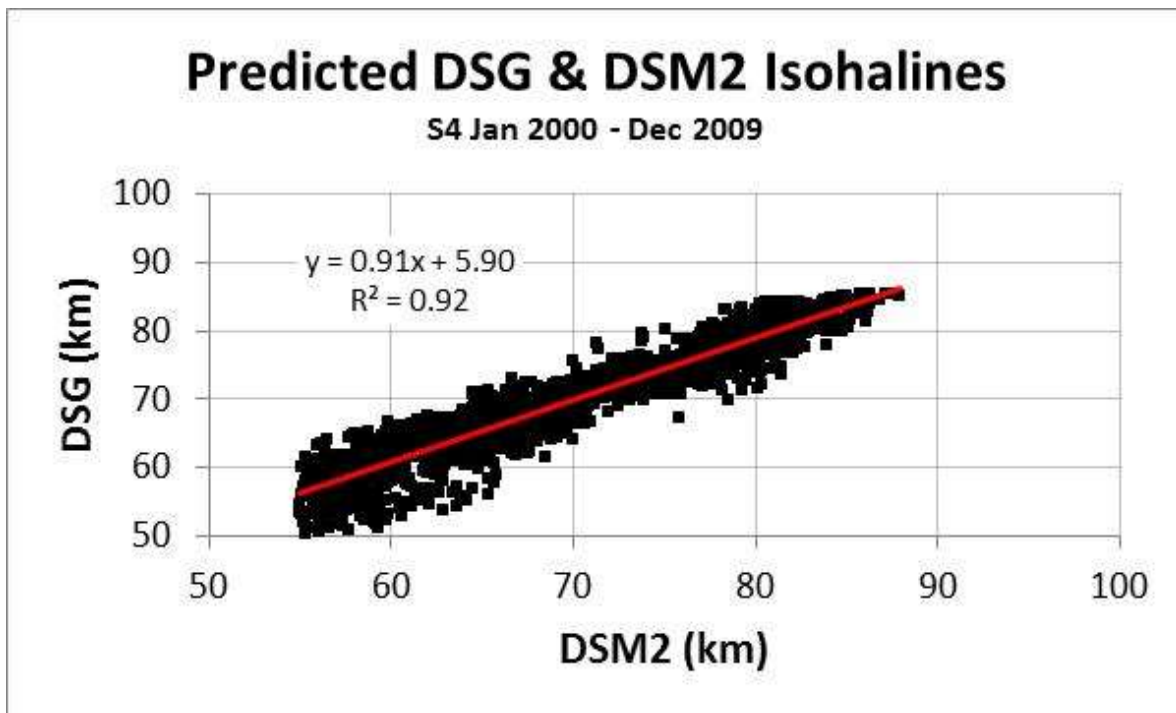


Figure A-7: DSG Predicted vs. DSM2 Interpolated 4 ppt Surface Isohaline Position: 2000-2009

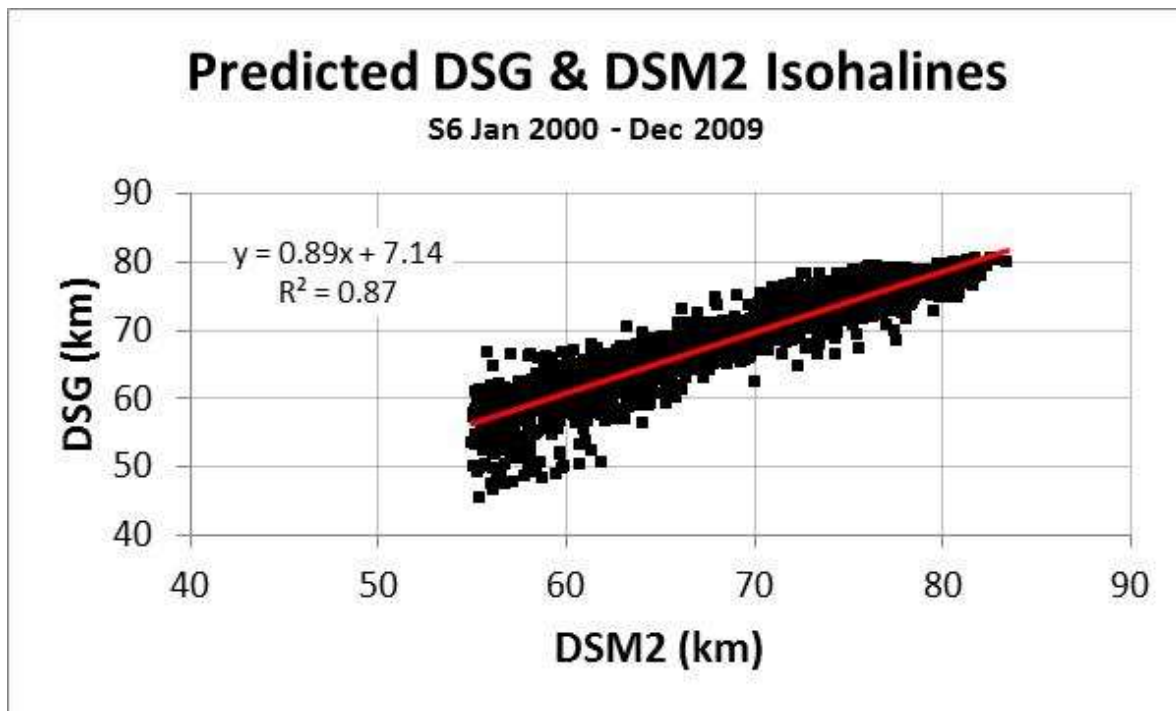


Figure A-8: DSG Predicted vs. DSM2 Interpolated 6 ppt Surface Isohaline Position: 2000-2009

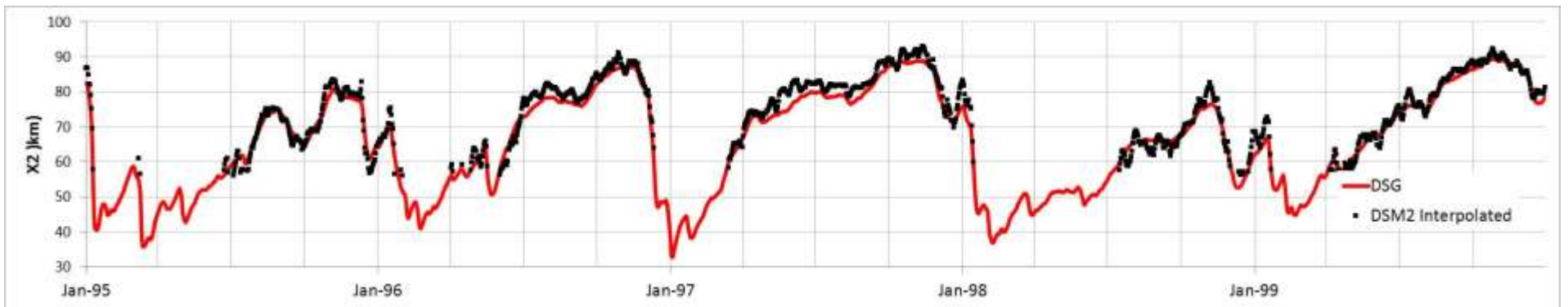
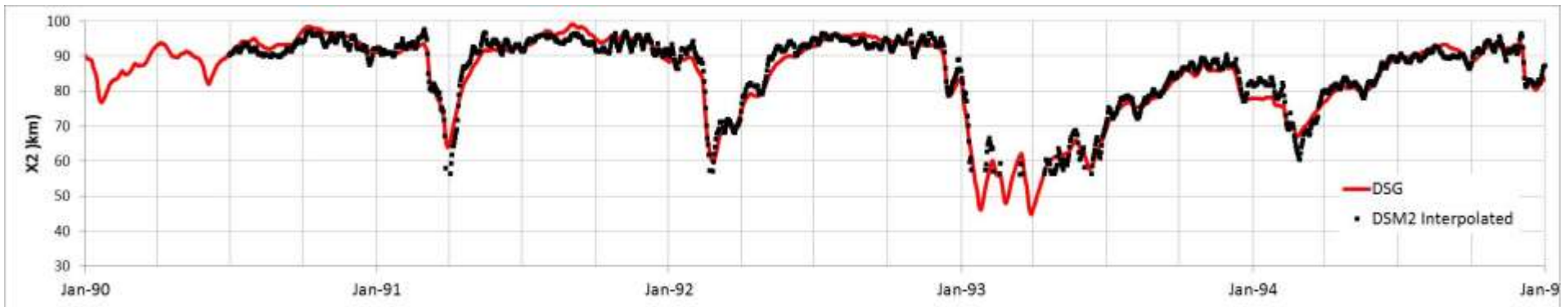


Figure A-9: Time Series of DSG Predicted and DSM2 Interpolated X2 Position: 1990-1999

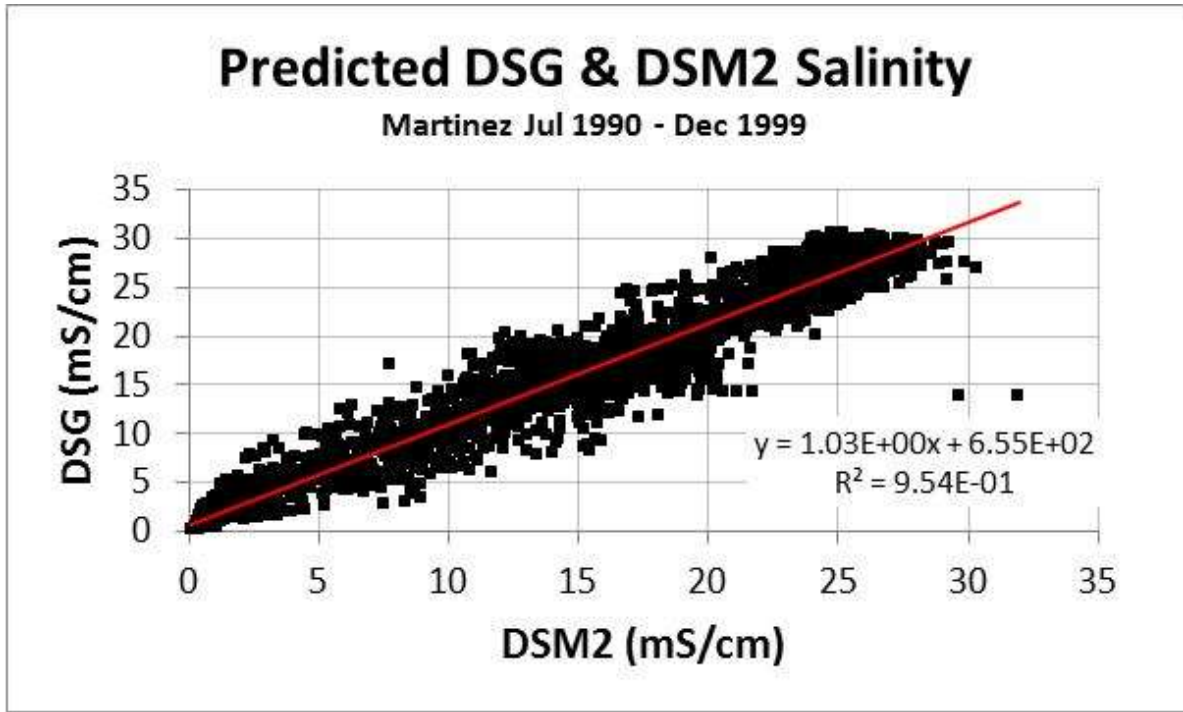


Figure A-10: DSG Predicted vs. DSM Surface Salinity at Martinez: 1990-1999

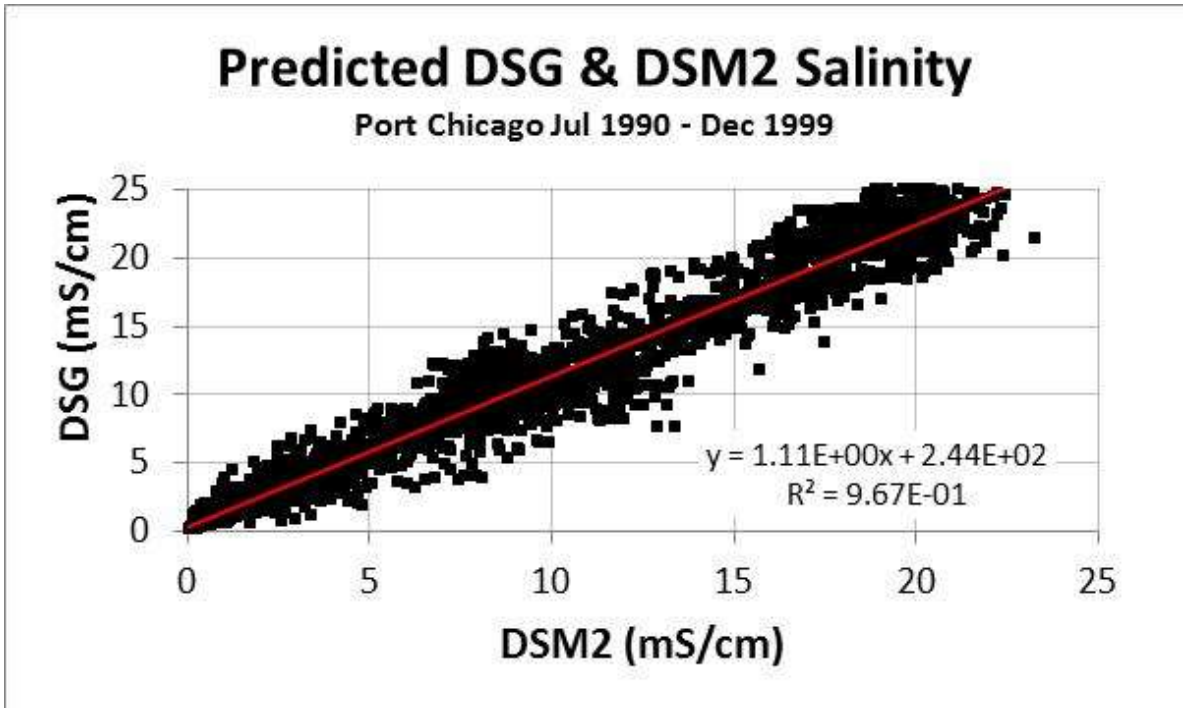


Figure A-11: DSG Predicted vs. DSM Surface Salinity at Port Chicago: 1990-1999

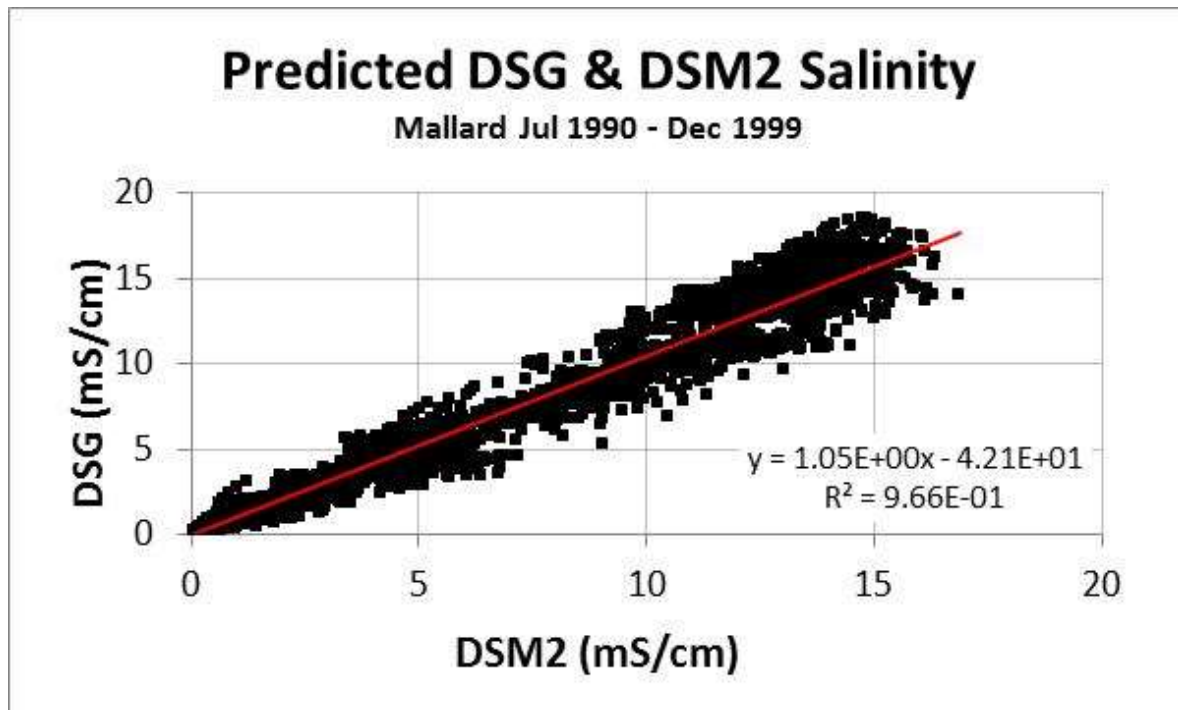


Figure A-12: DSG Predicted vs. DSM Surface Salinity at Mallard Island: 1990-1999

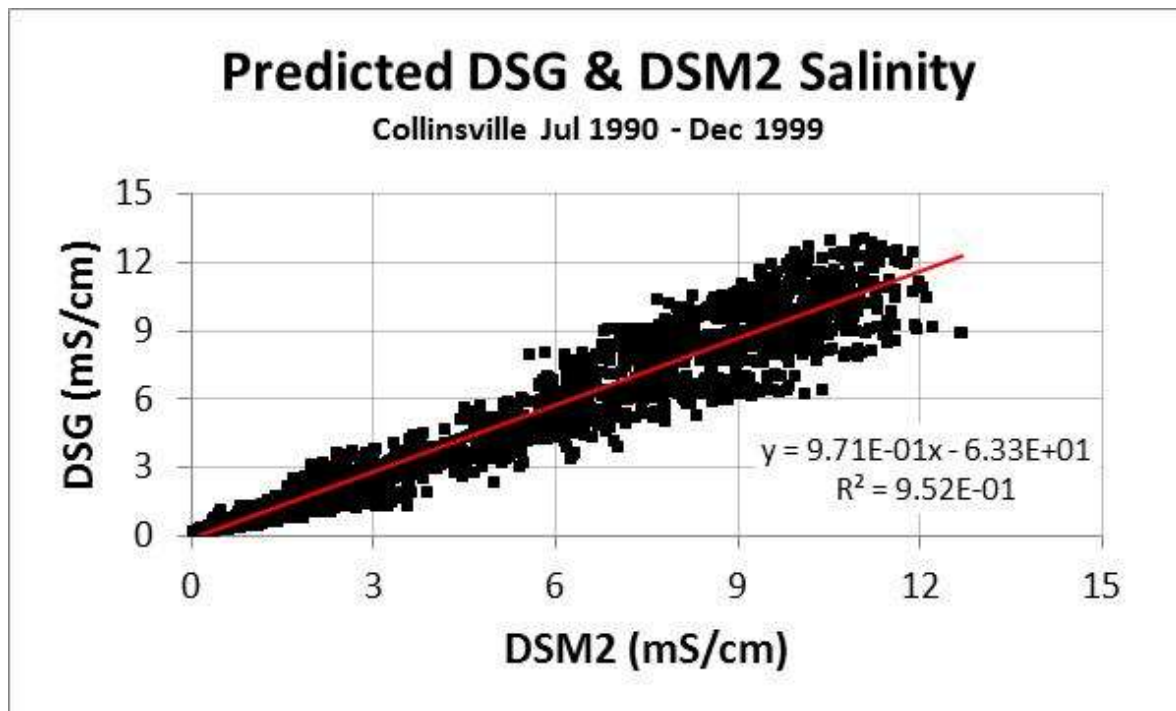


Figure A-13: DSG Predicted vs. DSM Surface Salinity at Collinsville: 1990-1999

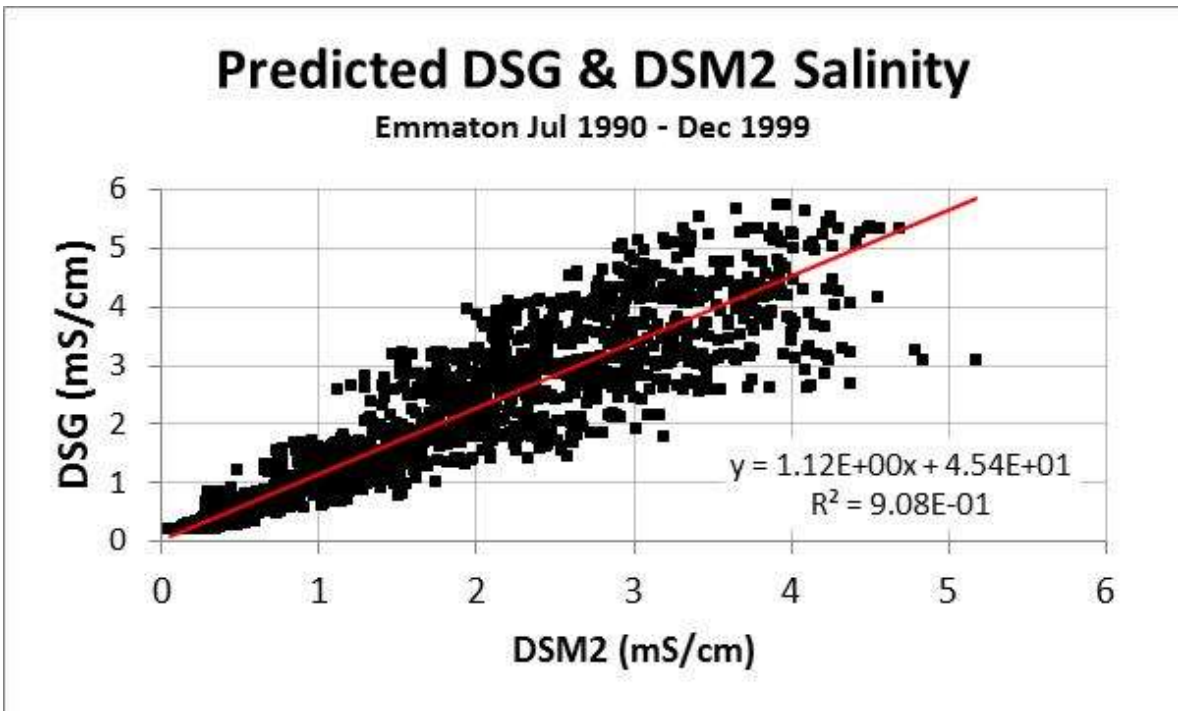


Figure A-14: DSG Predicted vs. DSM Surface Salinity at Emmaton: 1990-1999

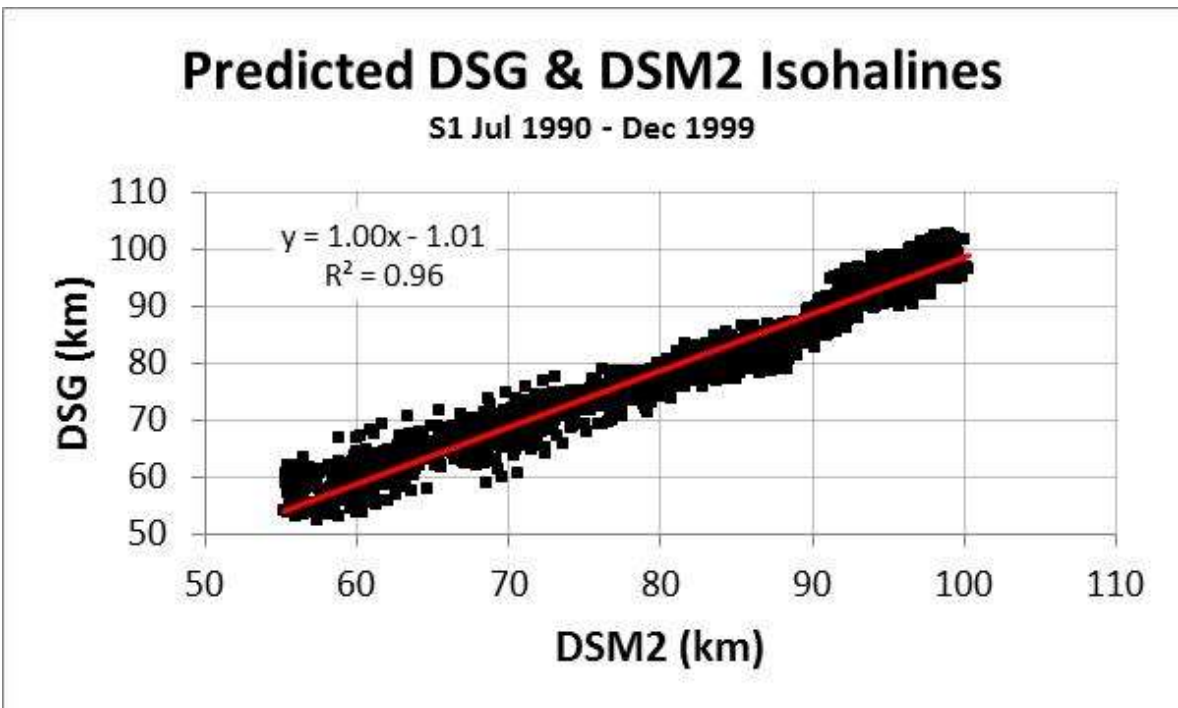


Figure A-15: DSG Predicted vs. DSM2 Interpolated 1 ppt Surface Isohaline Position: 1990-1999

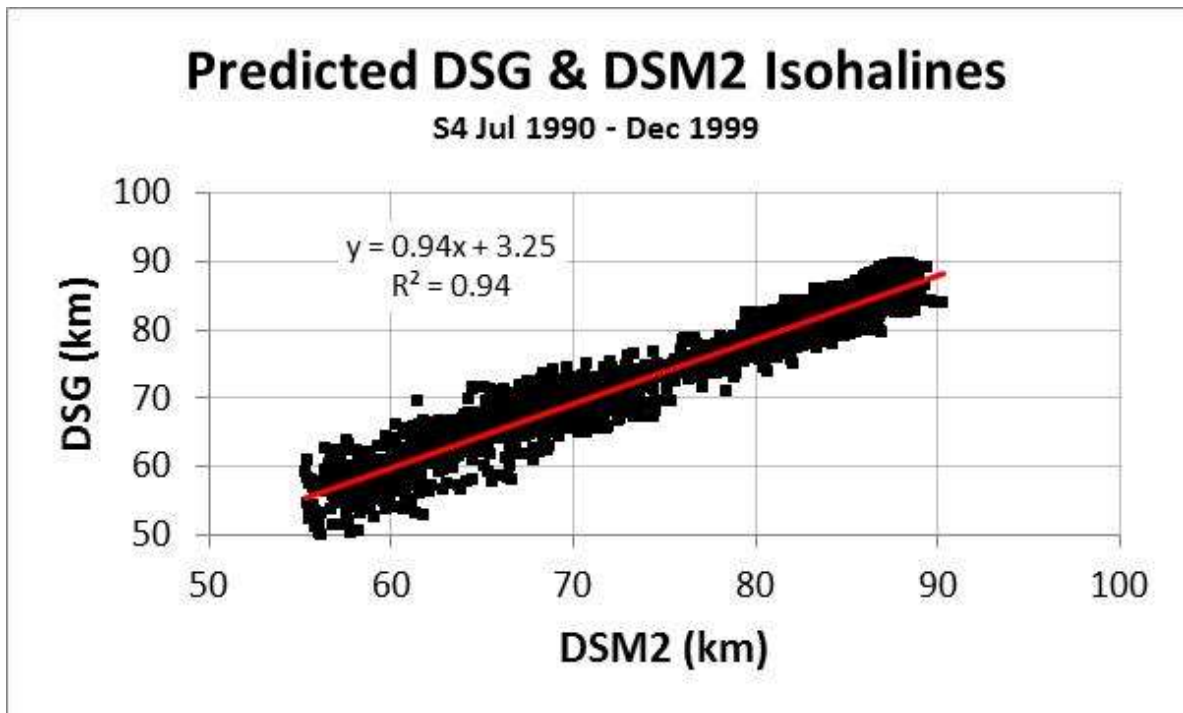


Figure A-16: DSG Predicted vs. DSM2 Interpolated 4 ppt Surface Isohaline Position: 1990-1999

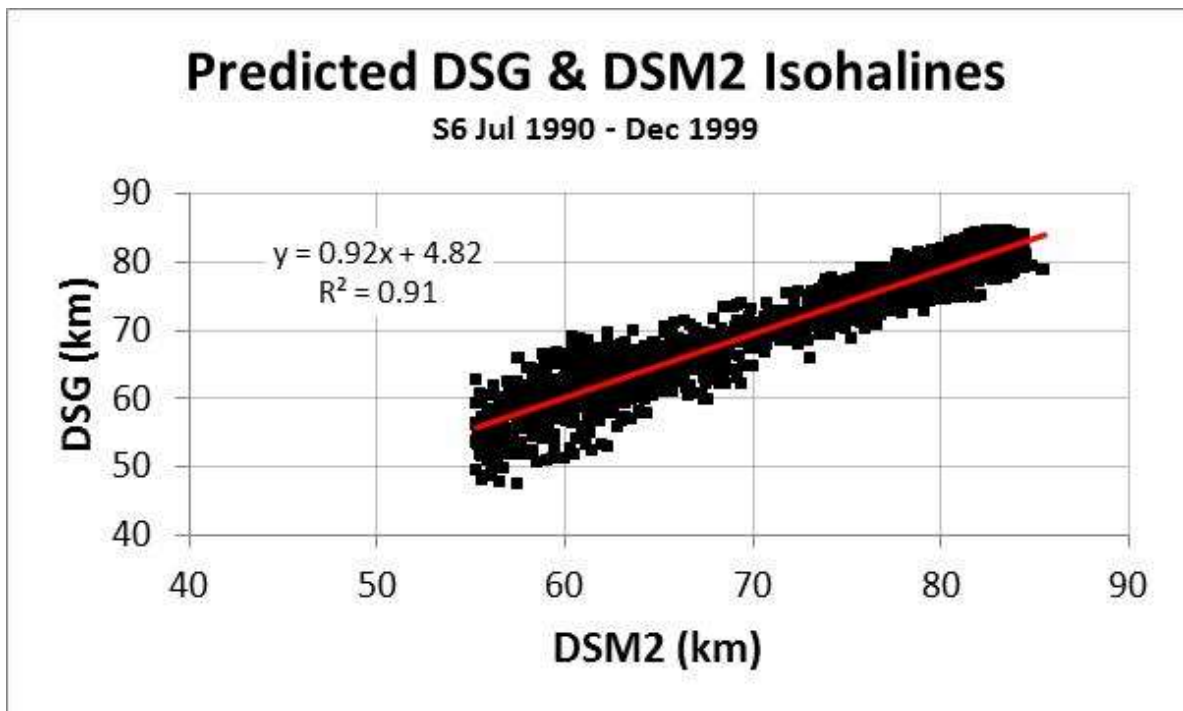


Figure A-17: DSG Predicted vs. DSM2 Interpolated 6 ppt Surface Isohaline Position: 1990-1999

Appendix B: Development of Daily Net Delta Outflow for the Period October 1921 through September 1929

The official record of net Delta outflow in DAYFLOW begins on October 1, 1929 (CDWR 2014). Salinity and isohaline data for the Suisun Bay and western Delta, as assembled by Roy et al. (2014) begins eight years earlier. To assist in validating these cleaned and filled salinity data and interpolated isohaline estimates, it was necessary to develop a daily Delta outflow record for this intervening period of October 1921 through September 1929. This appendix describes the methodology that was used to develop daily net Delta outflow values for this period and provides graphical results.

Paper records of daily inflows to the Delta from the Sacramento and San Joaquin basins (CDPW, 1931)² were scanned and digitized. The reported Sacramento basin values represent the sum of Delta inflows at Freeport and the Yolo Bypass. The reported San Joaquin basin values represent the sum of Delta inflows at Vernalis and east side Delta inflows from the Mokelumne, Cosumnes and Calaveras Rivers. Monthly averages were computed for each inflow and compared with official monthly inflow estimates (CDWR, 1957). A ratio between the official monthly inflows and the computed monthly averages were developed for the Sacramento and San Joaquin basin inflows. The daily inflows were then scaled upward or downward by these ratios to match the official monthly inflow values. Daily net Delta outflow was then computed as a difference between the scaled inflows and official monthly averaged net channel depletion estimates (CDWR, 1957).

Time series charts for Sacramento and San Joaquin basin daily inflows spanning the period October 1921 through September 1929 are provided in [Figure B-1](#). A similar chart for net Delta outflow is provided in [Figure B-2](#).

² Appendix D, Table 37

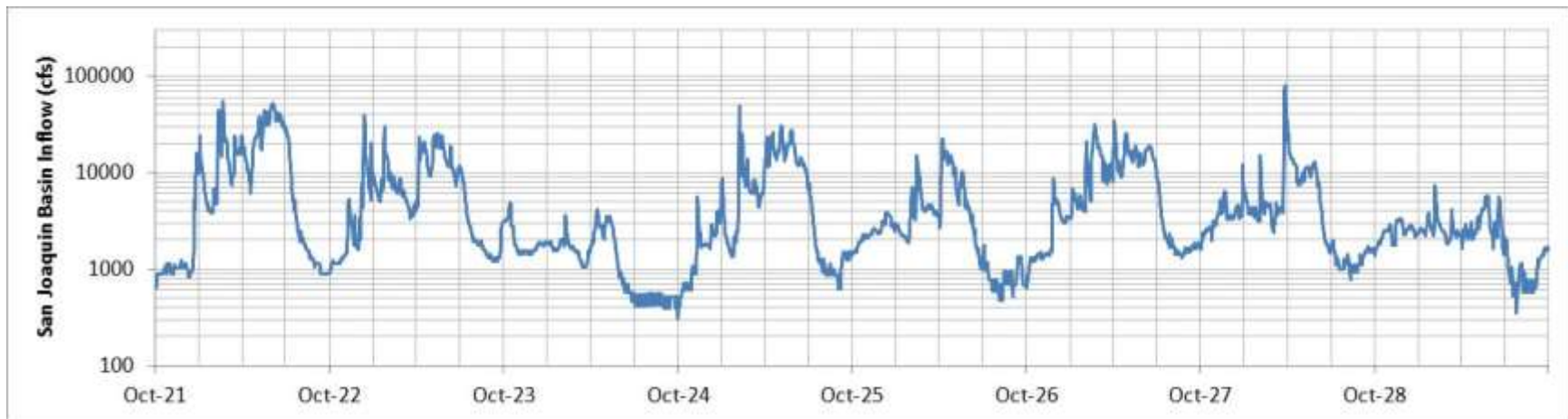
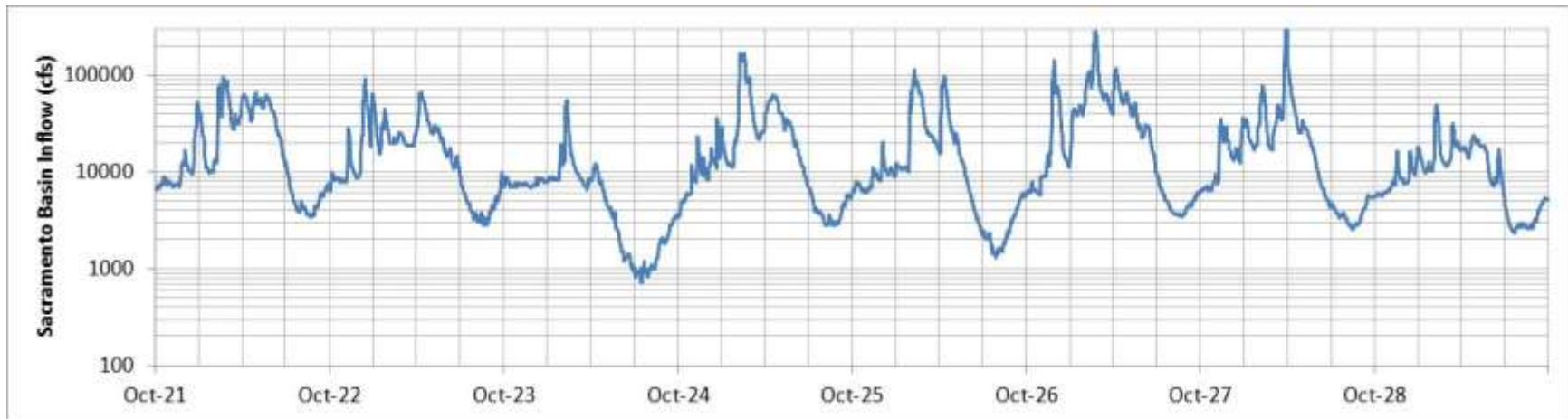


Figure B-1: Time Series of Delta Inflows October 1921 – September 1929

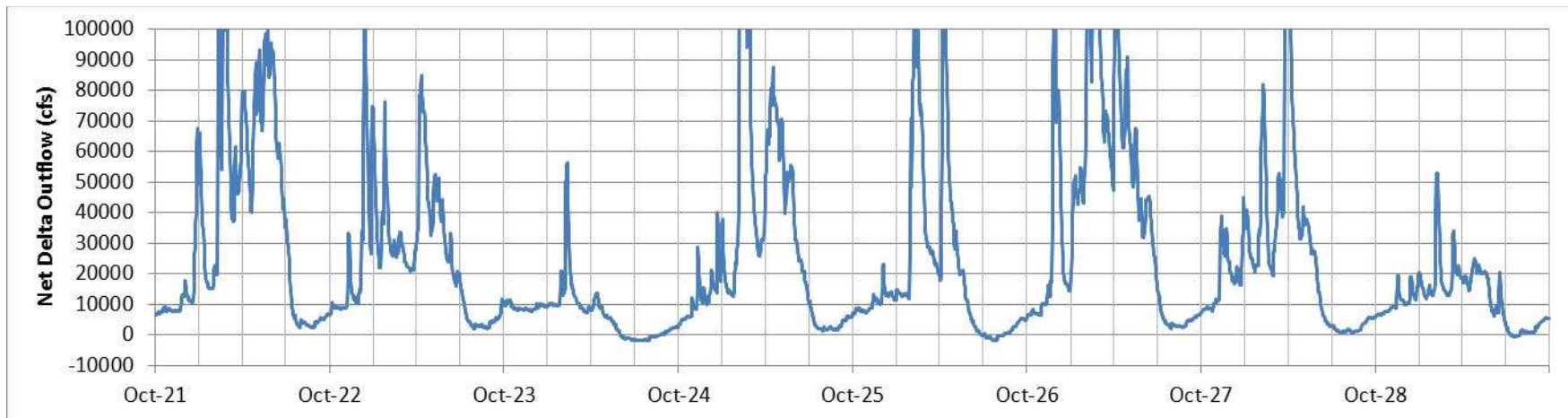


Figure B-2: Time Series of Delta Outflow October 1921 – September 1929

Appendix C: Scatter Plots – DSG Model Calibration with Observed Data

This appendix provides scatter plots comparing DSG estimates with observations of isohaline positions and salinity at the following locations for the 2000-09 calibration period: Martinez, Port Chicago, Mallard Island, Collinsville, Emmaton, Pittsburg, Antioch and Jersey Point.

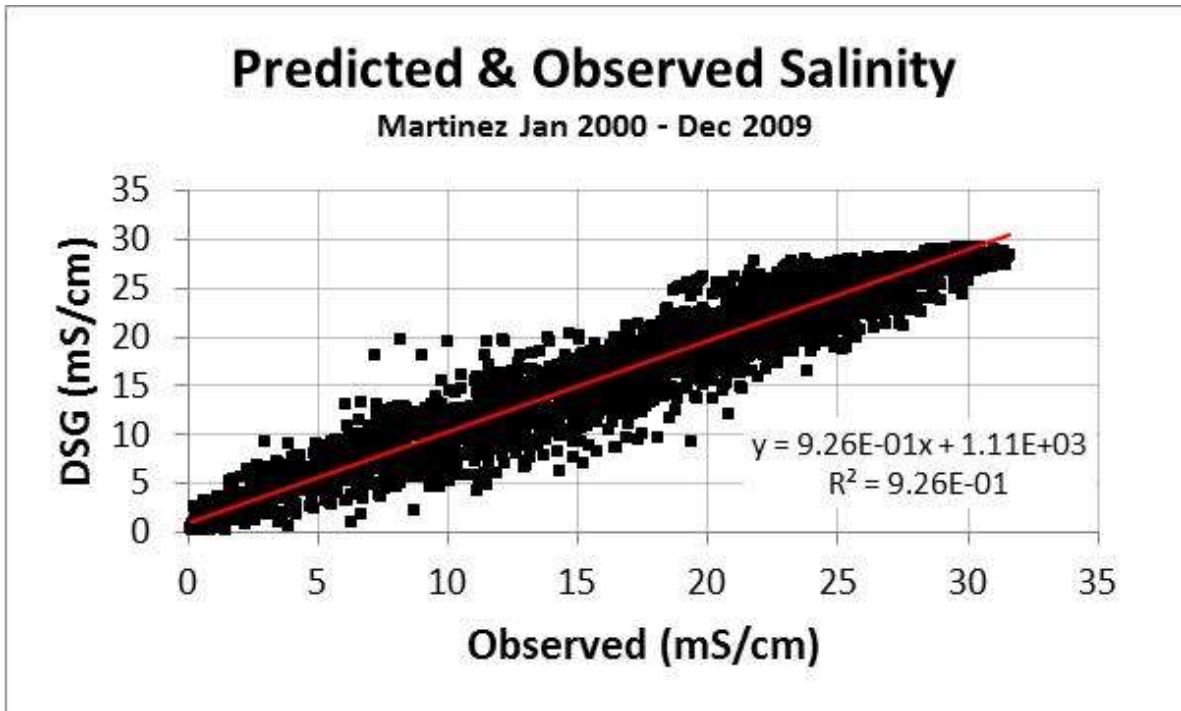


Figure C-1: DSG Predicted vs. Observed Surface Salinity at Martinez: 2000-2009

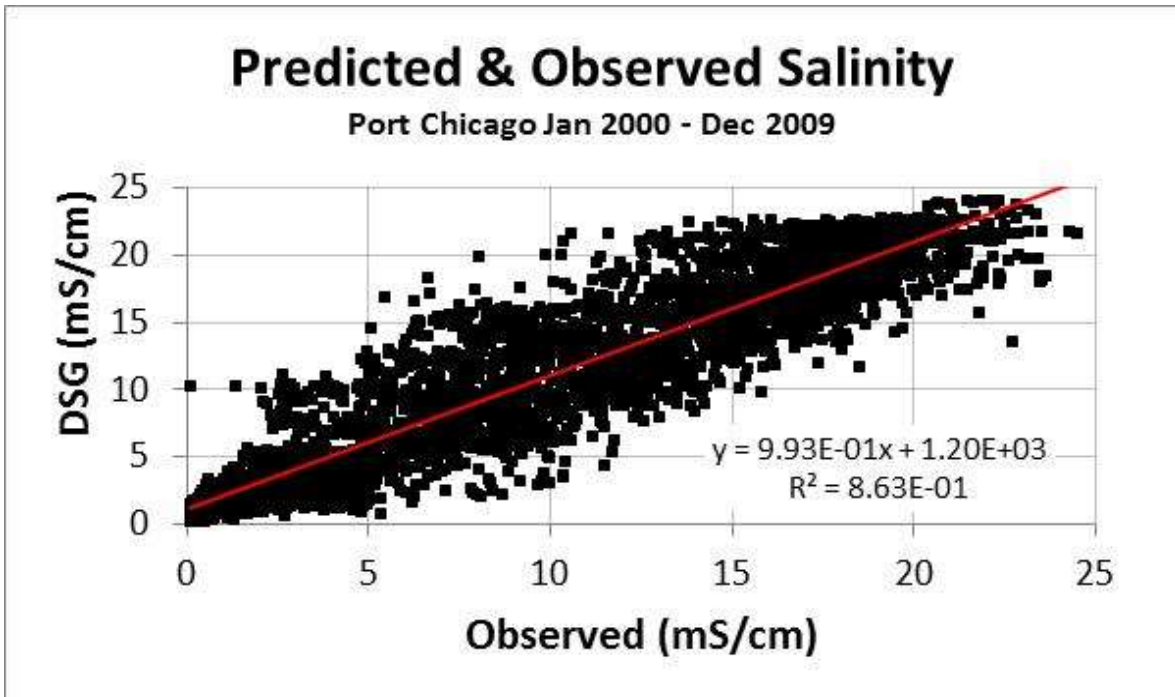


Figure C-2: DSG Predicted vs. Observed Surface Salinity at Port Chicago: 2000-2009

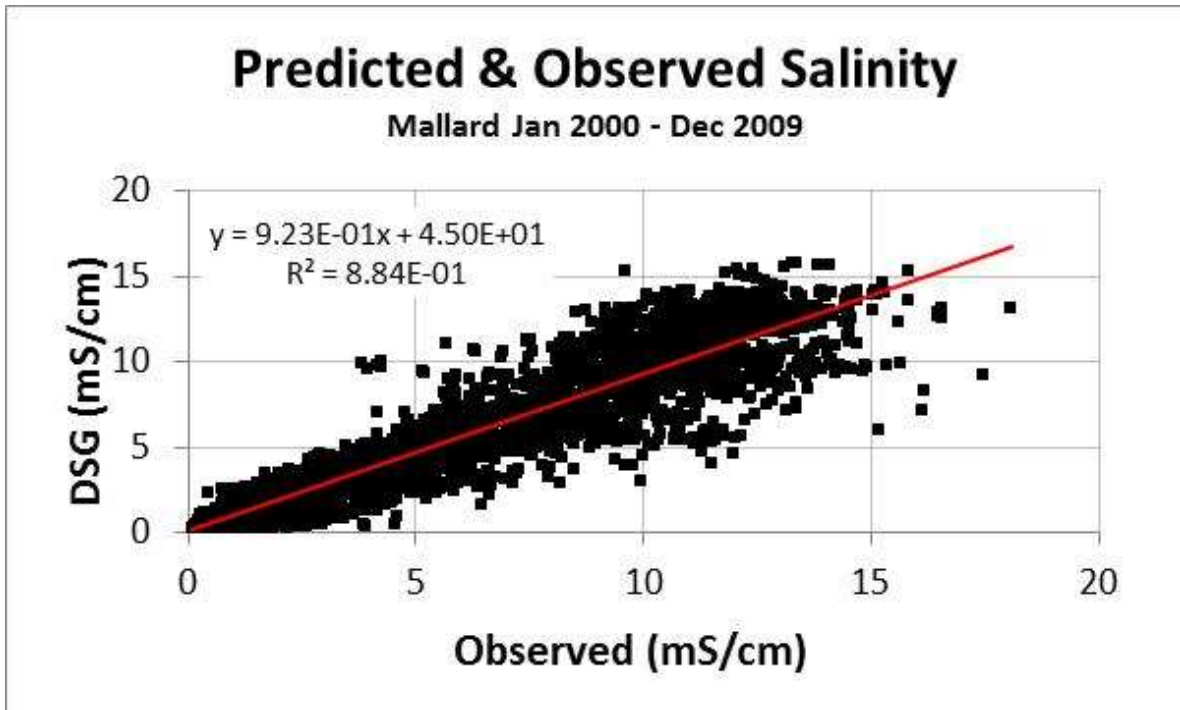


Figure C-3: DSG Predicted vs. Observed Surface Salinity at Mallard Island: 2000-2009

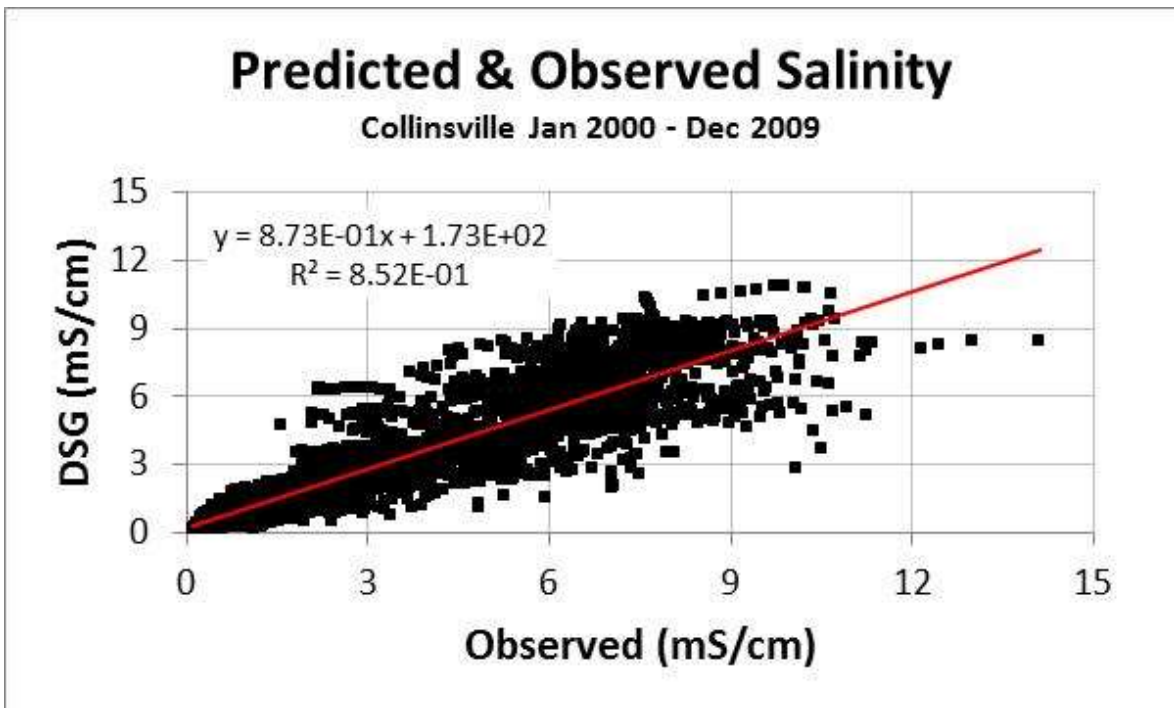


Figure C-4: DSG Predicted vs. Observed Surface Salinity at Collinsville: 2000-2009

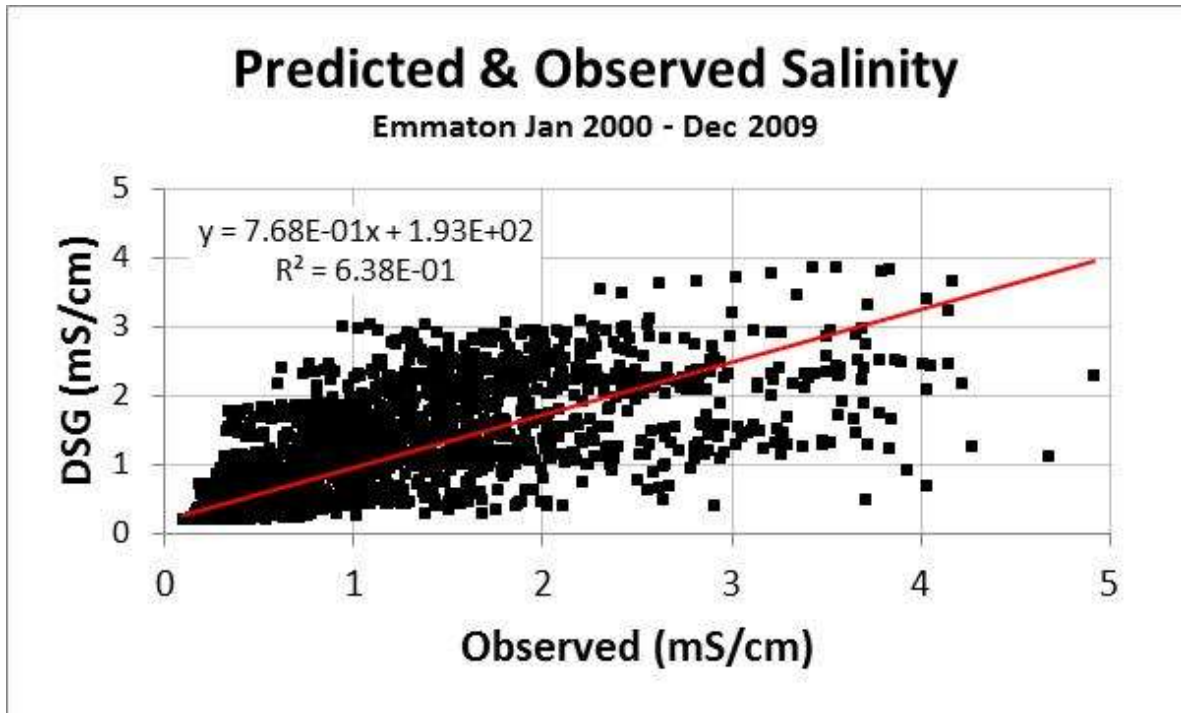


Figure C-5: DSG Predicted vs. Observed Surface Salinity at Emmaton: 2000-2009

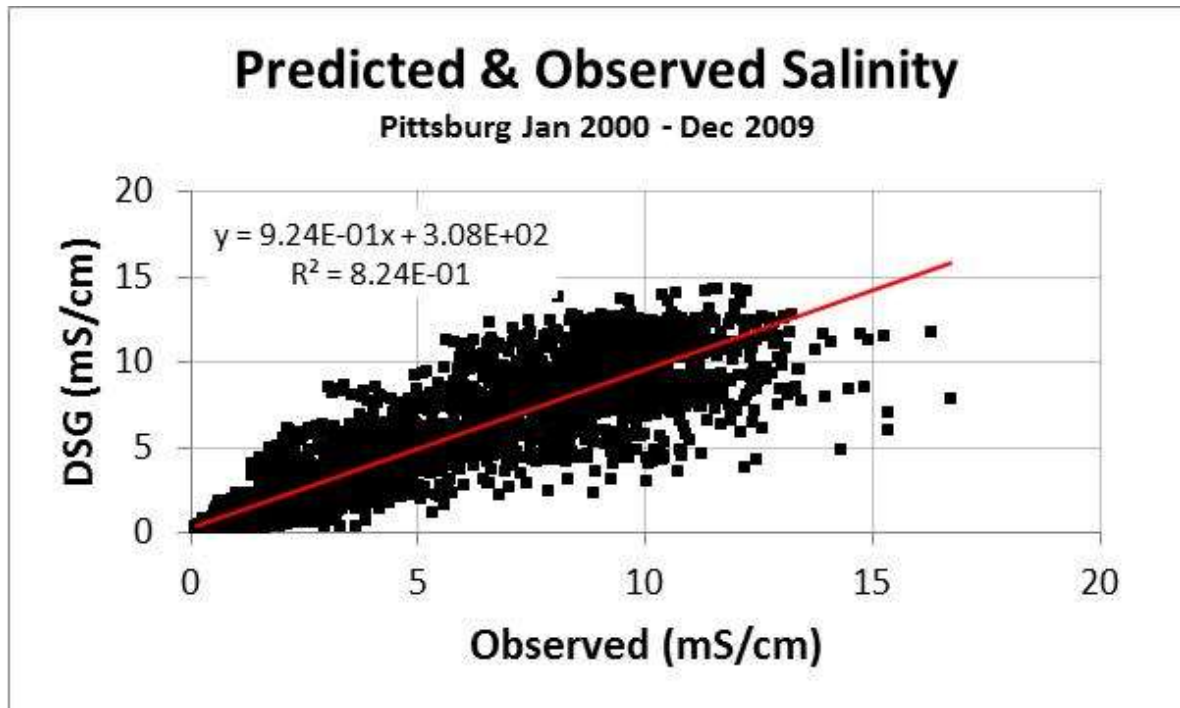


Figure C-6: DSG Predicted vs. Observed Surface Salinity at Pittsburg: 2000-2009

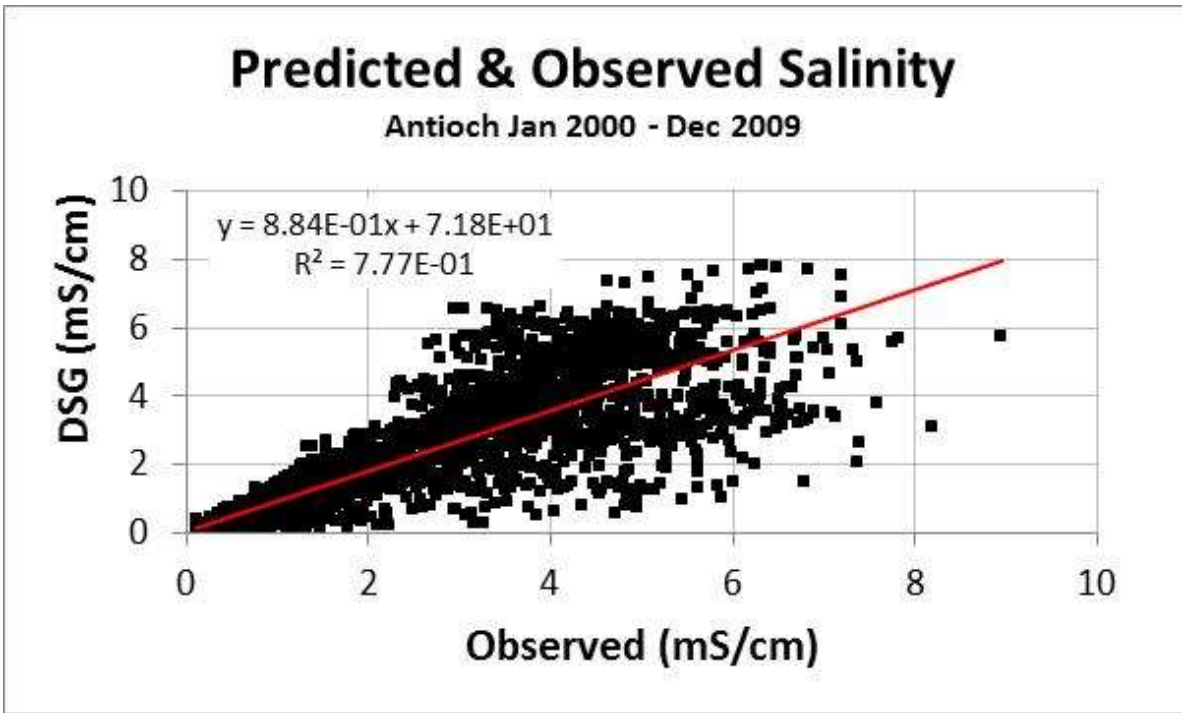


Figure C-7: DSG Predicted vs. Observed Surface Salinity at Antioch: 2000-2009

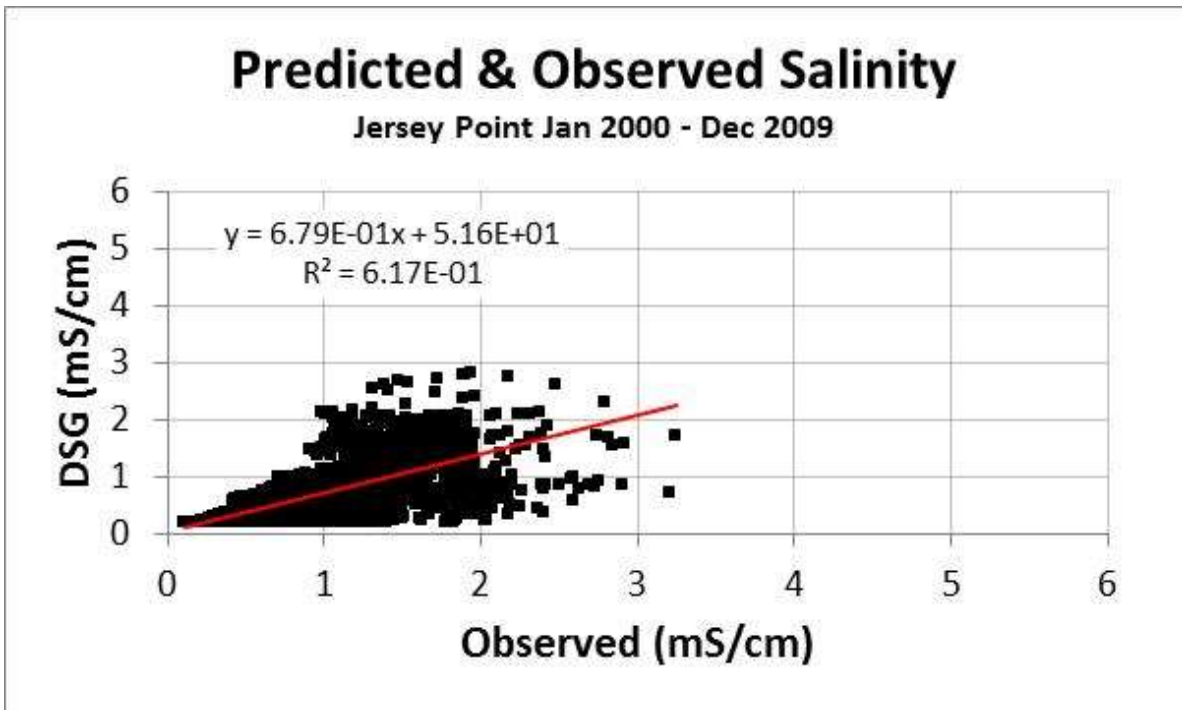


Figure C-8: DSG Predicted vs. Observed Surface Salinity at Jersey Point: 2000-2009

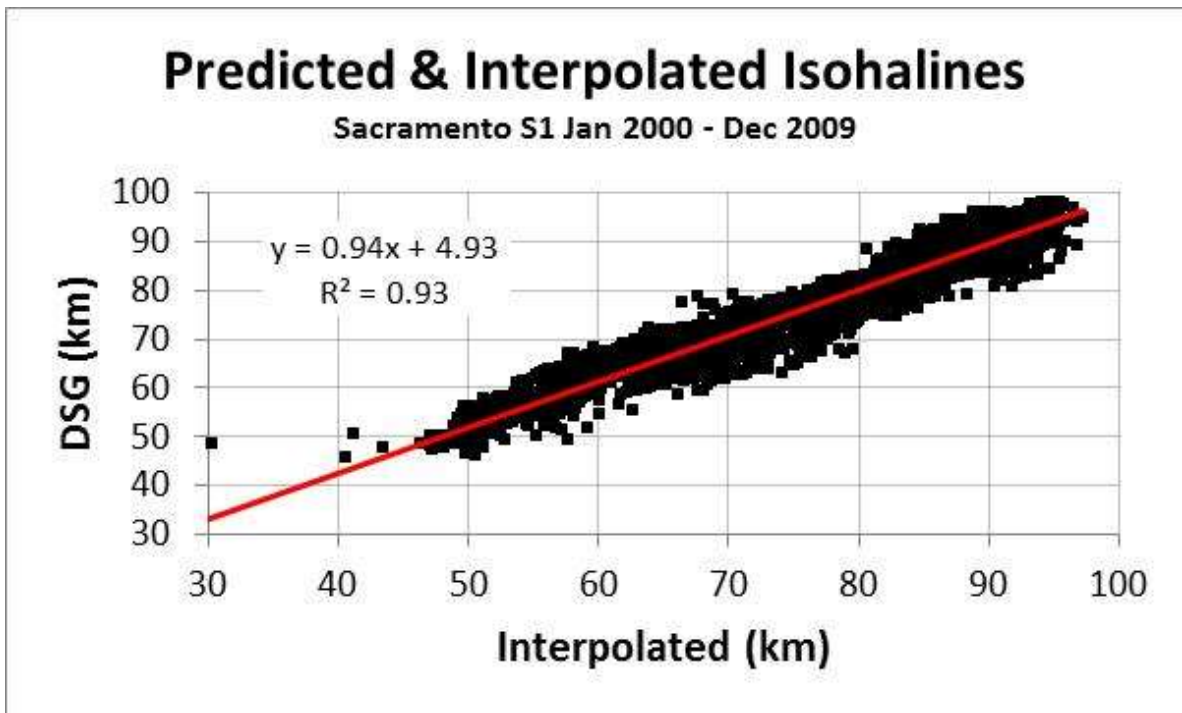


Figure C-9: DSG Predicted vs. Sacramento Branch Interpolated 1 ppt Surface Isohaline Position: 2000-2009

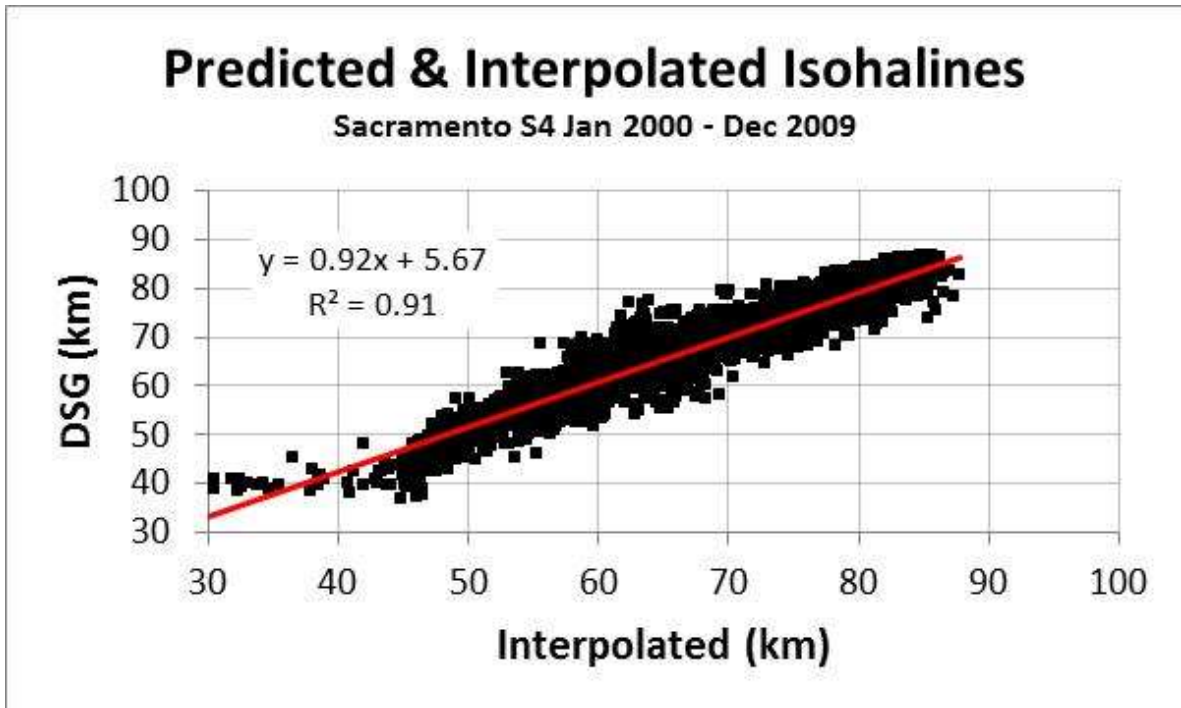


Figure C-10: DSG Predicted vs. Sacramento Branch Interpolated 4 ppt Surface Isohaline Position: 2000-2009

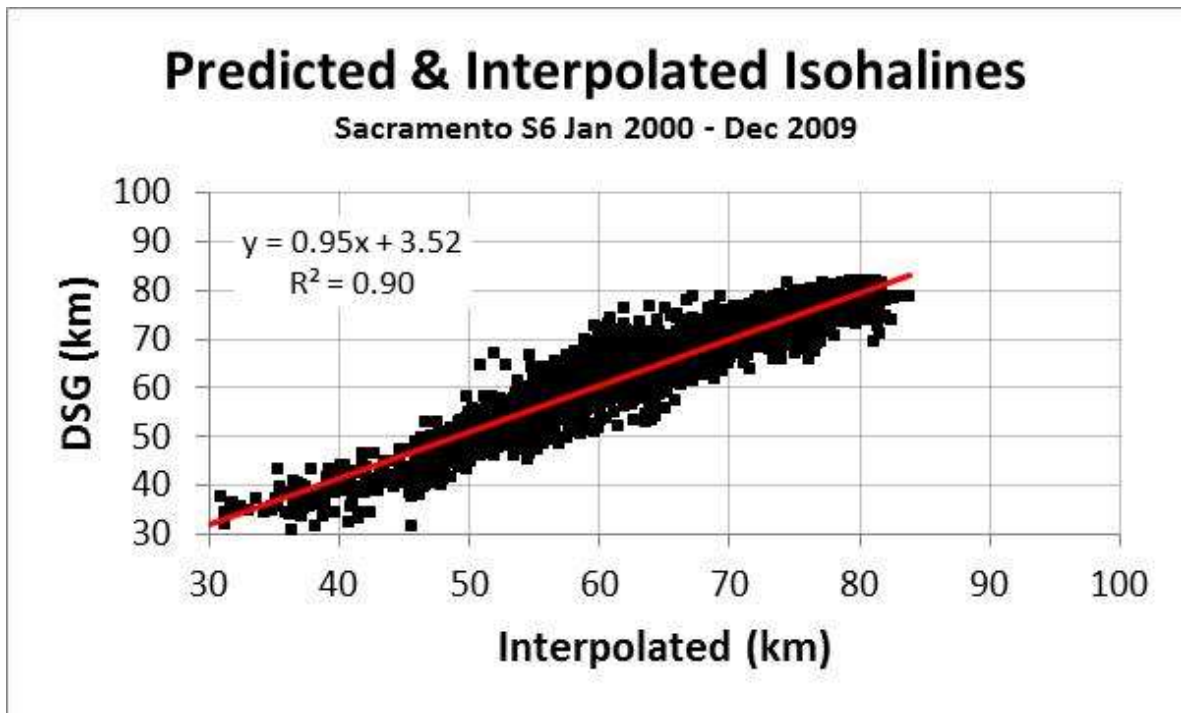


Figure C-11: DSG Predicted vs. Sacramento Branch Interpolated 6 ppt Surface Isohaline Position: 2000-2009

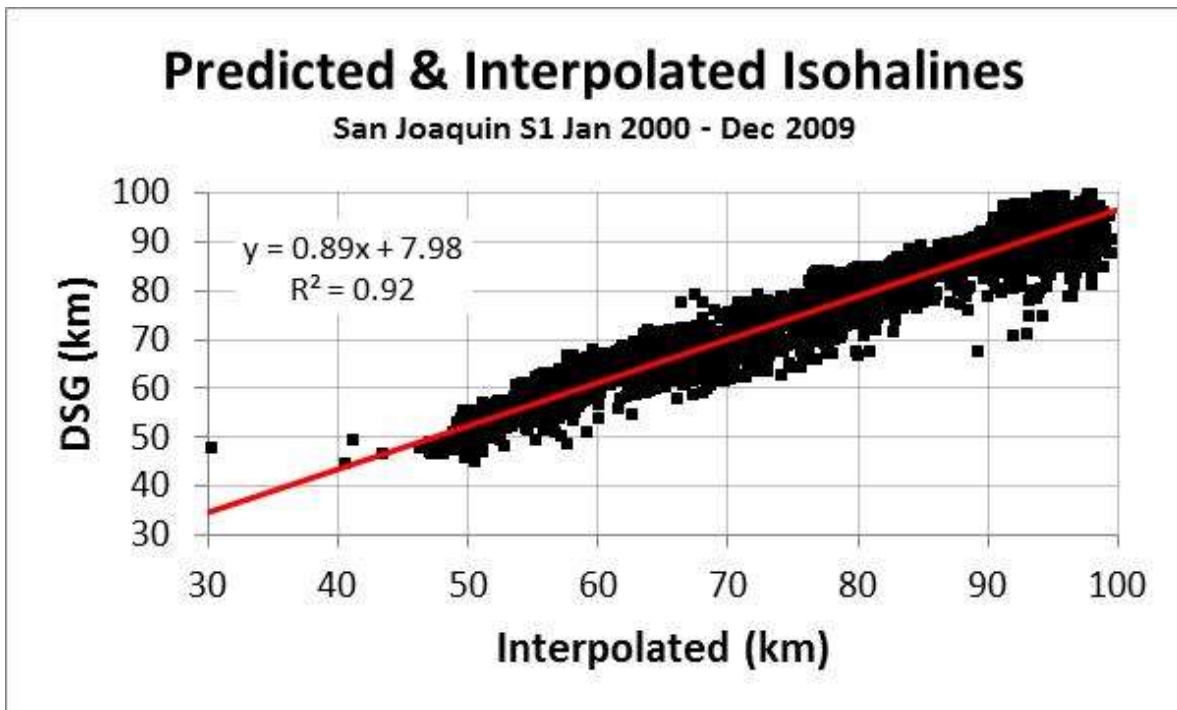


Figure C-12: DSG Predicted vs. San Joaquin Branch Interpolated 1 ppt Surface Isohaline Position: 2000-2009

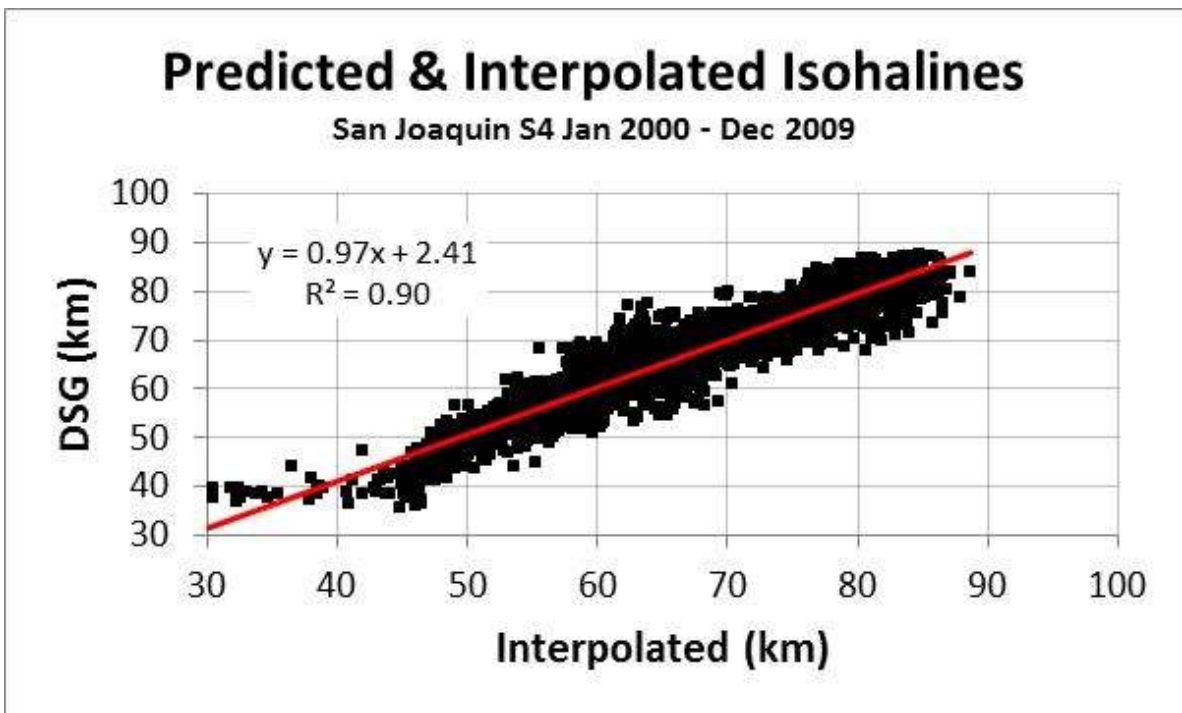


Figure C-13: DSG Predicted vs. San Joaquin Branch Interpolated 4 ppt Surface Isohaline Position: 2000-2009

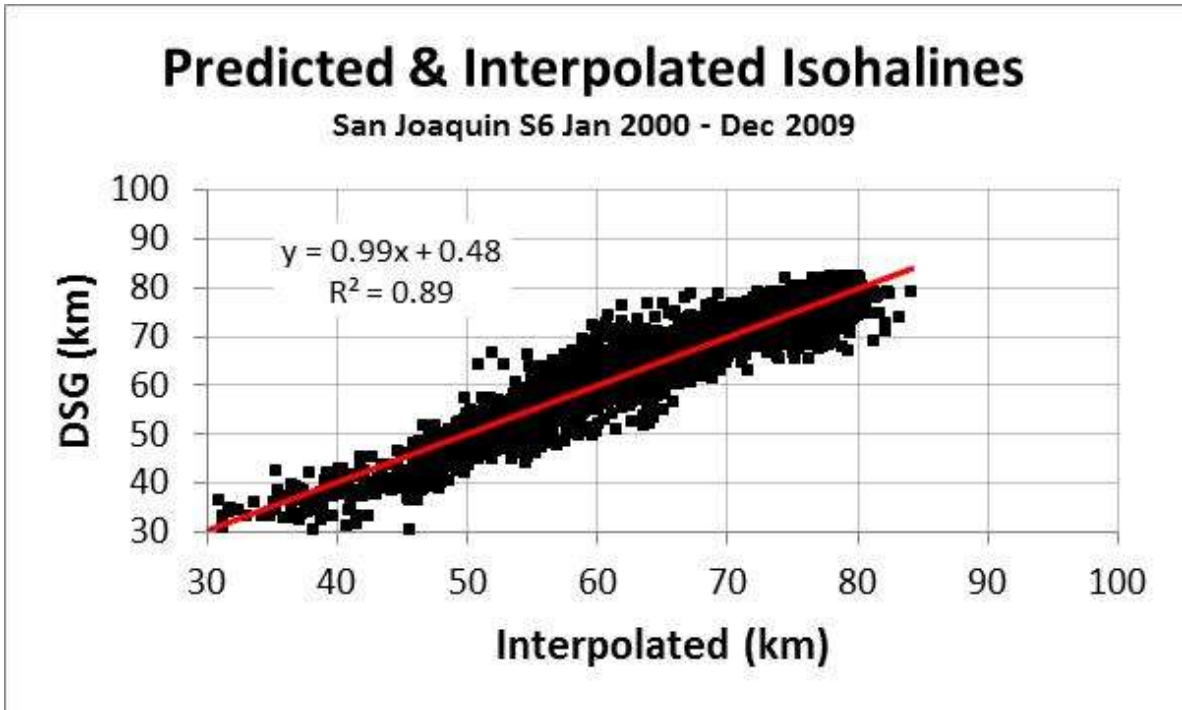


Figure C-14: DSG Predicted vs. San Joaquin Branch Interpolated 6 ppt Surface Isohaline Position: 2000-2009

Appendix D: Time Series Plots – DSG Model Validation with Interpolated X2 Data

This appendix provides time series plots comparing DSG and observed (i.e. interpolated) X2 position for the Sacramento and San Joaquin River branches for the validation period by decade: 2010-13, 1990-99, 1980-89, 1970-79, 1960-69, 1950-59, 1940-49, 1930-39 and 1920-29.

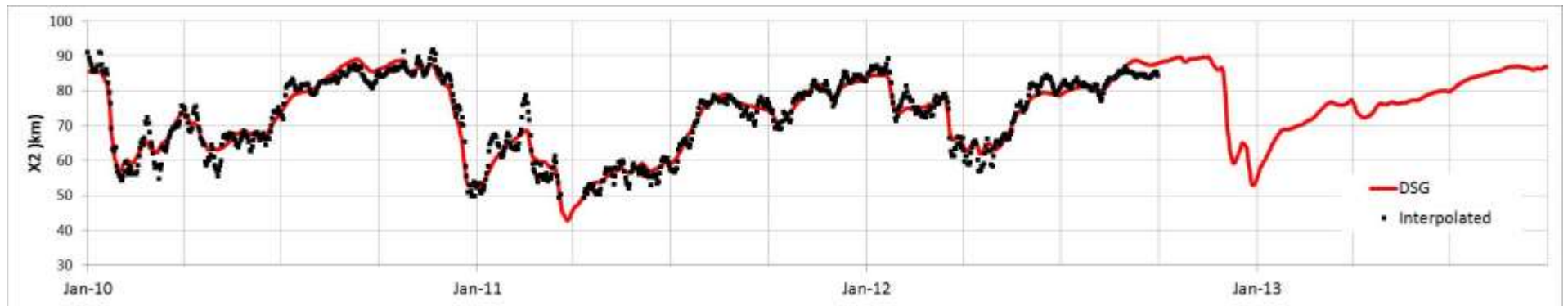


Figure D-1: Time Series of DSG Predicted and Interpolated Sacramento Branch X2 Position: 2010-2013

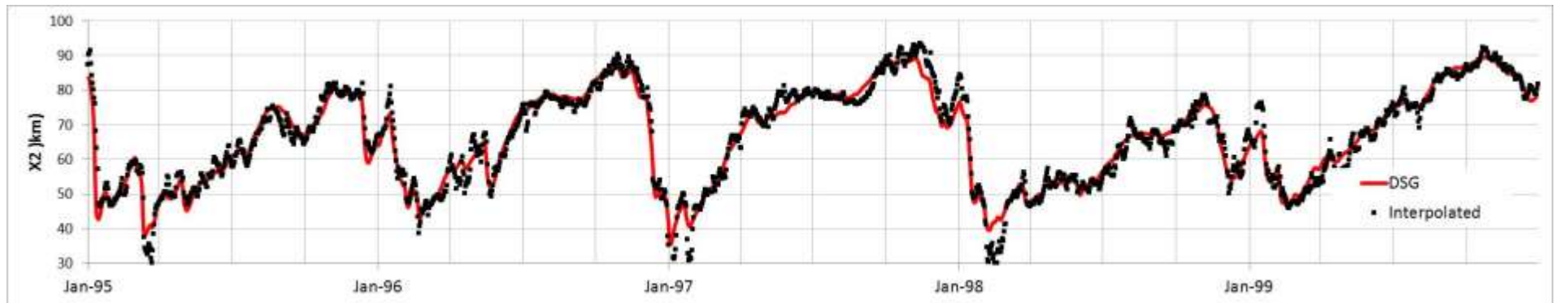
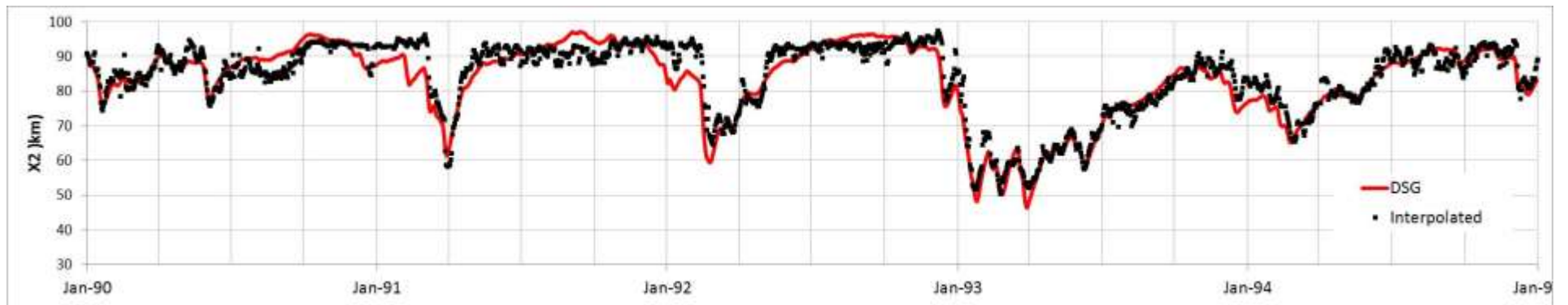


Figure D-2: Time Series of DSG Predicted and Interpolated Sacramento Branch X2 Position: 1990-1999

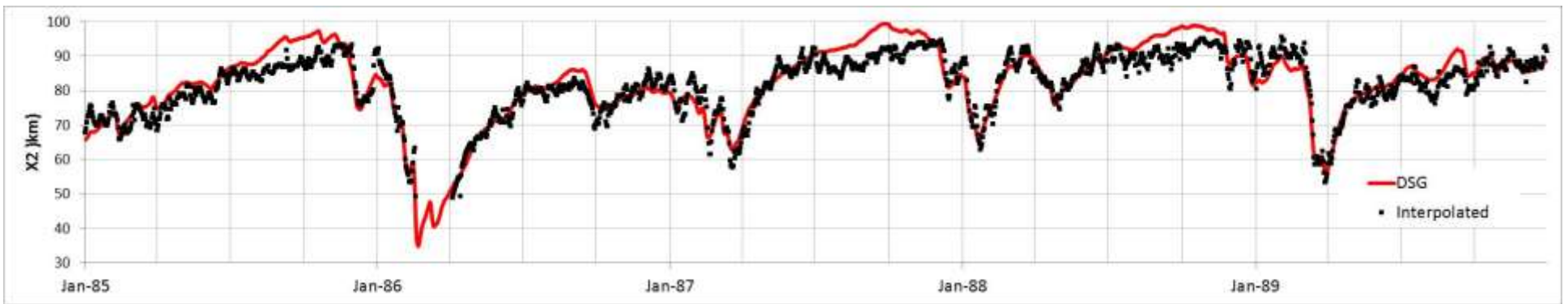
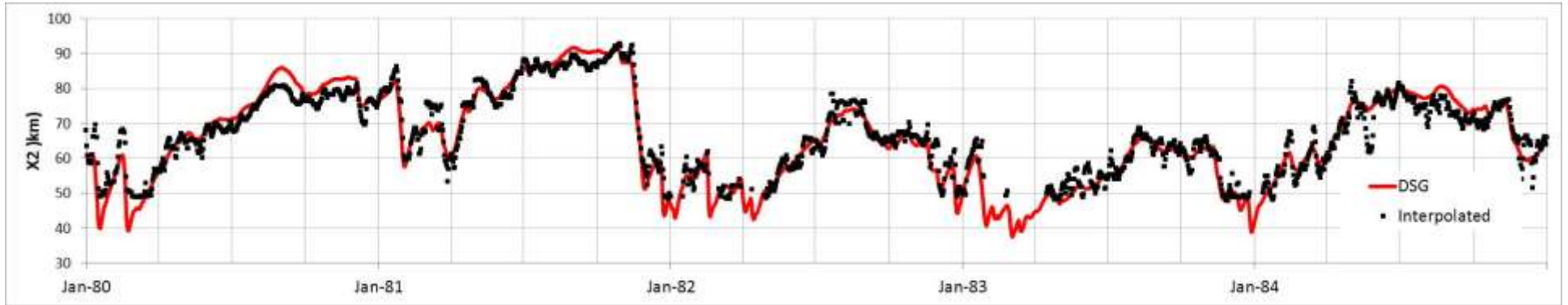


Figure D-3: Time Series of DSG Predicted and Interpolated Sacramento Branch X2 Position: 1980-1989

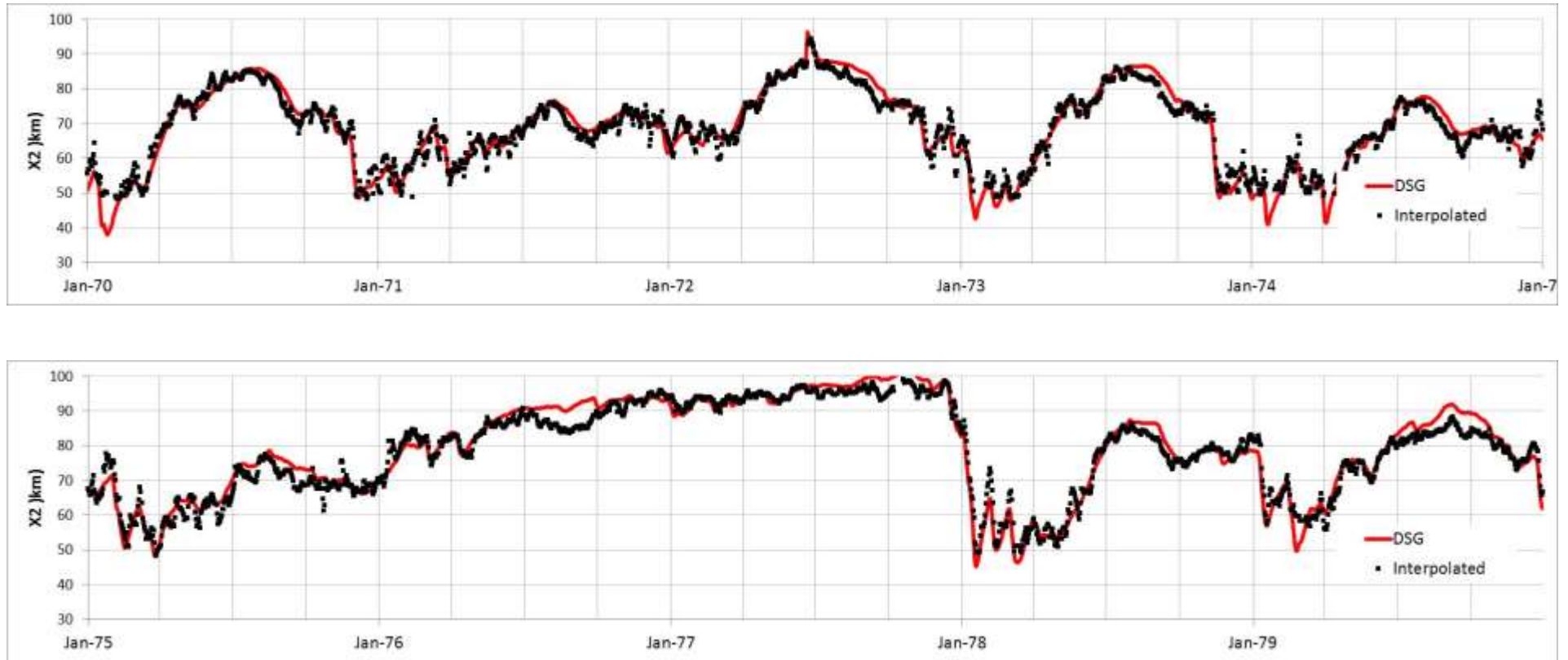


Figure D-4: Time Series of DSG Predicted and Interpolated Sacramento Branch X2 Position: 1970-1979

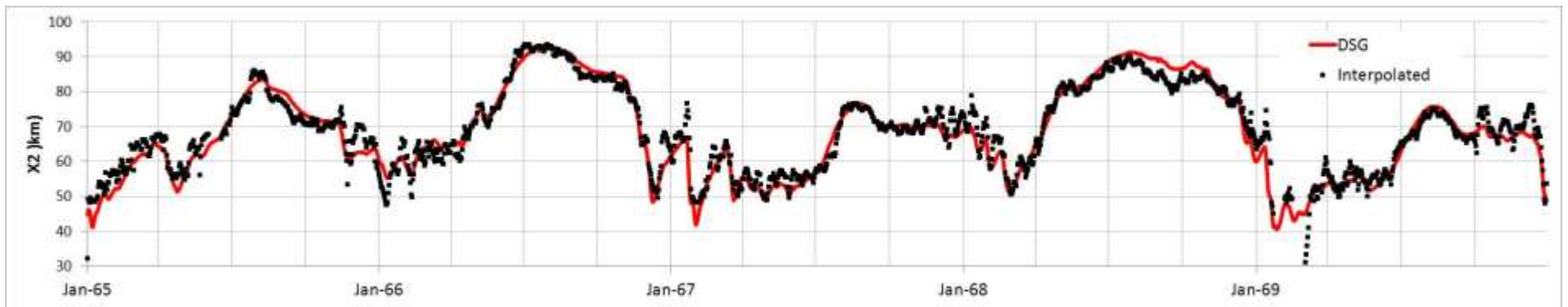
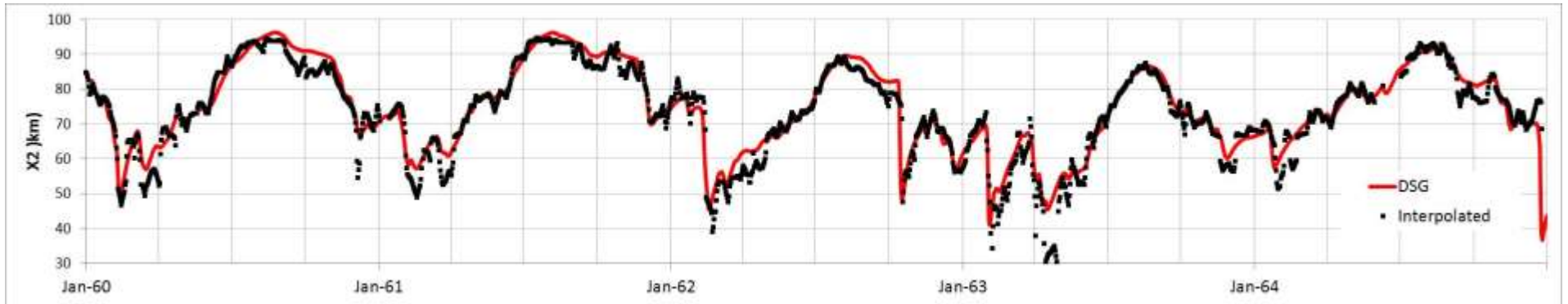


Figure D-5: Time Series of DSG Predicted and Interpolated Sacramento Branch X2 Position: 1960-1969

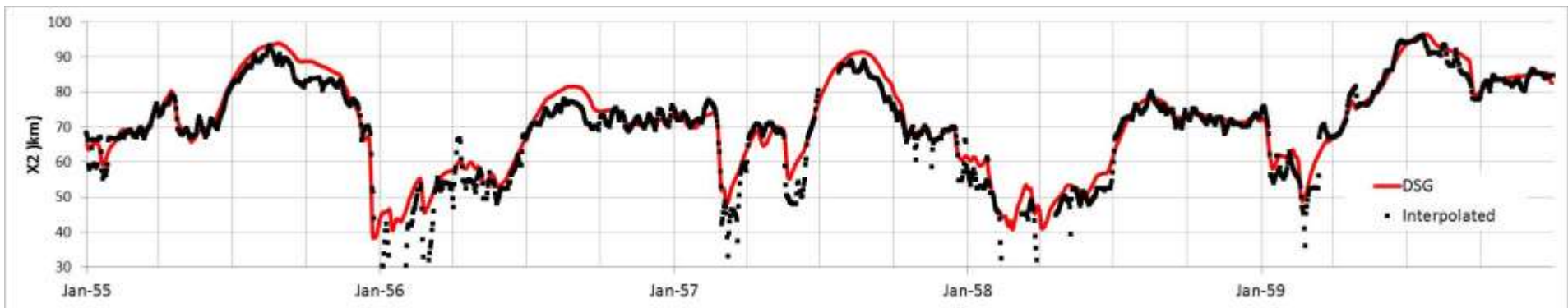
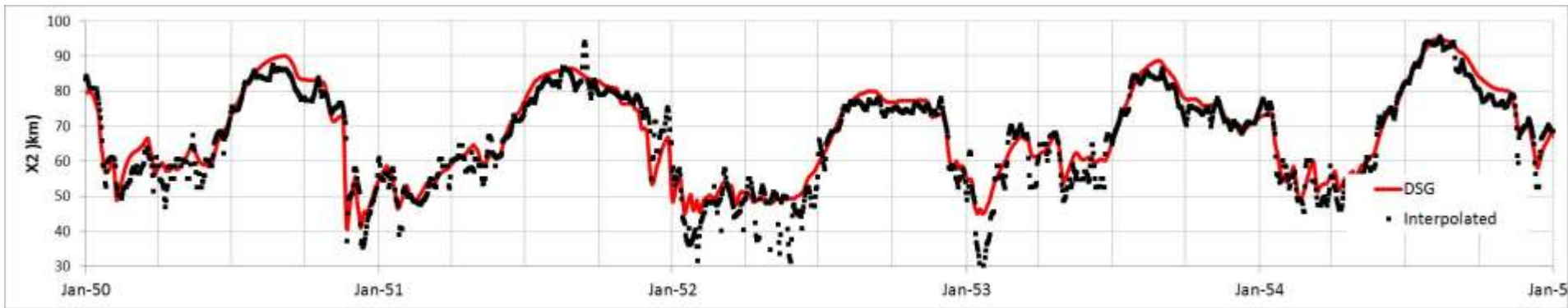


Figure D-6: Time Series of DSG Predicted and Interpolated Sacramento Branch X2 Position: 1950-1959

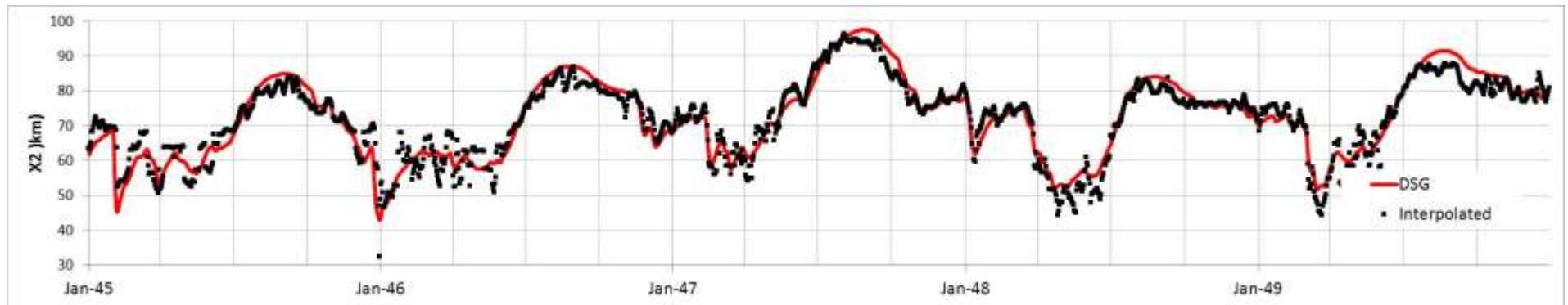
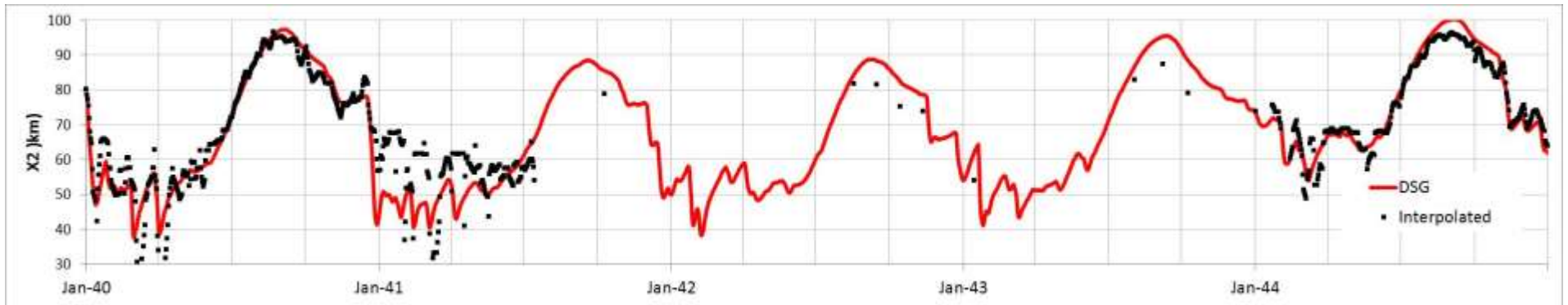


Figure D-7: Time Series of DSG Predicted and Interpolated Sacramento Branch X2 Position: 1940-1949

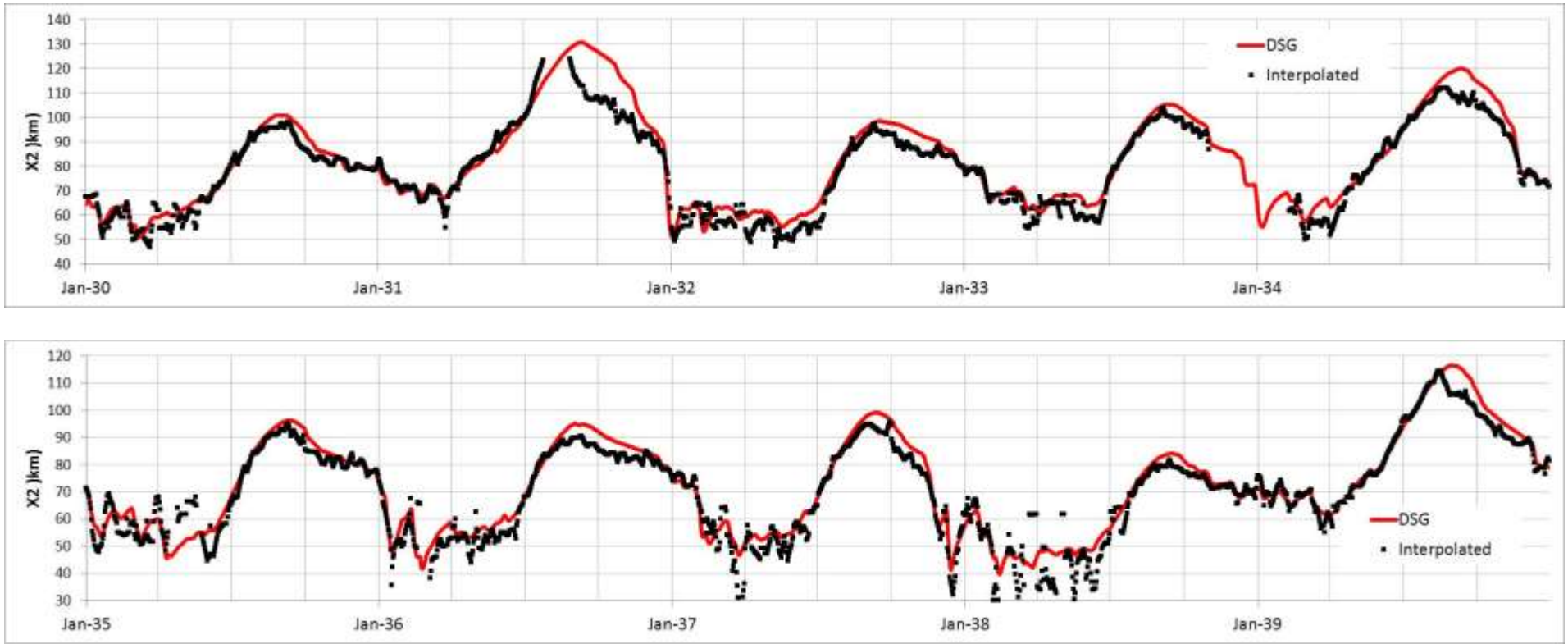


Figure D-8: Time Series of DSG Predicted and Interpolated Sacramento Branch X2 Position: 1930-1939

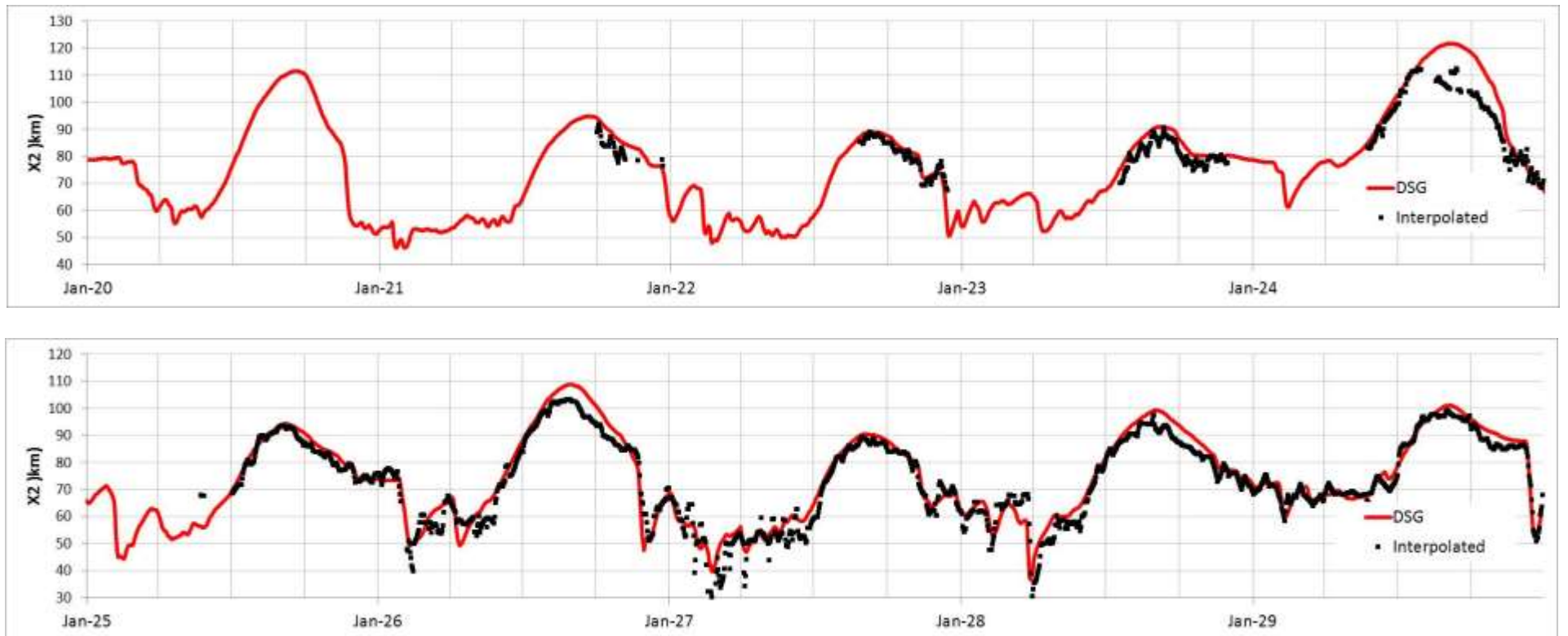


Figure D-9: Time Series of DSG Predicted and Interpolated Sacramento Branch X2 Position: 1920-1929

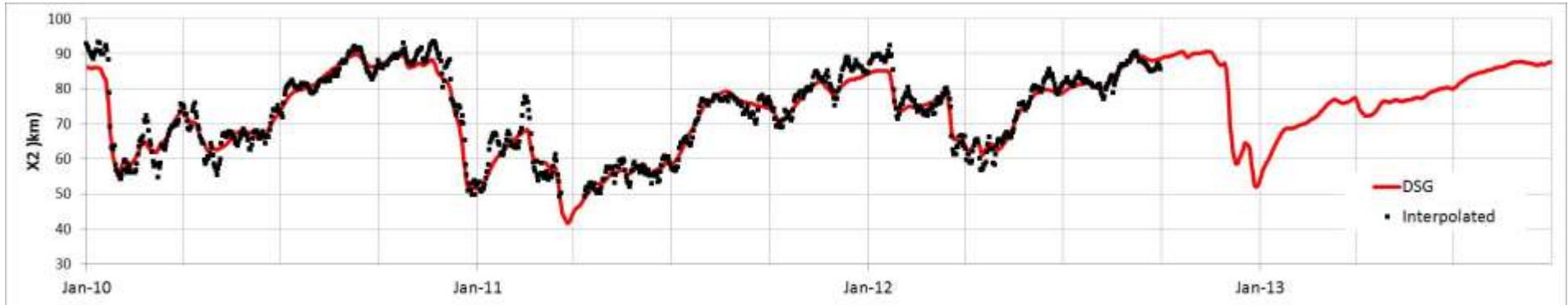


Figure D-10: Time Series of DSG Predicted and Interpolated San Joaquin Branch X2 Position: 2010-2013

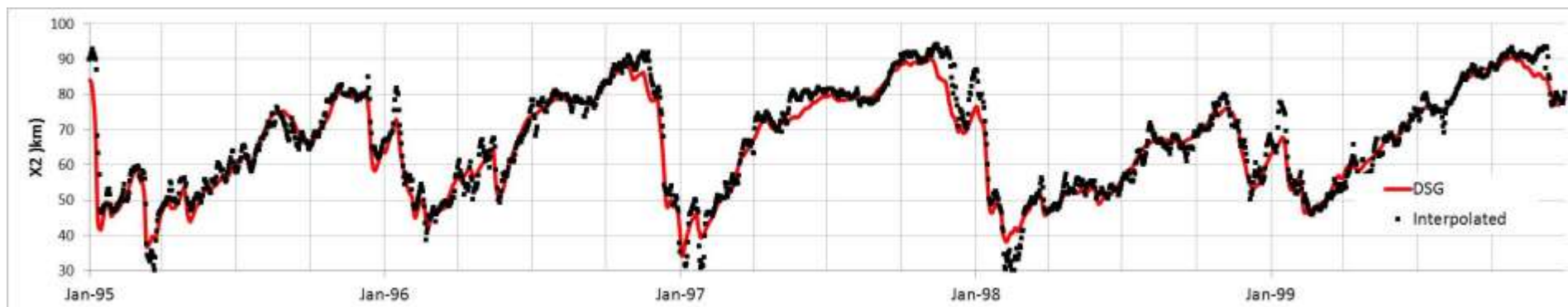
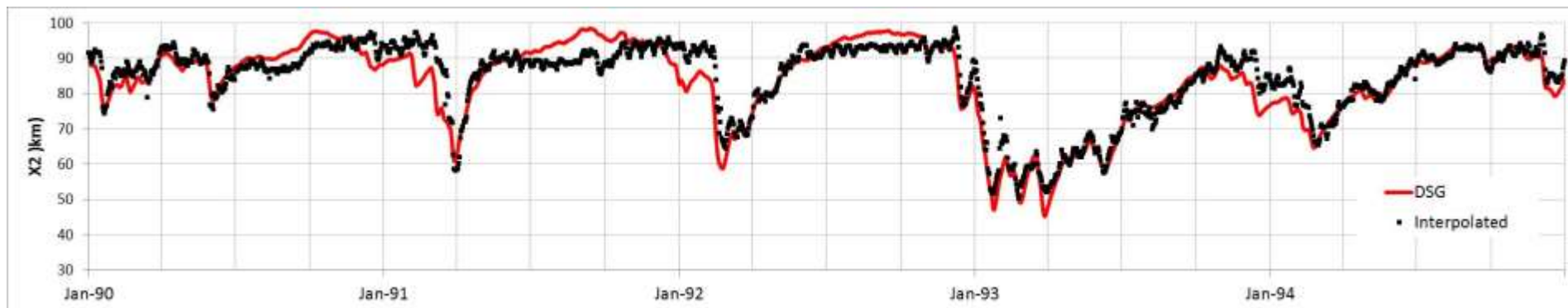


Figure D-11: Time Series of DSG Predicted and Interpolated San Joaquin Branch X2 Position: 1990-1999

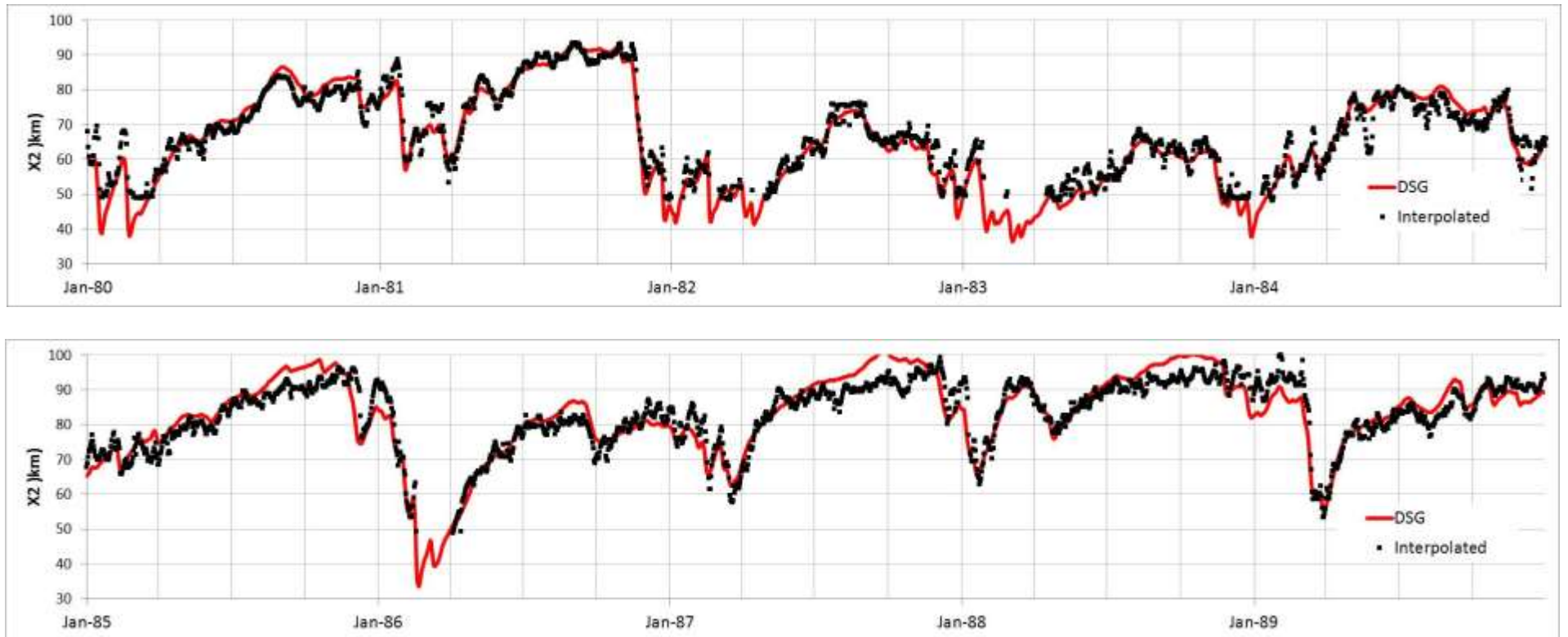


Figure D-12: Time Series of DSG Predicted and Interpolated San Joaquin Branch X2 Position: 1980-1989

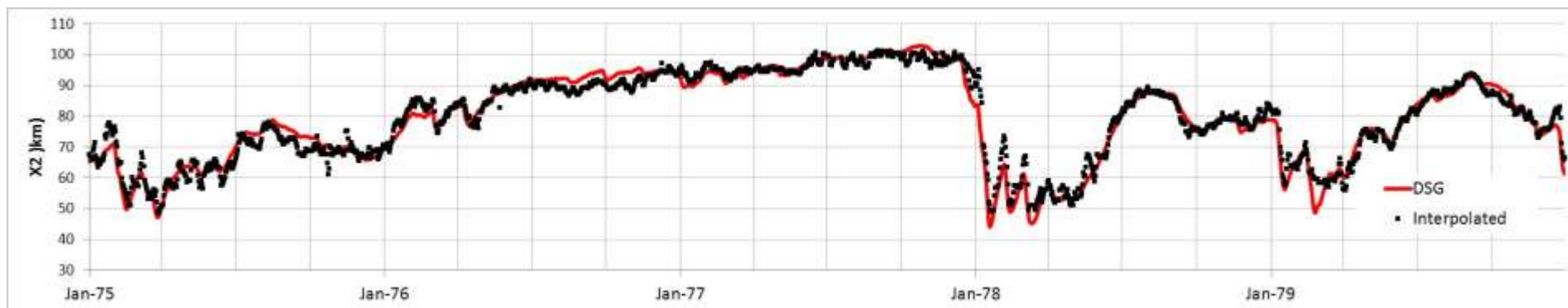
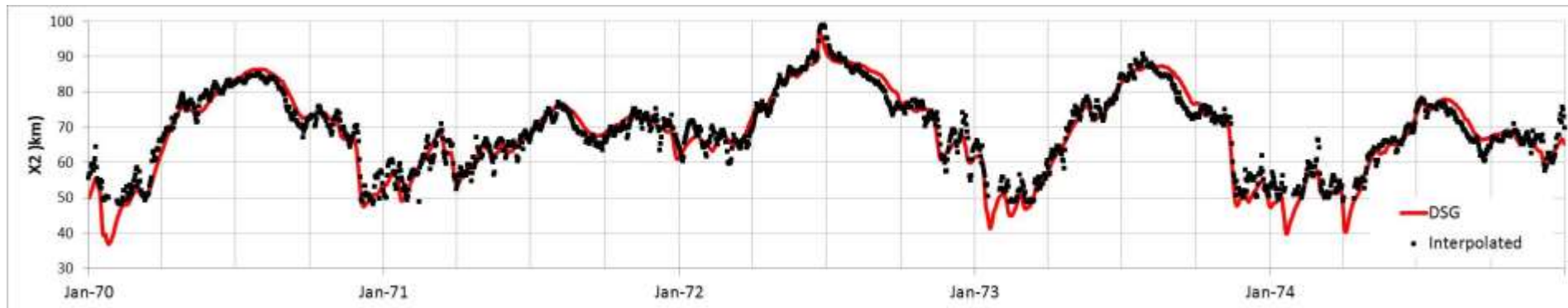


Figure D-13: Time Series of DSG Predicted and Interpolated San Joaquin Branch X2 Position: 1970-1979

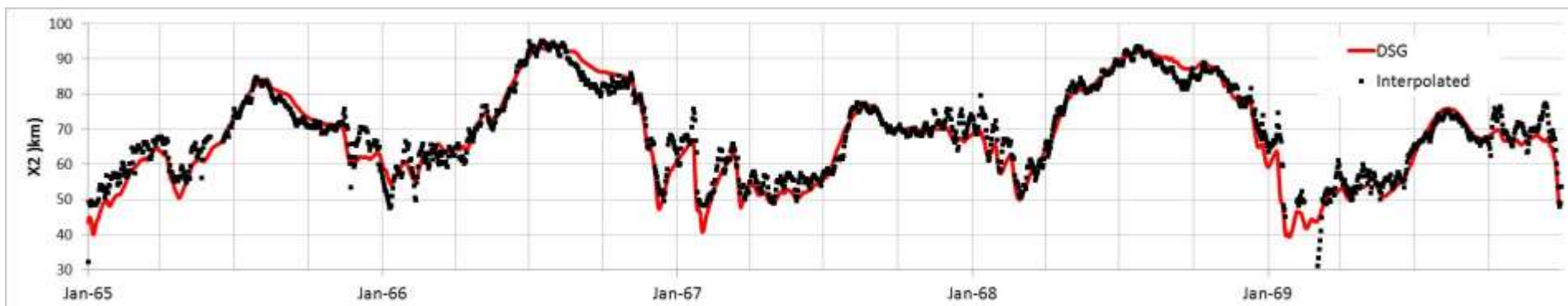
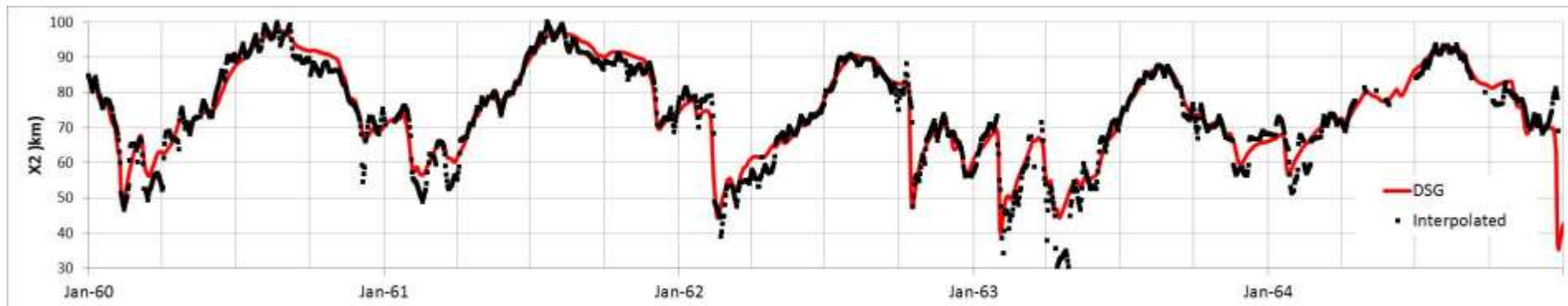


Figure D-14: Time Series of DSG Predicted and Interpolated San Joaquin Branch X2 Position: 1960-1969

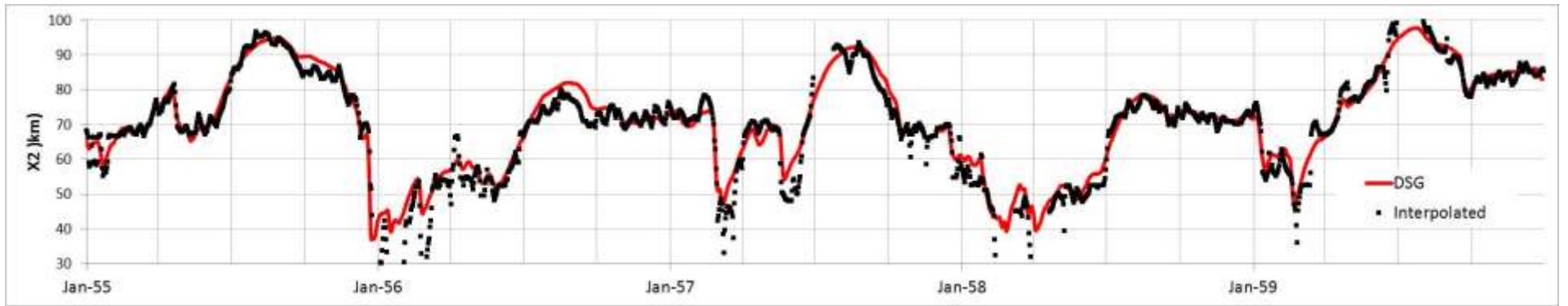
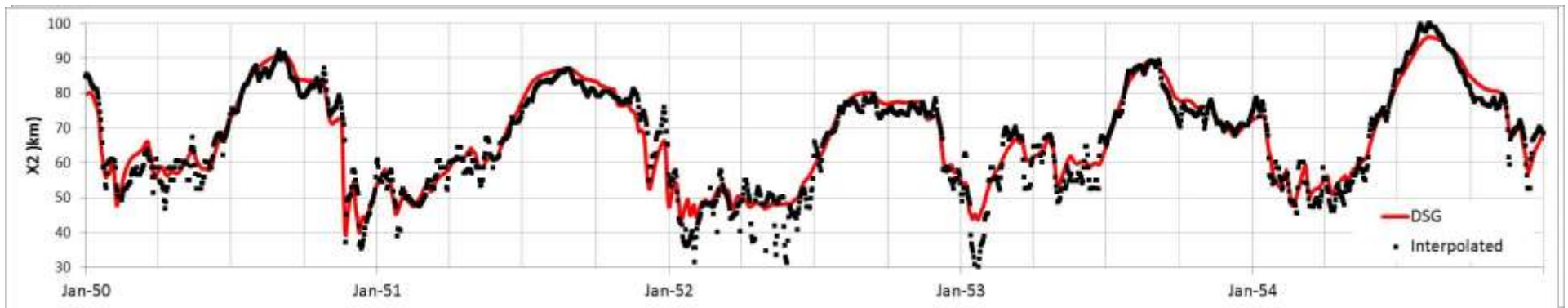


Figure D-15: Time Series of DSG Predicted and Interpolated San Joaquin Branch X2 Position: 1950-1959

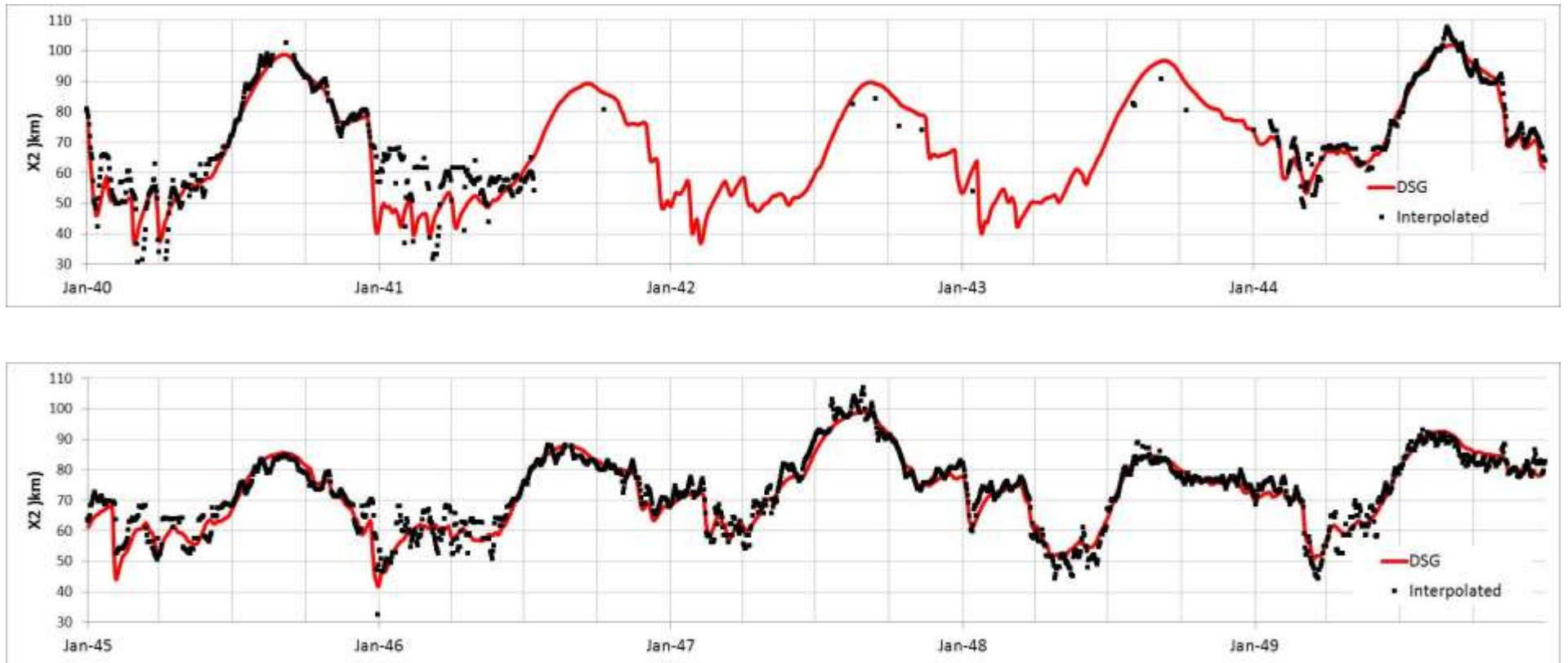


Figure D-16: Time Series of DSG Predicted and Interpolated San Joaquin Branch X2 Position: 1940-1949

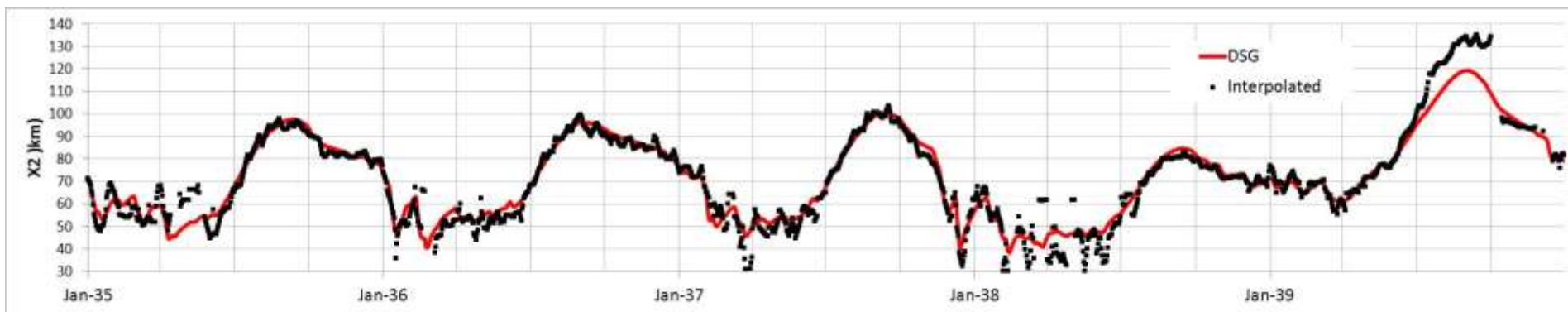
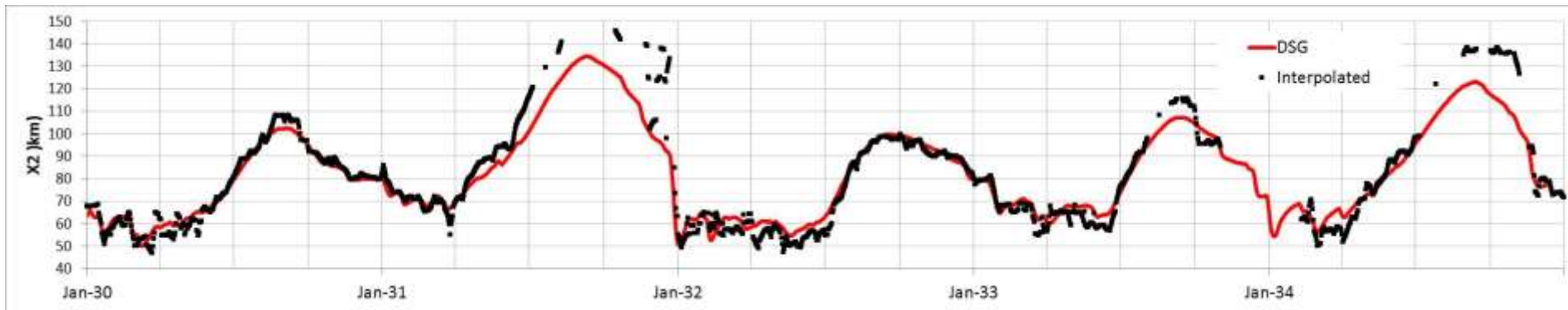


Figure D-17: Time Series of DSG Predicted and Interpolated San Joaquin Branch X2 Position: 1930-1939

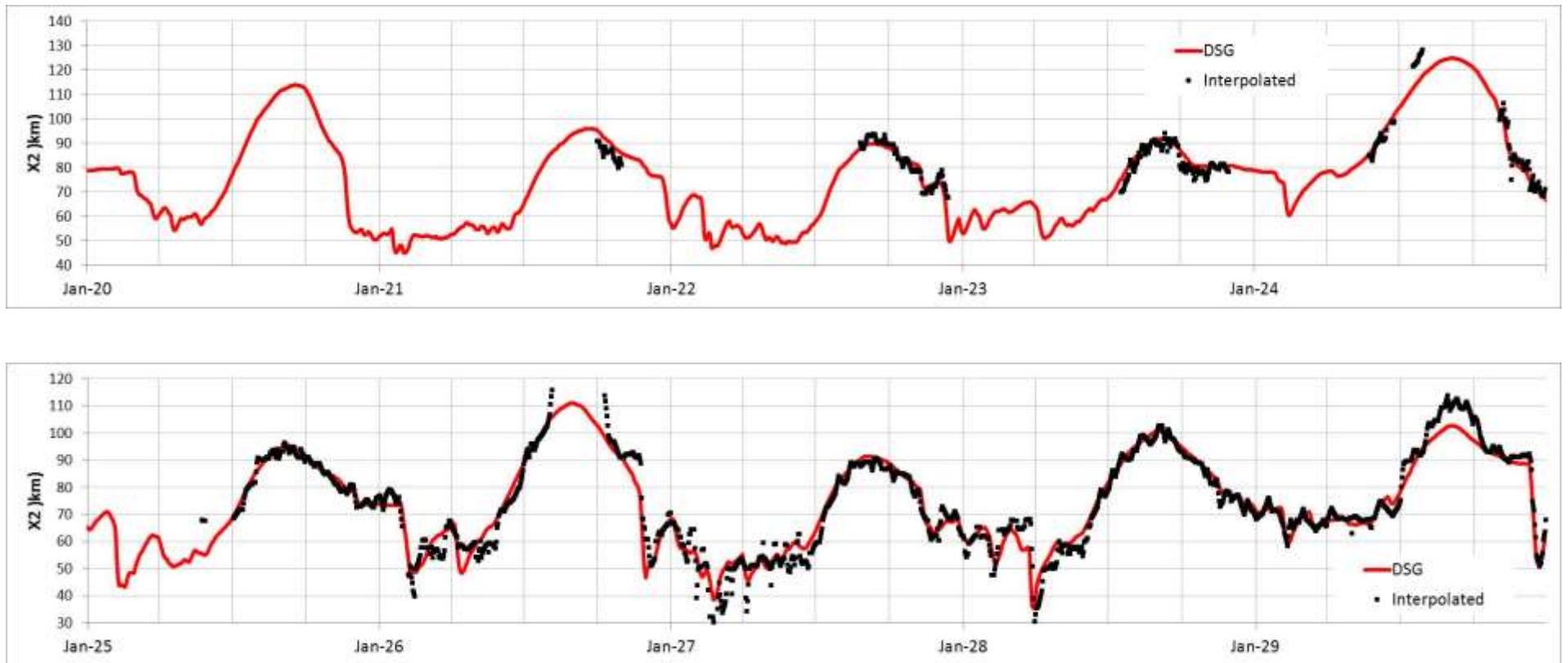


Figure D-18: Time Series of DSG Predicted and Interpolated San Joaquin Branch X2 Position: 1920-1929

Appendix E: Time Series Plots – DSG Model Validation with Observed Salinity Data

This appendix provides time series plots comparing DSG and observed salinity for the validation period by decade (2010-13, 1990-99, 1980-89, 1970-79, 1960-69, 1950-59, 1940-49, 1930-39 and 1920-29) at the following locations: Martinez, Port Chicago, Mallard Island, Collinsville, Emmaton, Pittsburg, Antioch and Jersey Point.

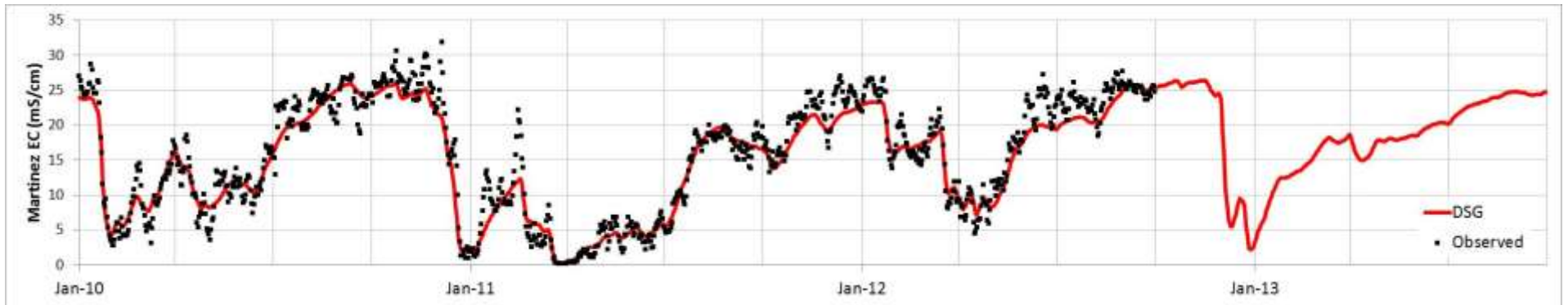


Figure E-1: Time Series of DSG Predicted and Observed Surface Salinity at Martinez: 2010-2013

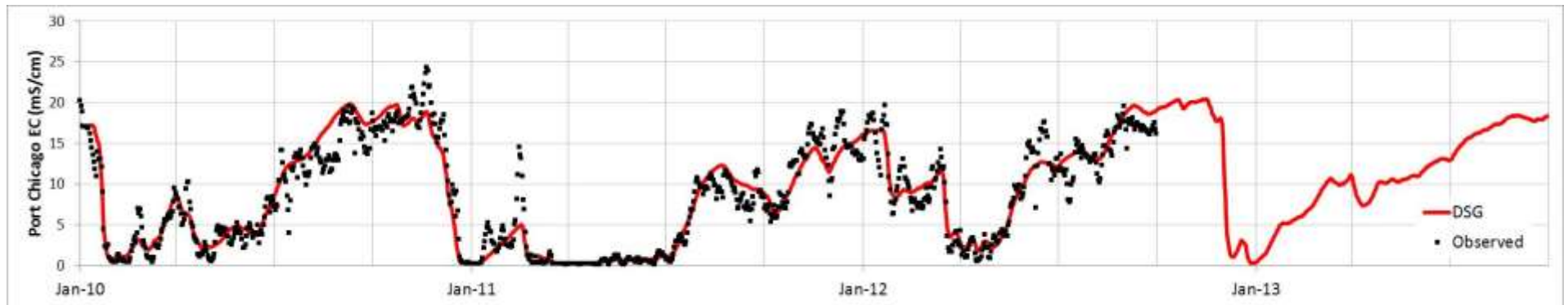


Figure E-2: Time Series of DSG Predicted and Observed Surface Salinity at Port Chicago: 2010-2013

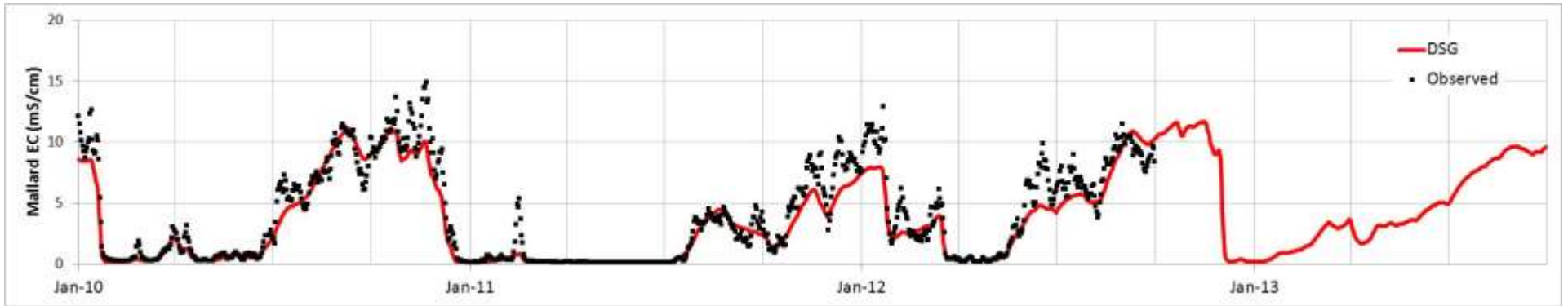


Figure E-3: Time Series of DSG Predicted and Observed Surface Salinity at Mallard Island: 2010-2013

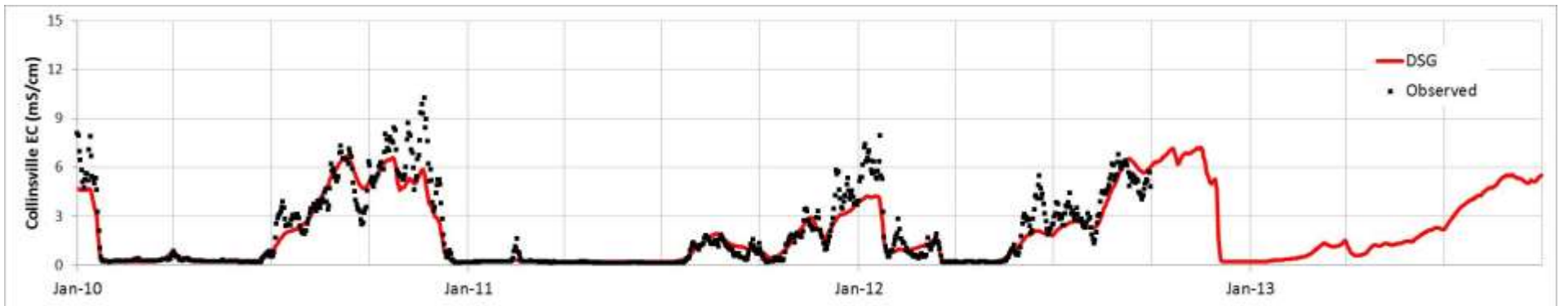


Figure E-4: Time Series of DSG Predicted and Observed Surface Salinity at Collinsville: 2010-2013

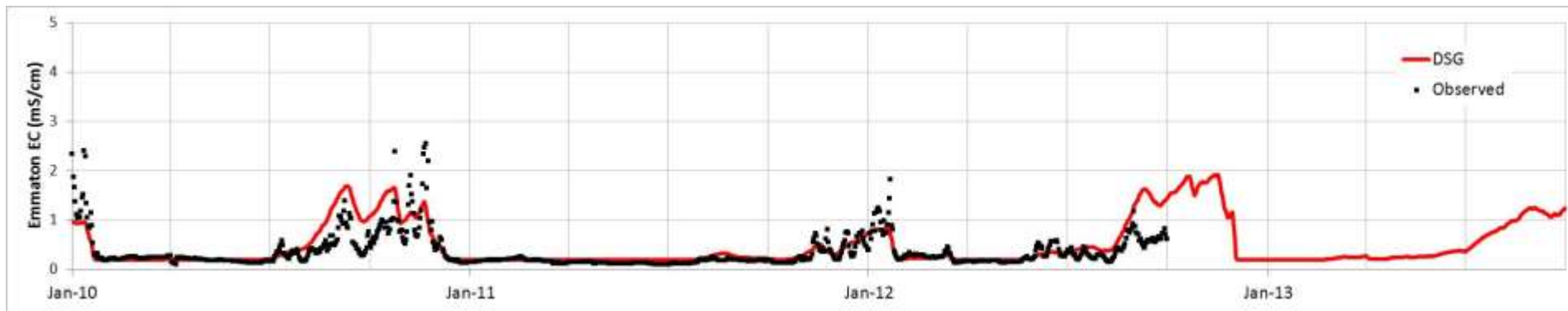


Figure E-5: Time Series of DSG Predicted and Observed Surface Salinity at Emmaton: 2010-2013

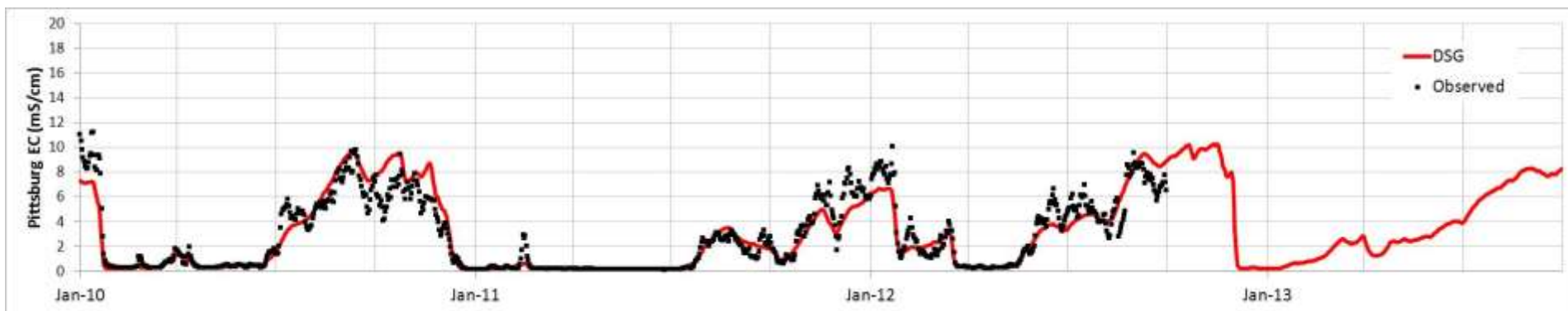


Figure E-6: Time Series of DSG Predicted and Observed Surface Salinity at Pittsburg: 2010-2013

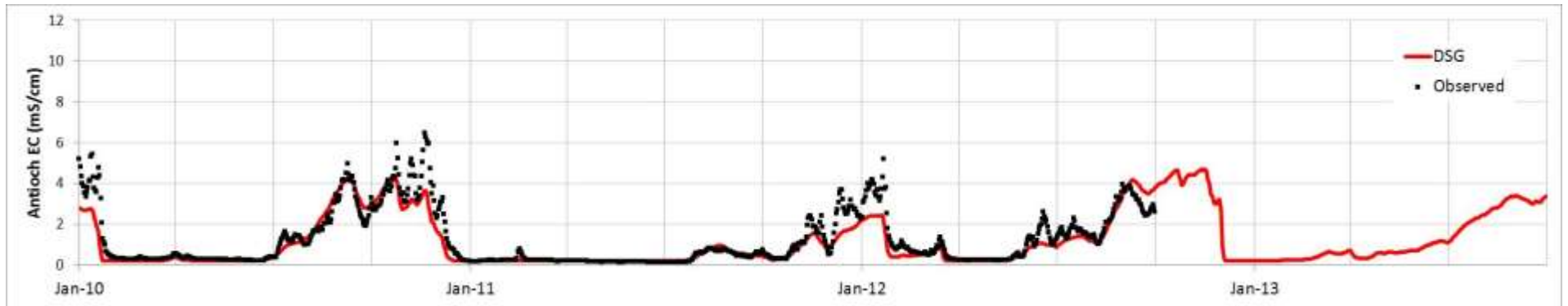


Figure E-7: Time Series of DSG Predicted and Observed Surface Salinity at Antioch: 2010-2013

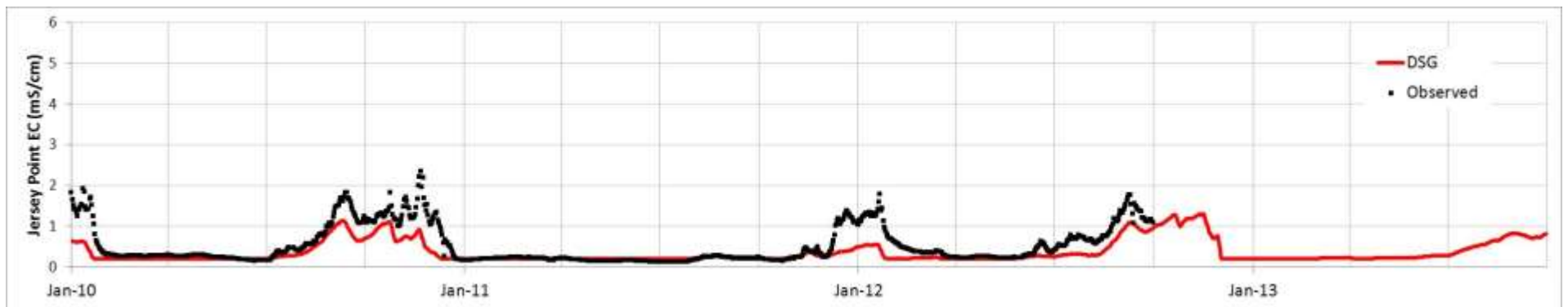


Figure E-8: Time Series of DSG Predicted and Observed Surface Salinity at Jersey Point: 2010-2013

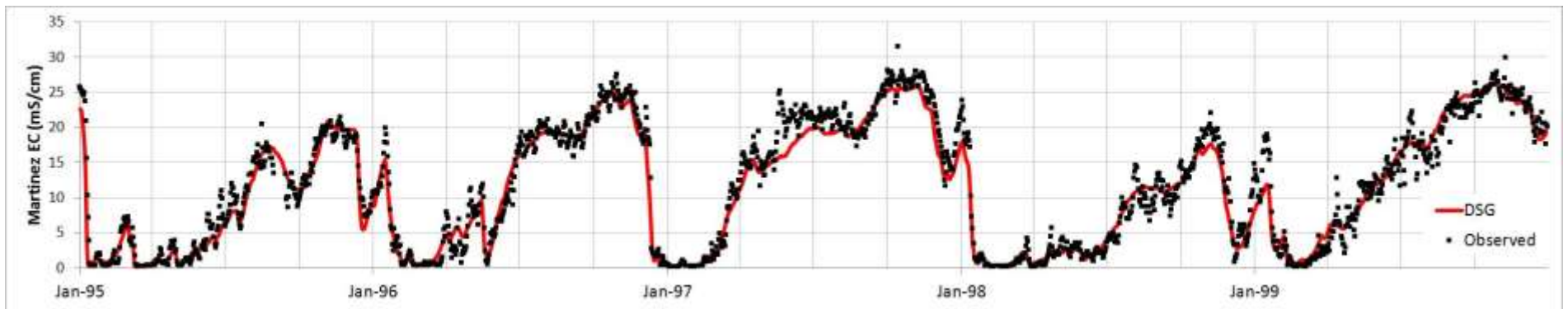
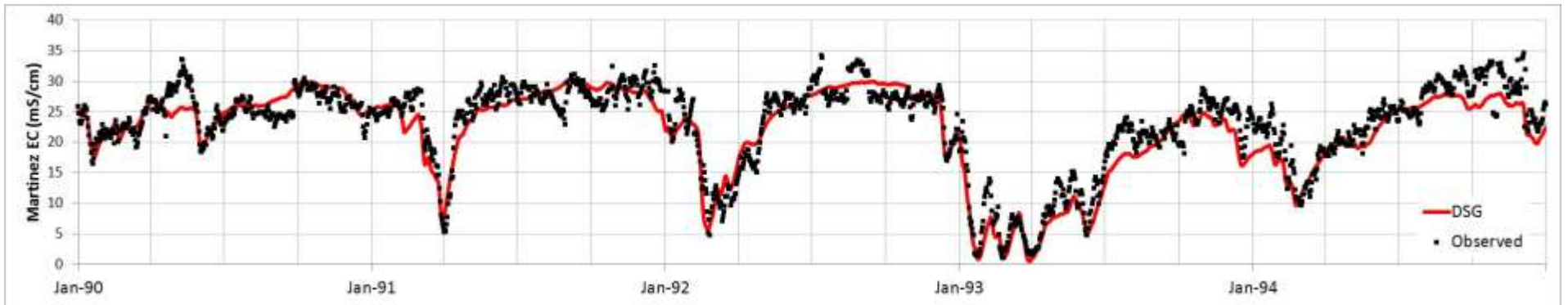


Figure E-9: Time Series of DSG Predicted and Observed Surface Salinity at Martinez: 1990-1999

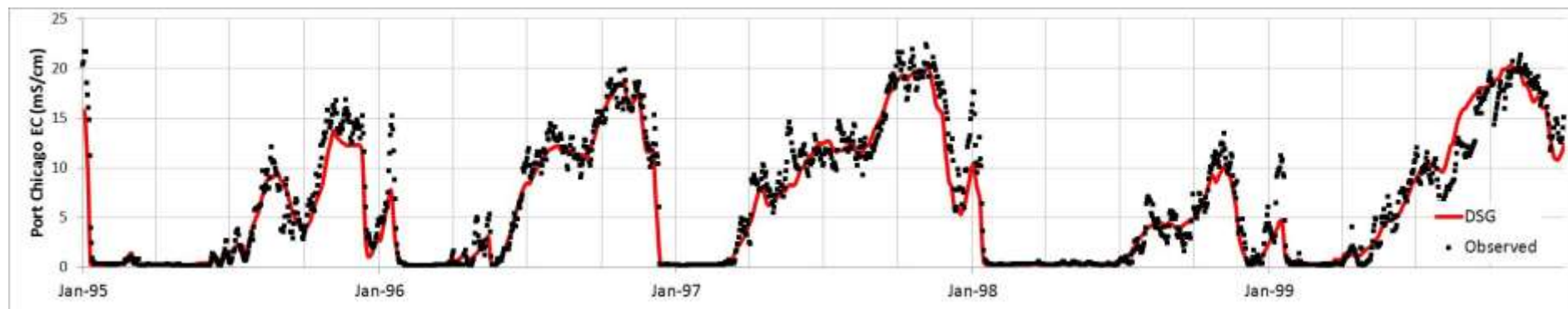
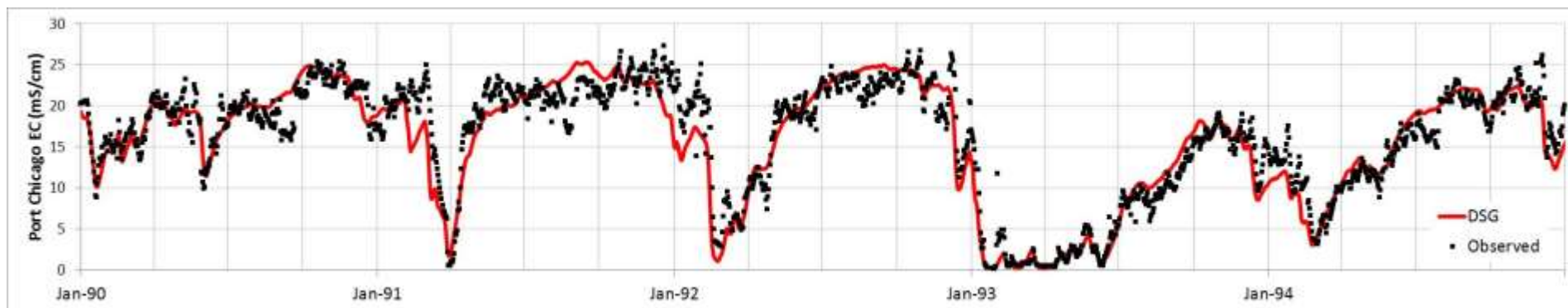


Figure E-10: Time Series of DSG Predicted and Observed Surface Salinity at Port Chicago: 1990-1999

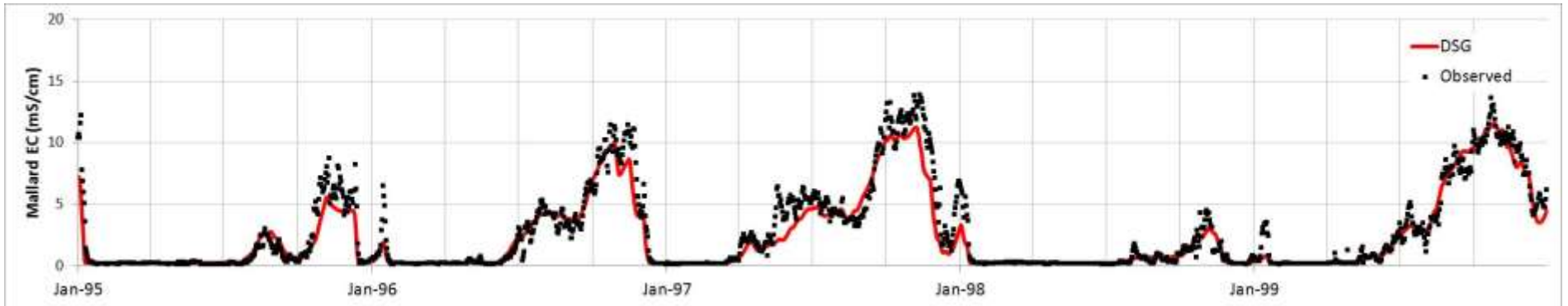
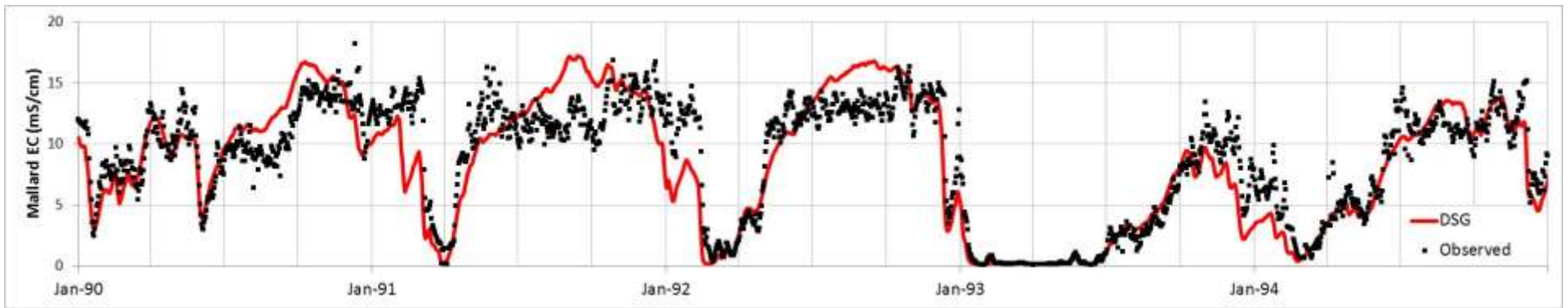


Figure E-11: Time Series of DSG Predicted and Observed Surface Salinity at Mallard Island: 1990-1999

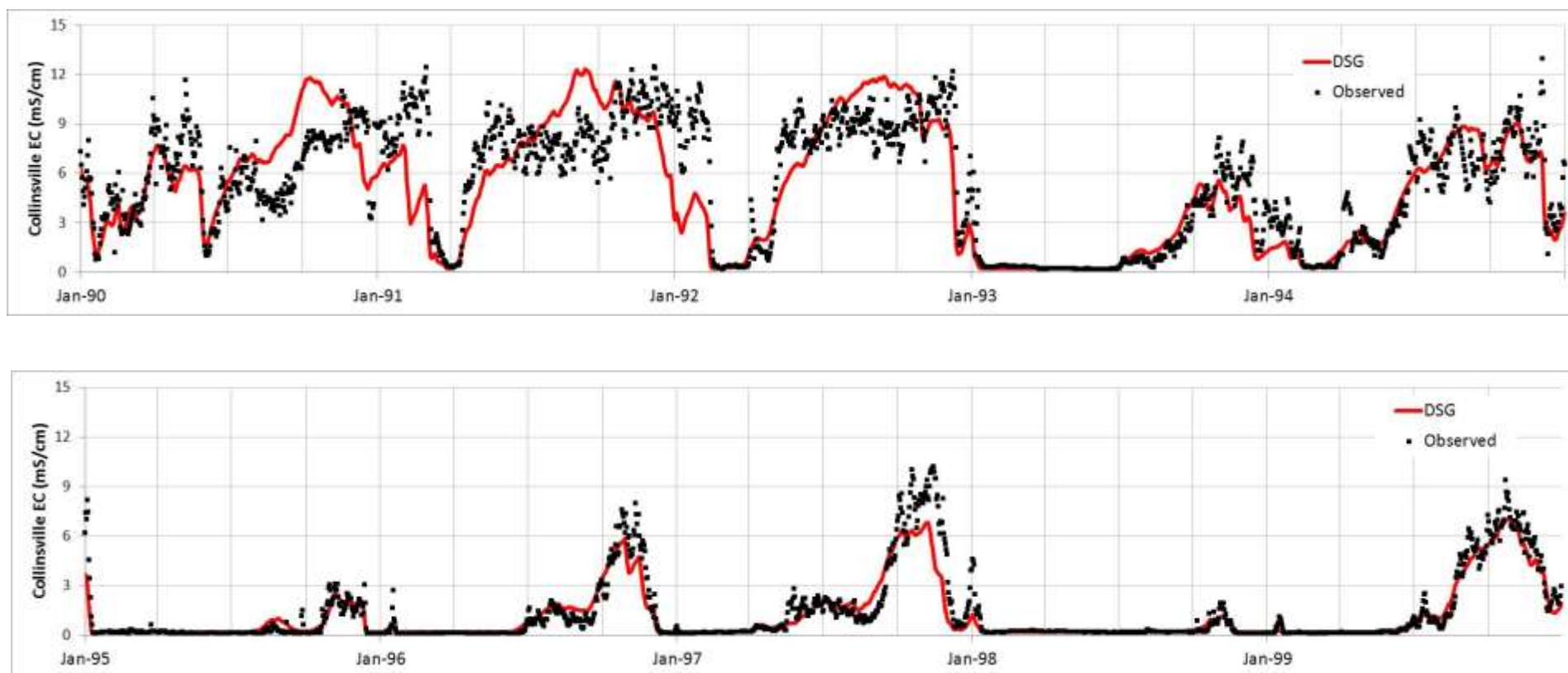


Figure E-12: Time Series of DSG Predicted and Observed Surface Salinity at Collinsville: 1990-1999

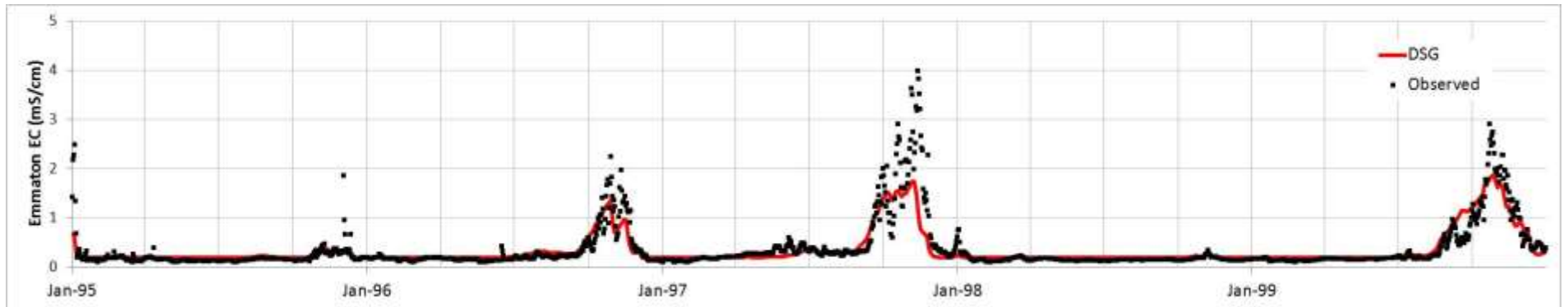
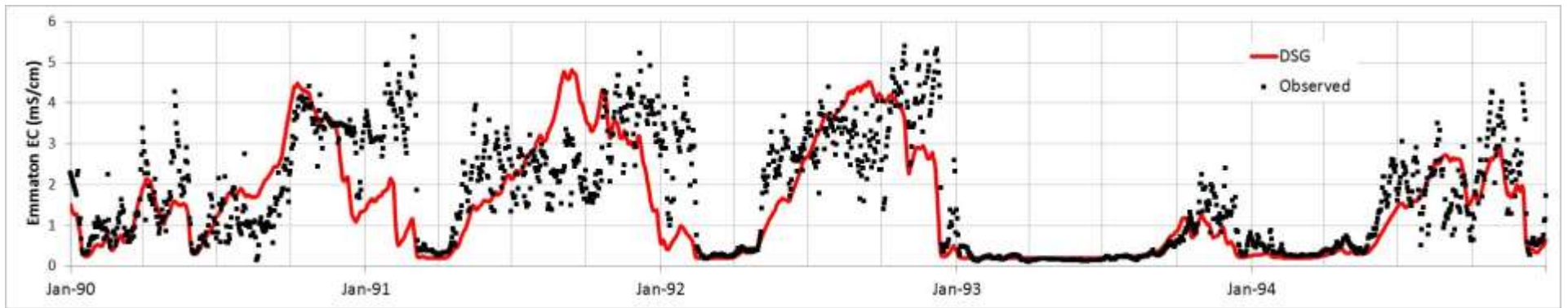


Figure E-13: Time Series of DSG Predicted and Observed Surface Salinity at Emmaton: 1990-1999

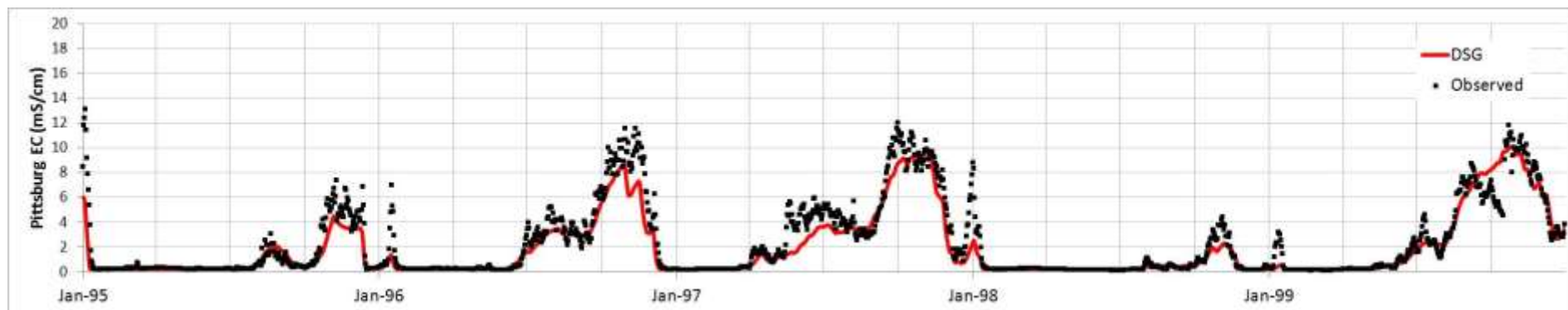
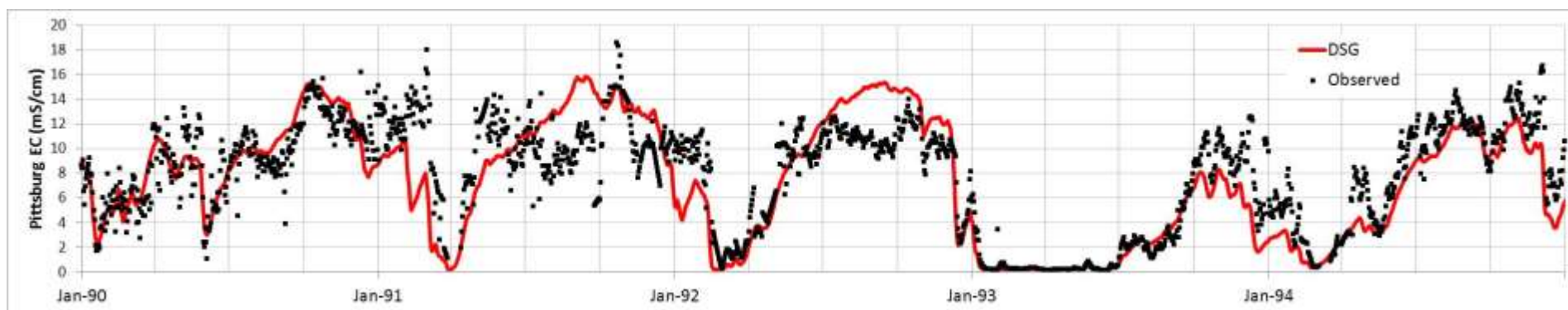


Figure E-14: Time Series of DSG Predicted and Observed Surface Salinity at Pittsburgh: 1990-1999

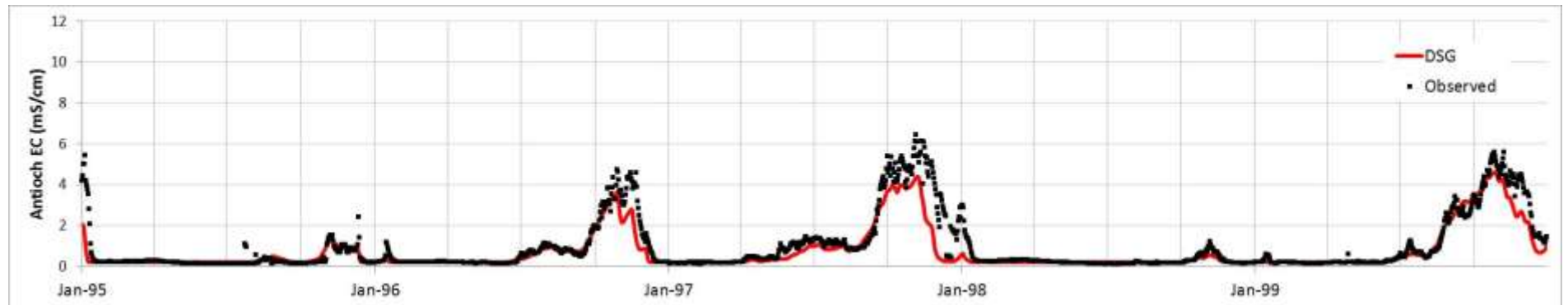
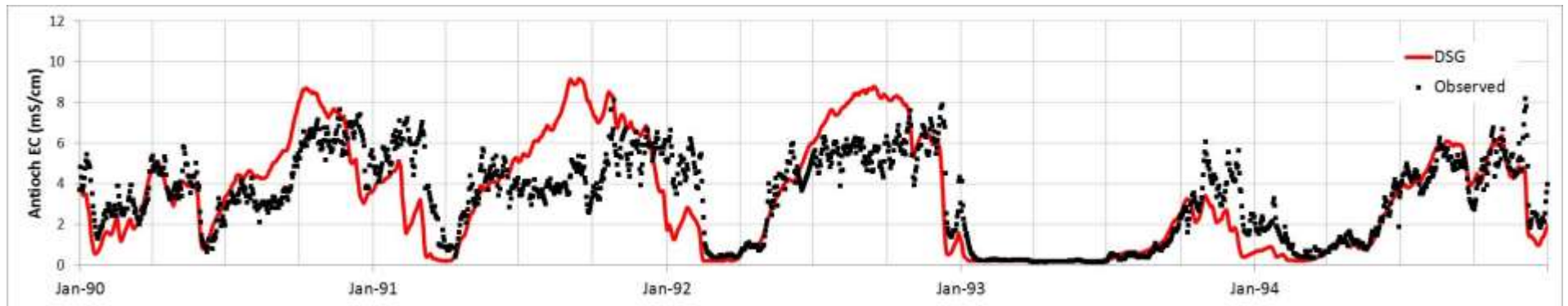


Figure E-15: Time Series of DSG Predicted and Observed Surface Salinity at Antioch: 1990-1999

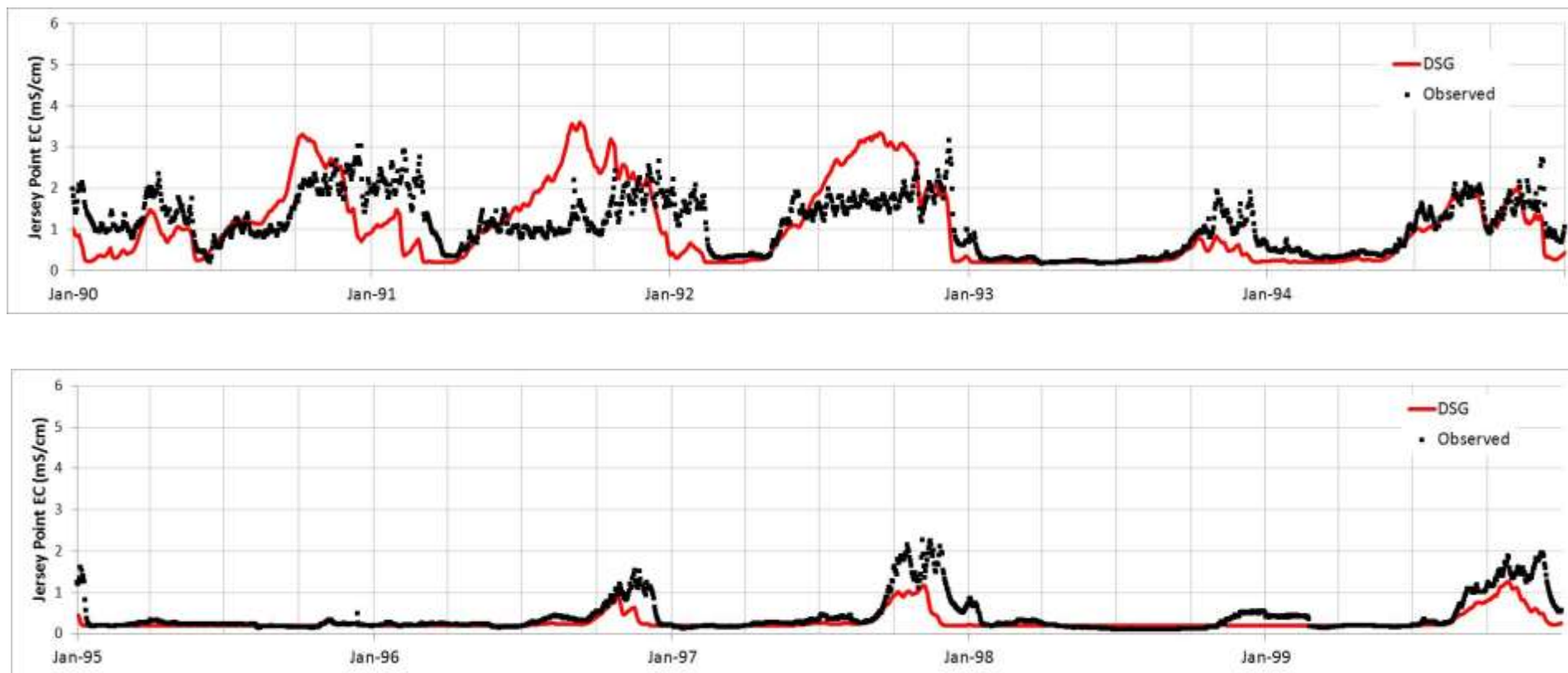


Figure E-16: Time Series of DSG Predicted and Observed Surface Salinity at Jersey Point: 1990-1999

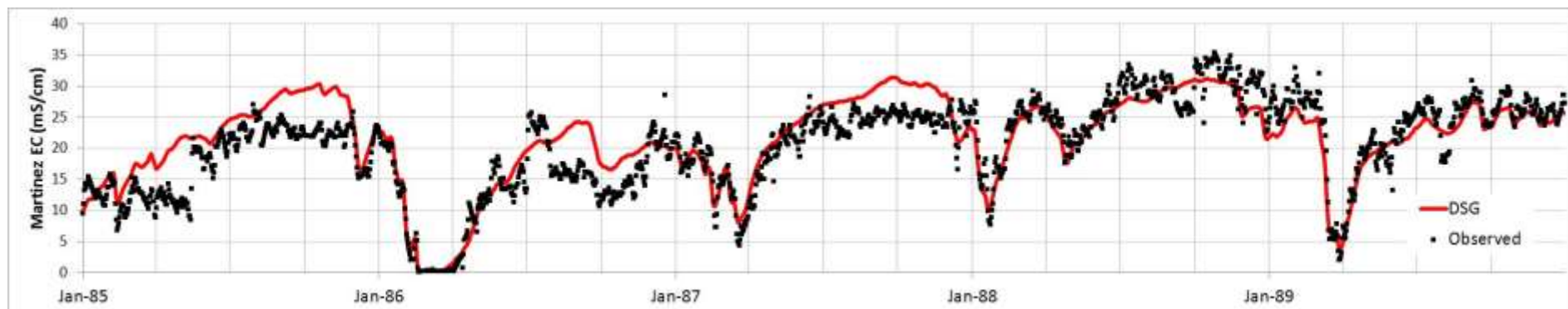
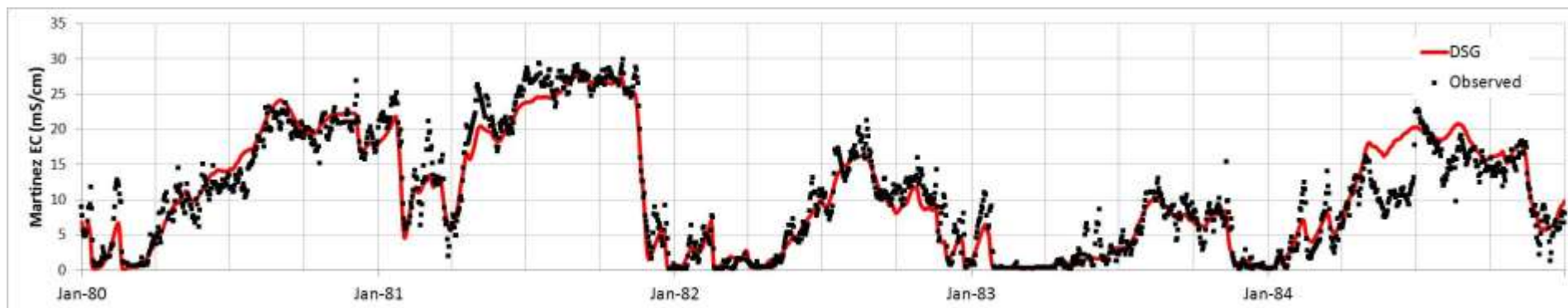


Figure E-17: Time Series of DSG Predicted and Observed Surface Salinity at Martinez: 1980-1989

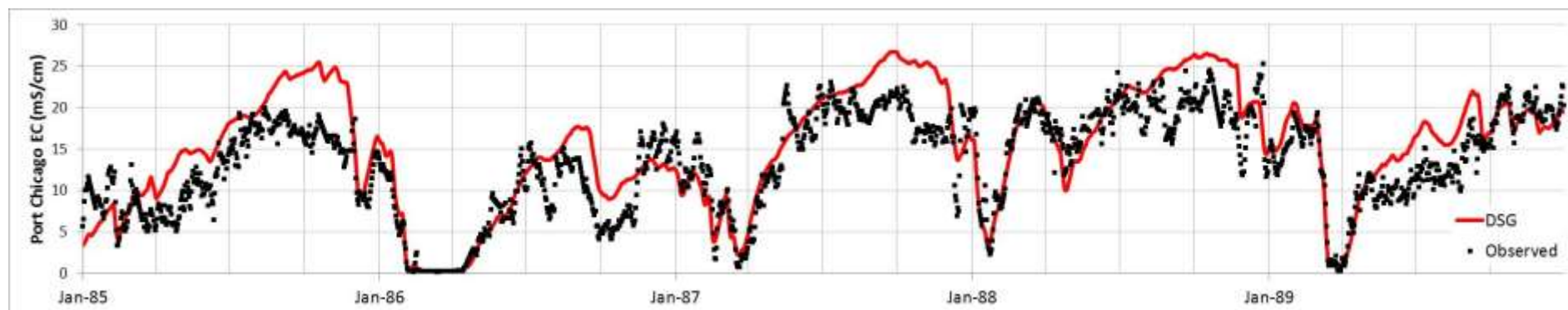
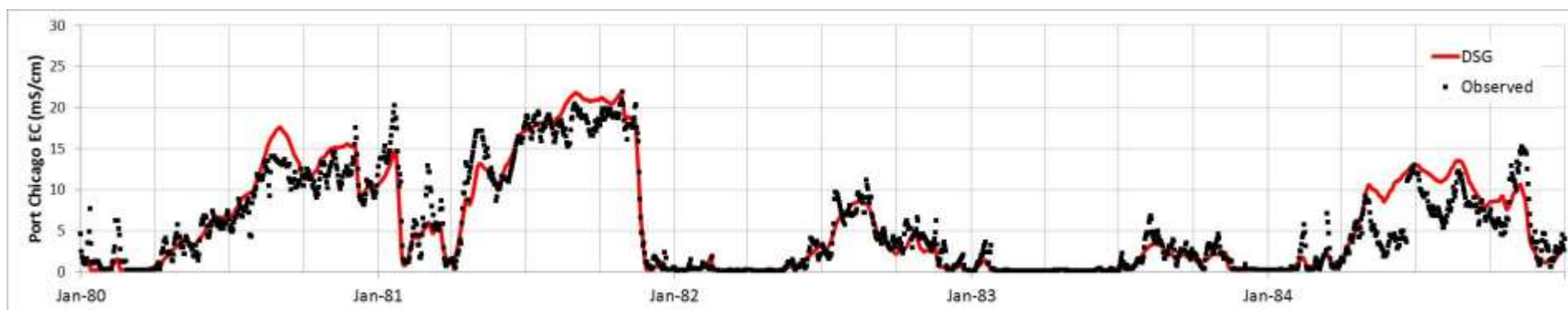


Figure E-18: Time Series of DSG Predicted and Observed Surface Salinity at Port Chicago: 1980-1989

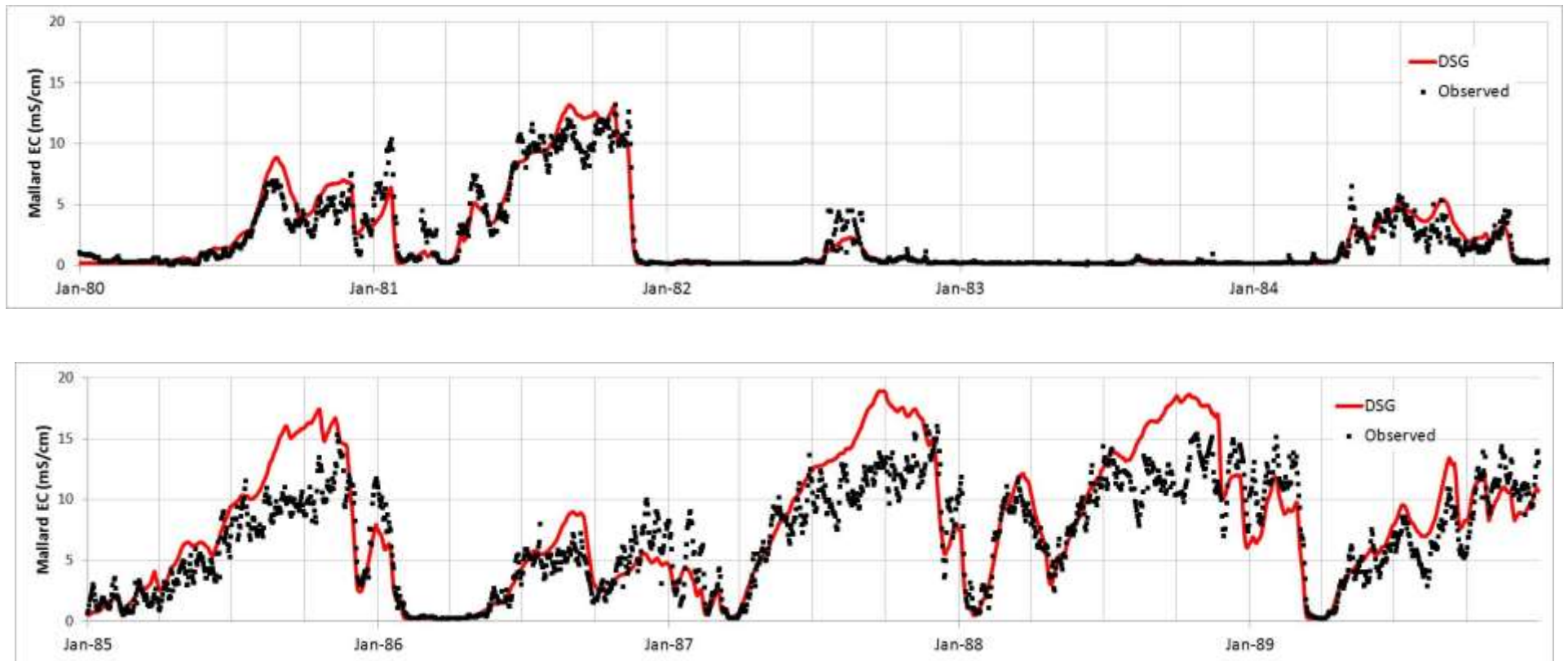


Figure E-19: Time Series of DSG Predicted and Observed Surface Salinity at Mallard Island: 1980-1989

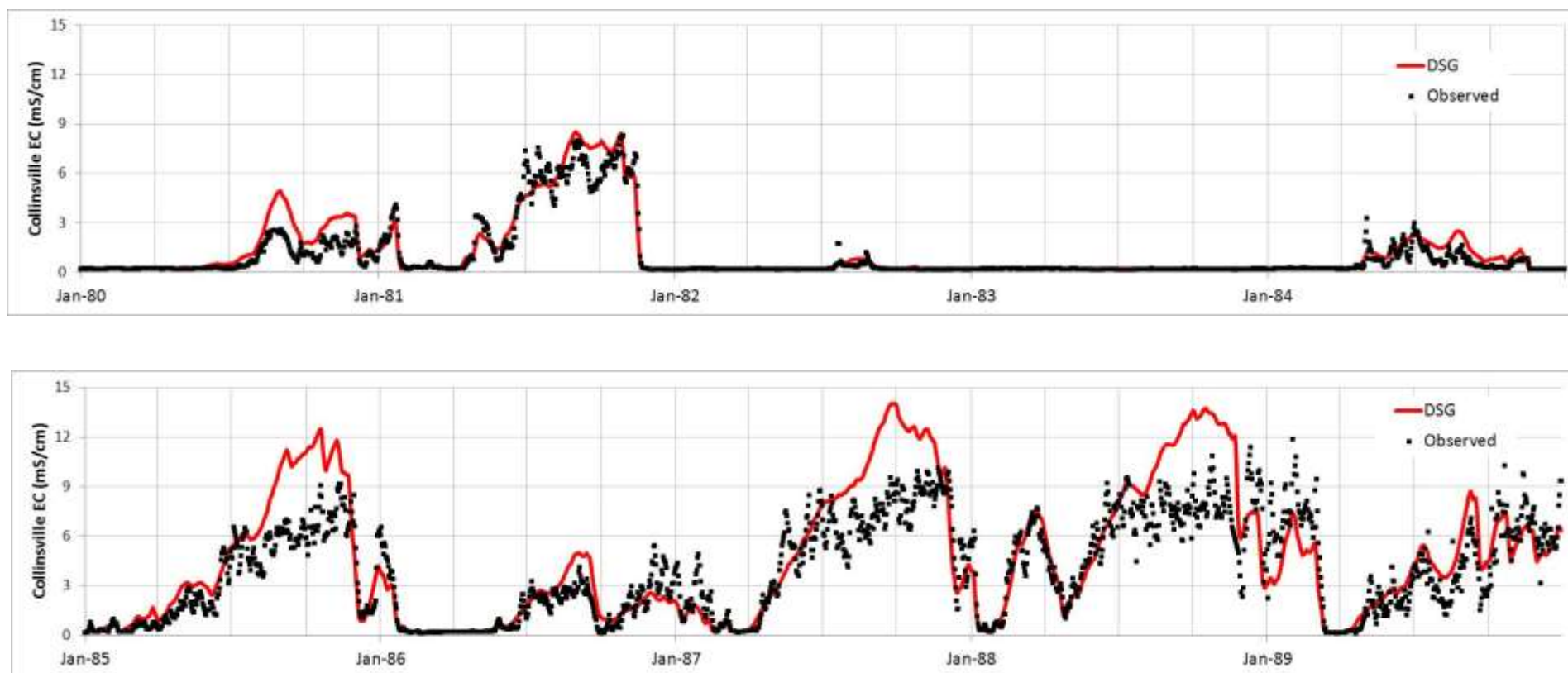


Figure E-20: Time Series of DSG Predicted and Observed Surface Salinity at Collinsville: 1980-1989

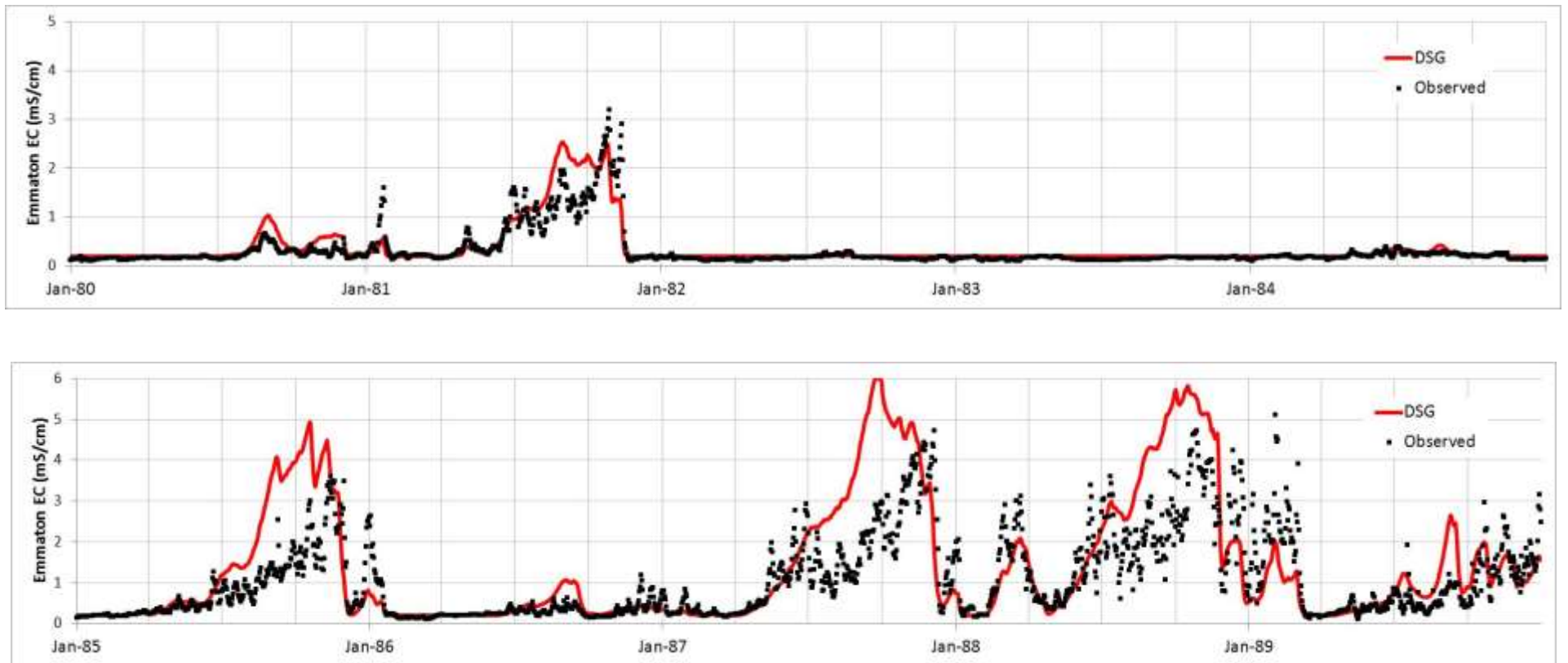


Figure E-21: Time Series of DSG Predicted and Observed Surface Salinity at Emmaton: 1980-1989

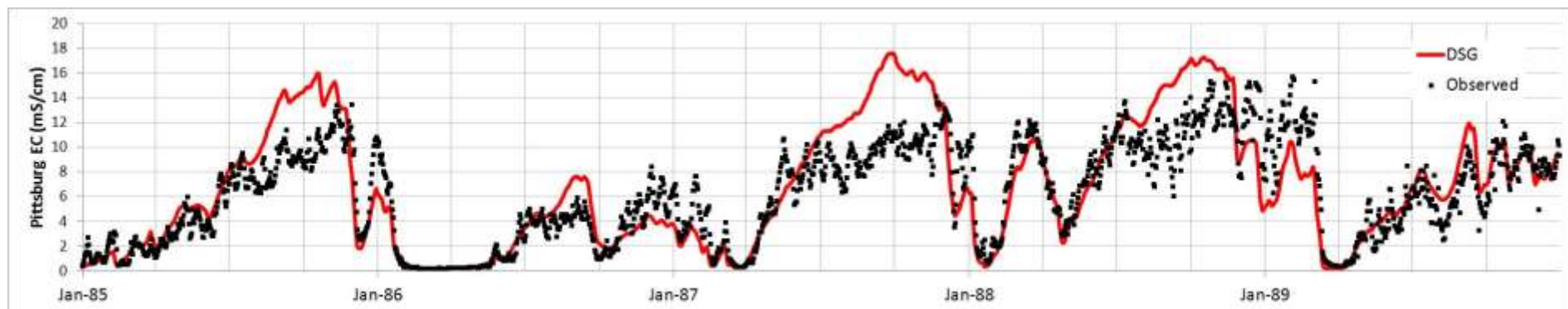
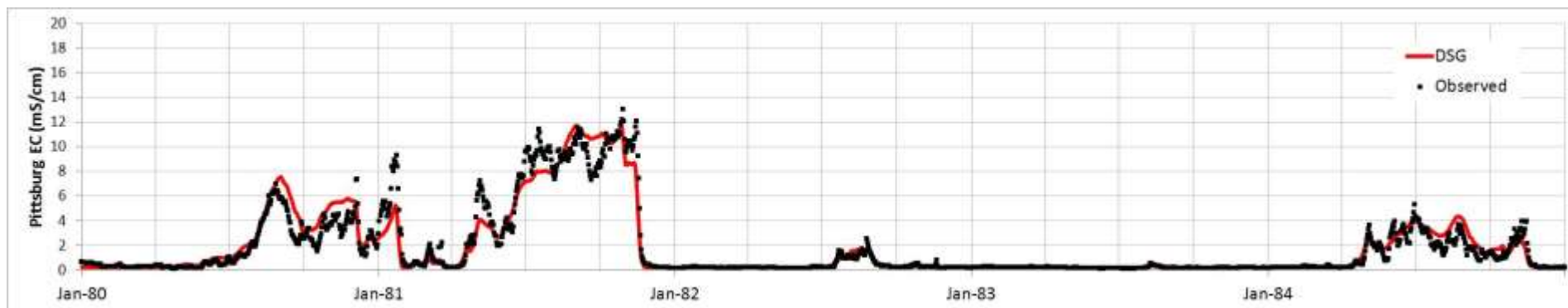


Figure E-22: Time Series of DSG Predicted and Observed Surface Salinity at Pittsburg: 1980-1989

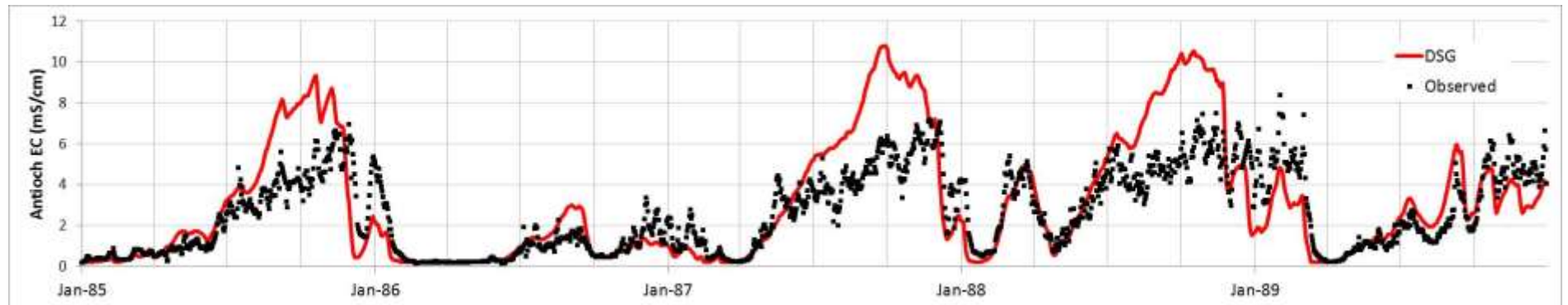
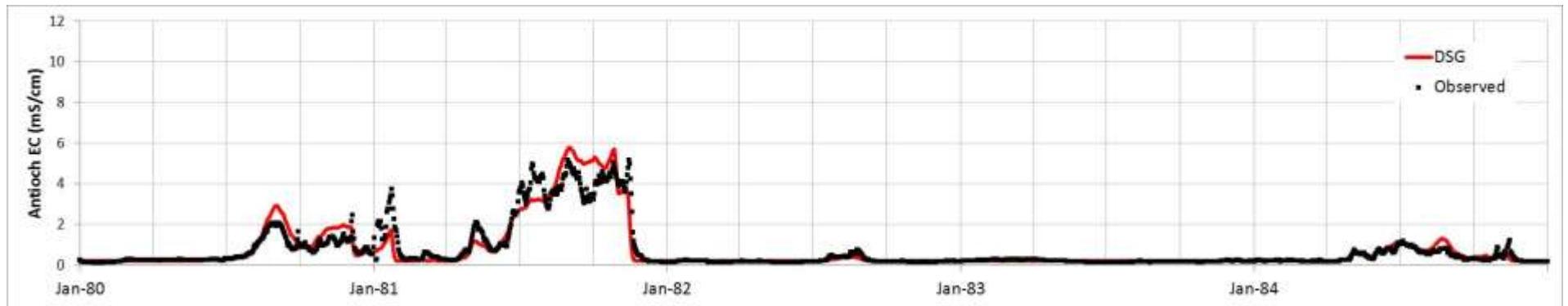


Figure E-23: Time Series of DSG Predicted and Observed Surface Salinity at Antioch: 1980-1989

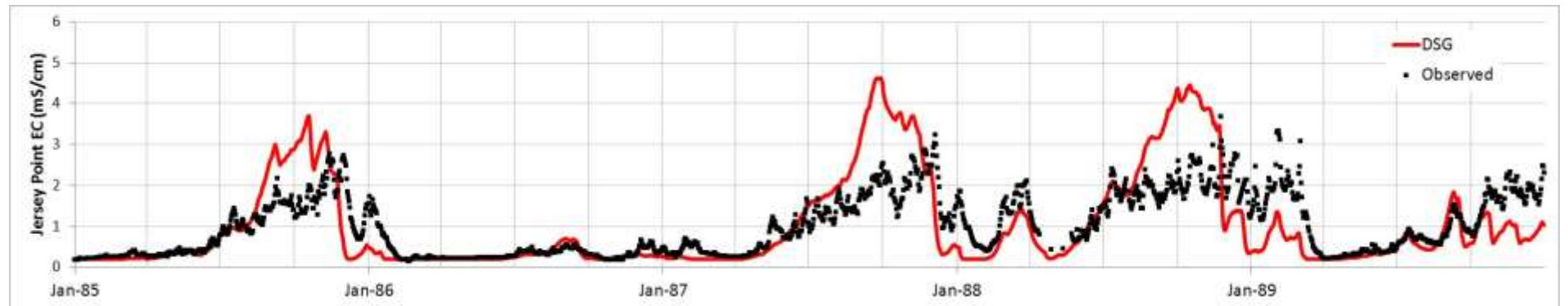
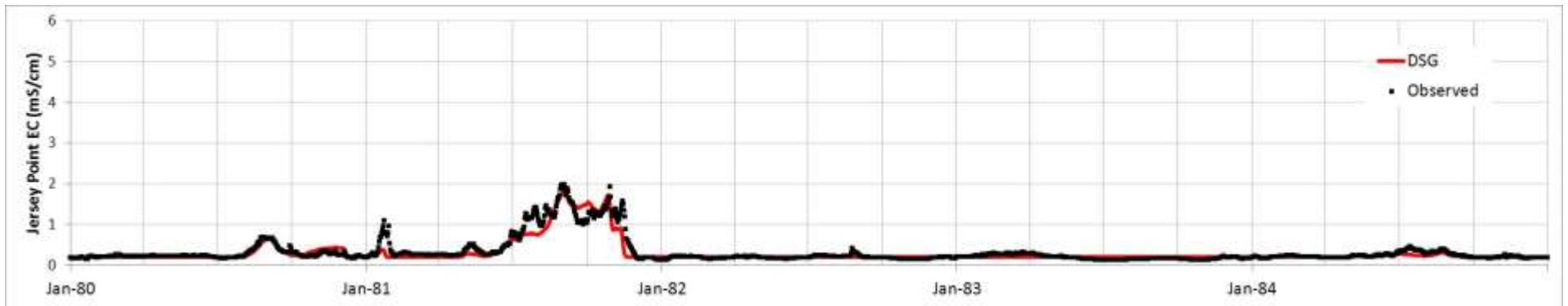


Figure E-24: Time Series of DSG Predicted and Observed Surface Salinity at Jersey Point: 1980-1989

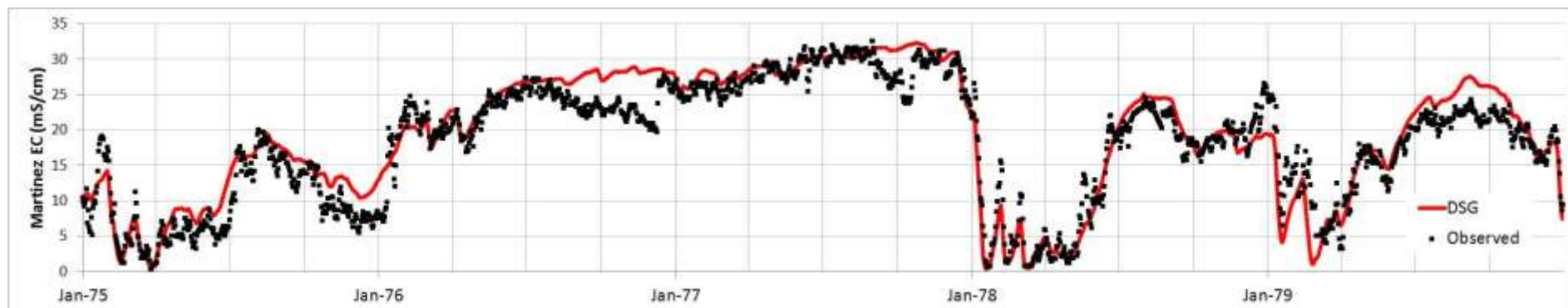
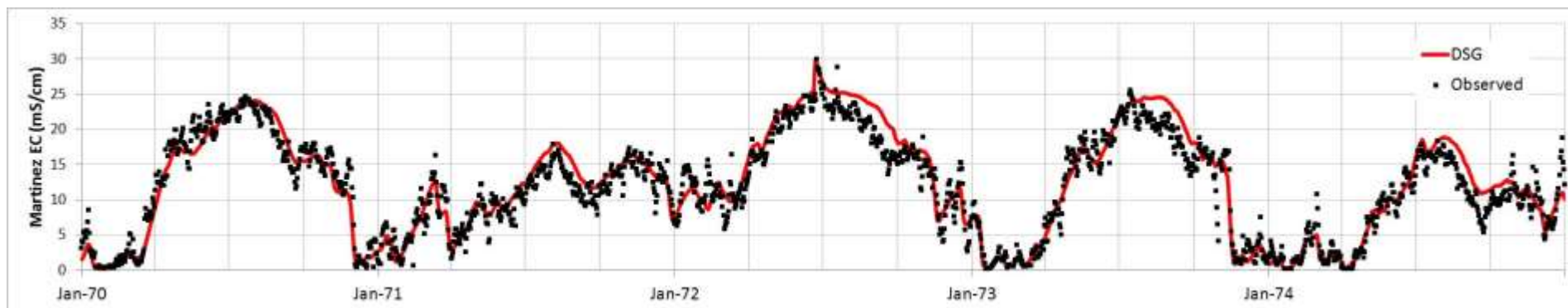


Figure E-25: Time Series of DSG Predicted and Observed Surface Salinity at Martinez: 1970-1979

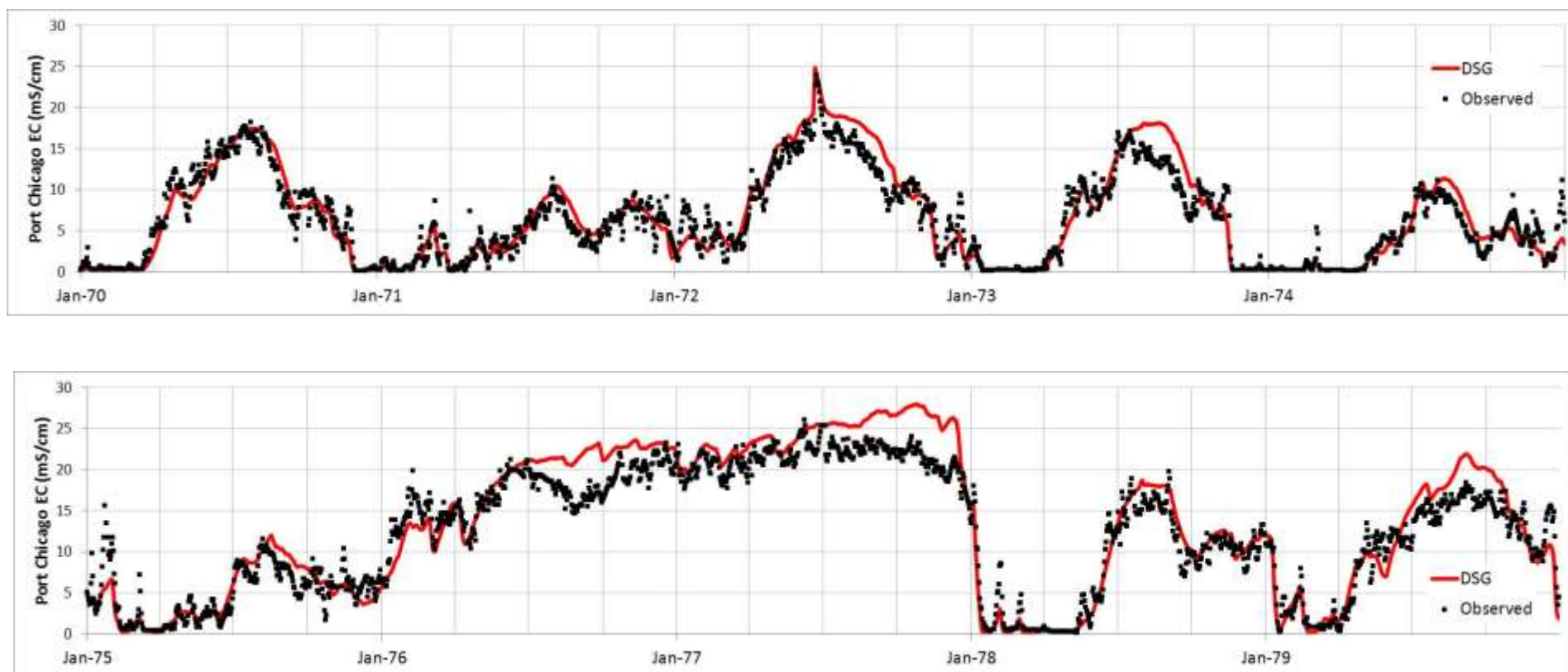


Figure E-26: Time Series of DSG Predicted and Observed Surface Salinity at Port Chicago: 1970-1979

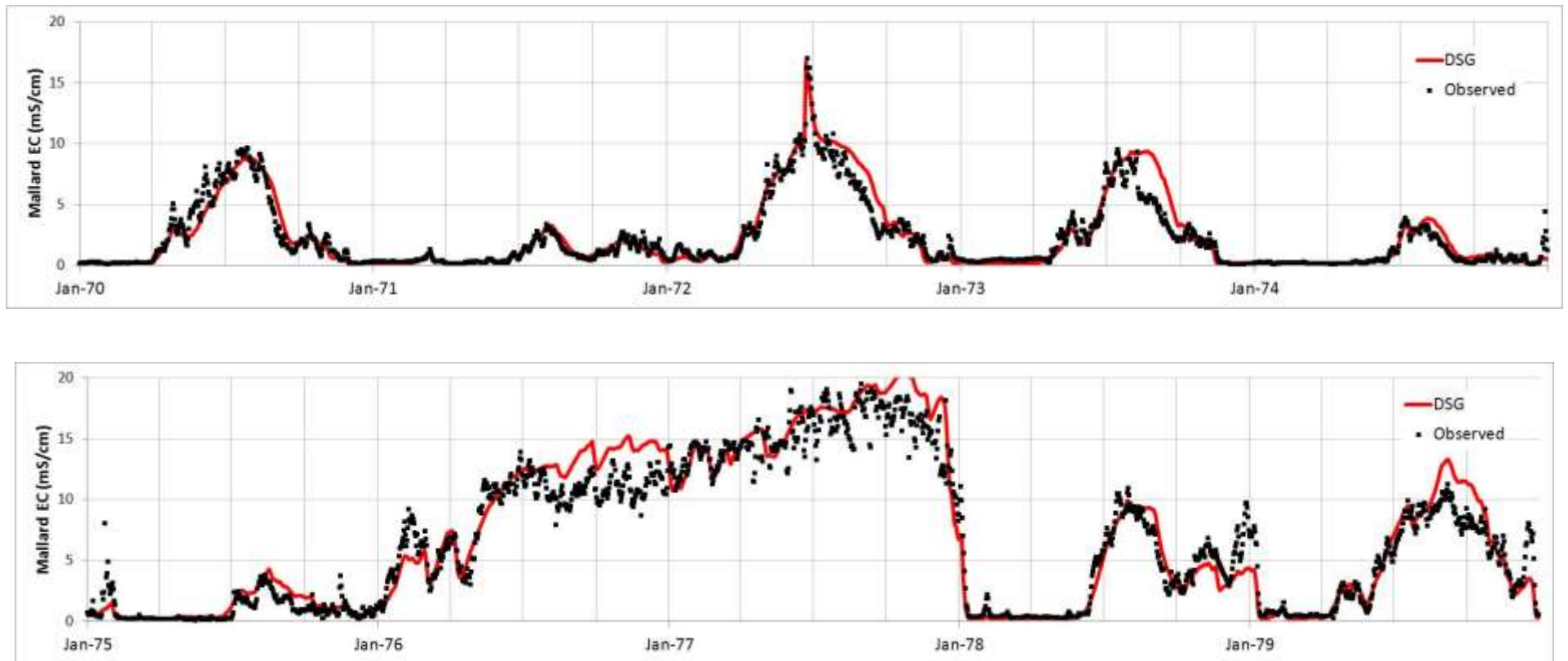


Figure E-27: Time Series of DSG Predicted and Observed Surface Salinity at Mallard Island: 1970-1979

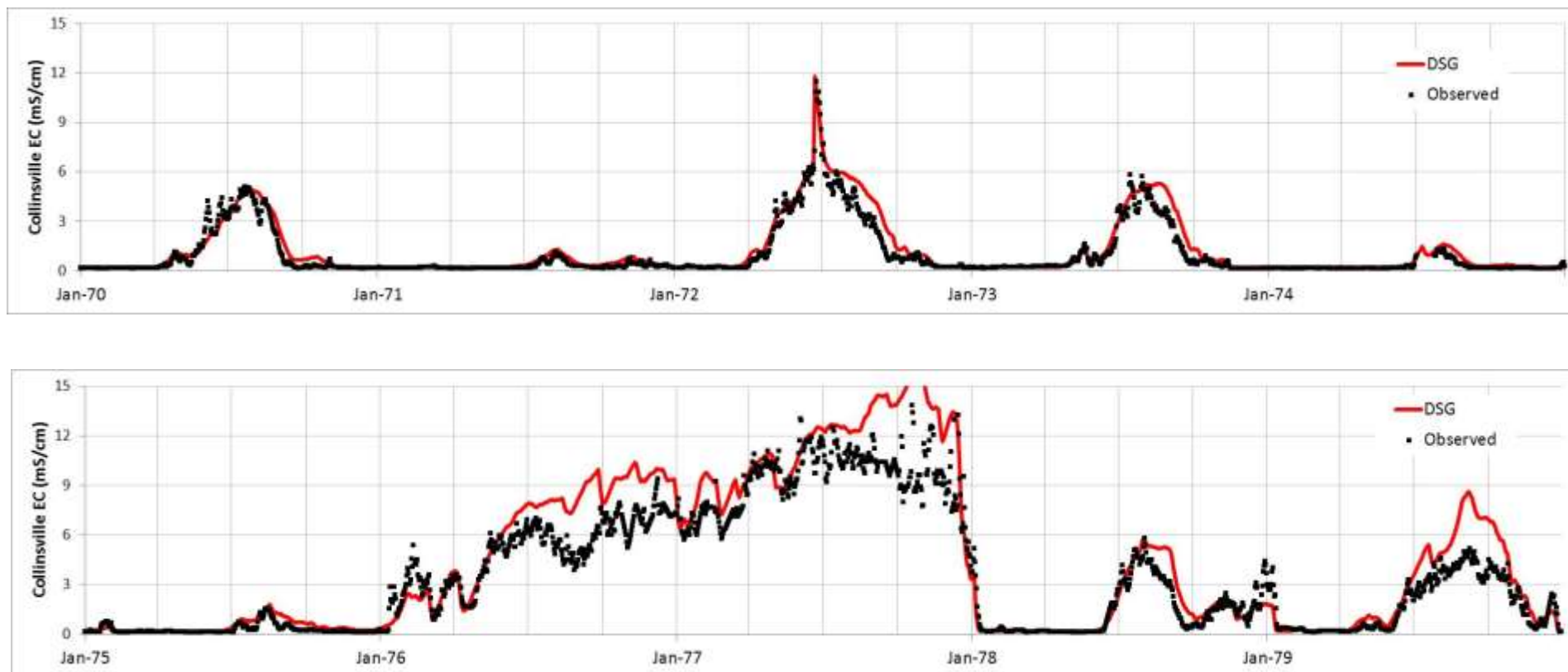


Figure E-28: Time Series of DSG Predicted and Observed Surface Salinity at Collinsville: 1970-1979

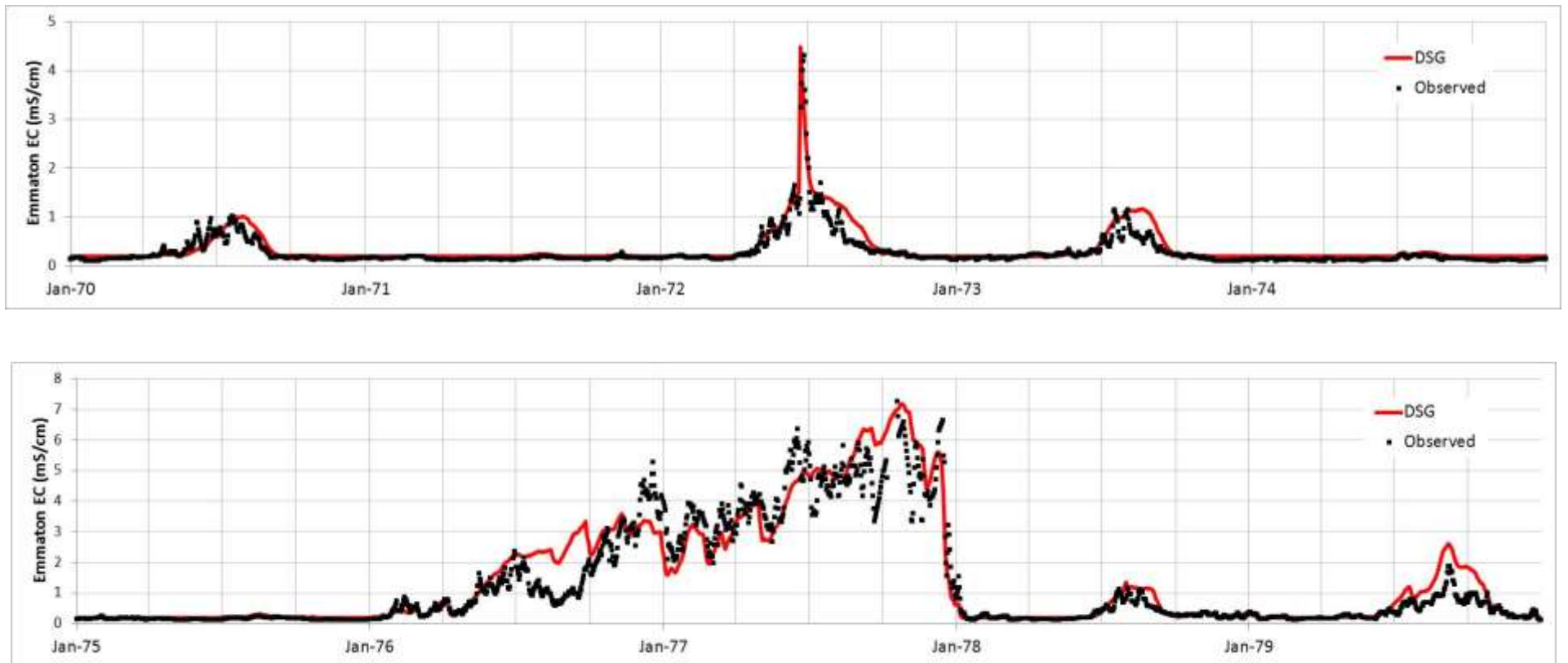


Figure E-29: Time Series of DSG Predicted and Observed Surface Salinity at Emmaton: 1970-1979

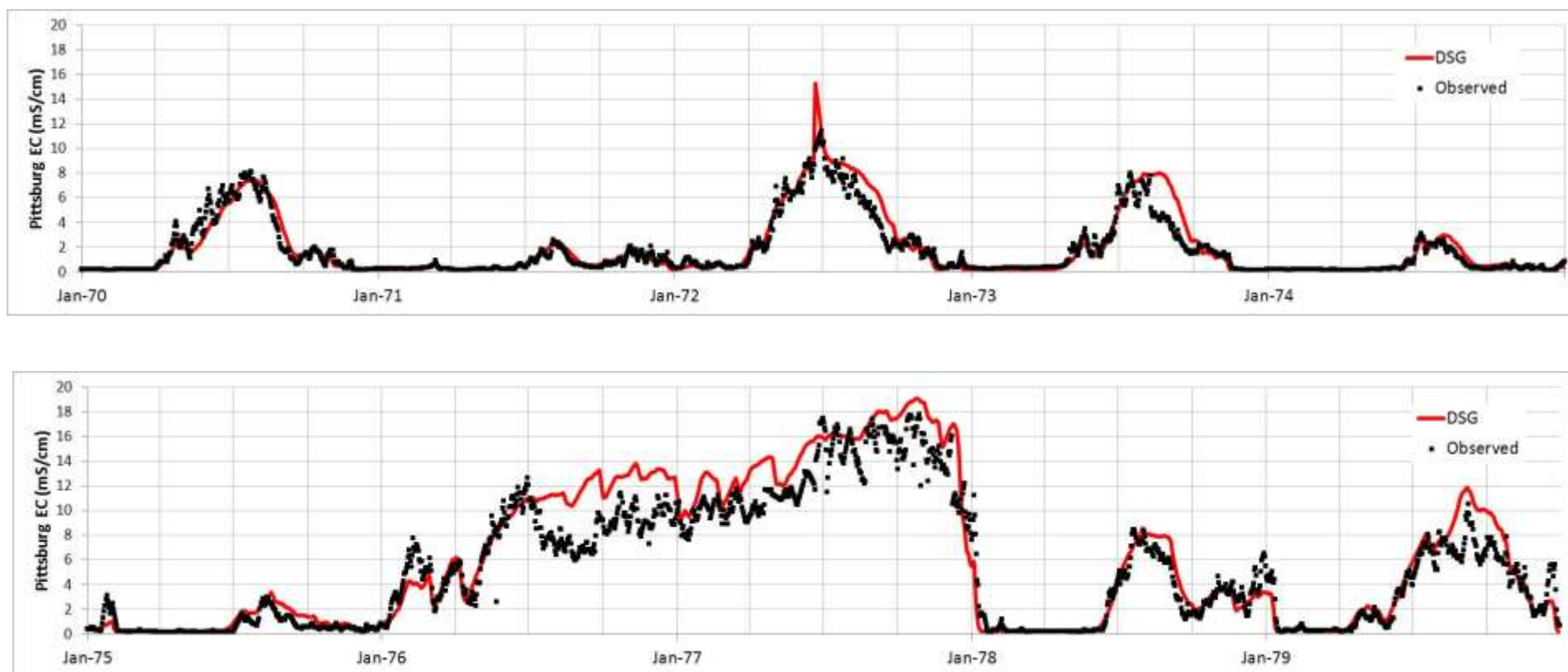


Figure E-30: Time Series of DSG Predicted and Observed Surface Salinity at Pittsburg: 1970-1979

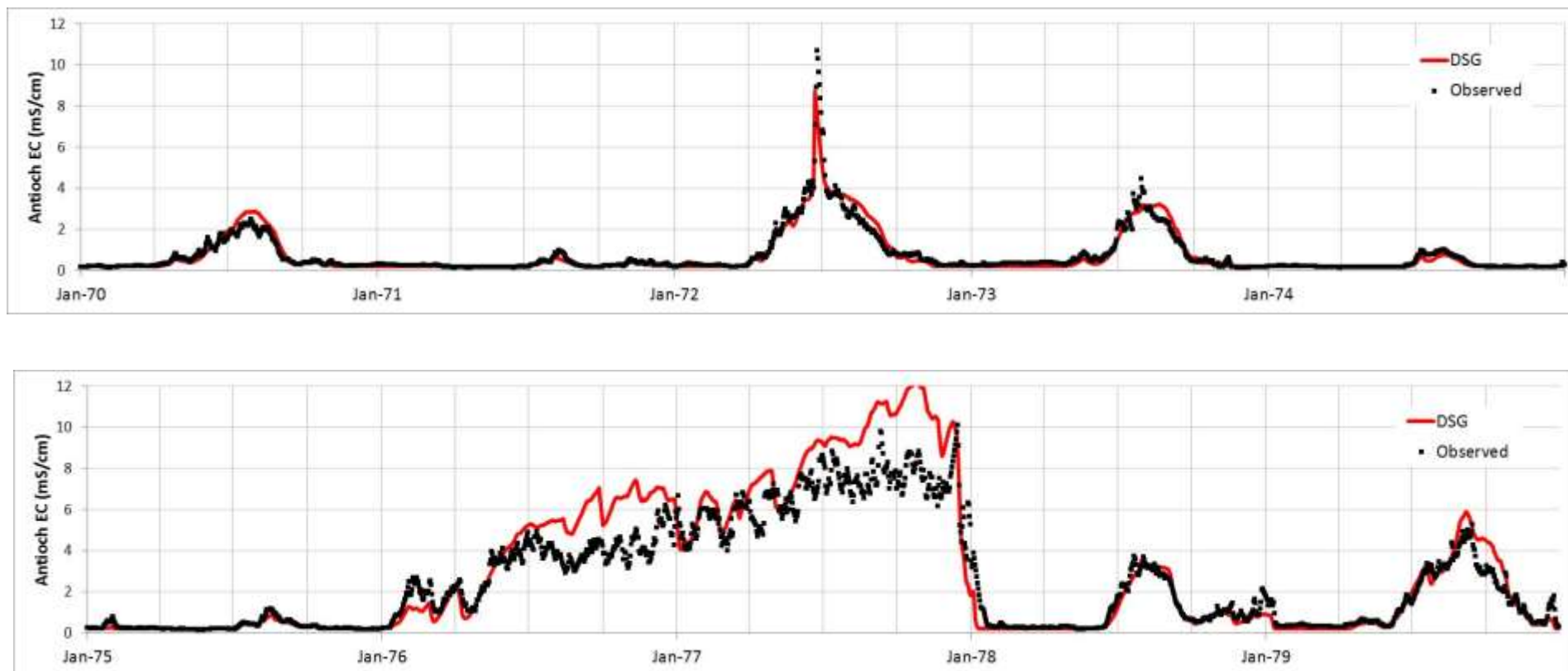


Figure E-31: Time Series of DSG Predicted and Observed Surface Salinity at Antioch: 1970-1979

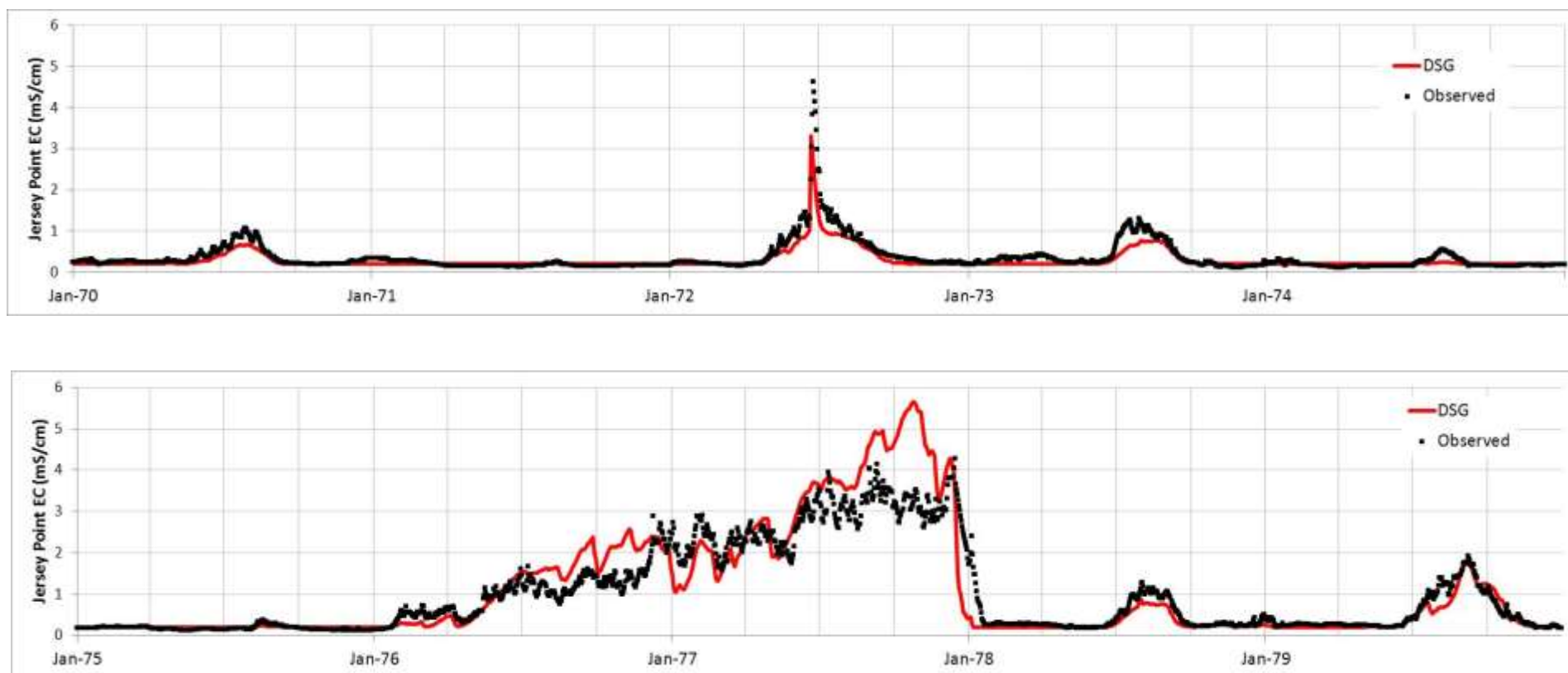


Figure E-32: Time Series of DSG Predicted and Observed Surface Salinity at Jersey Point: 1970-1979

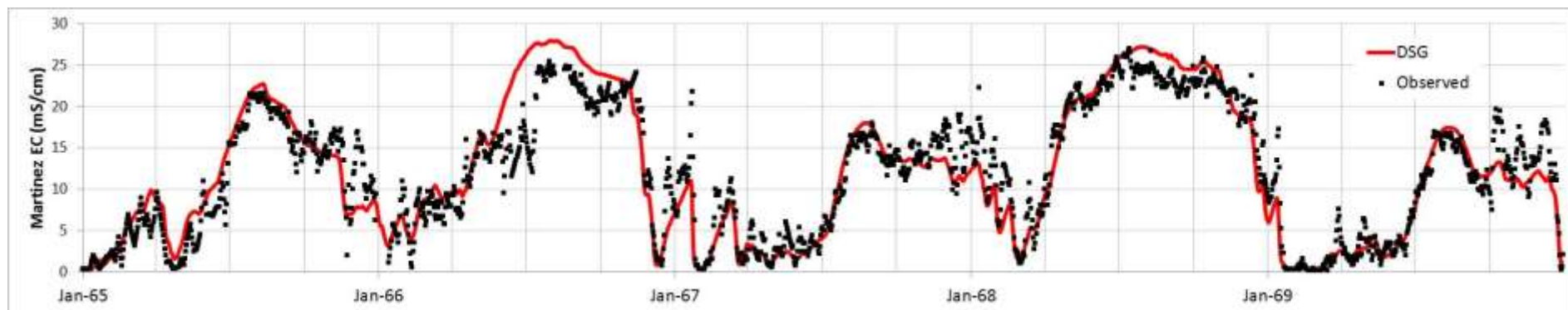
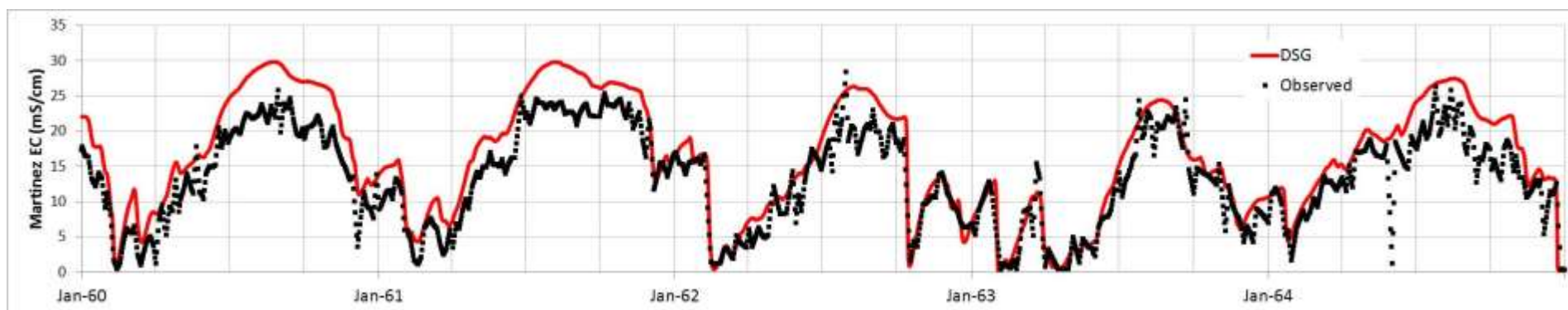


Figure E-33: Time Series of DSG Predicted and Observed Surface Salinity at Martinez: 1960-1969

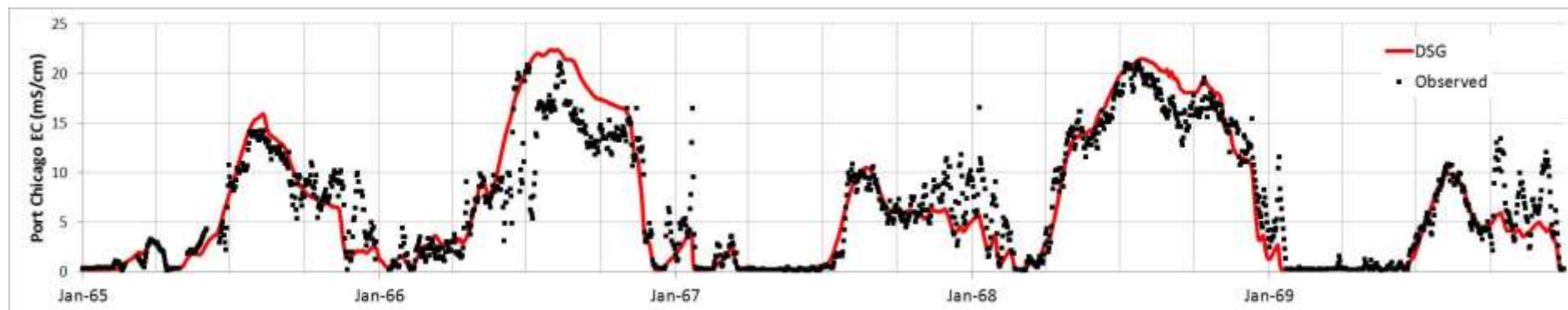
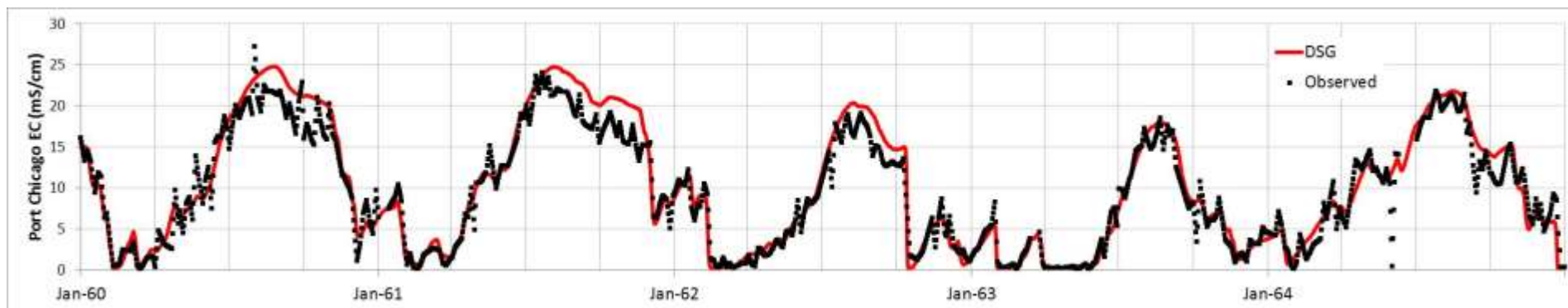


Figure E-34: Time Series of DSG Predicted and Observed Surface Salinity at Port Chicago: 1960-1969

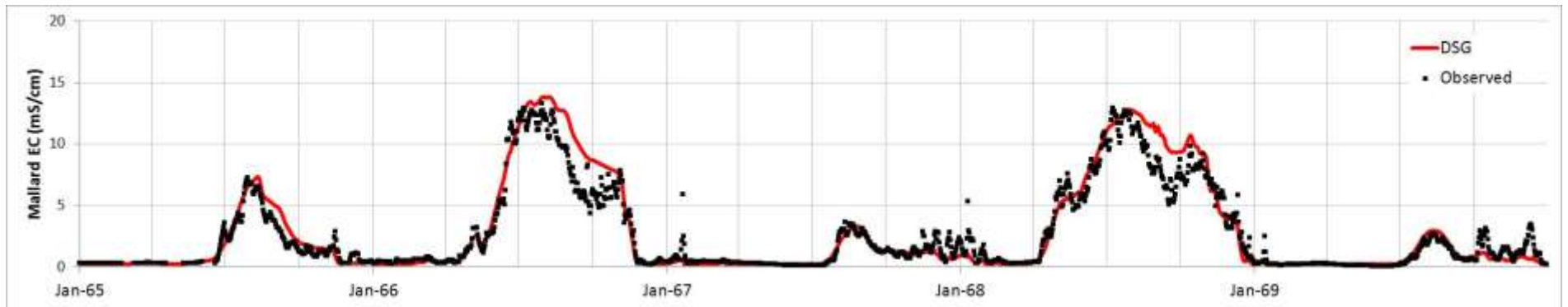
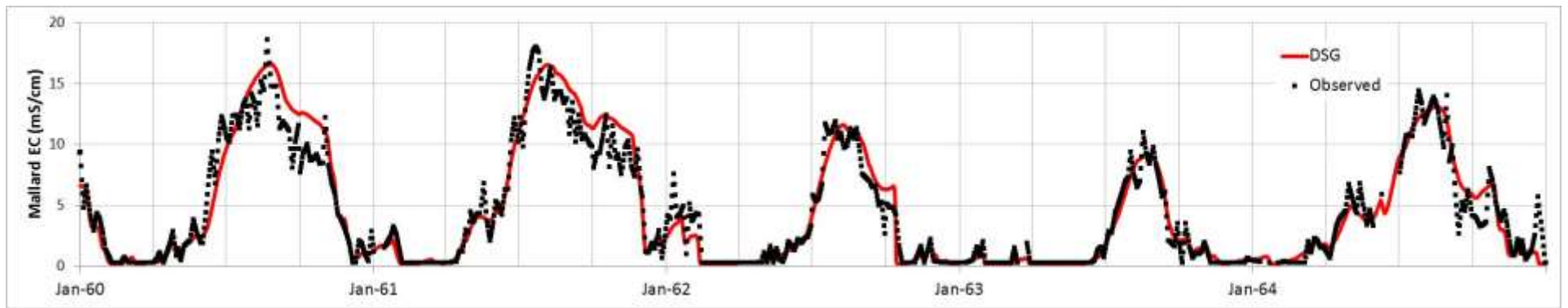


Figure E-35: Time Series of DSG Predicted and Observed Surface Salinity at Mallard Island: 1960-1969

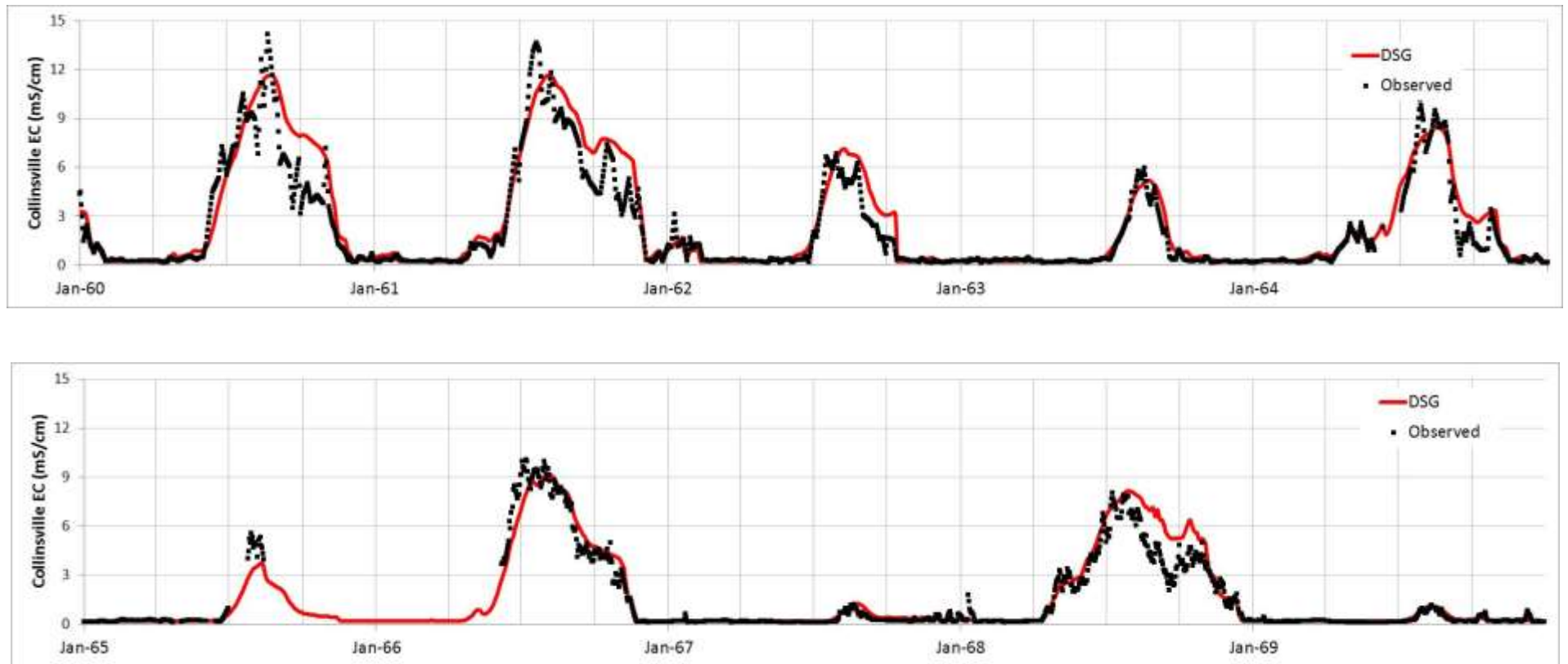


Figure E-36: Time Series of DSG Predicted and Observed Surface Salinity at Collinsville: 1960-1969

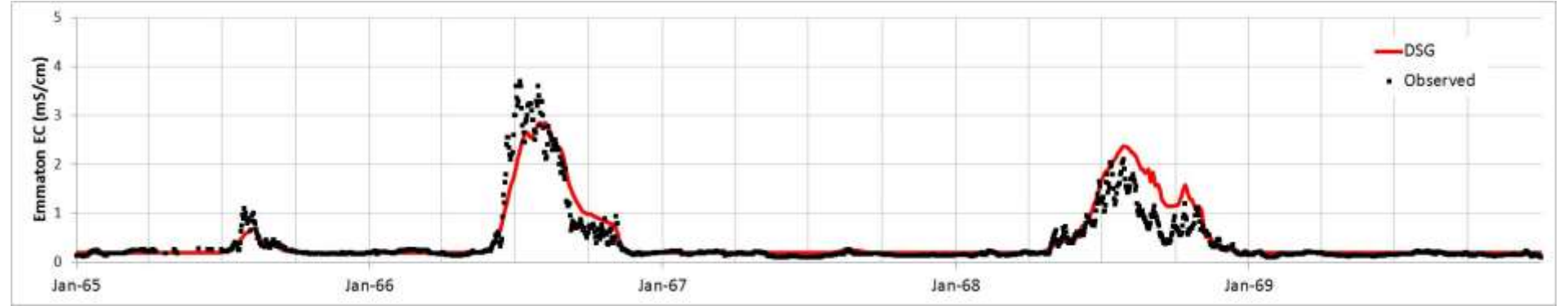
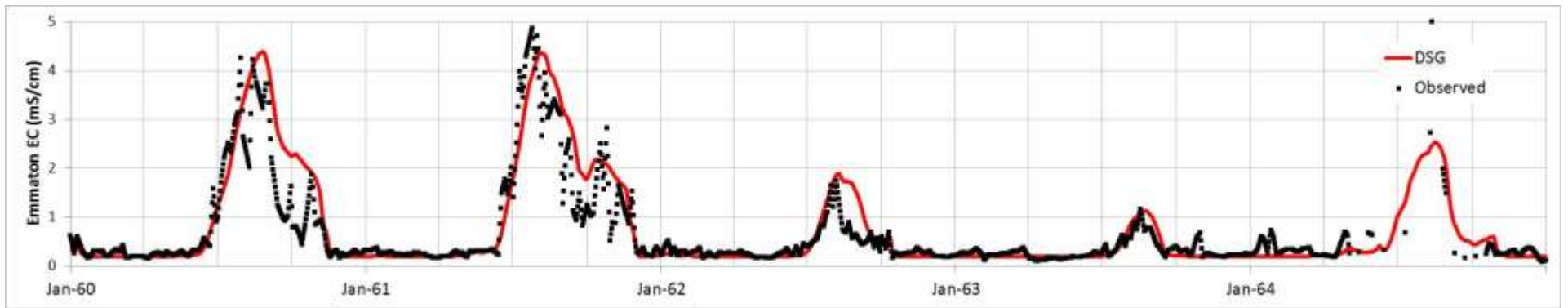


Figure E-37: Time Series of DSG Predicted and Observed Surface Salinity at Emmaton: 1960-1969

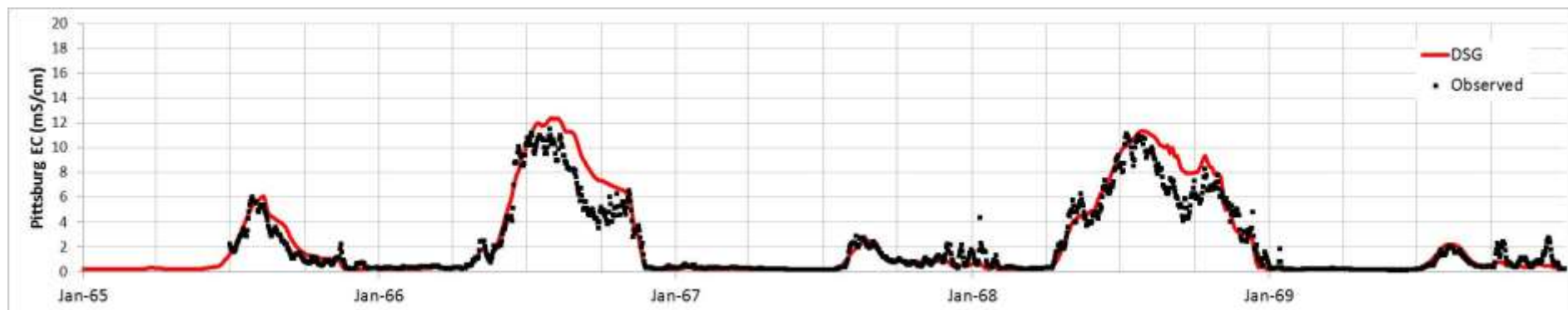
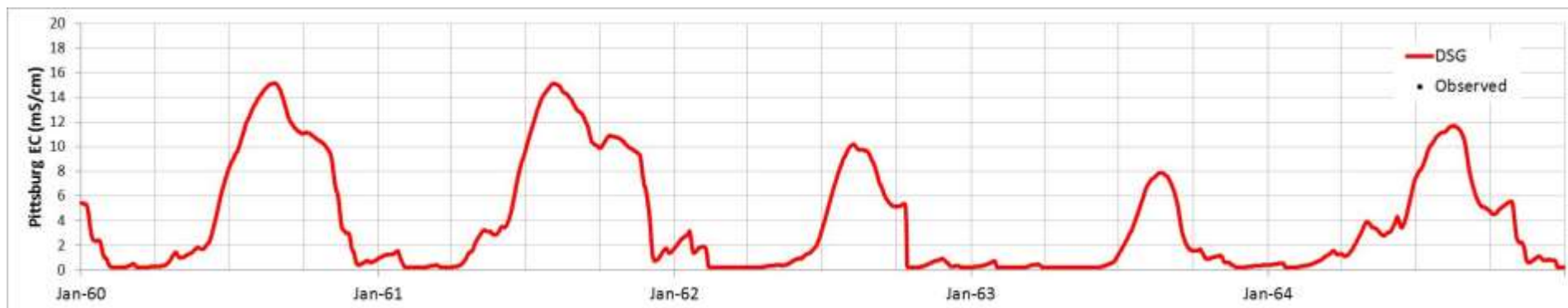


Figure E-38: Time Series of DSG Predicted and Observed Surface Salinity at Pittsburg: 1960-1969

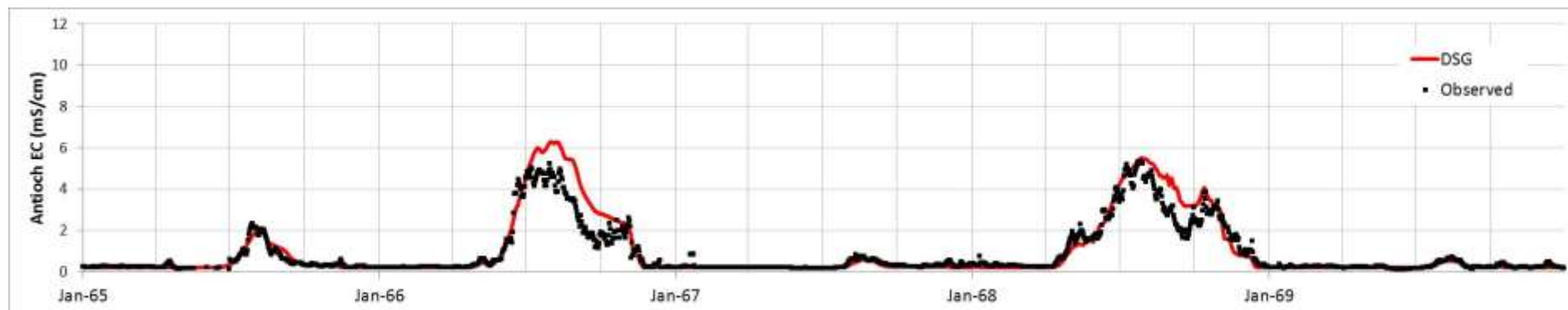
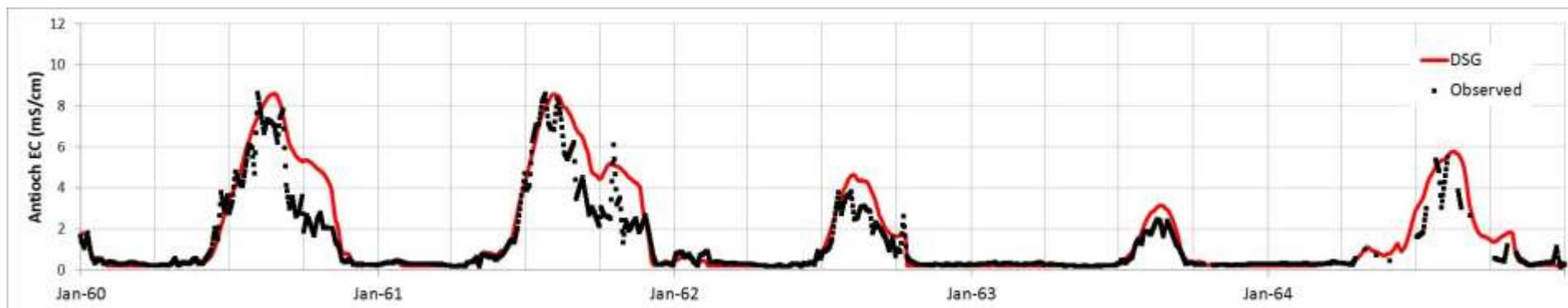


Figure E-39: Time Series of DSG Predicted and Observed Surface Salinity at Antioch: 1960-1969

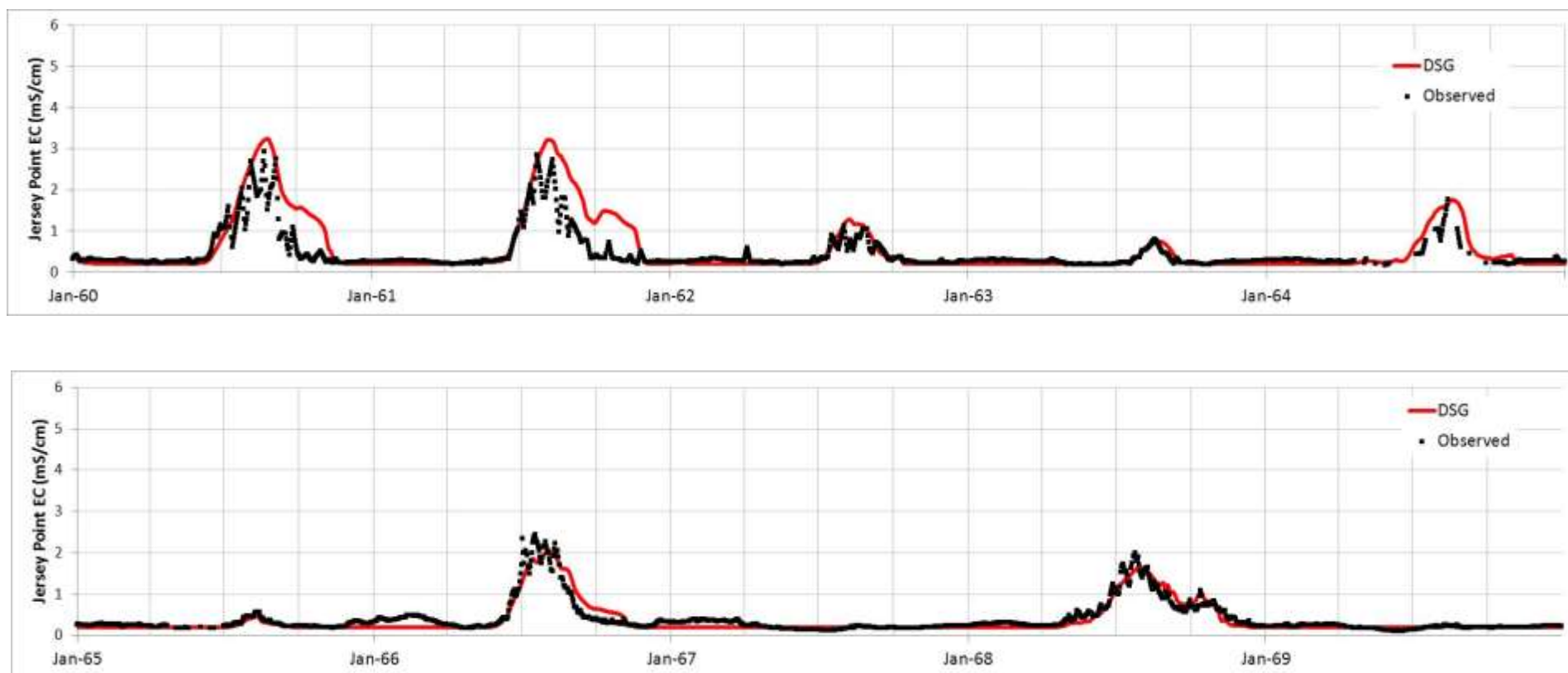


Figure E-40: Time Series of DSG Predicted and Observed Surface Salinity at Jersey Point: 1960-1969

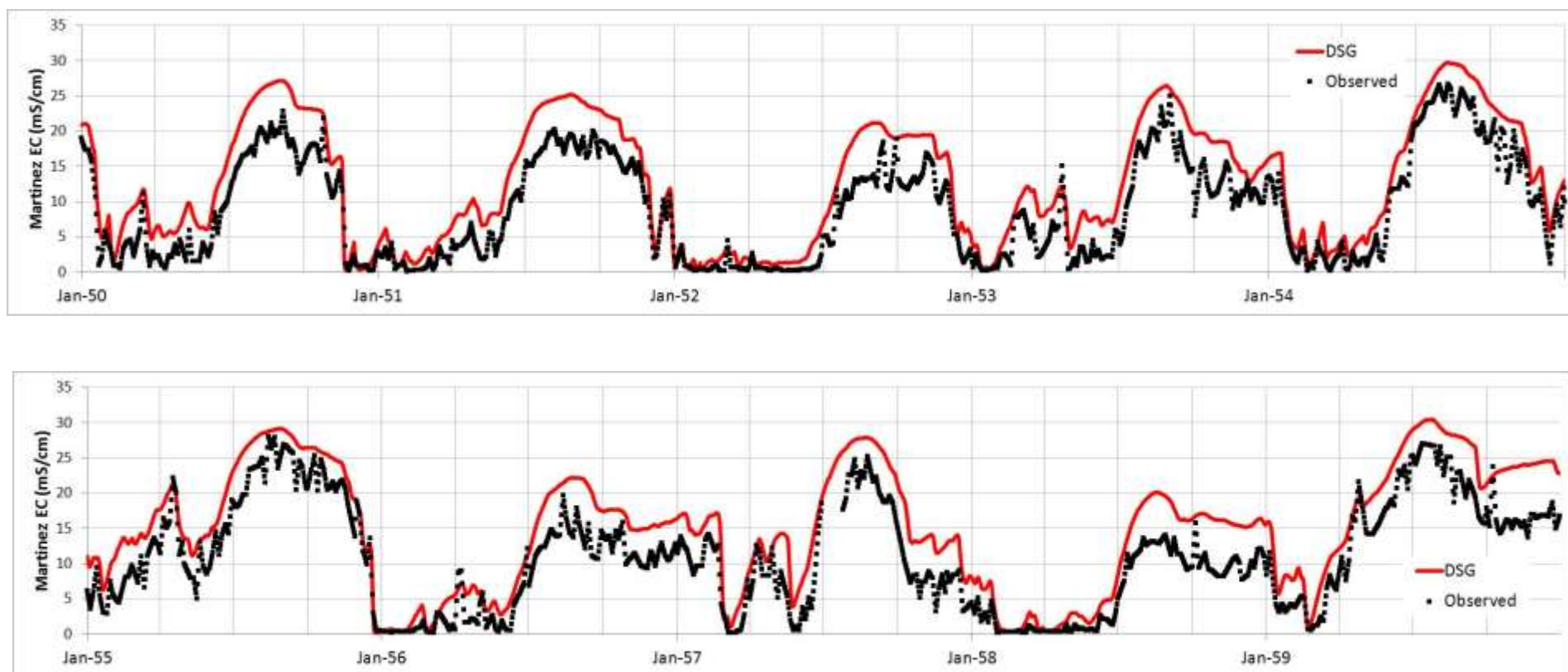


Figure E-41: Time Series of DSG Predicted and Observed Surface Salinity at Martinez: 1950-1959

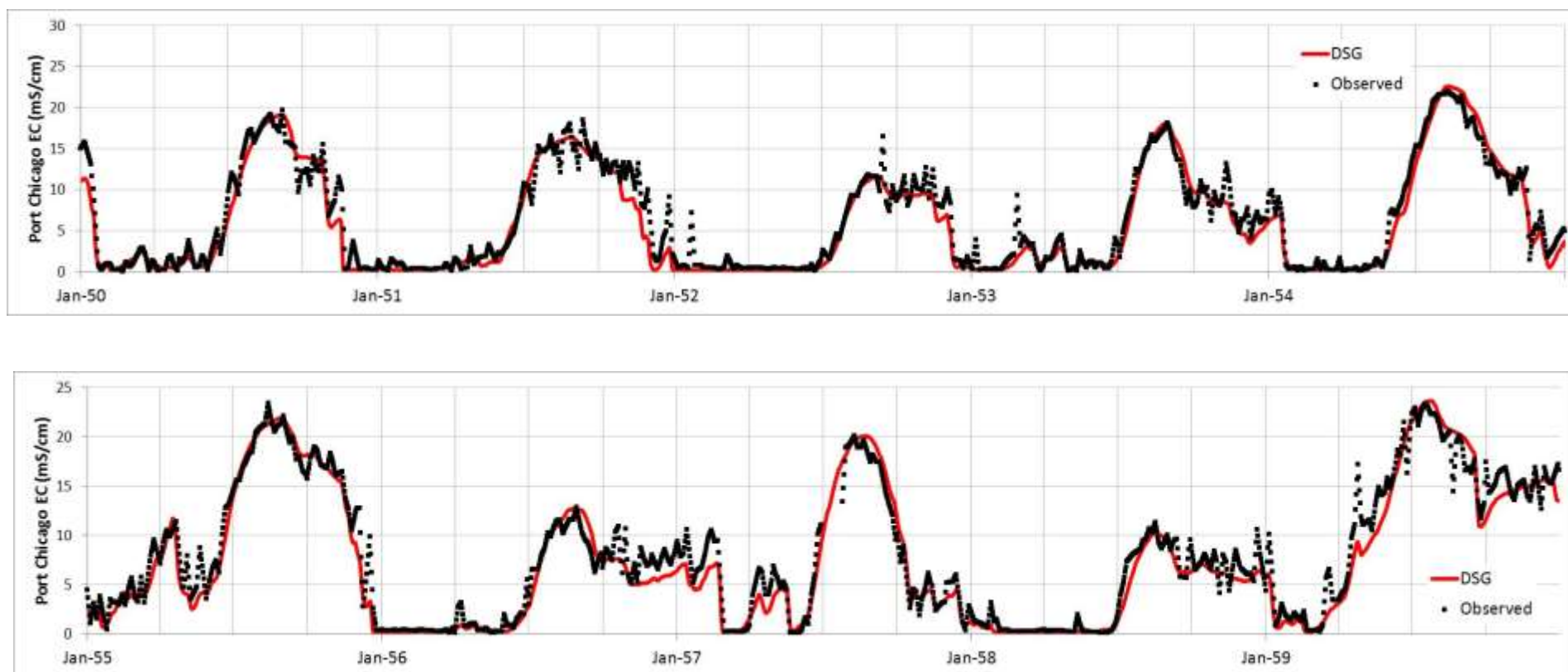


Figure E-42: Time Series of DSG Predicted and Observed Surface Salinity at Port Chicago: 1950-1959

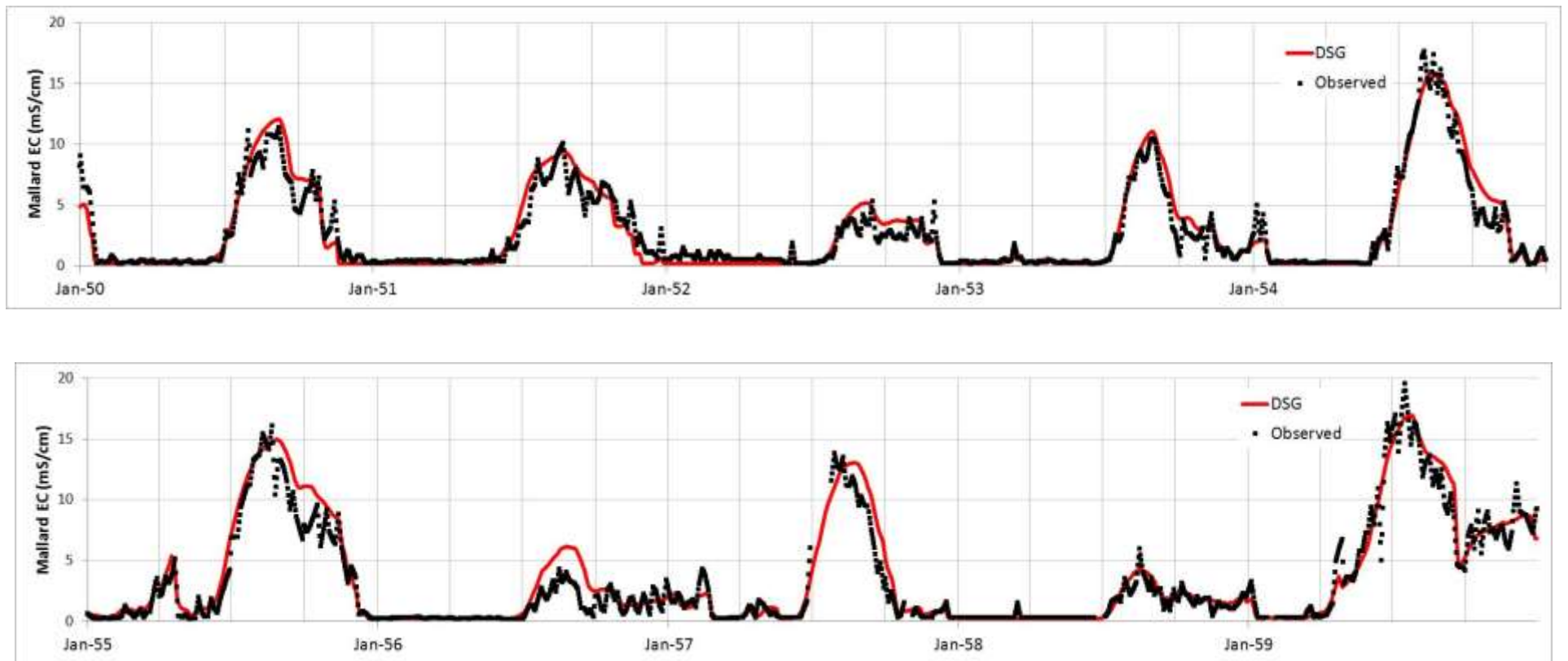


Figure E-43: Time Series of DSG Predicted and Observed Surface Salinity at Mallard Island: 1950-1959

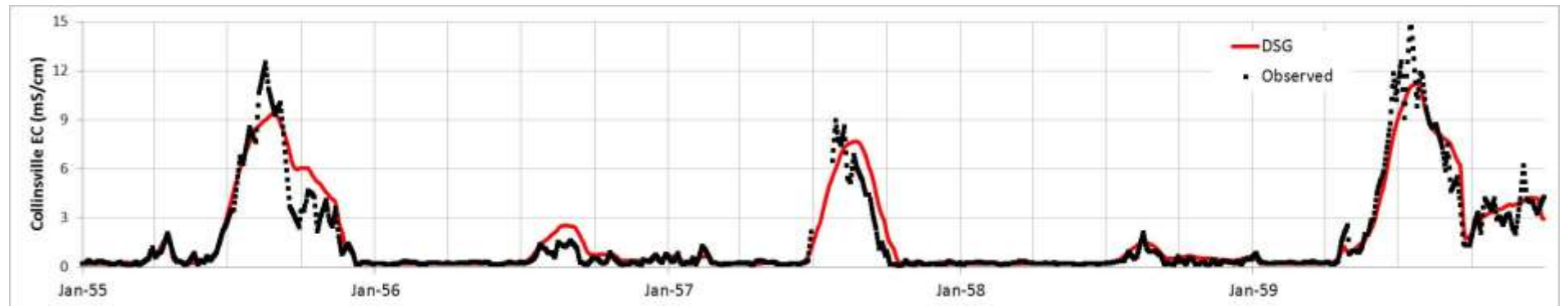
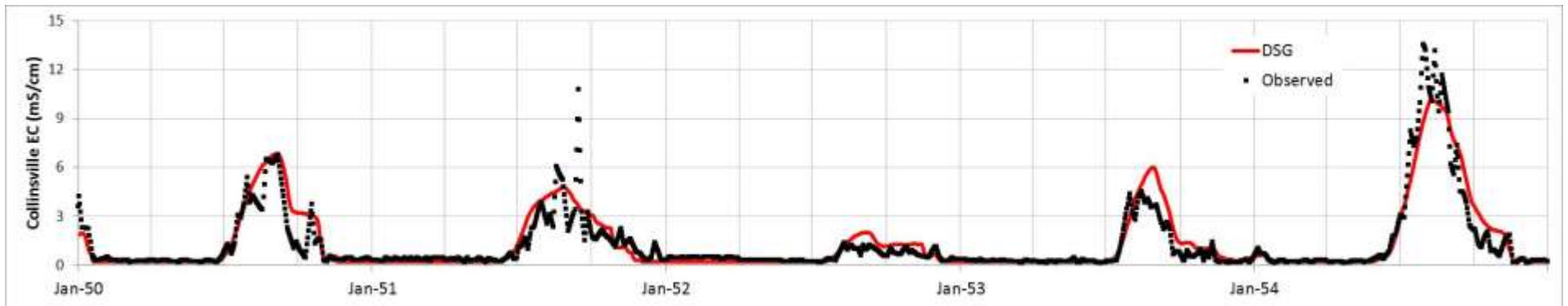


Figure E-44: Time Series of DSG Predicted and Observed Surface Salinity at Collinsville: 1950-1959

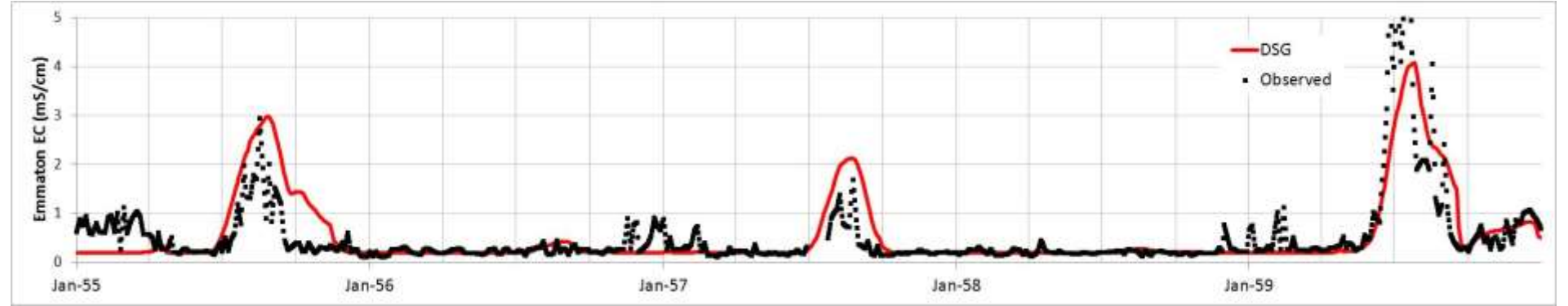
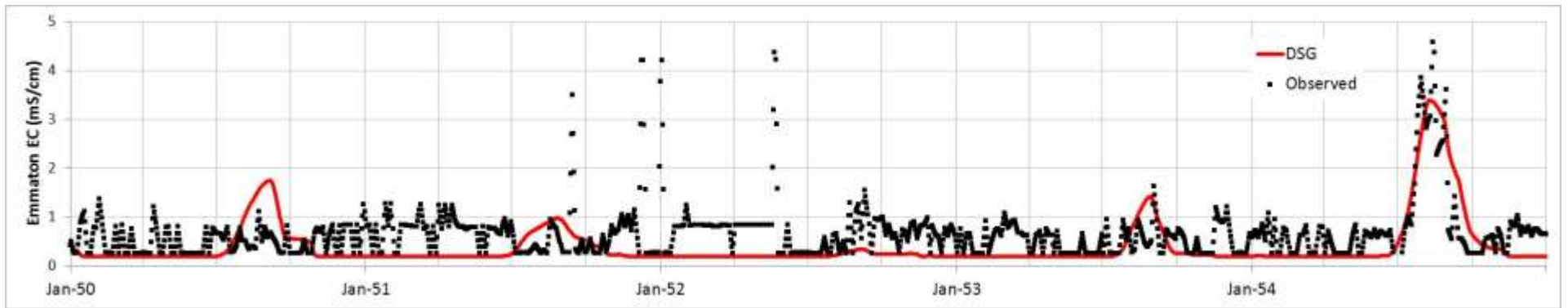


Figure E-45: Time Series of DSG Predicted and Observed Surface Salinity at Emmaton: 1950-1959

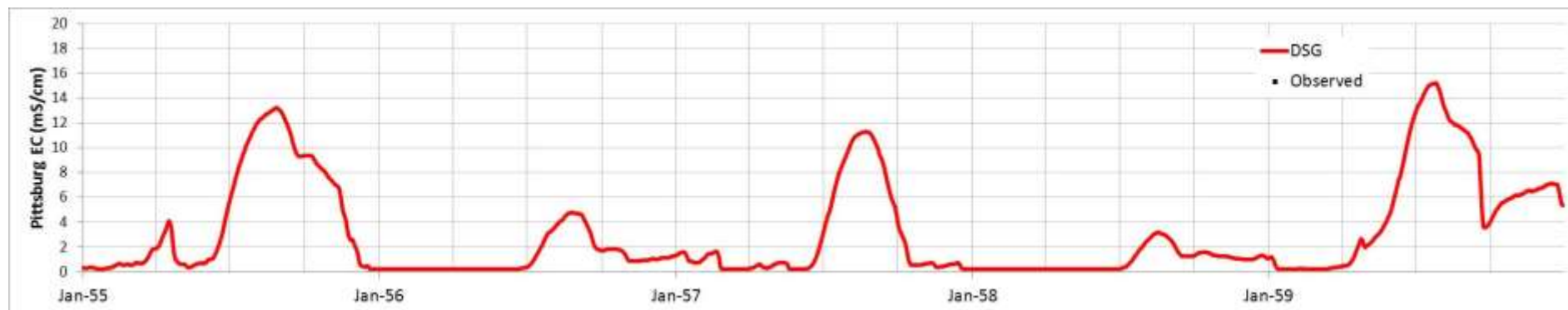
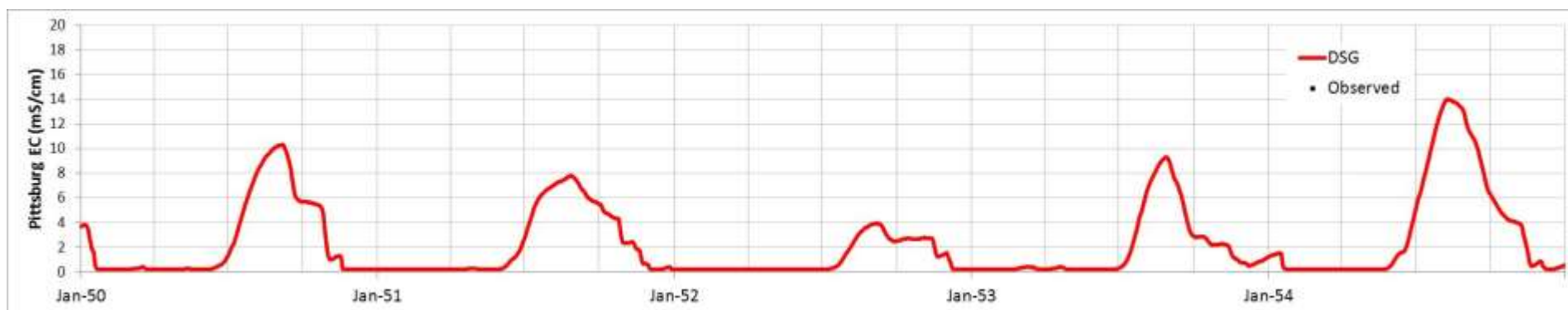


Figure E-46: Time Series of DSG Predicted and Observed Surface Salinity at Pittsburg: 1950-1959

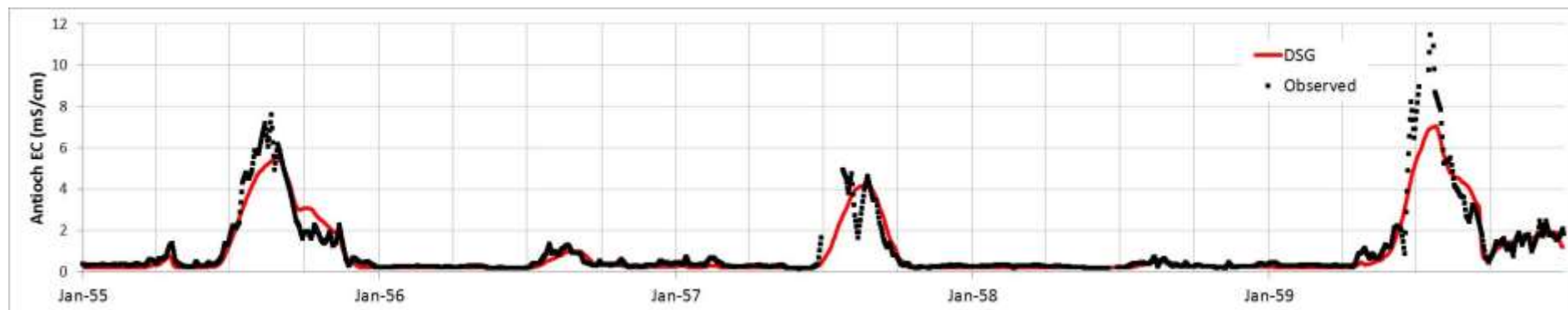
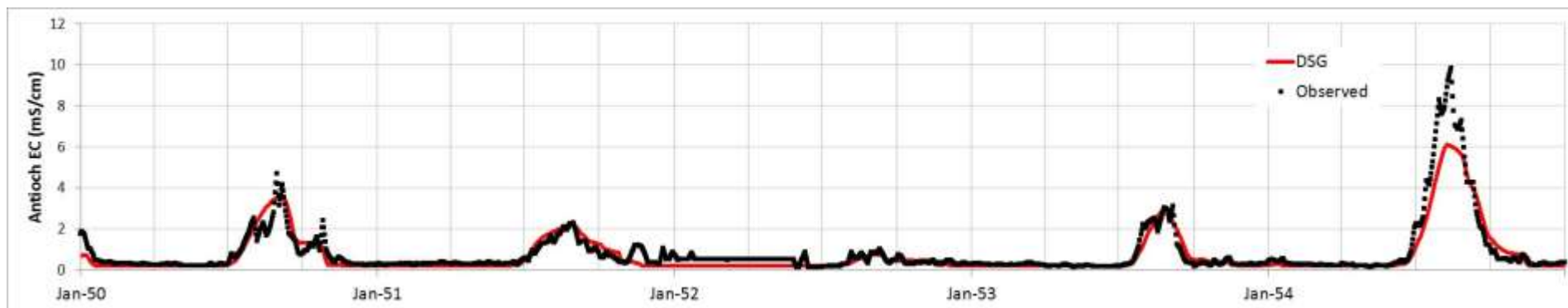


Figure E-47: Time Series of DSG Predicted and Observed Surface Salinity at Antioch: 1950-1959

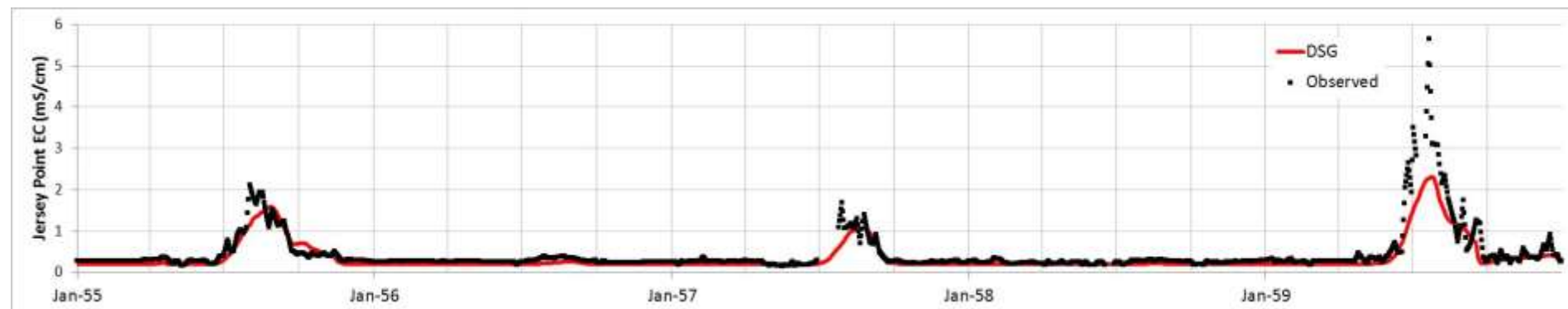
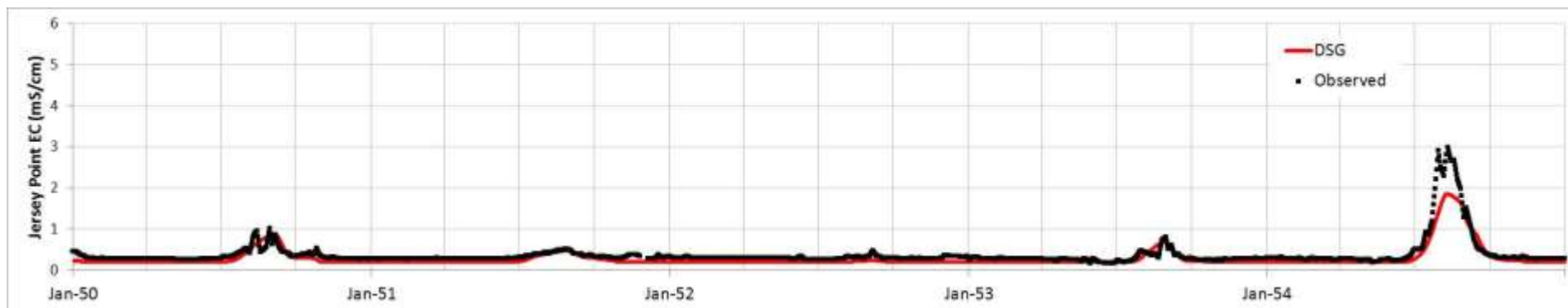


Figure E-48: Time Series of DSG Predicted and Observed Surface Salinity at Jersey Point: 1950-1959

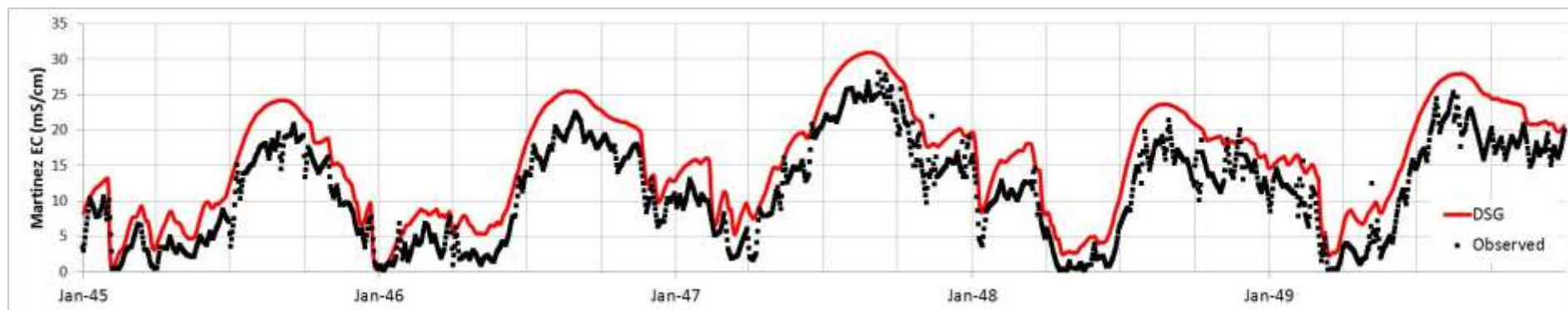
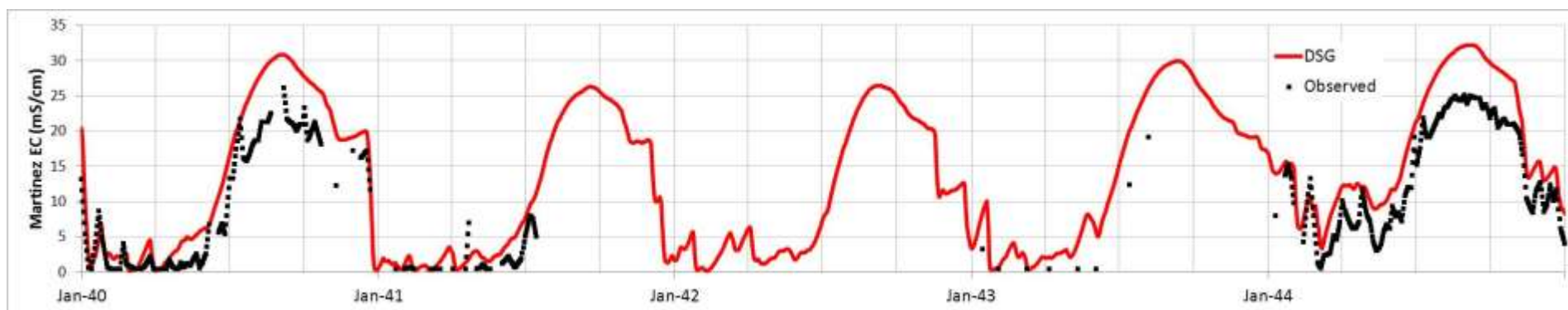


Figure E-49: Time Series of DSG Predicted and Observed Surface Salinity at Martinez: 1940-1949

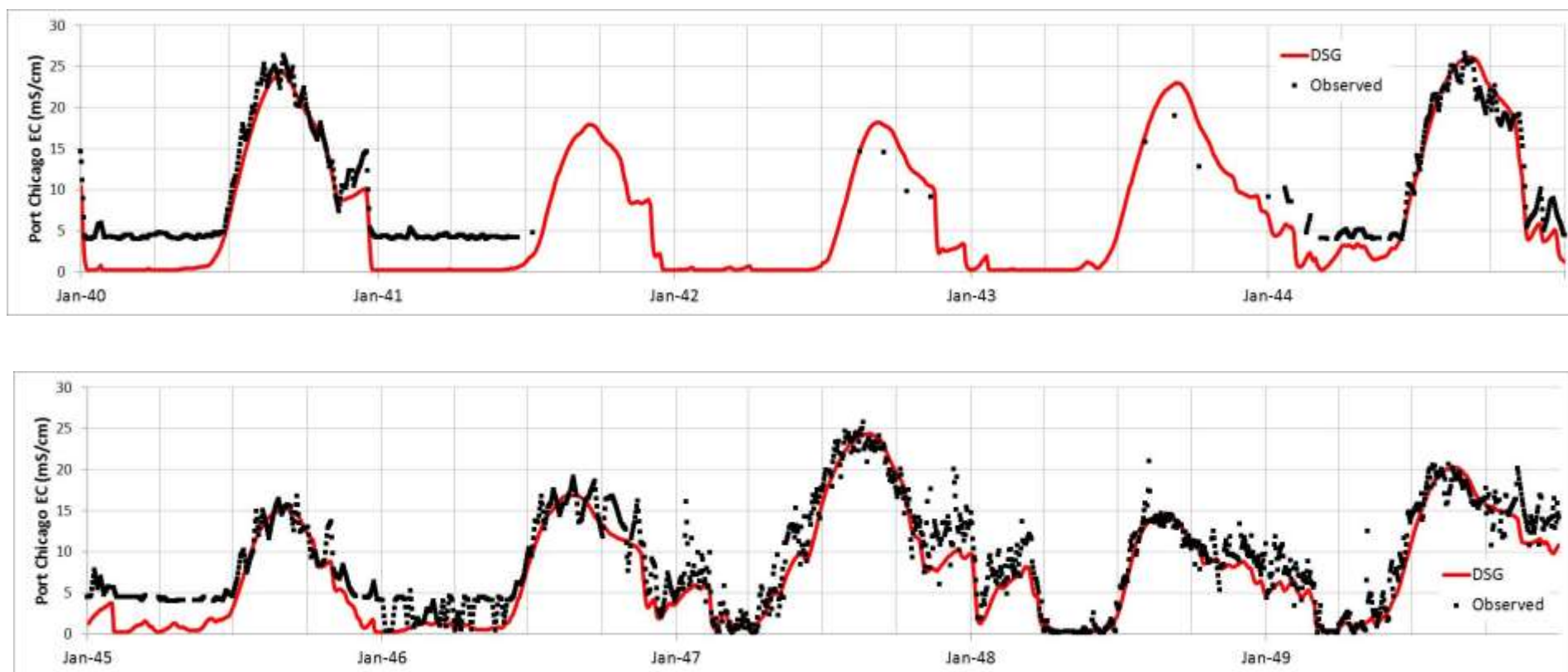


Figure E-50: Time Series of DSG Predicted and Observed Surface Salinity at Port Chicago: 1940-1949

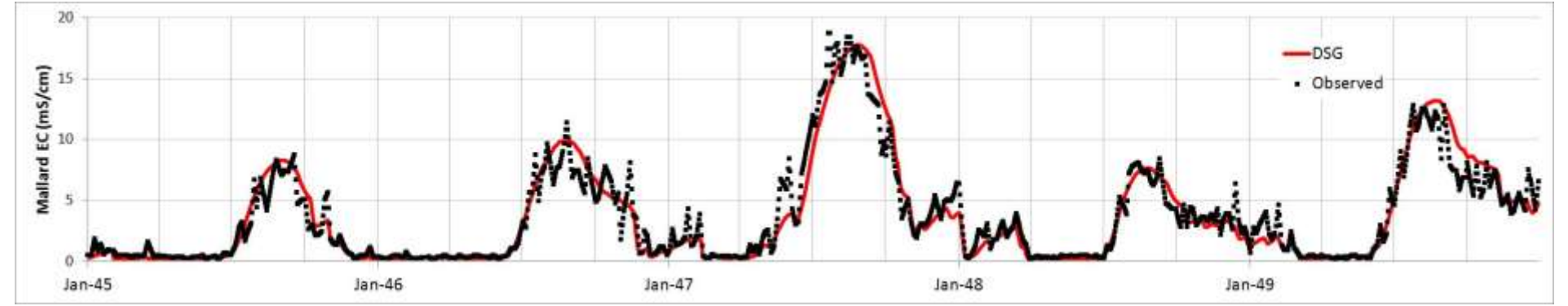
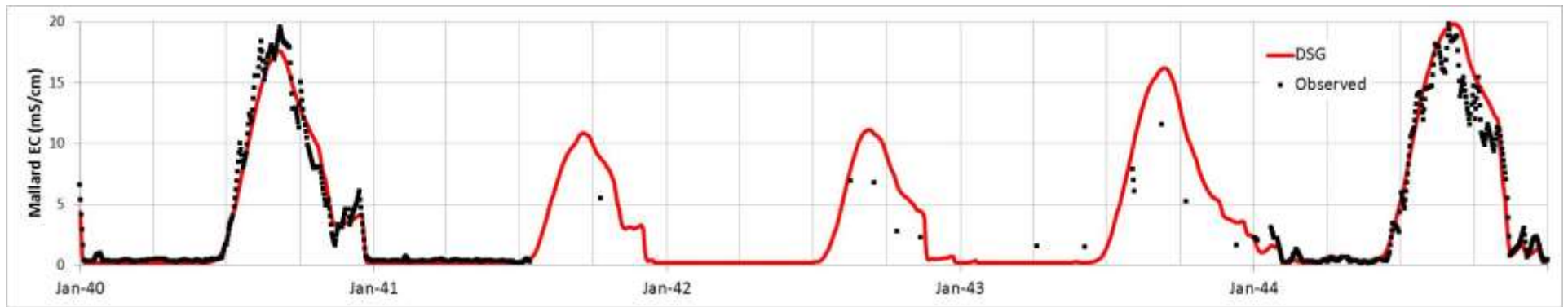


Figure E-51: Time Series of DSG Predicted and Observed Surface Salinity at Mallard Island: 1940-1949

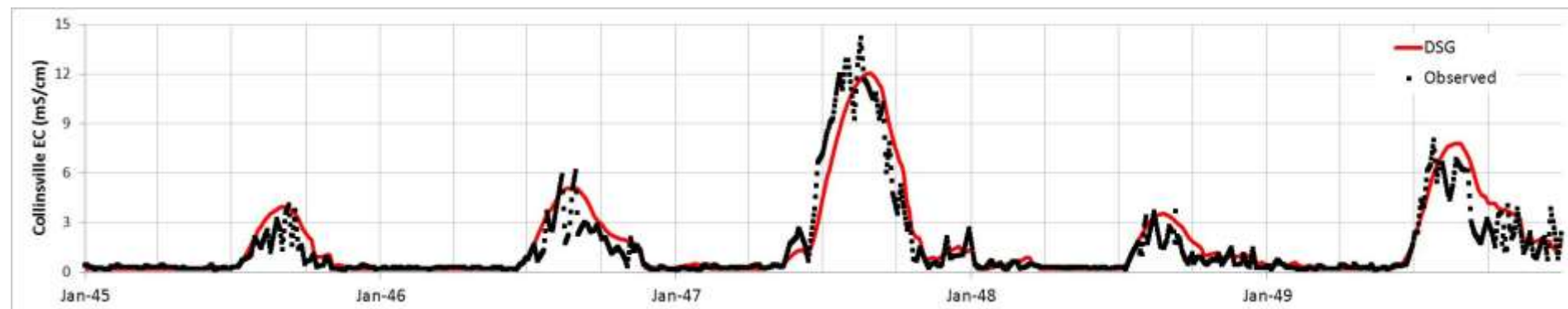
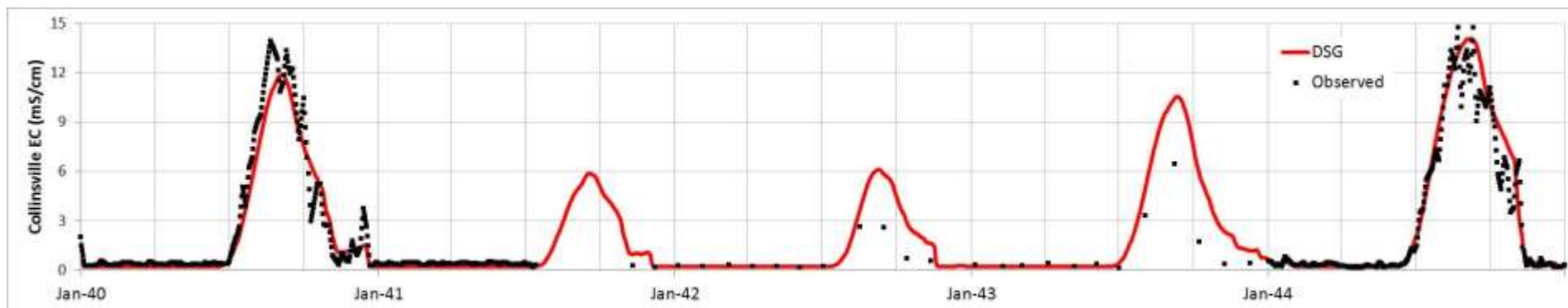


Figure E-52: Time Series of DSG Predicted and Observed Surface Salinity at Collinsville: 1940-1949

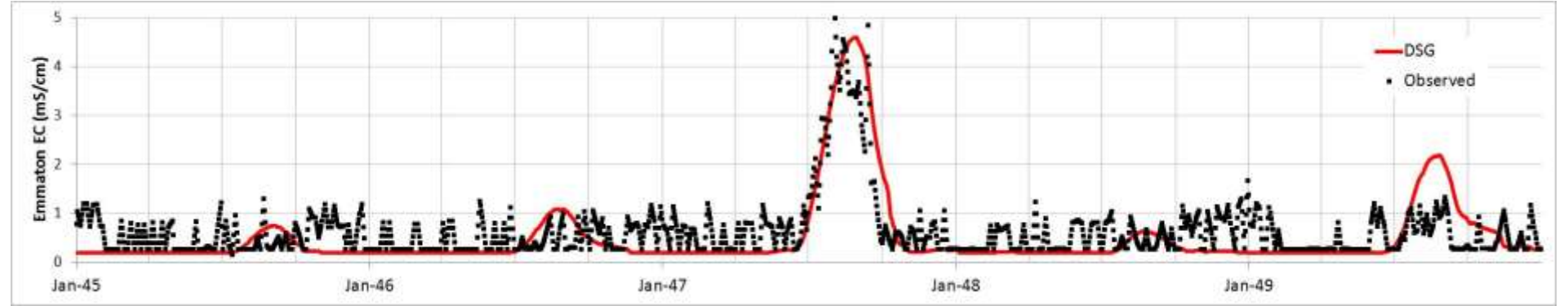
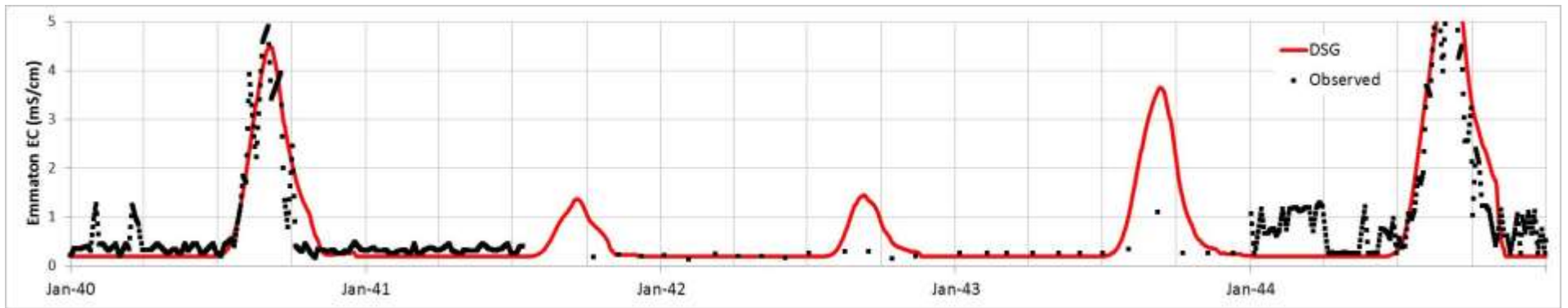


Figure E-53: Time Series of DSG Predicted and Observed Surface Salinity at Emmaton: 1940-1949

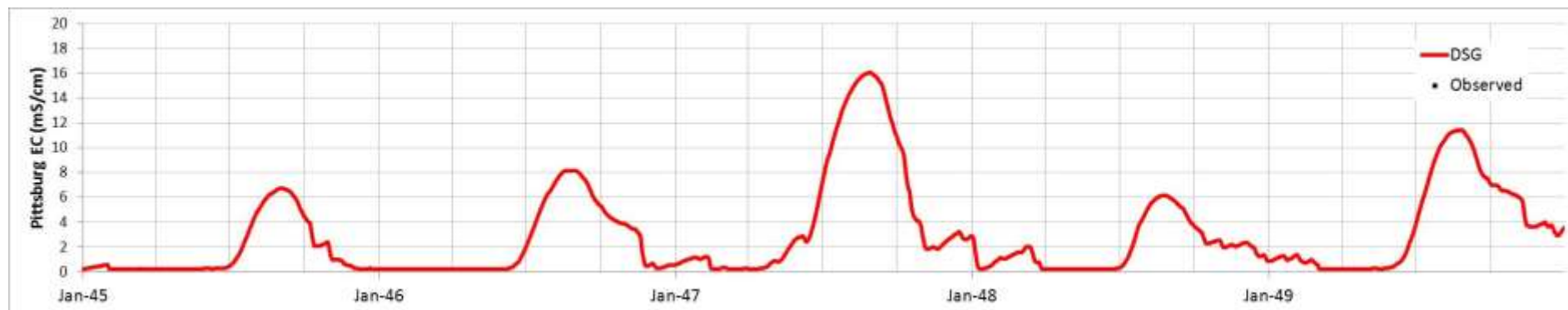
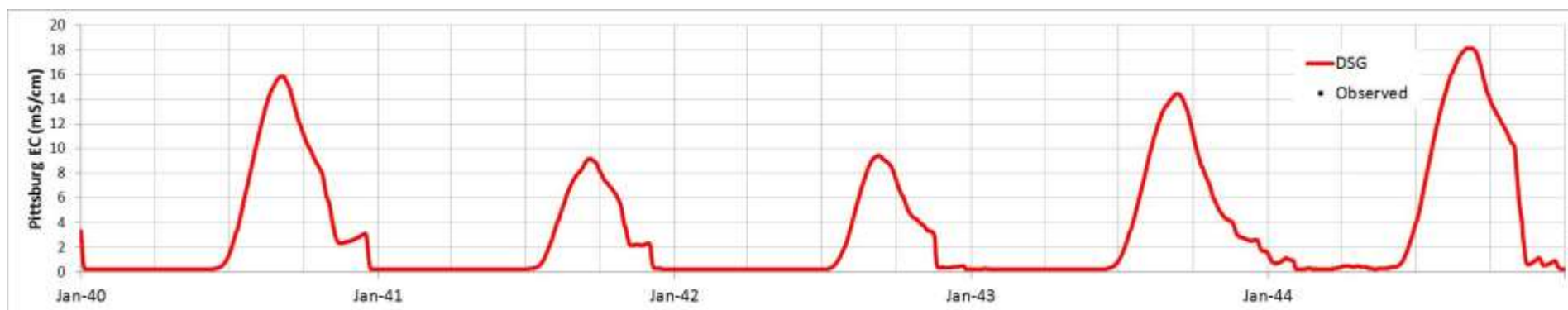


Figure E-54: Time Series of DSG Predicted and Observed Surface Salinity at Pittsburg: 1940-1949

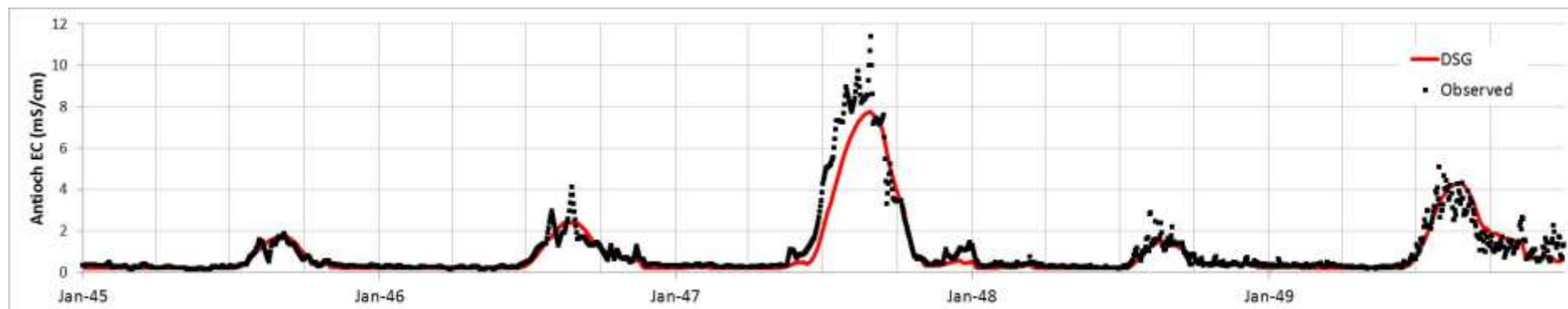
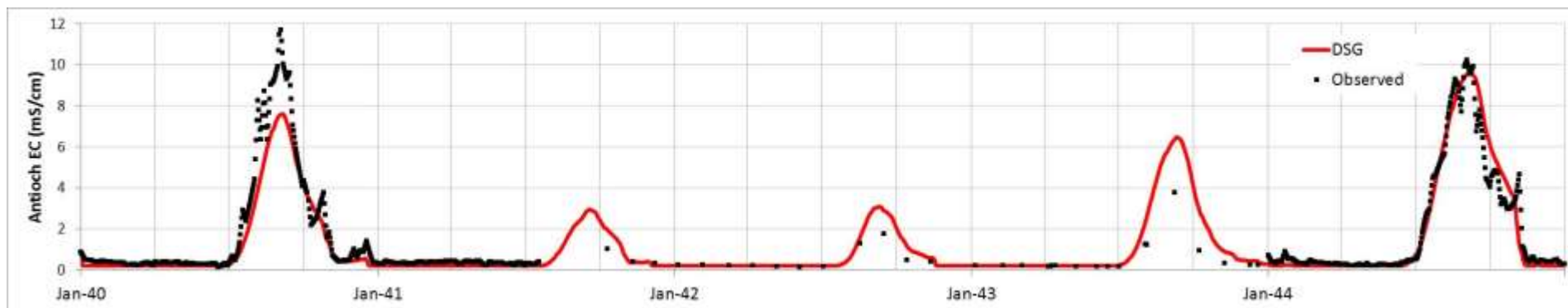


Figure E-55: Time Series of DSG Predicted and Observed Surface Salinity at Antioch: 1940-1949

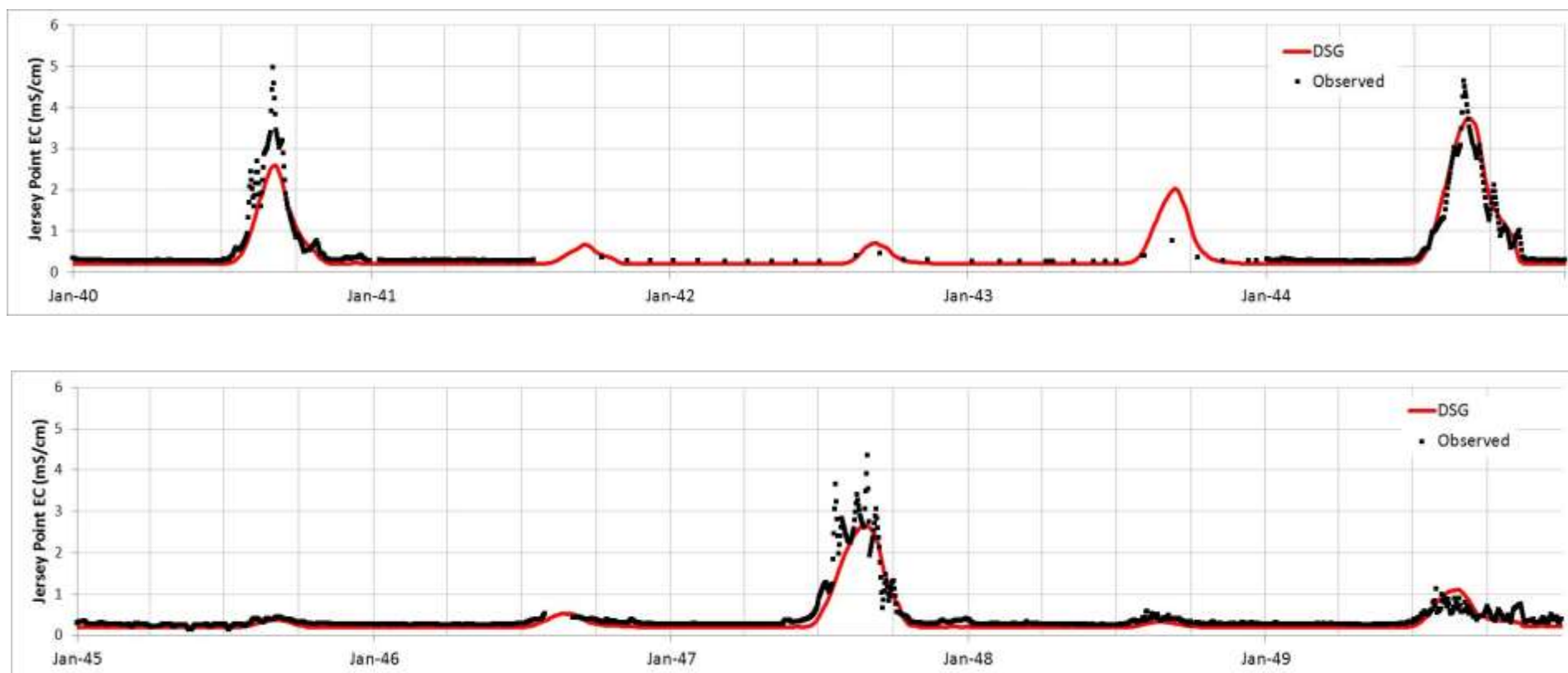


Figure E-56: Time Series of DSG Predicted and Observed Surface Salinity at Jersey Point: 1940-1949

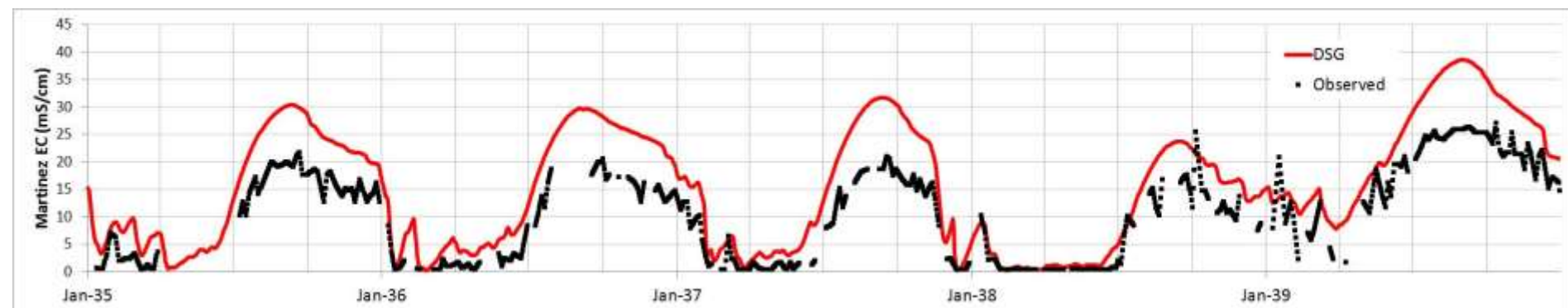
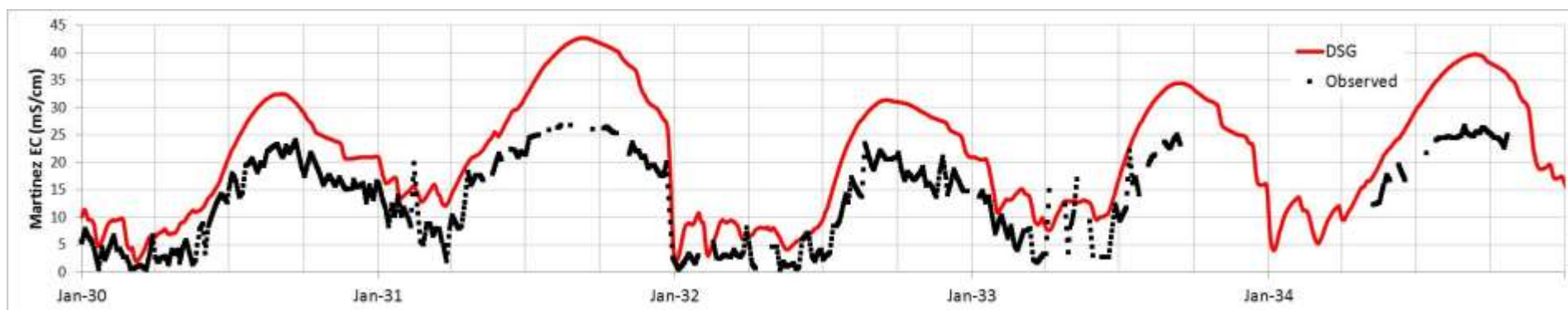


Figure E-57: Time Series of DSG Predicted and Observed Surface Salinity at Martinez: 1930-1939

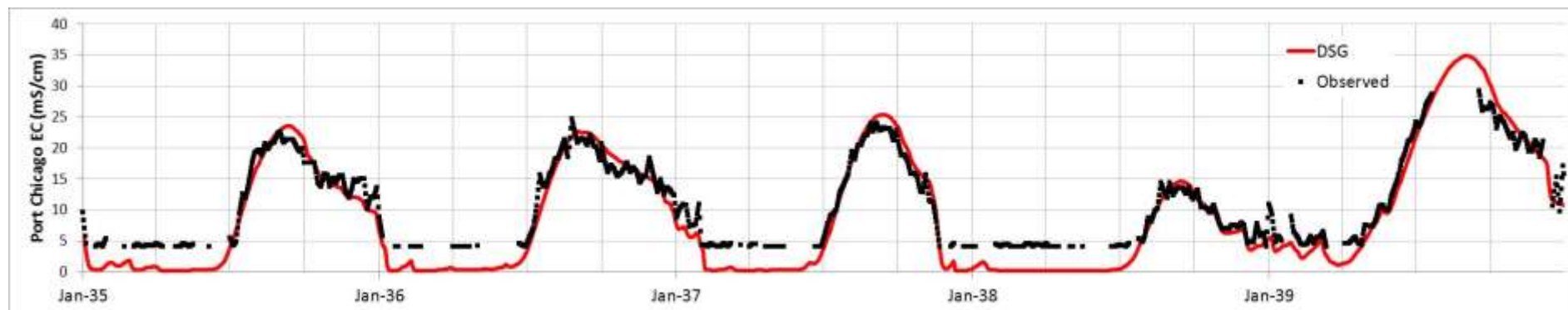
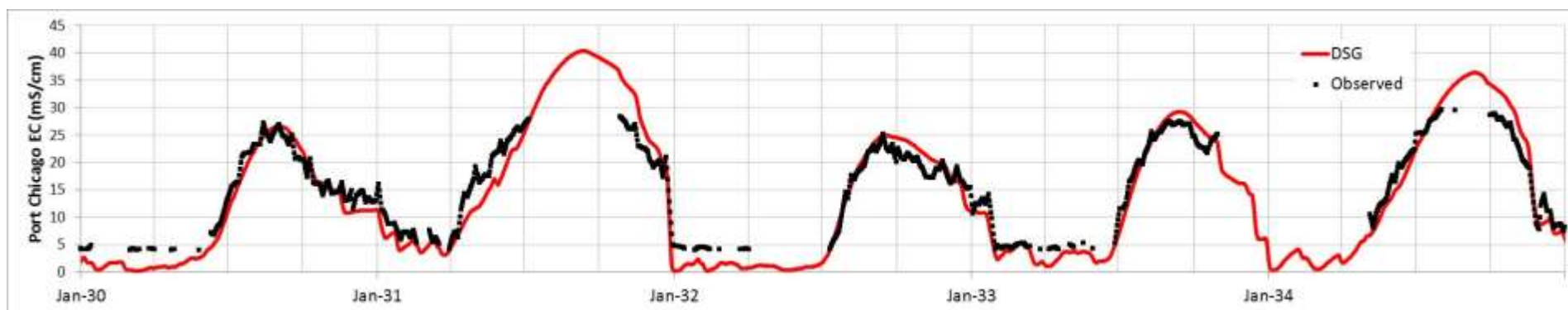


Figure E-58: Time Series of DSG Predicted and Observed Surface Salinity at Port Chicago: 1930-1939

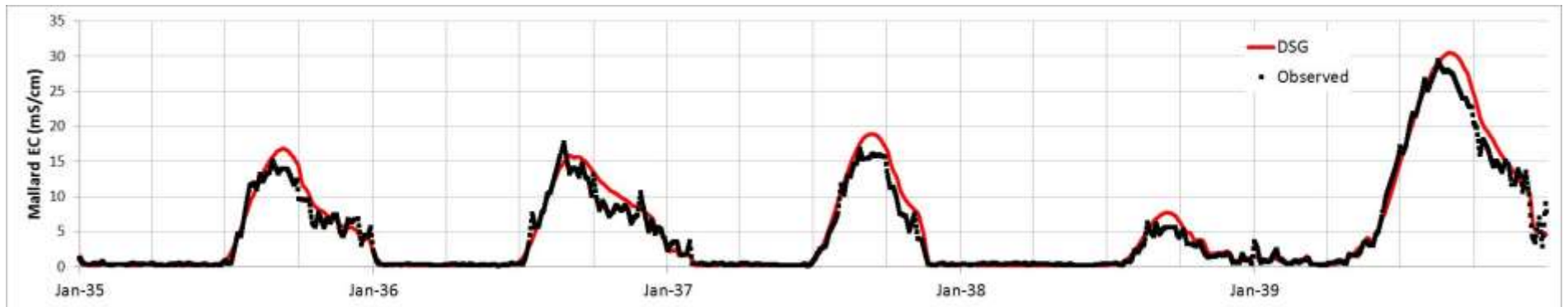
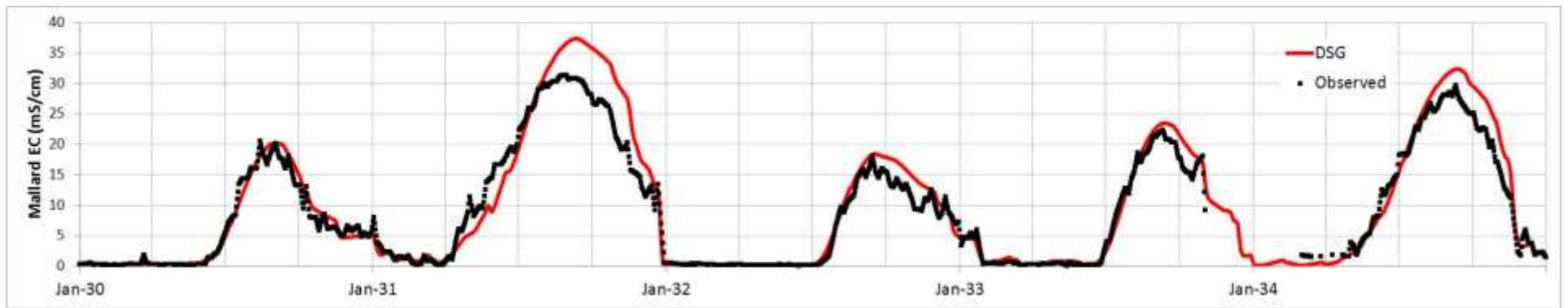


Figure E-59: Time Series of DSG Predicted and Observed Surface Salinity at Mallard Island: 1930-1939

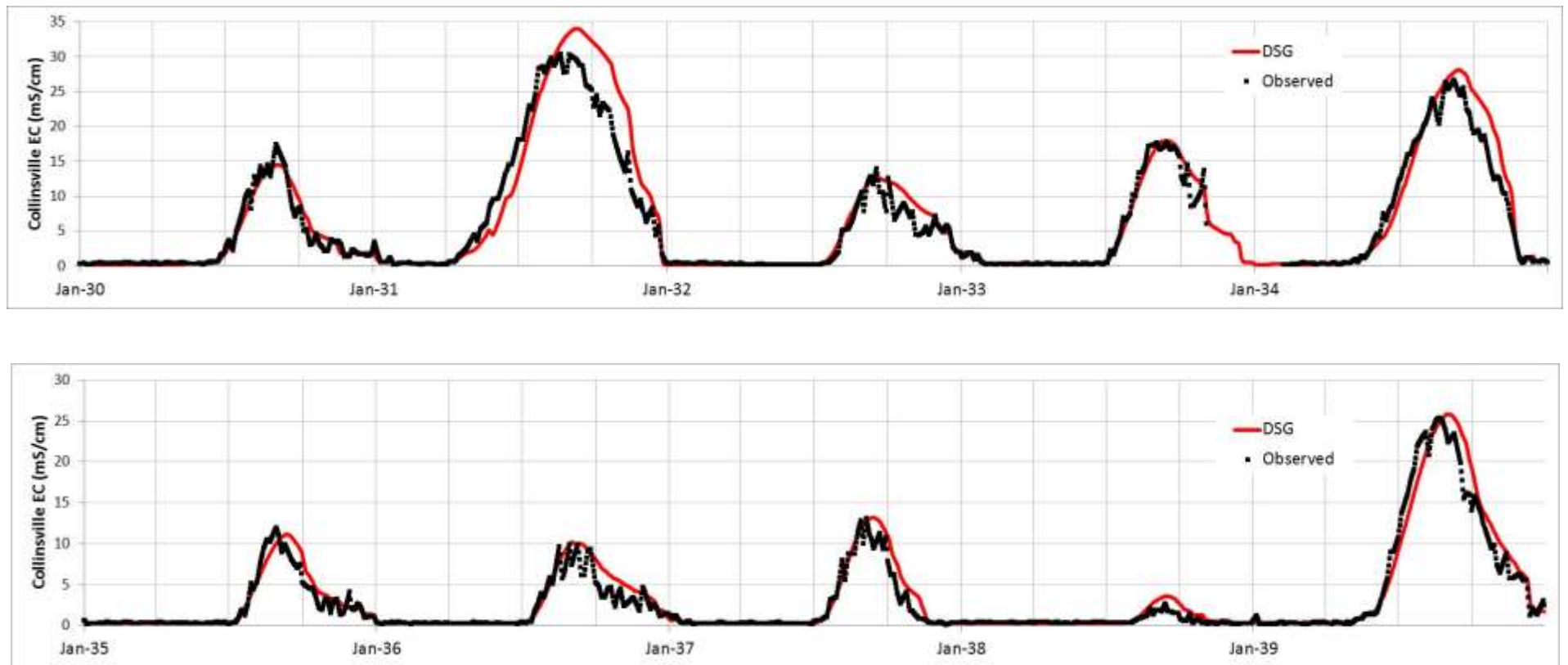


Figure E-60: Time Series of DSG Predicted and Observed Surface Salinity at Collinsville: 1930-1939

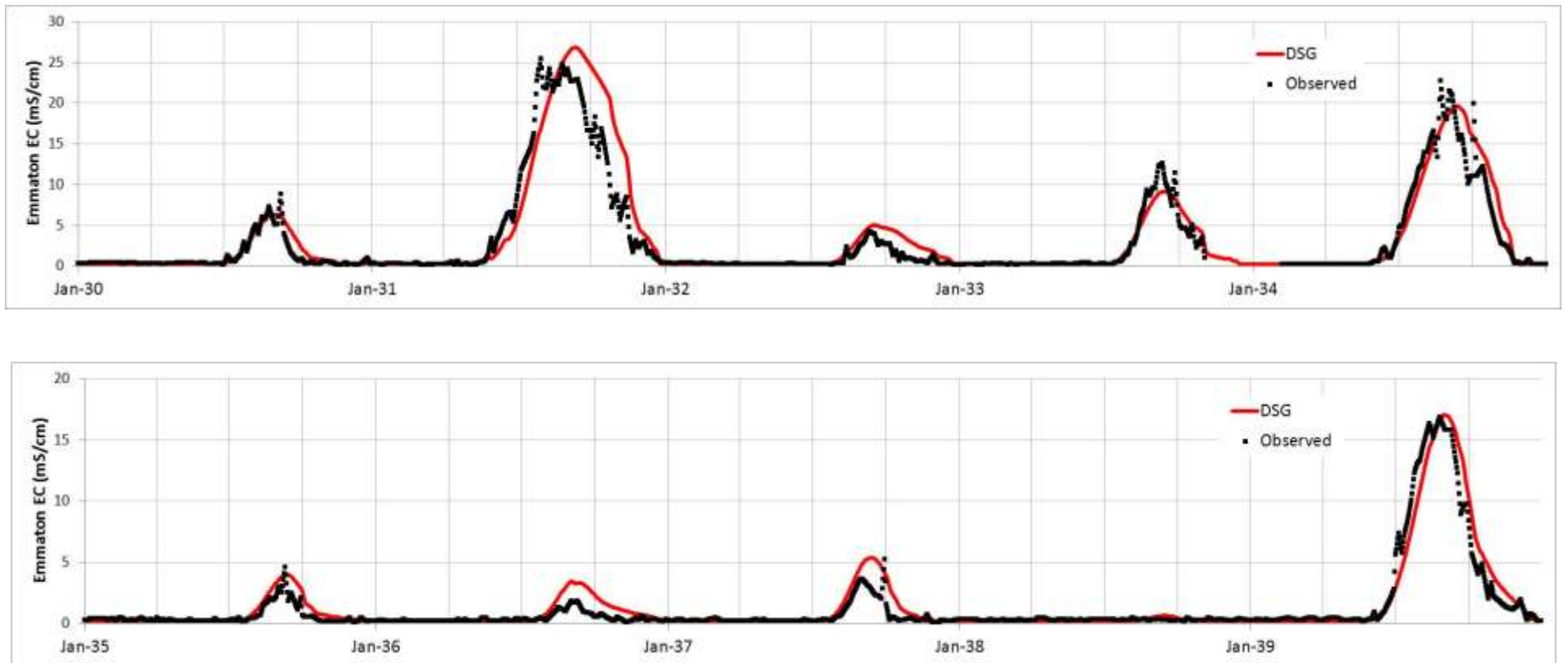


Figure E-61: Time Series of DSG Predicted and Observed Surface Salinity at Emmaton: 1930-1939

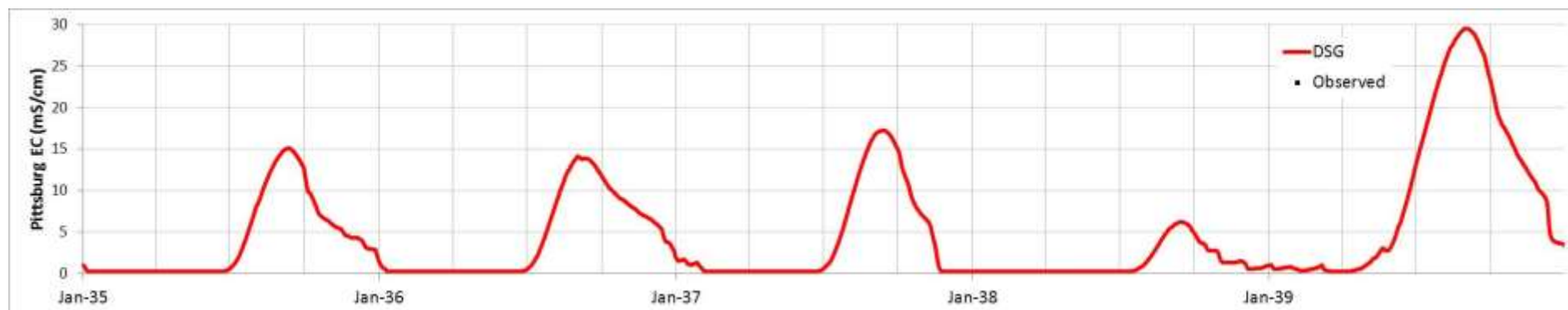
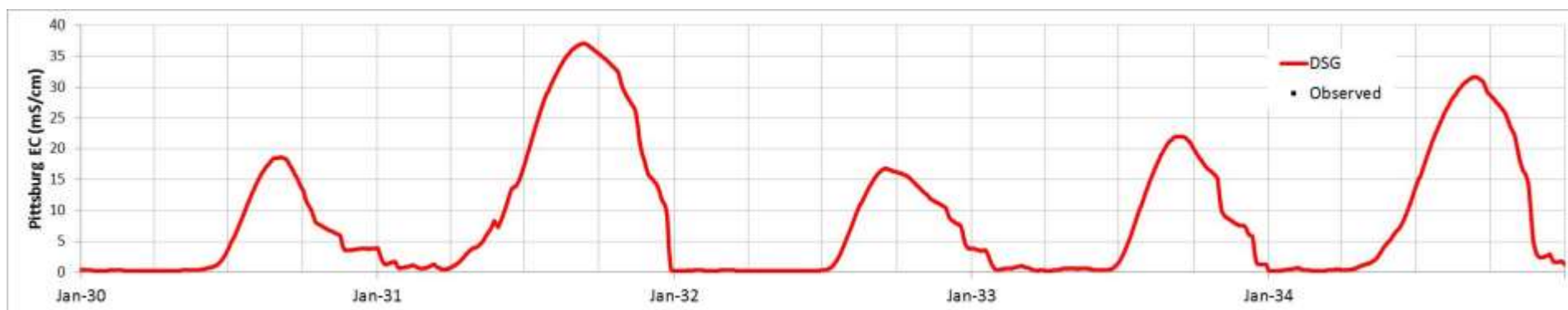


Figure E-62: Time Series of DSG Predicted and Observed Surface Salinity at Pittsburg: 1930-1939

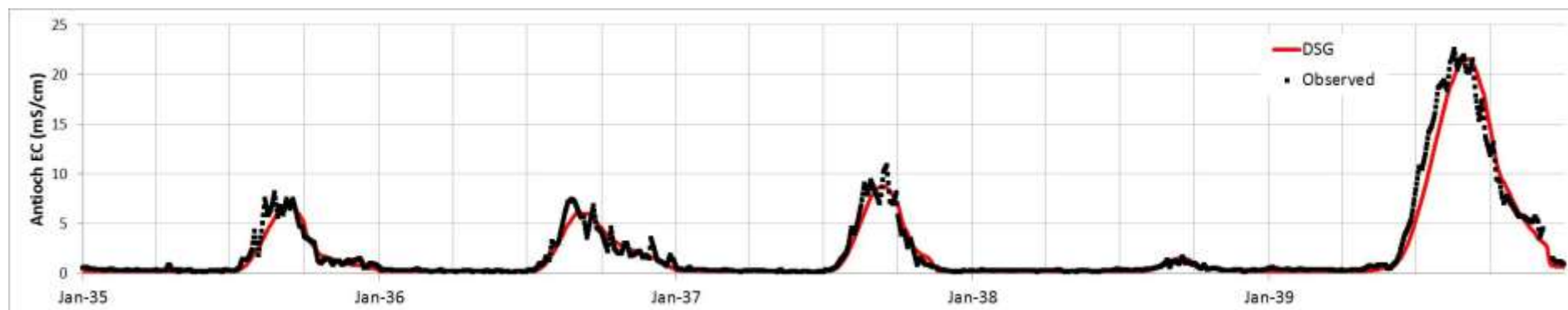
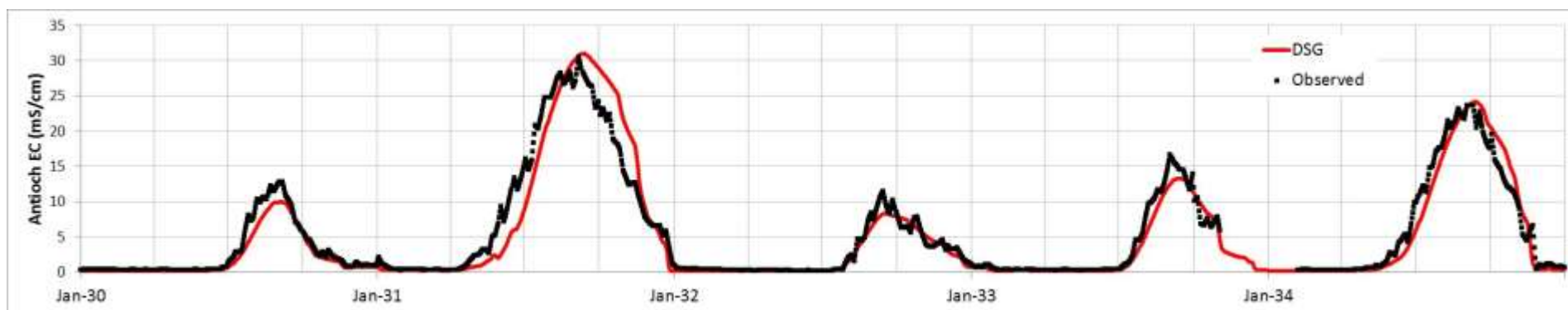


Figure E-63: Time Series of DSG Predicted and Observed Surface Salinity at Antioch: 1930-1939

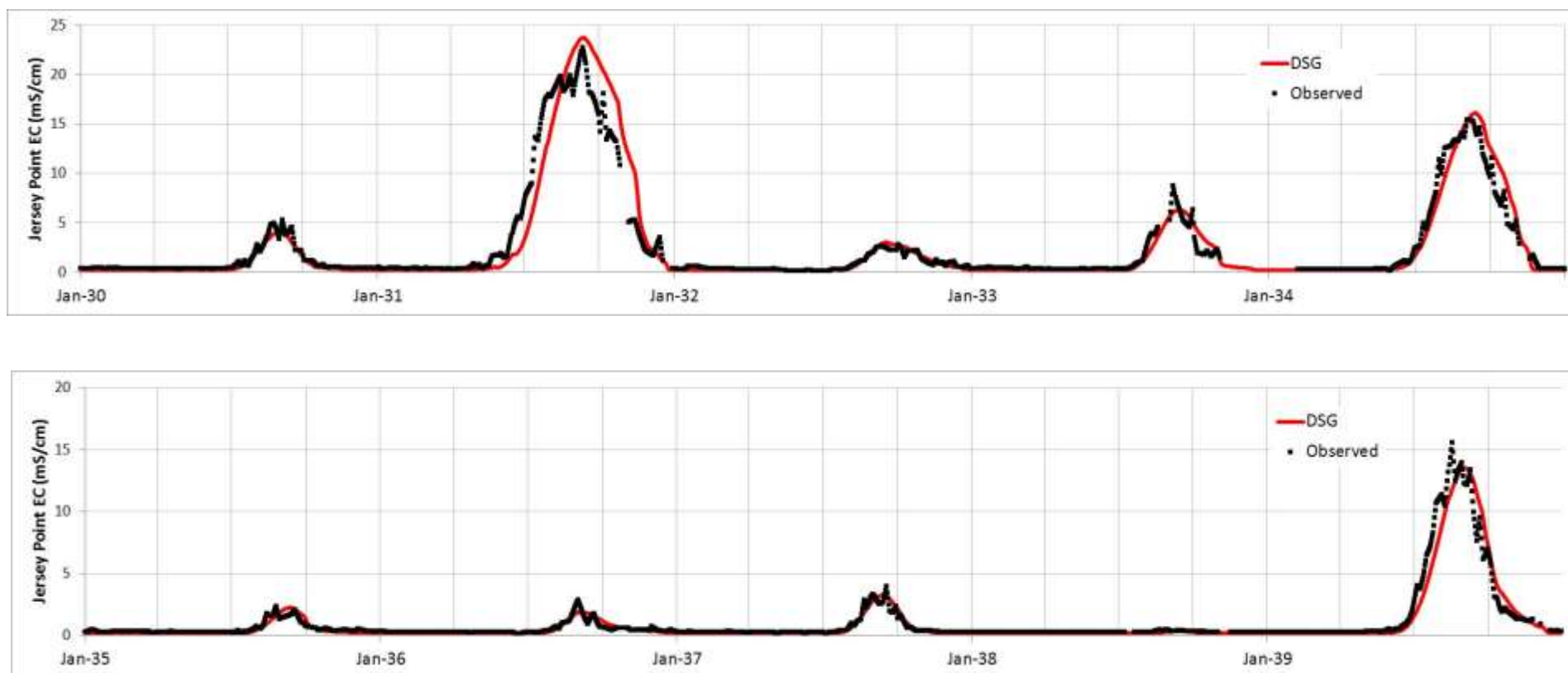


Figure E-64: Time Series of DSG Predicted and Observed Surface Salinity at Jersey Point: 1930-1939

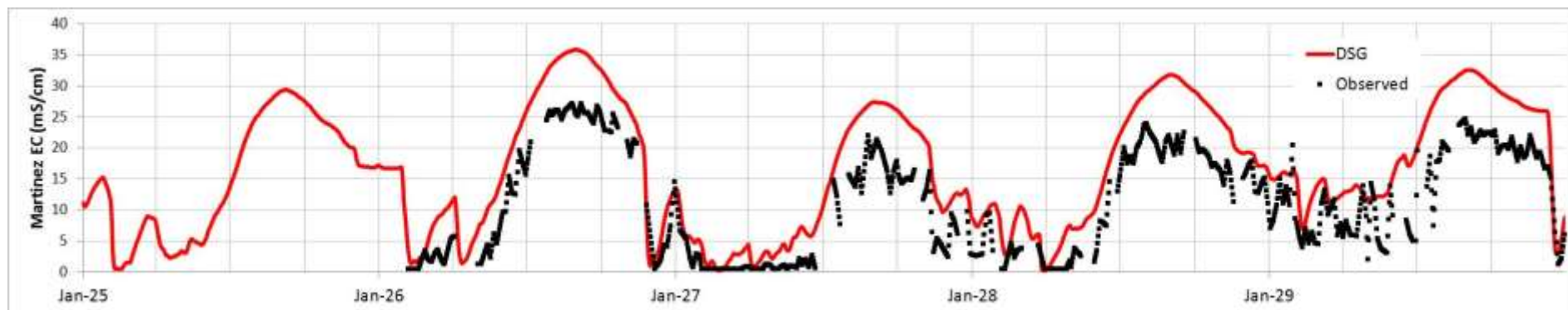
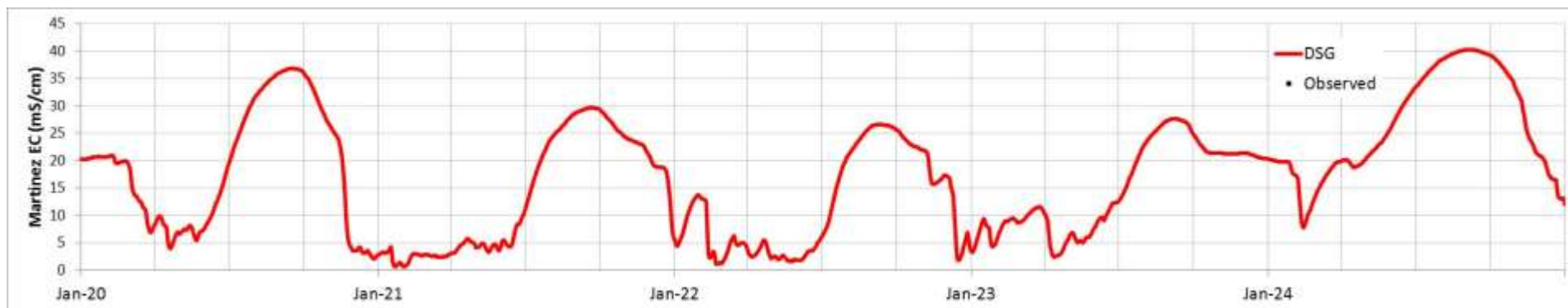


Figure E-65: Time Series of DSG Predicted and Observed Surface Salinity at Martinez: 1920-1929

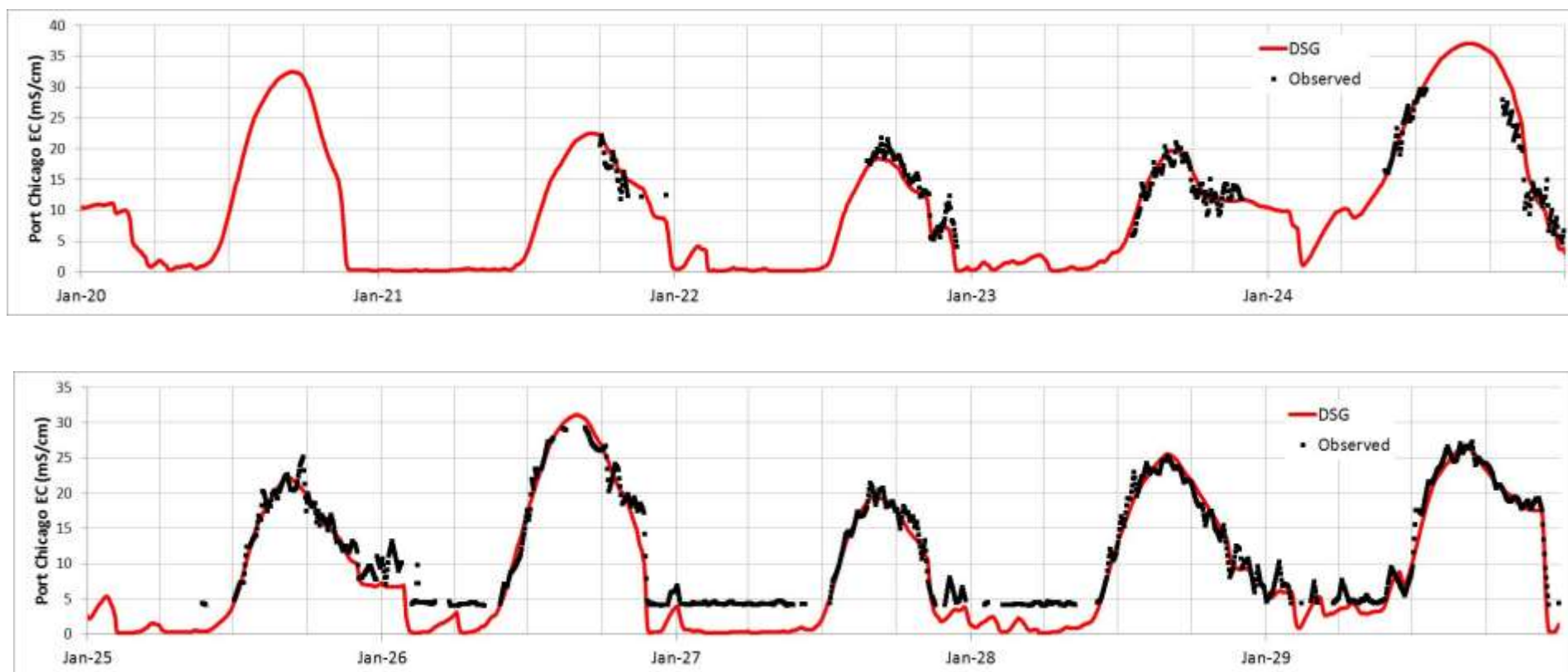


Figure E-66: Time Series of DSG Predicted and Observed Surface Salinity at Port Chicago: 1920-1929

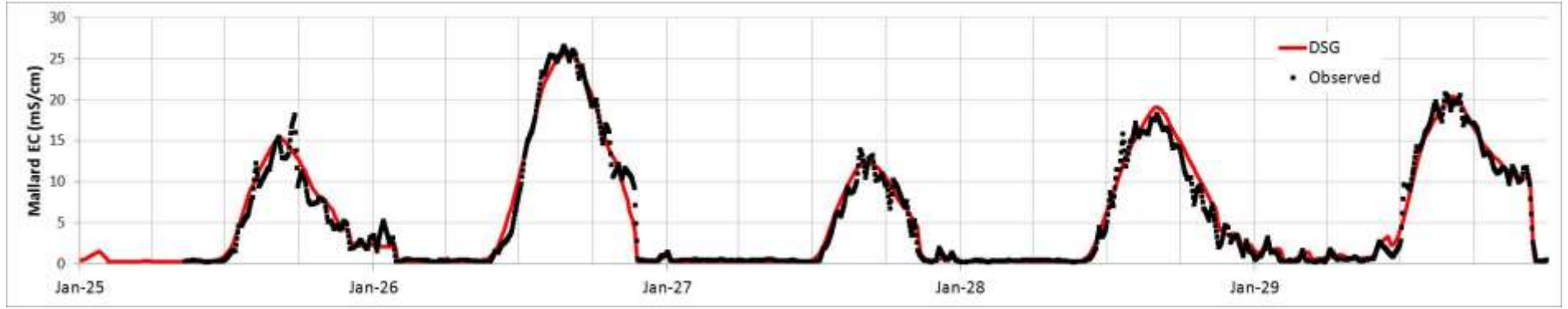
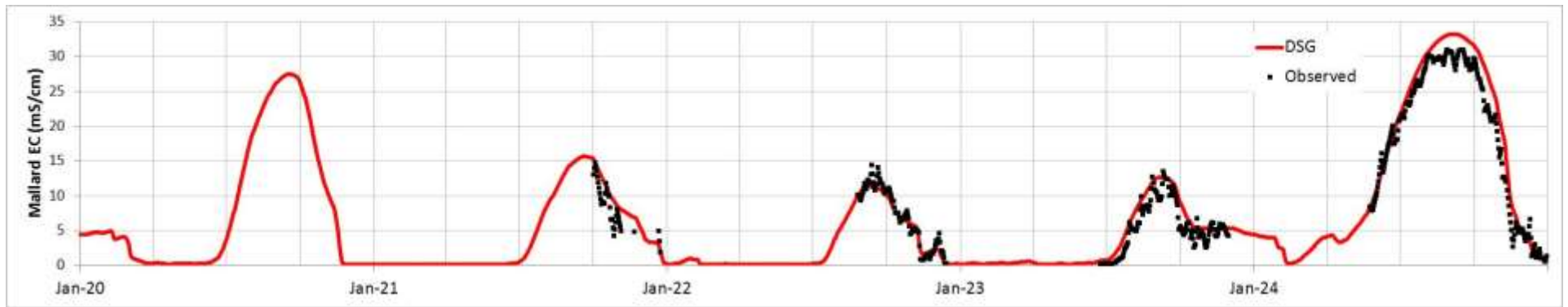


Figure E-67: Time Series of DSG Predicted and Observed Surface Salinity at Mallard Island: 1920-1929

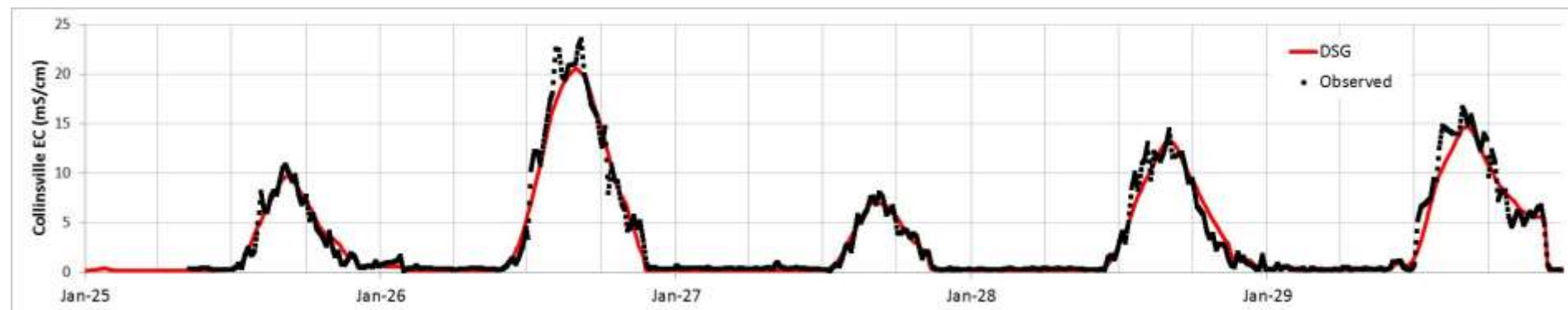


Figure E-68: Time Series of DSG Predicted and Observed Surface Salinity at Collinsville: 1920-1929

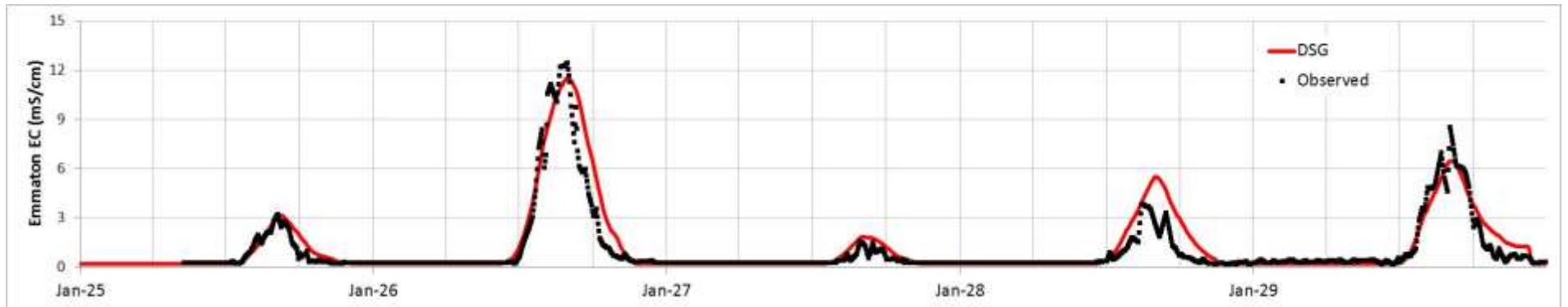
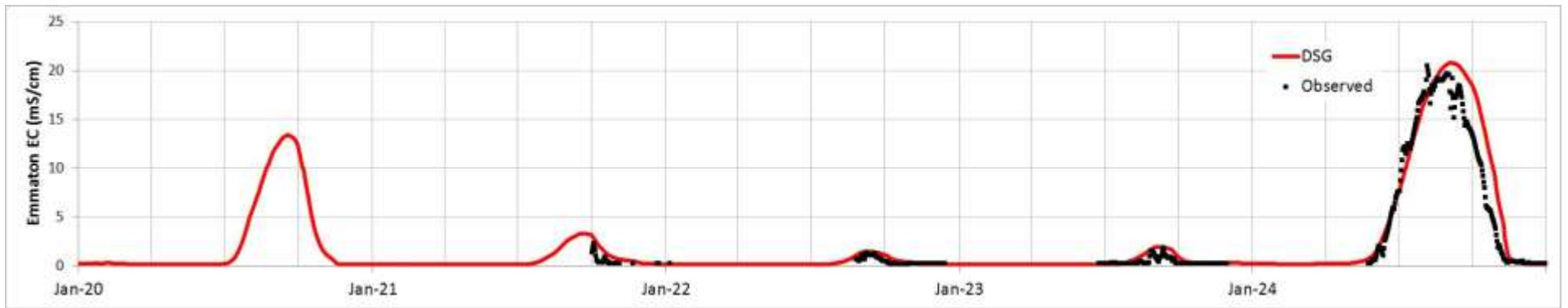


Figure E-69: Time Series of DSG Predicted and Observed Surface Salinity at Emmaton: 1920-1929

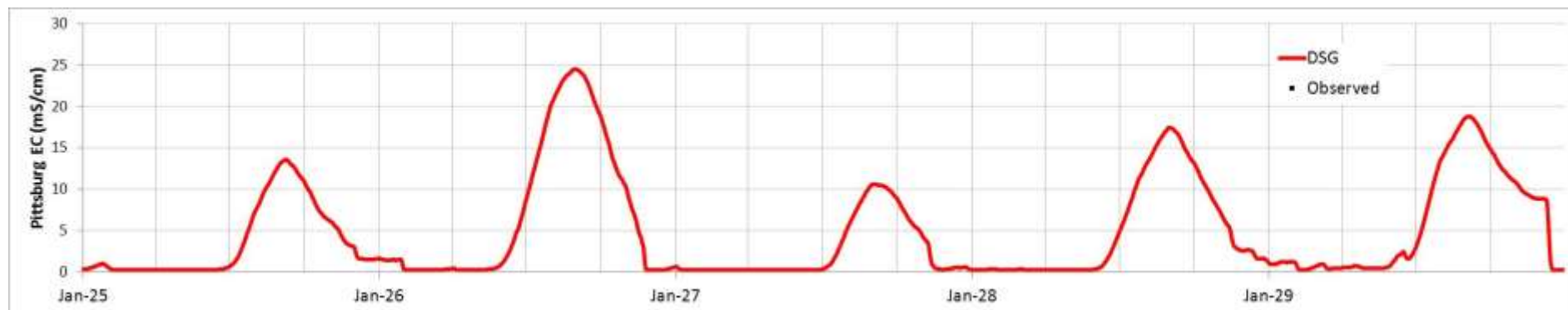
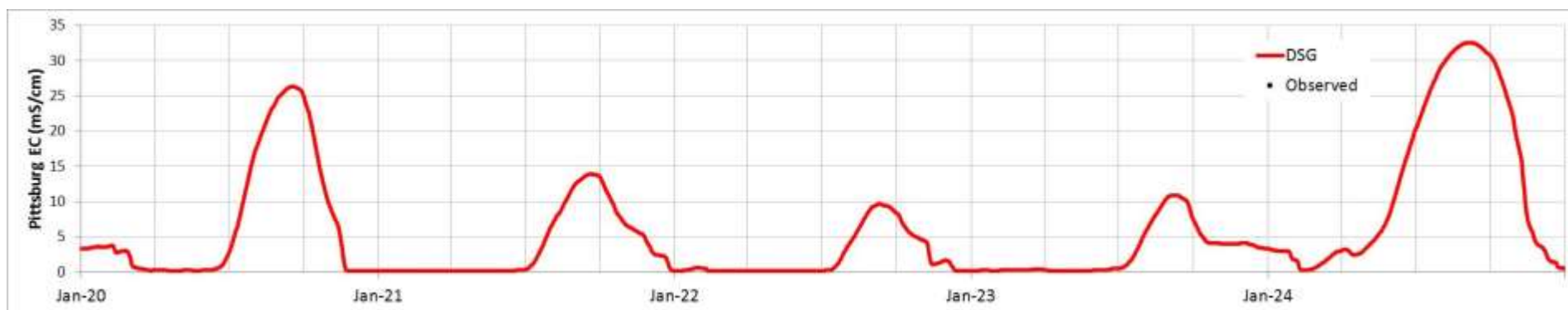


Figure E-70: Time Series of DSG Predicted and Observed Surface Salinity at Pittsburg: 1920-1929

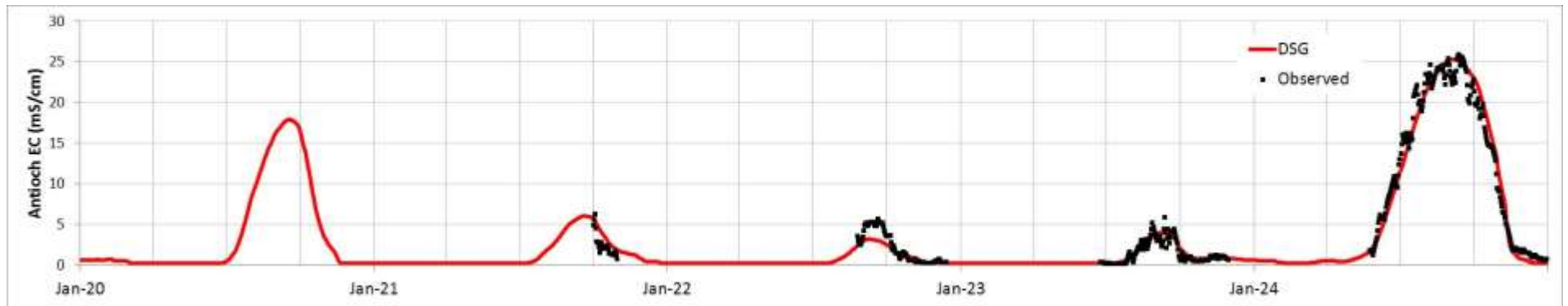


Figure E-71: Time Series of DSG Predicted and Observed Surface Salinity at Antioch: 1920-1929

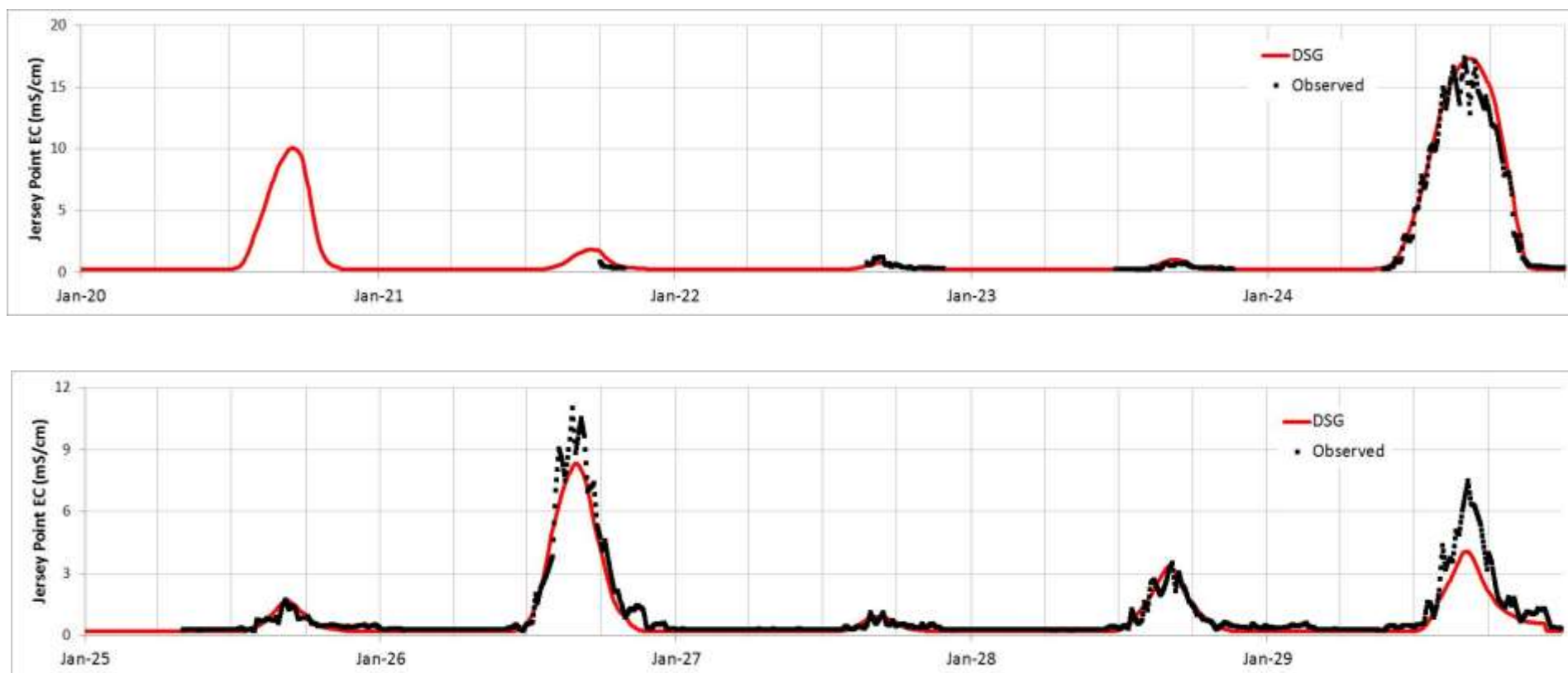


Figure E-72: Time Series of DSG Predicted and Observed Surface Salinity at Jersey Point: 1920-1929

Appendix F: Time Series Plots – DSG Salinity Predictions Using Interpolated X2 Values

This appendix provides time series plots comparing DSG and observed salinity at the following locations for the 2000-09 calibration period: Martinez, Port Chicago, Mallard Island, Collinsville, Emmaton, Pittsburg, Antioch and Jersey Point. The DSG estimates shown in these plots are computed from observed (i.e. interpolated) X2 values rather than X2 values estimated from antecedent outflow.

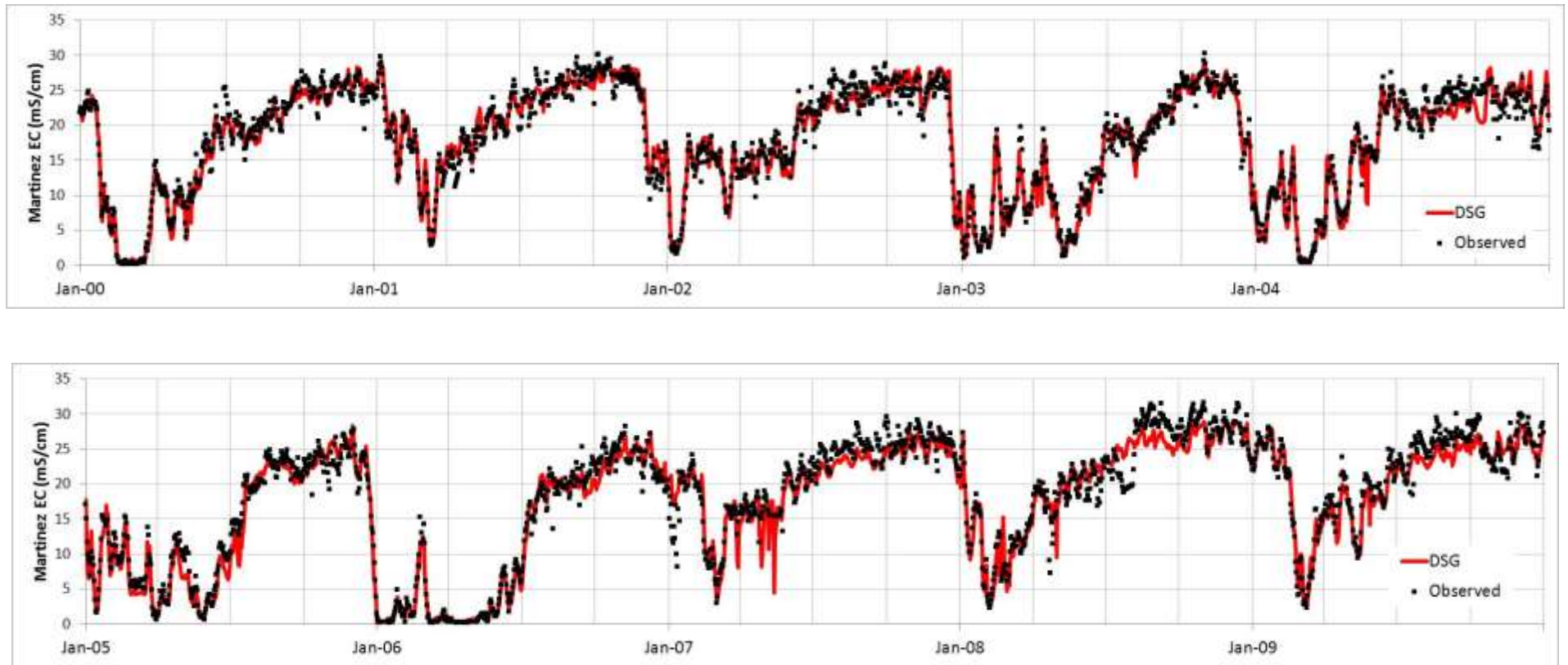


Figure F-1: Time Series of DSG Predicted (Using Interpolated X2) and Observed Surface Salinity at Martinez: 2000-2009

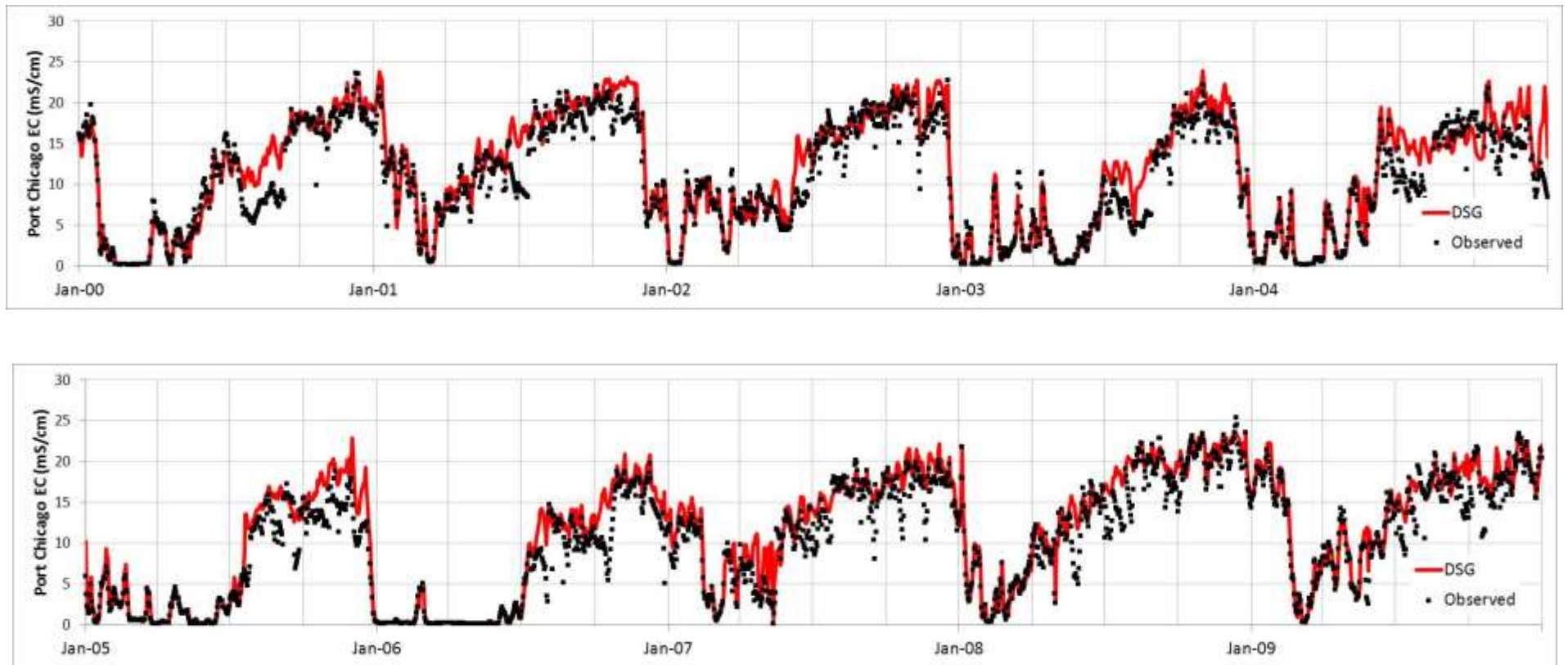


Figure F-2: Time Series of DSG Predicted (Using Interpolated X2) and Observed Surface Salinity at Port Chicago: 2000-2009

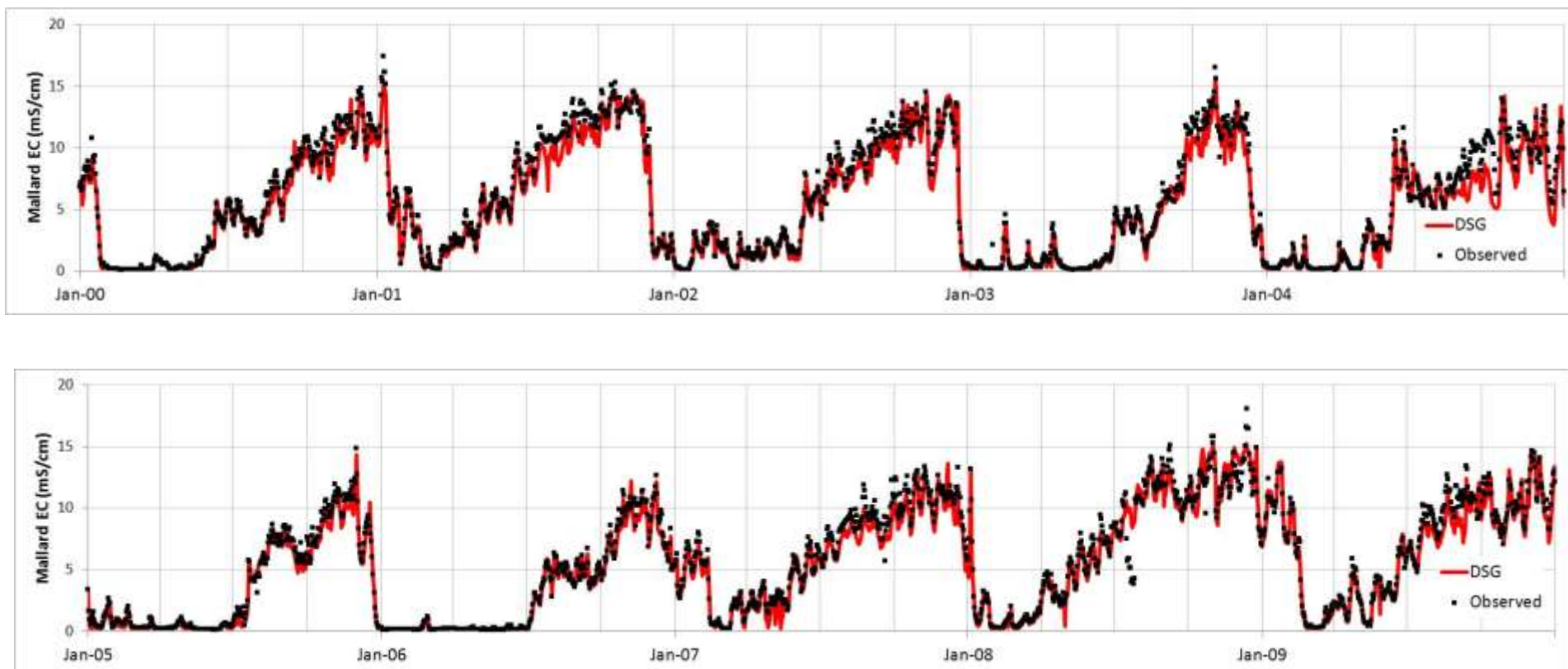


Figure F-3: Time Series of DSG Predicted (Using Interpolated X2) and Observed Surface Salinity at Mallard Island: 2000-2009

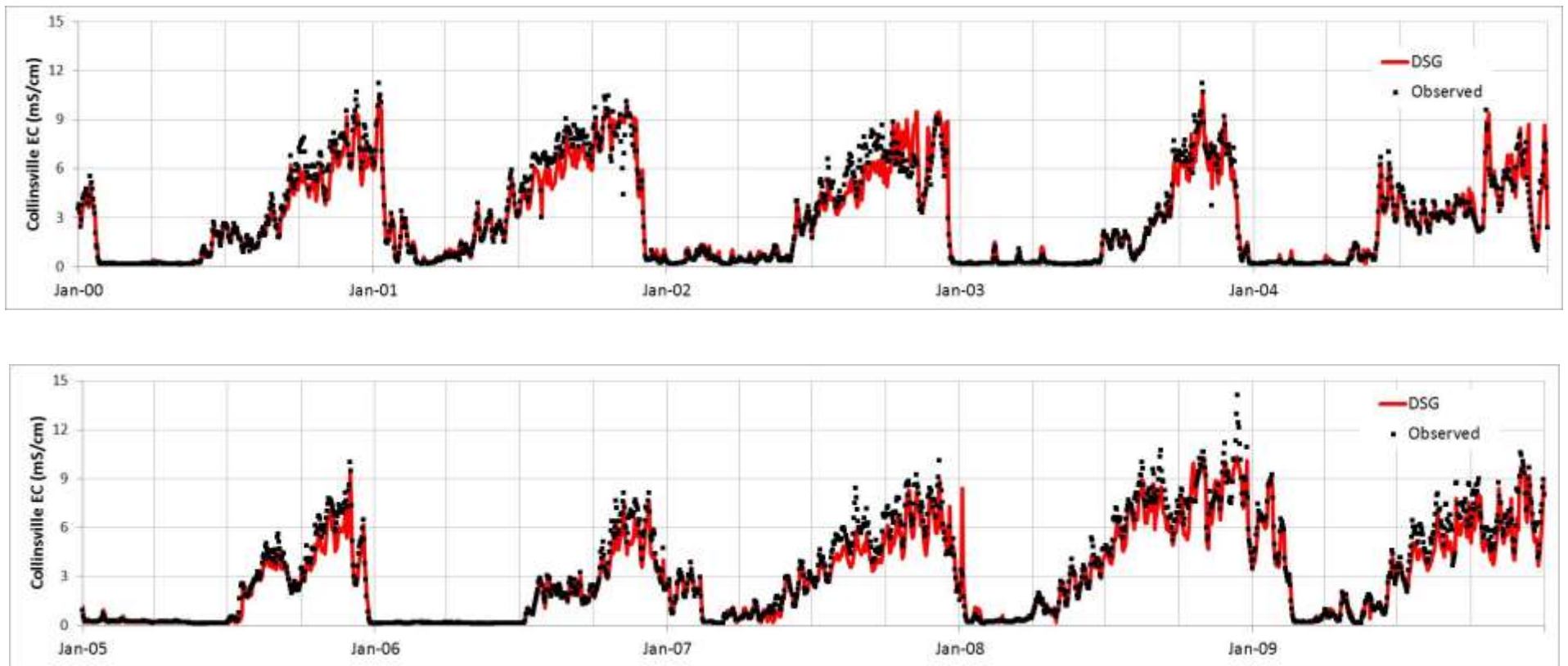


Figure F-4: Time Series of DSG Predicted (Using Interpolated X2) and Observed Surface Salinity at Collinsville: 2000-2009

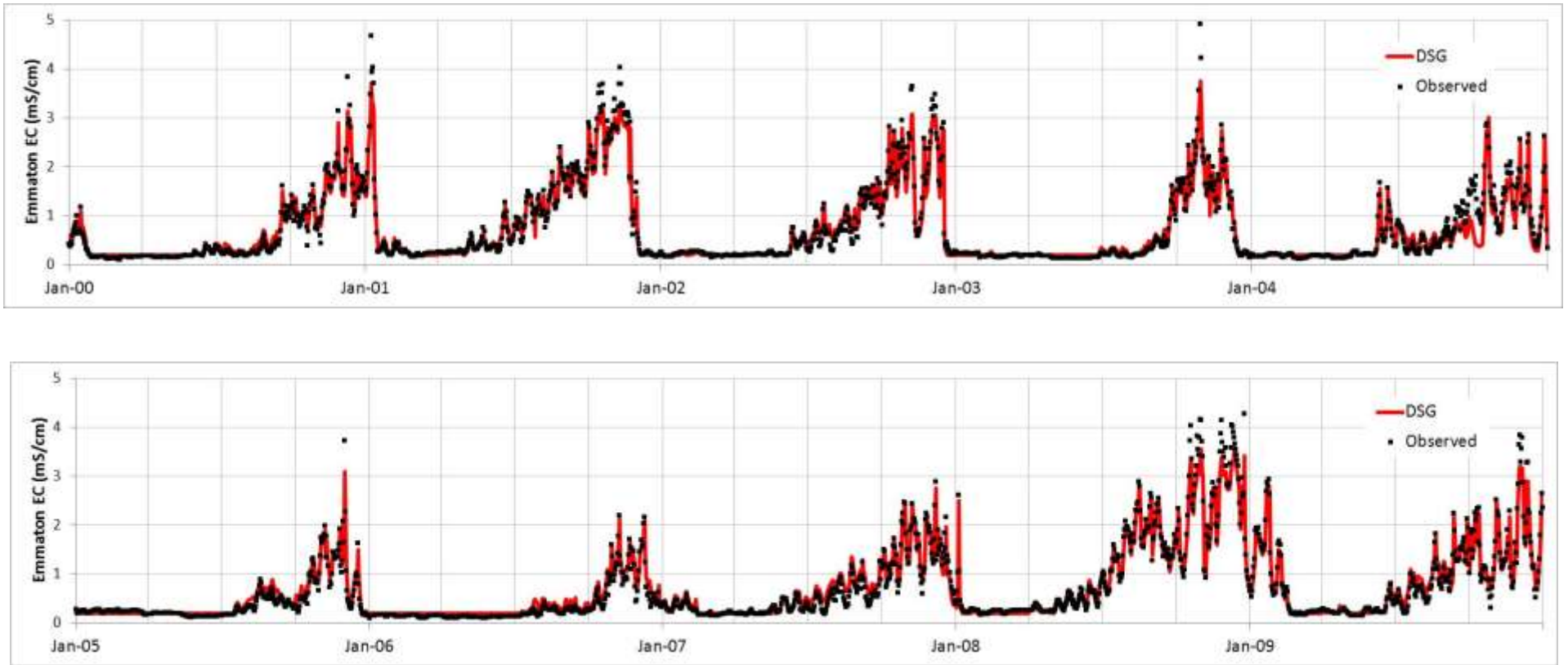


Figure F-5: Time Series of DSG Predicted (Using Interpolated X2) and Observed Surface Salinity at Emmaton: 2000-2009

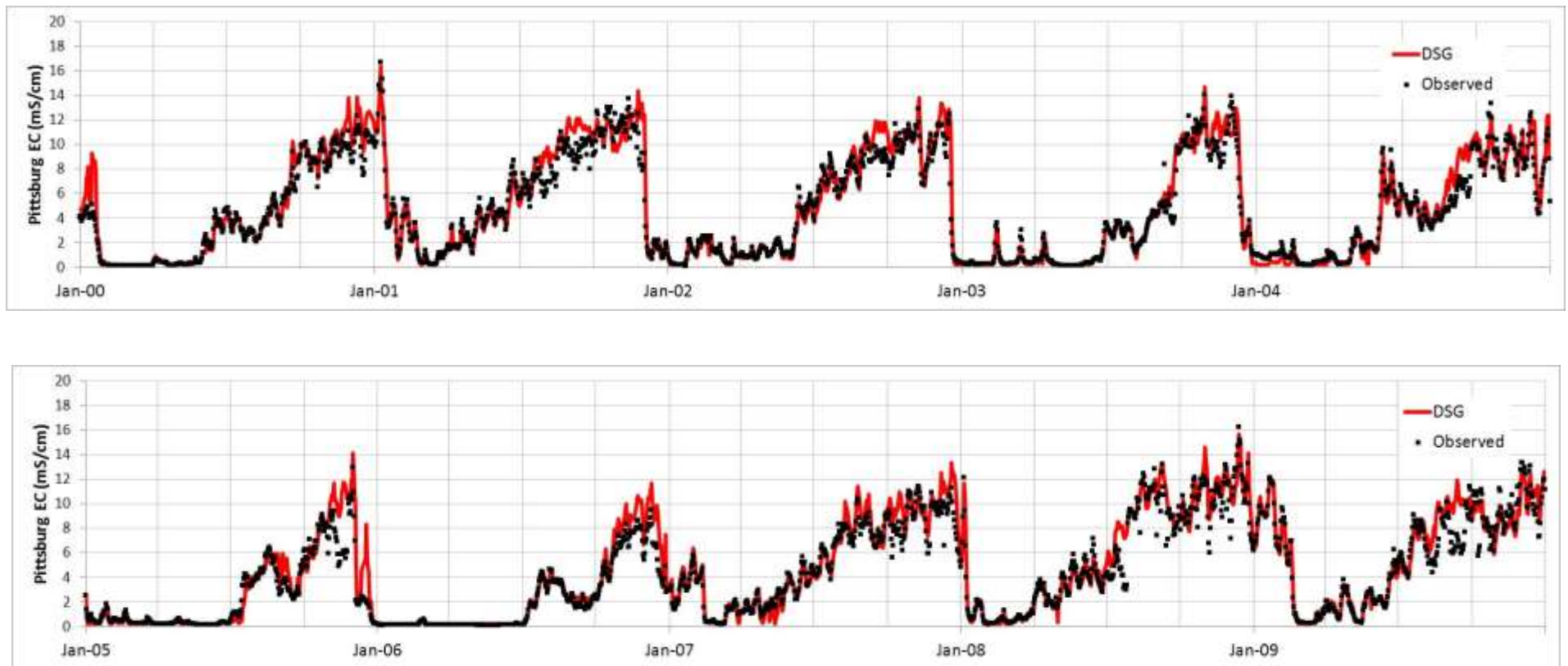


Figure F-6: Time Series of DSG Predicted (Using Interpolated X2) and Observed Surface Salinity at Pittsburg: 2000-2009

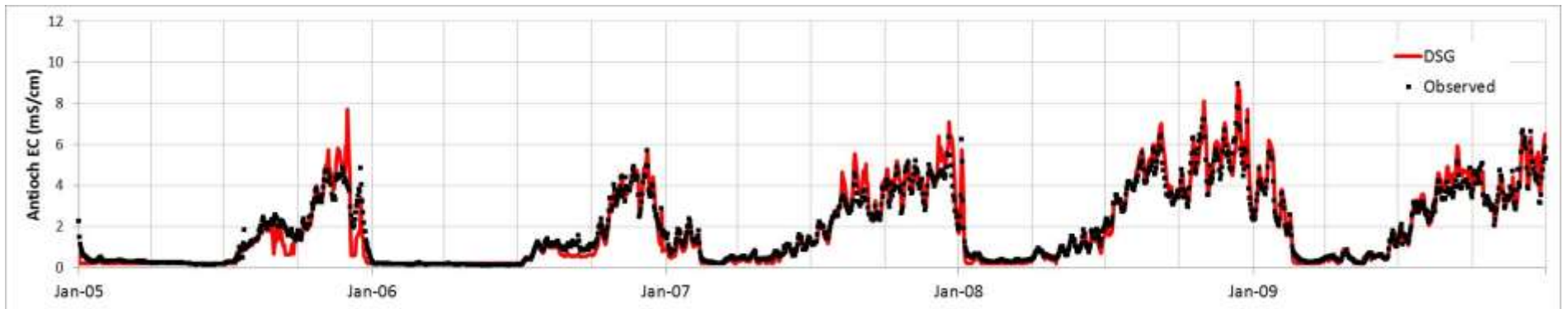
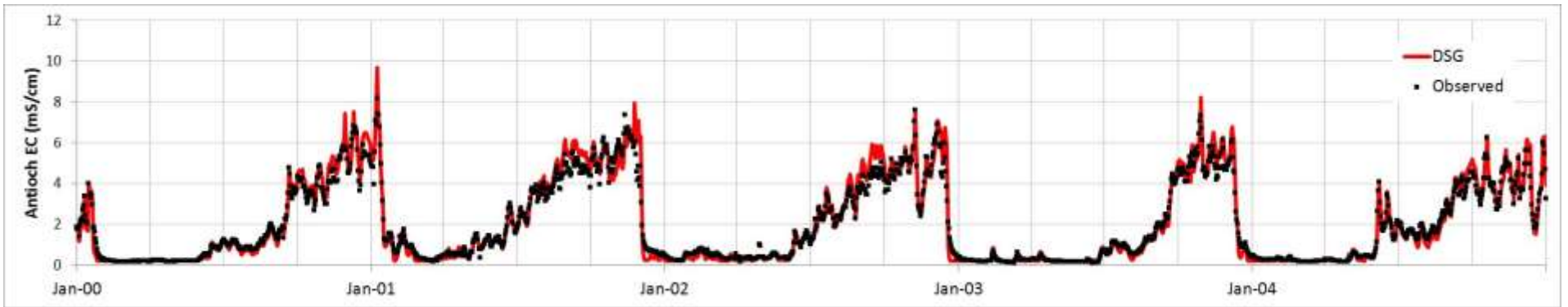


Figure F-7: Time Series of DSG Predicted (Using Interpolated X2) and Observed Surface Salinity at Antioch: 2000-2009

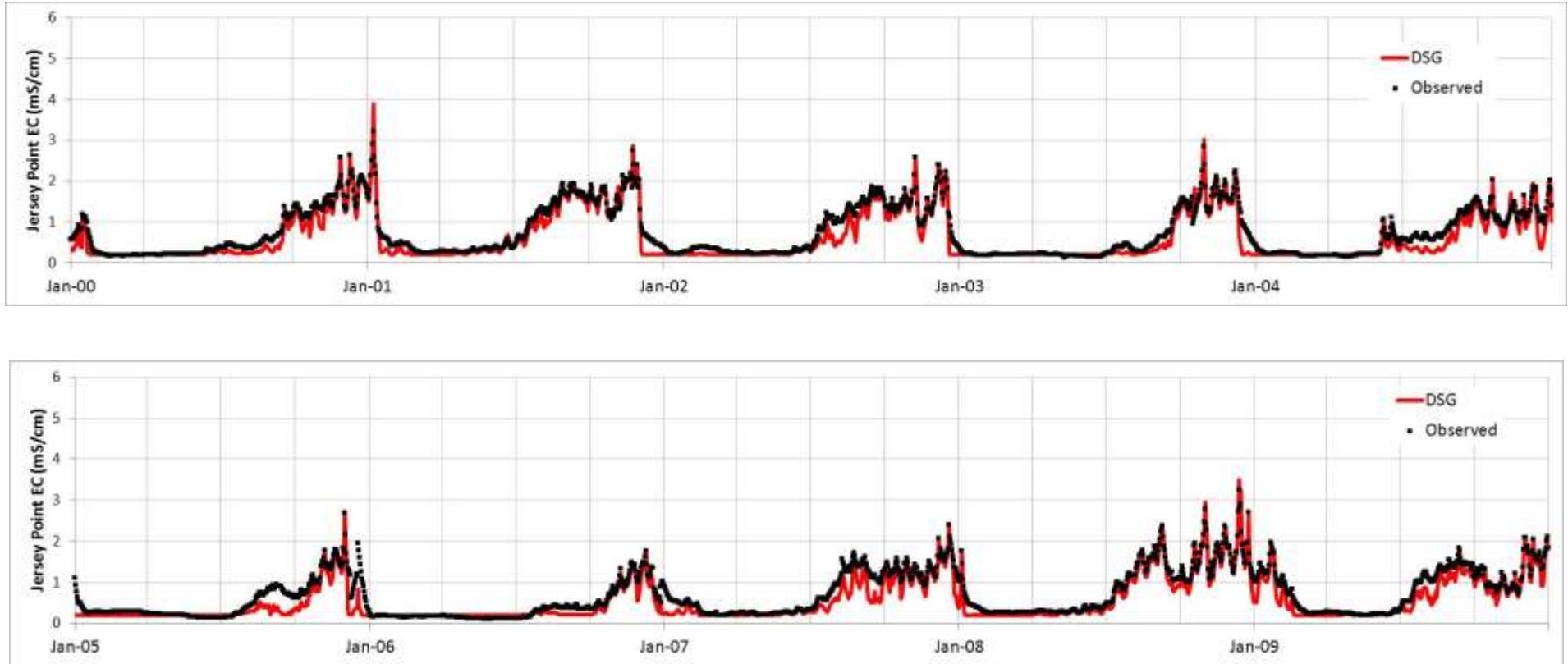


Figure F-8: Time Series of DSG Predicted (Using Interpolated X2) and Observed Surface Salinity at Jersey Point: 2000-2009